Department für Pferde, Musculoskeleteal Research Unit (MSRU)
Vetsuisse Faculty, University of Zurich

Director: Prof. Dr. med. vet. Anton Fürst, Dipl. ECVS, FTA für Pferde

Scientific supervision was provided by
Dr. med. vet. Gisela Kuhn

Interaction of mechanical loading with osteoporosis treatment in ovariectomized mice

INAUGURAL-DISSERTATION
to be awarded the Doctoral Degree of the
Vetsuisse Faculty, University of Zurich

submitted by

Claudia Weigt

Veterinarian
from Karl-Marx-Stadt, today Chemnitz, Germany

2013

Approved by the Vetsuisse Faculty as inaugural dissertation on proposal from

Prof. Dr. med. vet. Brigitte von Rechenberg, examiner

Prof. Dr. Ralph Müller, co-examiner

Zurich,

Dean of Vetsuisse Faculty
University of Zurich

Table of Contents

Summary 5
Zusammenfassung 6
1 Introduction 7
1.1 Motivation 7
1.2 Aim 9
1.3 Experimental setup 10
2 Literature review 11
2.1 Bone 11
2.1.1 Bone cells and their function 11
2.1.2 Bone remodeling 13
2.1.3 Impairment of bone remodeling 15
2.2 Osteoporosis as a health problem 18
2.2.1 Types of Osteoporosis and their pathogenesis 20
2.2.2 Pharmacological treatment 27
2.3 Bone and biomechanics 32
2.3.1 Bone mechanobiology 32
2.3.2 Mechanical intervention in osteoporosis 34
2.4 Animal models in postmenopausal osteoporosis and mechanobiology 37
2.4.1 Animal models in postmenopausal osteoporosis 37
2.4.2 Animal models for unloading and loading 40
2.4.3 Quantitative assessment of bone remodeling 44
2.4.4 Ethical aspects of animal models 46
3 Materials and Methods 49
3.1 Experimental setup 49
3.2 Animals 51
3.3 Ovariectomy 51
3.4 Pinning procedure 53
3.5 Loading and pharmacological treatment 56
3.6 CT-measurements 58
3.7 Image processing and evaluation 59
3.8 Physiome map 62
3.9 Statistical analysis 63
4 Results 64
4.1 Outcome of ovariectomy and pinning operation 64
4.2 Effect of ovariectomy 66
4.3 Loading in ovariectomized mice 70

4.4 Loading in pharmacological treated ovariectomized mice 87
4.4.1 PTH studies 87
4.4.2 Bisphosphonate study 106
4.5 Physiome map 124
5 Discussion 139
5.1 Model, Methods and experimental design 139
5.2 Results 143
5.2.1 Loading in ovariectomized mice 143
5.2.2 Loading in pharmacological treated ovariectomized mice 147
5.2.3 Comparison PTH and Bisphosphonates 154
6 Outlook 159
7 List of references 163
Acknowedgments 181
Curriculum Vitae 182

Summary

Osteoporosis, characterized by bone loss and increased fracture risk, is usually treated with exercises and medication. However, exact interactions of different treatments are not fully known yet. This study investigated the interaction of mechanical load on the 6th caudal vertebra (CV) and bisphosphonate (BIS) or PTH treatment in ovariectomized (OVX) mice. *In vivo* micro-CT measurements of the 6th CV were performed before OVX and during treatment. From the CT images static and dynamic bone parameters were evaluated. An OVX induced bone loss was observed. Loading improved all static parameters in OVX animals, except for trabecular number. BIS treatment had comparable effects as loading for most parameters. However, trabecular number increased. Adding loading to BIS treatment improved static parameters even more. PTH treatment caused similar or better results as combined BIS treatment and loading. When loading was combined with PTH treatment the improvement of the static parameters exceeded all other groups. For the dynamic parameters it can be said, that loading increased formation parameters and decreased resorption parameters. PTH increased formation parameters the most, while BIS related to similar formation parameters as vehicle. BIS treatment revealed its anticatabolic action in the resorption parameters. Bone resorption rate was reduced, as well as mineral resorption rate.

Zusammenfassung

Die Behandlung von Osteoporose, welche durch Knochenmasseverlust und ein erhöhtes Frakturrisiko charakterisiert ist, erfolgt meist medikamentös und mit Sport. Das genaue Zusammenspiel verschiedener Behandlungsmethoden ist jedoch noch ungenügend erforscht. Diese Studie untersuchte die Interaktion von mechanischer Belastung (LOAD) des 6. Schwanzwirbels (SW) und der Behandlung mit Bisphosphonaten (BIS) oder PTH in ovariektomierten (OVX) Mäusen. Vor der OVX OP, sowie jeweils während der Behandlung wurden micro-CT-Aufnahmen des 6. SW angefertigt. Mit Hilfe dieser Aufnahmen wurden statische und dynamische Knochenparameter berechnet. OVX verursachte einen Knochenmasseverlust. Durch LOAD wurden alle statischen Paramter, ausser trabecular number verbessert. Ähnliche Effekte wurden nach der Behandlung mit BIS festgestellt, allerdings nahm hier die Anzahl der Trabekel zu. BIS Behandlung zusammen mit LOAD führte zu noch besseren statischen Parametern. Die Ergebnisse nach PTH Behandlung waren ähnlich oder besser als bei BIS und LOAD zusammen. Die grösste Verbesserung der Parameter wurde bei der Kombination von PTH und LOAD gesehen. Bei den dynamischen Parametern stiegen durch LOAD die Aufbauparameter und sanken die Resorptionsparameter. Unter PTH Behandlung stiegen die Aufbauparameter am stärksten an. Die antikatabolische Wirkungsweise von BIS wird bei den Resorptionsparametern deutlich, welche reduziert werden.

1 Introduction

1.1 Motivation

Osteoporosis is a major health problem, worldwide. It occurs mainly in the developed countries, and affects about 75 million people in Europe, USA and Japan. The World Health Organization (WHO) called it an "epidemic of the 21st century"[1]. As mainly elderly people, who represent a rapidly growing subpopulation, are suffering from this disease, the number of osteoporosis patients will increase dramatically in the future. Cooper et al. estimated, that in Europe the population of people aged 65 years or older will increase from 68 million in the year 1990 to over 133 million in 2050. An even greater increase in the elderly population is expected for Asia. Here the number will rise from 145 million in 1990 to 894 million in 2050 [2]. The number of osteoporosis patients is expected to increase to a similar extend.

The causes for osteoporosis can be manifold, but the consequences are always similar: Bone architecture is slowly deteriorated and bone mass is lost, resulting in an increased risk for fractures. In the past, according to WHO a bone was considered to be osteoporotic when the bone mineral density (BMD) was 2.5 standard deviations or more below the young adult mean [3]. Consequently, due to reduced BMD, bone rigidity is impaired and fractures may occur. However, as bone mineral density not always correlates with mechanical stability the definition of osteoporosis changed to be a combination of bone loss and increased fracture risk [4]. Patients with fractures have to be hospitalized and sometimes need intensive care afterwards. The life time risk to experience a hip fracture is one in six in white women. In comparison, the life time risk for breast cancer is one in nine [5]. Women after menopause are the largest patient group affected by osteoporosis, because decreasing estrogen levels can cause rapid bone loss. In women older than 45 years, osteoporosis is the reason for spending more days in hospital than many other diseases such as diabetes, myocardial infarction or breast cancer [6]. In Switzerland in the year 2000 62,535 people had to be hospitalized for fractures. Among these fractures 51% in women and 24% in men were caused by osteoporosis [7]. In Europe there were about four million new fractures in the year 2000, which is one fracture every eight seconds. About 3.79 million of them were considered to be caused by osteoporosis. Costs for all osteoporotic fractures in Europe were €36 billion in the year 2000 and are expected to rise up to €76 billion in the year 2050 due to the increasing elderly population [8, 9]. Mortality rates are up to 20-24% in the first year after experiencing a hip fracture and are still elevated for at least 5 years. Additionally, among survivors about 40 % are not able to walk independently and 60 % still require assistance one year after the fracture

occurred [10-12]. Hence osteoporosis has a tremendous impact not only on national health care systems, but also on the personal wellbeing of the patients. Therefore, the demand to fully understand the mechanisms leading to bone loss and to find effective treatment options is high.

However, as bone physiology is a complex and precisely regulated process, there are still a lot of questions that need to be answered. Different cell types are orchestrated by many endocrine and paracrine signals to maintain bone mass. The most important cells are osteoclasts, responsible for bone resorption, and osteoblasts, responsible for bone formation. Only if bone resorption and bone formation are in balance, a stable bone mass can be maintained. During childhood bone mass is increasing and reaches the peak bone mass at time of adolescence. Starting at the age of about 25 to 30 years, bone mass is decreasing again. This bone loss continues also in healthy persons for the rest of the life time [13, 14].

A common measure to try to prevent the onset of osteoporosis is to induce a high peak bone mass and maintain this by the application of food with high calcium and vitamin D content. Furthermore, bone mass can be improved by physical activity. This is important not only during childhood and adolescence, but also during the adult life. It has been shown that physical activity can reduce the risk of osteoporosis and fractures. Therapeutic exercise can increase or maintain bone mineral density in postmenopausal women and improve strength and function, even in elderly patients who already experienced hip replacement after a hip fracture [15-20]. Once osteoporosis is diagnosed, several pharmacological treatments are available. There are two different strategies how such medication acts on bone: Anabolic drugs target osteoblasts and increase bone formation, while antiresorptive drugs act on osteoclasts and impede bone resorption. So far the European Medicines Agency EMEA approved only one anabolic drug for osteoporosis treatment in Europe: Teriparatide, an analogue of the parathyroid hormone (PTH). It increases both bone formation and - with a certain delay - bone resorption. However, after about two years, bone remodeling parameters go back to baseline levels [21]. Moreover, in a rat study an incidence of osteosarcoma development occurred after treating the animals with high dose PTH for two years [22]. Due to these facts, teriparatide is approved for a treatment period of two years only in humans. However, within these two years a tremendous increase in bone mineral density, bone mass, bone strength, bone formation and bone micro architectural parameters can be observed in both human and animal studies [23-31]. For the second strategy, antiresorptive treatment, several medications are on the market. Bisphosphonates are the most commonly used drugs but there are also hormone replacement therapy, selective estrogen receptor modulators,

calcitonin and denosumab, an antibody that interrupts pro-resorptive signaling, available. Bisphosphonates have a high affinity to bone mineral and accumulate in osteoclasts. Therefore, they have a very long half-life. The biggest concern about bisphosphonates, besides having side effects like nausea, headache or bone pain, is that they are suspected to cause atypical femoral fractures and osteonecrosis of the jaw [32, 33]. Nevertheless, bisphosphonates show good results in improving deteriorated bone architecture and strength [34-40].

It has been shown that with the appropriate treatment the risk of vertebral fracture can be reduced by 30-65 % [41]. However, patient adherence (the number of days a medication is taken) and patient compliance (the number of doses taken divided by the number of doses prescribed), are often poor. This can be due to side effects, simply forgetting to take the medication or unpleasant way of administration, as PTH, for example, has to be administered daily with a subcutaneous injection. A drug with good compliance is Zolendronate, a newly developed bisphosphonate that has to be administered just once a year via infusion [39].

Therefore, there is a great demand to further improve the available drugs. However, neither the pathways inducing osteoporosis nor the mechanisms of the drugs and their interaction with mechanical loading are fully understood yet. Hence, research has to focus on investigating these mechanisms closer in order to provide better medication.

1.2 Aim

The aim of this thesis was to investigate the effect of combined pharmacological treatment and mechanical loading on bone remodeling in ovariectomized mice.

Ovariectomized mice are a common model for postmenopausal osteoporosis. First it was studied if the ovariectomized mice are susceptible to loading. The second aim was to study the effect of different pharmacological treatments in combination with mechanical loading. Both pharmacological strategies were investigated. The influence of an anabolic drug, namely PTH and an anticatabolic treatment, namely bisphosphonates, both in combination with loading was examined. To illustrate the effects at different time points of bone loss, all experiments were performed at an early and a late time point after ovariectomy. During all experiments the changes in static and dynamic bone parameters were monitored with *in vivo* micro-CT. With a method recently developed at our institute [42] not only bone microstructure, also bone formation and resorption can be monitored over time at a three dimensional level with *in vivo* micro-CT . This is a great advantage compared to conventional methods as histology and histomorphometry. With histology and histomorphometry data can

only be acquired from cross sectional studies, because the bones have to be processed and cannot be observed in living animals. Furthermore, only single slices can be evaluated at a two dimensional level. Now, with *in vivo* micro- CT it is possible to perform longitudinal studies and monitor the effect of treatment over a longer period of time. Moreover, the entire bone can be evaluated at a three dimensional level. Finally all experiments were summarized in a physiome map. With this summary the outcomes of the different experiments can be compared directly. A physiome map provides a powerful evaluation tool but could also be the basis to add data of future experiments. Furthermore, it can serve as input for computer simulations to be able to predict changes in bone morphology and bone morphometry due to diseases and due to different types of treatments.

1.3 Experimental setup

In all studies C57Bl/6J mice were ovariectomized (OVX) or sham operated (SHM) at the age of 15 weeks. In an earlier study at our institute, we investigated the time course of bone loss in OVX mice [43]. During this experiment ovariectomized mice were scanned biweekly for twelve weeks. It was shown that between two and eight weeks after ovariectomy a phase of rapid bone loss occurred, which was followed by a phase of slow bone loss where a plateau is reached. Between ten and twelve weeks after ovariectomy bone mass is kept stable at a very low level [43]. Based on these results, our experiments were performed in two series which differ in the starting point for the treatment. In the early loading series, treatment was started during the rapid bone loss period, five weeks after surgery. In the other experimental series, the late loading experimental series, treatment and loading started eleven weeks after ovariectomy. Three studies were performed in each experimental series. One study investigated the effect of loading on ovariectomized compared to sham operated mice to test whether OVX mice are mechanosensitive at all. In a second study, PTH or vehicle were injected and both were combined with loading. The last study investigated the effect of the combination of bisphosphonate or vehicle treatment and loading. All treatments were applied over four weeks. The pharmacological treatment was performed only in OVX mice, because treatment of mice with normal bone mass was not in the scope of our project. In all studies non-loaded mice were used as controls. At the beginning of each study ten mice were assigned to each group.

The effect of pharmacological treatment in combination with loading was monitored with *in vivo* micro-CT in all studies. During the course of each study *in vivo* micro-CT scans were performed four times in total. The first scan was done before ovariectomy, the second at the

start of the loading and treatment period and the last two with a time lag of two weeks in the middle and at the end of the loading and treatment period.

Due to *in vivo* micro-CT measurements all studies could be performed in a longitudinal fashion. With longitudinal studies the number of animals can be reduced. Furthermore the fact that all animals show inter-individually different reactions to the different treatment types can be overcome.

2 Literature review

2.1 Bone

The human skeleton consists of about 200 bones of different shapes, length and function. However, the principle composition of a bone is always the same. It consists of a compact outer shell, called cortical bone, which contributes about 80% of the whole skeletal mass. Inside the bones there is a three dimensional network of trabeculae and in-between there is the bone marrow. With this construction bone is resistant and strong but still light weighted. The material which bone is made of consists of about 80 % dry matter, splitting up into 30% organic material, such as collagen and 70% inorganic material, mainly hydroxyapatite. With just 20% water content, bone has extremely little water compared to other organs. The functions of bone are manifold. Most obviously bones are responsible to give stability and shape to the entire body. As bones are very solid, they protect vital sensitive organs, such as the brain, heart and lungs. Furthermore, production of new blood cells is located in the bones. In new born humans hematopoiesis is almost exclusively located in the red bone marrow, which is present in all bones at that time point. As humans get older, the red bone marrow turns into yellow bone marrow in many bones and hematopoiesis is only located in some bones (e.g. pelvis), where red bone marrow is still remaining. Another very important function of bone is to keep the mineral metabolism of calcium and phosphate in homeostasis and to regulate blood pH by secreting buffer substances. It also serves as a reservoir for other minerals, such as magnesium and sodium. Furthermore some toxic substances can be cleared from the blood by binding in the bone matrix.

2.1.1 Bone cells and their function

Bone is a complex structure that has to be organized properly. In order to preserve healthy bone, different cells work together. The most important cells are osteoclasts, responsible for bone resorption, osteoblasts, responsible for bone formation and osteocytes, which are

embedded in the bone matrix and serve as mechanosensors. During bone remodeling, these cells are organized in the so called bone multicellular unit (BMU). In BMUs osteoclasts form a resorption cavity by resorbing bone. This cavity is filled later by osteoblasts with newly formed bone.

As just mentioned, osteoclasts are the bone resorbing cells. They derive from hematopoietic stem cells and form large multinucleated cells. To resorb bone, they lower the pH by secreting hydrogen ions after attaching to the bone surface. This dissolves the mineral salts within the bone. Furthermore secreted proteolytic enzymes dissolve the organic matrix. With these processes osteoclasts form the resorption cavity. Osteoclasts are activated by PTH and inactivated by calcitonin.

Osteoblasts are the bone forming cells. To form the bone matrix they secret type I collagen and the non-collagenous protein osteocalcin. Osteoblasts derive from multipotential mesenchymal stem cells in the bone marrow. These cells can differentiate into different cell lines, like adipocytes, chondrocytes or osteoblasts. To differentiate into an osteoblast, the expression of the transcription factors Runx2 and osterix are important, whereas the expression of other transcription factors favors the differentiation into adipocytes or chondrocytes. Osteoblasts refill the resorption cavity. When the cavity is refilled with new bone matrix, osteoblasts die from apoptosis, get embedded into the matrix and turn into osteocytes, or become lining cells and stay at the bone surface.

Osteocytes develop from osteoblasts. They represent mature bone cells and are embedded in the mineralized bone matrix. Osteocytes account for the largest number of cells in the bone. They have long slender processes, which are connected with each other via small canaliculi. As they form a communication network with the help of these slender processes, osteocytes are also referred to as the "brain" of the bone [44]. Osteocytes can sense mechanical forces and their viability depends upon physiological levels of mechanical stimulation. If these levels drop, the cells go into apoptosis, which seems to be the trigger to recruit new osteoblasts and to generate a new bone multicellular unit (BMU) [45].

A fourth common bone cell type are bone lining cells. They evolve from osteoblasts and cover all inactive bone surfaces. These cells can re-differentiate into osteoblasts [46].

To orchestrate all bone cells, a number of local, systemic and central factors are necessary. Local factors are for example prostaglandins and nitric oxide which are produced by osteocytes. Others are several growth factors such as transforming growth factor beta (TGF-β), which are released from the dissolved bone matrix and exert their effects on osteoblast precursors by enhancing their differentiation or activation [47]. Systemic factors are sex

steroids, parathyroid hormone (PTH), calcitonin, vitamin D3 or cytokines. They derive directly from endocrine glands and immune cells and have different direct and indirect actions on bone cells [48]. At the central level, leptin, a hormone produced by fat cells, has been shown to have inhibitory effects on bone formation via binding to hypothalamic receptors. The antiosteogenic function is mediated by the sympathetic nervous system which favors bone resorption by increasing the expression of the ligand of transmembrane receptor activator of NF-κB (RANKL) in osteoblast progenitor cells [49].

Osteoclast differentiation is initiated and supported by several factors: Osteoblasts produce macrophage colony stimulating factor (M-CSF) and RANKL, a ligand to the transmembrane receptor activator of NF-κB (RANK). RANK is expressed in osteoclast precursors which then differentiate as soon as RANKL is present. The expression of RANK in osteoclasts and RANKL in osteoblasts is stimulated by M-CSF. Binding of RANKL to RANK is not only important for the differentiation of osteoclast precursors, but also for their fusion to multinucleated cells and the activity and survival of osteoclasts [47]. Osteoblasts also produce osteoprotegerin (OPG) which is a decoy receptor for RANKL and inhibits osteoclast differentiation. Thus, the RANKL/OPG ratio is important for osteoclast differentiation and regulates the activity of RANK in osteoclast precursors [50].

The number of osteoblasts is dependent on the lineage specification process. When differentiation of osteoblast precursors proceeds, replication gets less, the cells mature and acquire differentiated characteristics. Replication, differentiation, and survival of osteoblast progenitors is influenced by several autocrine and paracrine factors such as Wnt proteins, bone morphogenic protein, several growth factors (TGF-β, IGF-1, FGF-2) and interleukins. Many of these growth factors are produced by osteoblasts and deposited in the bone matrix to be released during osteoclastic bone resorption [51]. Osteocytes also produce many factors regulating bone remodeling. These factors are for example, nitrogen oxide and prostaglandins, but also sclerostin, the product of the SOST gene. Sclerostin prevents binding of Wnt to its receptor and therefore has a restraining effect on osteoblast differentiation [52].

2.1.2 Bone remodeling

Bone is remodeled during the entire life time. The remodeling serves different purposes, for example optimizing bone microarchitecture or release of calcium. Harold M. Frost defines remodeling as “processes which turn over lamellar bone; it does not cause large changes in its quantity, geometry or size and it continues throughout life.” In contrast, to modeling, which he defines as “bone resorptive and formative processes which are associated primarily with

growth (…) Modeling serves primarily to alter the amount of bone present, and to determine its geometry and size."[53]. Remodeling provides skeletal integrity and maintains the bones mechanical properties by replacing old bone with new resistant bone. During walking and load bearing, bone is exposed to loading throughout the whole life. Due to this loading small micro cracks can occur. A single micro crack does not affect the bone stability at all, but if damage accumulates, the strength of the bone becomes impaired and fractures may occur. Micro cracks are detected by osteocytes, which then trigger the remodeling.

Bone remodeling occurs in so-called basic multicellular units (BMU), where the osteoclast mediated bone resorption and the subsequent osteoblast mediated bone formation are coupled. BMUs have different morphological shapes in cortical and trabecular bone. In the cortex a cylindrical canal is formed, which is about 200 µm long in humans. At the tip osteoclasts form the "cutting cone" digging a tunnel by resorbing bone. They are followed by osteoblasts forming the "closing cone" and refilling the defect with new bone [54, 55]. In the trabecular bone, osteoclasts act first as well. However, they dig a trench rather than a tunnel. Therefore, a trabecular BMU can be morphologically regarded as half a cortical BMU [56].

The bone remodeling cycle consists of 5 steps: 1) initiation, 2) bone resorption, 3) reversal 4) bone formation, 5) mineralization. Bone remodeling is initiated by osteocytes and their secretion of signaling molecules. Lining cells are retracted and osteoclasts start resorbing bone. After some time, the reversal phase starts where pre-osteoblasts differentiate into osteoblasts. These cells assemble at the bottom of the resorption cavity and start formation of new bone by secretion of organic matrix (osteoid). While bone formation progresses some osteoblasts are entombed within the matrix and form osteocytes. However, most osteoblasts die by apoptosis. The whole process terminates when the cavity is refilled and the remaining osteoblasts turn into flat lining cells [51]. The secreted osteoid is later mineralized and represents the newly formed bone [57]. In humans, the resorption phase of the remodeling cycle stops after one or two months and is followed by an approximate 3 month period of bone formation [58]. The average bone formation rate per bone surface is 0.038 $\mu m^2/\mu m/d$ compared to 0.15 $\mu m^2/\mu m/d$ in mice. These different bone formation rates can be explained with the different osteoblast life spans, which is 10-12 days in mice but about 150 days in humans [51].

In healthy bones, resorption and formation are balanced with equal amounts of resorbed and newly formed bone. However, during the course of aging, remodeling tends to become unbalanced. In women at the age of 40 years and in men at the age of 50 years each BMU is slightly smaller than the cavity where it sits, leading to 10-30% negative imbalance at the

endosteal surface, covering the trabecular bone and the inner surface of the cortical bone and a zero or slightly positive imbalance at the periosteal surface, covering the outer surface of the cortical bone [59]. However, the number of BMUs is increasing in age. During aging, these processes lead to cortical thinning, increased cortical porosity, decreased trabecular thickness and decreased trabecular connectivity density [60].

2.1.3 Impairment of bone remodeling

Impairments of bone remodeling can occur at many different levels. Bone formation and resorption is unbalanced, when the activity or number of osteoblasts or osteoclasts is changing. The two processes can also be uncoupled, leading to excessive bone formation or resorption. While an imbalance can occur at any time in the remodeling cycle, whether during resorption or during formation, uncoupling happens only during the reversal phase, when bone resorption changes into bone formation. When formation and resorption are coupled and balanced, the activation frequency (the number of newly formed BMU within a certain bone volume and specified time) can still be changed. An increasing activation frequency results initially in net bone resorption until formation is up-regulated and a steady state is reached with overall increased bone turnover [53]. All mechanisms in bone remodeling are linked together tightly. Therefore, diseases arising from impairments in remodeling will always present in a heterogeneous fashion, combining different aspects of impaired bone remodeling.

Osteopetroses (Marble bone disease) are a group of inherited diseases that are characterized by increased bone density. Their prevalence is between 1 in 250 000 birth for autosomal recessive forms and 1 in 20 000 births for the autosomal dominant form. Osteopetroses are classified according to their malignancy, age of occurrence or partially on the responsible mutation. Only the main forms are presented here.

Infantile malignant osteopetrosis is the most severe form of the disease. It is transmitted autosomal recessive and caused in most cases by loss of function mutations of the proton pump (vATPase) or the chloride channel (ClC7) involved in the acid secretion of the osteoclast. The impairment of bone resorption results in missing marrow cavities (“bone in bone appearance”), compression of cranial nerves due to closure of their canals in the skull base and extramedullary blood formation. Without treatment, patients die within their first years because of pancytopenia and immunosuppression. The only known cure is bone marrow transplantation.

The autosomal dominant form of osteopetrosis is also called Albers-Schönberg-disease. This disease is often not diagnosed before adulthood. Typical clinical findings are abnormal

fractures and “sandwich vertebrae" on x-rays. The disease can be caused by mutations of the ClC-7, however the function of the channel is not completely lost, which allows a reduced osteoclast function and bone resorption. Therefore bone accumulates during growth, but remains stable afterwards [61].

Osteopetrosis with renal tubular acidosis is an autosomal recessively transmitted mutation of the gene encoding carbonic anhydrase II. This enzyme synthetizes the protons secreted by osteoclasts via the proton pump. As protons also result from other processes in the cell, acid secretion is not completely disabled. Therefore this disease is also called intermediate osteopetrosis. However as carbonic anhydrase II is also highly expressed in renal intercalated cells and cerebral neurons, defects of the enzyme result in renal tubular acidosis and cerebral calcification causing mental retardation.

Sclerostosis and Van Buchem disease (hyperostosis corticalis generalisata) are autosomal recessive inherited diseases that are characterized by an overproduction of bone mass, but normal bone resorption. Typical clinical findings in sclerostosis are generalized skeletal overgrowth, mainly apparent in the skull and the mandibles, and a large stature. The thickened sclerotic skull results in narrowed foramina of the cranial nerves. This leads to hearing loss, neurological pain and atrophy of the optical nerve. It is a rare disease found in the Afrikaner population in South Africa. The clinical findings of Van Buchem disease are similar, however milder than in sclerostosis. A skeletal overgrowth with enlarged jaw, skull and long bones can be found as well. The increased thickness of the skull results in hearing problems, neurological pain and rarely blindness. This disease is very rare as well and was found in a Dutch population. While for sclerostosis a mutation in the SOST gene was found resulting in complete absence of its gene product sclerostin, the cause for Van Buchem disease a deletion downstream of the SOST gene. This deletion only decreases the gene expression. Therefore clinical findings in Van Buchem disease are milder than in sclerostosis [62, 63].

Osteogenesis imperfecta (brittle bone disease, OI) is a genetic disorder affecting bone formation. It is caused by a variety of mutations of genes encoding collagen I. Depending on the mutated gene, the structure of the collagen molecule can be more or less disturbed. Therefore, eight different types of the disease are distinguished; however, the symptoms can vary widely between patients. Type I (osteogenesis imperfecta tarda) is the most common form of OI. Patients produce collagen with normal structure, but in insufficient quantities. Fractures occur typically in childhood, after puberty the bones become more stable. Scoliosis due to vertebral fractures is common, but no other deformations occur. Hearing loss is possible. Type II is the most severe form and leads to death in the perinatal period caused by

numerous fractures, especially multiple rib fractures, and underdeveloped lungs leading to respiratory failure. The most severe non-lethal form is type III. Typical clinical findings are short stature, blue sclera, limb and spine deformities, loose joints and respiratory problems. In OI type III the amount of formed collagen is enough, however the structure is damaged. Type IV is characterized by mild to moderate bone deformities, a shorter stature than average and not properly formed collagen. By studying histological sections of type IV patients, investigators noticed that some patients had a distinct pattern of the histological appearance of the bone, either "mesh-like" or "fish-scale-like". Furthermore these patients had other features in their medical history in common. Therefore type V and VI were introduced. The underlying cause for both types has not been identified yet; however it is not a collagen mutation. Type V is characterized by moderate to severe bone fragility. Typically after surgical interventions these patients develop a hyperplastic callus. Furthermore, the interosseus membrane between ulna and radius becomes calcified leading to a restricted forearm rotation. The histological appearance of bones is "mesh-like". In type VI a higher amount of osteoid was found in histology and the bones present with a “fish scale appearance”. Types VII and VIII are recessive forms of OI. Both of them are caused by defects of genes affecting collagen formation. Typical clinical findings for type VII involve short stature, short humerus and femur and coxa vera. Type VIII presents with severe growth deficiency and is lethal at an early stage in life. Most of the treatment of OI aims on controlling symptoms and maximizing independent mobility. Therefore, rehabilitation and also insertion of intramedullary rods, to straighten femora and tibia are most common. Pharmacological treatment, such as bisphosphonates, growth hormones or PTH has been applied with varying success. However none of them can cure osteogenesis imperfecta [64, 65].

Paget’s disease is a slowly progressing chronic disease, mostly affecting older people. The causing agent is not known; viral infections like measles, canine distemper respiratory syncytial virus or slow virus disease are discussed [66]. Genetic predisposition might also be involved. The disease presents with locally increased bone turnover and affects different skeletal areas to different degrees in an asymmetric fashion. The remodeling is accelerated regionally with increased activation of new BMUs and increased bone resorption and formation. The mineralization of the osteoid is normal but faster than in normal bones. As recently remodeled bone is replaced quite soon the mean tissue age is decreasing [67]. The symptoms are often quite mild and patients do not notice that they have Paget's disease, however severe bone pain can be associated with this disease as well.

An increased remodeling rate can be found as well in primary hyperparathyroidism. In this disease the secretion of PTH is up-regulated, independent of blood calcium levels. PTH acts as a bone remodeling enhancer and activates new remodeling sites, leading to decreased BMD. It also inhibits the activity of osteoblasts and therefore slightly decreases the mineral apposition rate [67, 68].

Osteomalacia or rickets in children is often caused by lack of sunlight resulting in reduced activation of vitamin D. Sometimes also insufficient intake of calcium and vitamin D itself can cause this disease. The mineralization rate is reduced and the mineralization lag time prolonged. Large volumes of unmineralized bone matrix can be found and the osteoid seams seem to be resistant to osteoclastic resorption. This increased osteoid volume is due to increased forming surface areas, increasing mineral apposition rate and prolonged mineralization lag times [67].

One of the most famous impairments in bone remodeling is osteoporosis. This term includes a number of remodeling disturbances which all result in a decrease in bone mass and an increase in fracture risk. Osteoporosis will be described in detail in the following paragraphs.

2.2 Osteoporosis as a health problem

The term Osteoporosis consists of the two Greek words “osteon”, which means “bone” and “poros”, which means “pore”. This disease is characterized by low bone mass and an impairment of the microarchitecture of the bone, leading to bone instability and high fracture susceptibility. The World Health Organization (WHO) defines bones as osteoporotic when the bone mineral density (BMD) is 2.5 standard deviations or more below the young adult mean [69]. However, a more recent definition includes the increased susceptibility to fractures because not only bone mass is found to influence bone strength. Many patients who experienced a fracture have to stay in hospital for a longer time or depend on nursery day care afterwards. This creates an enormous amount of costs every year for the health care systems. In the year 2000 costs for all osteoporotic fractures in Europe were about €36 billion. Due to the increasing elderly population these costs are expected to more than double to €76 billion by the year 2050 [8]. It is estimated that about 75 million people are affected by osteoporosis in Europe, USA and Japan [1]. In terms of days spent in hospital, osteoporosis accounts for more days than many other common diseases, such as diabetes, myocardial infarction or breast cancer in women older than 45 years. Having such a high impact on the society, a lot of research has been done in the past years to improve the understanding of the disease mechanisms and provide better treatment of osteoporotic patients.

Osteoporosis is often recognized as a disease typically affecting older women. It is often called “silent epidemic” because it develops over the years without the patients noticing it. Bone loss is gradual and painless and usually a low impact fracture is the first noticed symptom. The life time risk to have an osteoporotic fracture is almost 40% for a white women aged 50 years or older and just 13% for white man over 50 years of age [70]. Nevertheless, the fracture related mortality rate in men is higher than in women [2, 71]. While in men most of the osteoporotic cases are due to other diseases and medication, such as malabsorption of calcium and vitamin D or glucocorticoid intake, in women the main reason developing osteoporosis is the postmenopausal lack of estrogen [72].

To improve the treatment and identify osteoporotic patients already at an early stage, attention is increasingly focusing on evaluation of fracture risks [73-77]. Bone mineral density (BMD) and its decrease during aging is influenced by several factors. Riggs et al. could show that it depends for example on the skeletal site and on gender [78]. This study showed that the decrease in BMD of the proximal femur in men is just two third of that of women, whereas the decrease in BMD at the lumbar spine is one quarter of that of women. Another factor influencing BMD is the weight at the age of menopause but also weight loss, which seems to be even more important than baseline weight [79]. Patients with a higher baseline weight showed a reduced bone loss. The highest bone loss was found in women with 60 kg or less. This study also suggests that a sedentary life style leads to a higher bone loss while no significant decrease in BMD was found in active women. The baseline BMD at the age of menopause also seems to be important as women with a high baseline BMD showed a higher bone loss than those with low baseline BMD. However, osteoporosis is a multifactorial disease. Assessing just bone mineral density would neglect other important risk factors. Interestingly enough, many fractures occur in patients without densitometrical osteoporosis [80].

In big meta-analysis studies, fracture risks, which are independent of BMD were evaluated. These risks are for example parental history of fractures, with higher risks in patients having maternal than paternal fracture history. Also, if the patients themselves had experienced previous fractures, regardless if osteoporotic or not, fracture risk increased. Furthermore, alcohol intake and smoking increase fracture risk. The consumption of more than 2 units of alcohol per day was found to have already a significant effect [81-85].

Because so many factors with different degrees of impact contribute to the risk of fractures a tool called FRAX™ has been developed by the WHO to evaluate the risk of patients considering all risk factors [74]. This tool includes computer simulations that are based on the

analysis of cohort models from Europe, North America, Asia and Australia. It does not only take BMD at the femur into consideration but also clinical risk factors like gender, smoking, body weight, history of previous fractures and intake of medication.

2.2.1 Types of Osteoporosis and their pathogenesis

In 1947 Albright described two types of osteoporosis: postmenopausal osteoporosis, occurring right after menopause and senile osteoporosis affecting people later in life [86]. Because researchers did not find a bimodal distribution, this concept was not widely accepted. In the beginning of 1980s Riggs and Melton confirmed Albrights findings and renamed postmenopausal osteoporosis into Type I osteoporosis and senile osteoporosis into Type II osteoporosis [87]. Both, Type I and Type II osteoporosis belong to the primary osteoporoses where also the idiopathic osteoporosis, which affects mainly young people, can be added. The manifestation of primary osteoporosis is strongly influenced by the environment and lifestyle rather than determined polygenetically. The other big group of osteoporoses are the secondary osteoporoses. This kind of disease attributes to a secondary cause, such as malnutrition, anorexia, gastro intestinal disorders causing malabsorption, hypogonadism, hyperparathyroidism, thyrotoxicosis, immobilization, alcohol abuse, anticonvulsant drugs, corticosteroid therapy or radiation therapy. To distinguish between secondary and primary osteoporosis can be important for the choice of treatment. In secondary osteoporosis one should try to adjust the causes that lead to osteoporosis, whereas in primary osteoporosis the only chance is to treat the bone loss itself.

This chapter will first focus on the primary osteoporosis and give some insight into the pathogenesis of the different types. Later a short overview over some secondary causes for osteoporosis will be given.

Postmenopausal (Type I) osteoporosis

Menopause is a process with complex endocrine changes. It lasts for many years and finally leads to the end of menses. Pathognomonic for the reduction in ovarian function is the decrease in 17β-estradiol concentration, which is the major hormone during the women's productive life [88].

Due to the sex steroid deficiency, the bone remodeling is unbalanced and stimulated. The accelerated bone remodeling consequently leads to bone loss, as resorption is much faster than bone formation. This hormone dependent increase in progressive bone resorption is mainly present in the first 5-10 years after menopause and represents the main pathogenic

factor in postmenopausal osteoporosis, although age related bone loss and suboptimal skeletal development must not be neglected as contributing factors [89]. It is generally known that estrogens have their main effect on the reproductive organs of a woman and therefore many estrogen receptors are present in these organs. Nevertheless, estrogen receptors can also be found in bone marrow stromal cells, osteoblasts, osteoclasts and osteoclast progenitors albeit to a much lesser degree [90]. Estrogens have a protectoral effect by balancing bone resorption and formation. They act multi-effective on osteoclasts. Osteoclast formation is decreased, while their apoptosis is increased and the capacity of mature osteoclasts to resorb bone is reduced. Furthermore, estrogens show an antiapoptotic effect on osteoblasts [91, 92]. Bone resorption is also hindered by an estrogen related decrease in osteoclastogenesis which is currently regarded as the main mechanism of estrogen action [93]. The blockade of osteoclasts is achieved with several pathways and the stimulation of bone resorption after estrogen deficiency is mainly due to a cytokine driven increase in osteoclast formation. Proliferation and differentiation of osteoclasts is dependent upon an equilibrium of cytokines, which can act autocrine and paracrine, such as RANK ligand (RANKL) and macrophage colony-stimulating factor (M-CSF). These factors are produced by bone marrow stromal cells, osteoblasts and activated T-cells [94]. RANKL not only binds to RANK, which is expressed on the surface of osteoclasts and their precursors, but also to osteoprotegerin (OPG). This is a soluble decoy receptor produced by many hematopoietic cells. When osteoblastic cells where treated with 17β-estradiol, mRNA and protein levels of OPG increased dose dependently. Thus OPG is an important antiosteoclastogenic cytokine, because it binds RANKL and therefore hinders it's binding to RANK [94-96]. Several other cytokines are responsible for the up regulation of osteoclast formation. They are present in different conditions, such as inflammation, hyperparathyroidism or estrogen deficiency. One of these factors is tumor necrosis factor alpha (TNF-α), which enhances the stromal cell production of RANKL and M-CSF and augments the responsiveness of osteoclast precursors to RANKL. Moreover, it stimulates osteoclast activity and inhibits osteoblastogenesis [97, 98]. In a study performed on transgenic mice insensitive to TNF-α, ovariectomy failed to induce bone loss, as it also did in TNF-α knockout mice and mice lacking a TNF-α receptor. In normal animals, not the production of TNF- α but the number of TNF producing T-cells is up-regulated after ovariectomy, by promoting T-cell activation which results in increased T-cell proliferation and life span [99, 100]. The gene expression of TNF-α and M-CSF is inhibited by sufficient levels of estrogen [101, 102].

Another cytokine augmenting the effects of RANKL and M-CSF is interleukin 1 (IL-1). It is enhanced by TNF-α and also acts as a downstream effector of TNF-α as there is an IL-1 dependent and independent pathway for the osteoclastogenic effect of TNF-α [103]. It promotes RANKL expression and stimulates osteoclast life span and activity. By converging their pathways, TNF-α and IL-1 combine their effects and thus produce a potent signal for osteoclastogenesis and inhibition of osteoblast function. They also have potent antiapoptotic effects on osteoclasts and prolong their life span [95]. A study with ovariectomized rats showed that the levels of TNF-α and IL-1 increased after ovariectomy, while bone mineral density was decreasing. Blocking IL-1 and TNF-α led to inhibition of osteoclastogenesis, reduced osteoclast activity and stimulated bone formation [104]. Not only IL-1, but also IL-6 levels rise after menopause. Osteoclastogenesis is increased by high IL-6 levels, while the production of IL-6 is suppressed by estrogens. In IL-6 knockout mice bone loss after ovariectomy was prevented by averting the increase in osteoclast numbers [93]. Interleukin 7 (IL-7) is another cytokine and potent inducer of bone destruction. After ovariectomy it has been shown that IL-7 levels are significantly up regulated. When IL-7 was neutralized *in vivo*, ovariectomy induced bone loss was prevented and bone formation seemed to be stimulated [105].

In general, it can be said that the protective action of sex steroids is dependent on the ratio of RANKL to cytokine induced osteoclastogenesis and levels of OPG. With the loss of sex steroids, there is a lack of the apoptotic effect on osteoclasts and a dramatic increase of apoptosis in osteoblasts and osteocytes. Therefore, the activity of osteoclasts compared to the activity of osteoblasts is much higher than in normal subjects. [90].

As a result of the deeper cavities digged by osteoclasts, bone trabeculae become thinner and are resorbed eventually thus leading to reduced bone strength and a higher fracture risk [106]. For example in rats the compressive strength of a vertebral body and the bending strength of the femur have been found to be decreased after ovariectomy [107]. However, the literature about mineral content in osteoporotic bones is somewhat inconsistent. Some studies revealed no changes or slight decrease after loss of sex steroids, whereas others could show an increase of mineral content and an altered type of collagen and even a lack of collagen [108-110]. A study performed on ovariectomized rats revealed an increased stiffness, yield strength, yield strain, ultimate stress and an increased cross-sectional area at the tibia compared to normal rats. At the tissue level, the mineral content was elevated in contrast to the overall bone mineral density, which was reduced [106]. Another study observed a reduction of the mineral to matrix ratio in the center of bone trabeculae [111]. These studies taken together provide

strong evidence for changes at the tissue level during the development of osteoporosis. These changes also affect mechanical strength of osteoporotic bone. Precise mechanisms for the increase in tissue level properties, such as bone strength and stiffness and mineral content are still not completely clear. However, a computer simulation revealed that, if tissue stiffness is increasing, the bone structures changes to bones with lower bone mass and increased anisotropy, as it is typical for osteoporotic bones [112]. An alternative theory is that, as some trabeculae disappear during development of osteoporosis, the remaining trabeculae undergo a compensatory shift in mineral content to counteract the loss of structural strength [106]. However, this compensatory shift can only protect from osteoporotic fractures until a certain amount of bone loss. Afterwards, it is not sufficient anymore and osteoporotic fractures occur.

Senile (Type II) osteoporosis

Riggs et al. discovered that the BMD of healthy subjects at the age of 90 is about 50% less in the femur and about 40% less in the spine compared to 20 year old subjects. The authors showed that this decrease is linear in both sexes, but the rate of decrease was about two third lower in man than in women [78]. At the age of 75, the regression for the proximal femoral BMD had decreased to more than two standard deviations below that of a normal young adult. Senile osteoporosis usually occurs in people older than 75 years. It may affect half of the aging women and one fourth of aging men, giving a female to male ratio of 2:1 [78, 87]. Patients experience hip fractures as well as spine, pelvis or humerus fractures. In most of the elderly subjects, decreased calcium absorption was found, leading to decreased plasma calcium levels. The data about levels of vitamin D3 is somewhat inconsistent. Some studies found a decrease in vitamin D3 levels [113, 114], others found no change in vitamin D3 levels with age [115, 116]. Nevertheless, calcium absorption was only increased in women not having experienced vertebral fractures before. This leads to the hypothesis that the circulating vitamin D3 does not bind properly to the intestinal receptor in women having senile osteoporosis. Thus it hinders the active, vitamin D dependent transport of calcium, which results in calcium malabsorption [117-119]. A major difference to postmenopausal osteoporosis is the increased serum level of PTH [87]. This could possibly be due to the malabsorption of calcium leading to hypocalcaemia which induces a secondary hyperparathyroidism with increased PTH levels and increased bone turnover.

At the micro architectural level of bone, there are three generally accepted processes leading to bone loss in senile osteoporosis. This bone loss appears in all compartments of the bone. The most important process is the bone loss in the trabecular region. The second one is the

continued net bone resorption at the endocortical surface and the third process is occurring in the cortex by a decrease of cortical bone [120]. As a result of the endosteal resorption the cortex becomes porous at the interface to the cancellous bone. When the endosteal resorption continues, the remaining structures are more the shape of trabeculae. Consequently these structures are accounted for cancellous bone [121-123].

It has been shown that the rate of bone loss varies at different skeletal sites throughout life. Trabecular bone loss, for example already starts at young adulthood in men and women, while cortical bone loss begins perimenopausal in women and after the age of 75 years in men [124]. Rates of trabecular bone loss were found to be similar at peripheral sites (distal radius and distal tibia) in postmenopausal women compared to premenopausal women. Nevertheless, in women in the lumbar spine the rate was 60% higher than at the peripheral sites. Similar findings could be seen in men where the rates of trabecular bone loss at peripheral sites were similar to those in younger men. However, in the lumbar spine a twofold greater rate was found in older men. In the cortical area another scenario appeared in both sexes. In premenopausal women no significant bone loss was found, in young men just a very low, but significant bone loss. This bone loss accelerated substantially in subjects over 50 years, it even increased 2-4 fold in men after the age of 50. This shows that there is a constant loss of bone throughout adult life, which is accelerated in elderly people in the cortical area leading to a deteriorated micro architectural structure of the bones.

While trabecular bone volume is decreasing, bone marrow adipose tissue is increasing and can fill up to 90% of the bone marrow cavity [125]. As both, osteoblasts and adipocytes derive from mesenchymal stem cells and can differentiate into each other, it has been postulated that pluripotent mesenchymal stem cells, located in bone marrow stroma are redirected from the osteogenic program to the adipogenic program, thus leading to reduced numbers of osteoblasts in elderly people [126].

Not only the loss in bone mass, but also the micro architectural changes in the trabecular region need to be taken into consideration. Their importance for the development of osteoporosis and subsequent fractures was first highlighted by Parfitt [127]. He investigated the structural changes with age and showed that the decrease in trabecular plate density rather than plate thickness had the main contribution to the decrease in bone volume. This leads to the conclusion that with age the mainly continuous trabecular network, which is typical for young people, is transformed into a mainly discontinuous network being typical for the elderly. While studies for trabecular separation (Tb. Sp) all come to the same conclusion [128-130], findings for trabecular thickness (Tb. Th) are more controversial. One study did

not see any significant decrease [131] while others could show a significant decrease either in all trabeculae [132] or in the horizontal trabeculae only [128, 129]. In a study using micro-computed tomography Tb. Sp and Tb. Th were studied globally and locally at a three dimensional level [133]. Here an increase in Tb. Sp was found. In Tb. Th no age-related changes were seen at a global level but at the local level, where the thickness was investigated separately for plates and rods. In the lumbar spine of elderly subjects, Tb. Th was increased at both levels. As Stauber et al. also saw a decreasing number of rods, they hypothesized that with age the trabeculae first become thinner and eventually vanish. In the lumbar spine, trabeculae are rod like already in very young people. As during aging rods become thinner and very thin rods eventually vanish, the trabecular bone structure is transformed to longer and on average thicker rods. In the femoral head trabeculae are plate like the entire life. Changes during aging occur as thinning and perforation of the plates, leading to new plates. As at the same time interconnecting trabeculae are lost, connectivity density can either increase or decrease. Therefore, Stauber et al. stated that the femoral head is not a good skeletal site to study age related changes.

According to the quantum concept [59] there is a balance between the amount of bone resorbed from the surface by osteoclasts and the refilling of the cavity by the osteoblasts. An imbalance in these two processes results in bone loss. Parfitt stated that rapid bone loss, which usually occurs after menopause, is due to deep osteoclastic penetration of the bone, whereas slow bone loss, which is typical for senile osteoporosis is due to a shallower deposition of bone by osteoblasts [127]. This decrease in osteoblast activity is due to a decreased number of osteoblasts, shorter lifespan and higher frequency of apoptosis [57]. Osteoblast number is not only reduced by increased adipogenesis, but also because of an increased apoptosis of osteoblast precursor cells, shown in SAMP6 mice, which age prematurely [134]. In another study performed with mice it was shown that osteoblastic cells from aged animals have a much greater potential to induce osteoclastogenesis than cells from younger animals. This is associated with a higher expression of RANKL and M-CSF, which both contribute to the recruitment and formation of osteoclasts [135]. This mechanism shifts the imbalance of osteoblasts and osteoclasts even more towards osteoclasts in elderly subjects.

Idiopathic osteoporosis

Idiopathic diseases are diseases with unknown causes. They are diagnosed after excluding all other possible reasons.

The idiopathic juvenile osteoporosis was first described in detail by Dent and Friedman in 1965 [136]. As it is an extremely rare disease, not even 200 cases have been reported in literature [137]. It affects young children, with no gender predilection between 8 and 14 years and is in contrast to the other types of osteoporosis self limitating. Before its limitation it is an acute disease which runs for 2-4 years [138]. During this acute phase growth arrests and multiple fractures occur. Typical symptoms are a gradual onset of pain in the back, the hip, knee, feet, difficulties and slowness in walking and an abnormal gait [139]. Often the children have vertebral compression fractures and fractures of the long bones. Wedge shaped, biconcave vertebrae are found as well. In radiologic studies, new abnormal formed bone may be present in the metaphyseal areas, which appear as a radiolucent submetaphyseal band and represent the so called "neo osseous osteoporosis" which is typical for idiopathic juvenile osteoporosis [137]. The bone mineralization rate is below the normal [140] and bone turnover measured in terms of activation frequency and bone surface-based remodeling parameters is much lower in affected than in healthy children [141]. The pathogenesis of the disease is unknown. Because of its close relationship to puberty, the influence of hormonal factors has been taken into consideration, but no direct evidence has been found. To diagnose idiopathic juvenile osteoporosis any secondary causes for osteoporosis, such as treatment with steroids, have to be excluded.

Secondary osteoporosis

Secondary osteoporosis means by definition that the bone loss results from a specific, well-defined primary clinical disorder or is a side effect of treatment. It is reversible, once the disease is treated or causative treatment is stopped. To treat secondary osteoporosis, the cause for bone loss has to be determined first. Differing numbers about the prevalence of secondary osteoporosis can be found in literature. It is estimated that in about 20 % of the postmenopausal osteoporosis cases another underlying secondary cause is the actual reason. In men, secondary osteoporosis is about 64 % of all cases [142, 143]. As there is a huge variety of underlying diseases, just a few will be explained in more detail in this paragraph. Diseases are for example endocrine disorders, such as Cushing syndrome, diabetes mellitus, hyperthyroidism, hyperparathyroidism or gastrointestinal diseases, gastrectomy, chronic active hepatitis, alcohol related liver diseases, malabsorption syndromes, pancreatic

insufficiency or any other diseases, for instance leukemia, multiple myeloma, amyloidosis, multiple sclerosis and rheumatoid arthritis.

2.2.2 Pharmacological treatment

The intention of every osteoporosis treatment is to reduce the fracture risk of a patient and increase the quality of life. Usually BMD is measured to monitor the success of treatment, but not all reduction in fracture risk can be explained by this parameter. Also bone quality is an important parameter, but as this is difficult to measure, BMD is still the standard measure in clinics [144].

Medical management strategies in osteoporosis treatment include change of life style, such as to quit smoking, moderate intake of alcohol, adequate protein, calcium and vitamin D intake and the avoidance of immobility [41]. However, these measures are only supportive to the pharmacological treatment.

Pharmacological treatment of osteoporosis can follow two different strategies: Antiresorptive drugs aim at the maintenance of the existing bone by decreasing or stopping the net bone loss, while anabolic drugs increase bone mass. Most of the drugs available on the market are antiresorptive drugs, such as bisphosphonates, calcitonin, hormone replacement therapy and selective estrogen receptor modulators (SERM). These drugs reduce the activation frequency, which represents the number of remodeling events, in trabecular and cortical bone. If the surface based remodeling is reduced, the number of weak spots is reduced as well, which lowers the chances to create discontinuities in the trabecular network [47]. A new drug was approved by the FDA in the U.S. and also in the European Union in the year 2010. Denosumab is a RANKL antibody that blocks the binding of RANKL to its receptor RANK. This imitates OPG function and therefore suppresses bone resorption by inhibiting the development and activity of osteoclasts [145]. Anabolic drugs of which PTH is the best known example increase bone turnover and change the balance towards a net bone gain. As bone resorption and formation are coupled processes, it has always to be kept in mind that by modulating one of the processes, the other is also affected. This means that antiresorptive drugs not only impair osteoclast function but secondly also osteoblast function. Furthermore when administering anabolic drugs a subsequent increase in osteoclast activity can be seen [47]. Therefore, an ideal drug would stimulate osteoblasts and inhibit osteoclasts at the same time. Strontium ranelate is such a drug stimulating bone formation and inhibiting bone resorption, however its mechanism of action is not known so far. But *in vitro* studies revealed that it can activate calcium sensing receptors in osteoblasts because of its similarities to

calcium. Activation of these receptors has positive effects on pre-osteoblast replication and differentiation, collagen type I synthesis and bone matrix mineralization. Furthermore, OPG levels are increased and RANKL decreased, leading to inhibition of osteoclast differentiation and activity [146].

Antiresorptives – Bisphosphonates

The most common antiresorptive drugs are bisphosphonates. Bisphosphonates are compounds derived from pyrophosphates where the two phosphate groups are connected via a carbon group (P-C-P). They are resistant to enzymatic degradation. Therefore, they show a very long half-life in the body, which can be in bone even as long as the half-life of the tissue itself. Bisphosphonates have a high affinity to bone mineral and inhibit the crystallization of calcium carbonate and calcium phosphate. The inhibition of osteolysis is mediated by a reduced number of osteoclasts and bone forming units. Bisphosphonates accumulate in osteoclasts and show four mechanisms of action [147]: First they inhibit the recruitment of precursors, secondly the adhesion of osteoclasts to bone is impaired, then osteoclast activity is inhibited and finally osteoclast apoptosis is induced [147, 148]. Meanwhile two generations of bisphosphonates are available. The second generation, such as zolendronate and risendronate contains a nitrogen atom in its alkyl chain, which is not present in the first generation, represented by etidronate or clodronate. Bisphosphonates of the first generation are incorporated into non-hydrolysable cytotoxic ATP analogues in osteoclasts and cause apoptosis of these cells. Bisphosphonates containing a nitrogen atom are more potent than the first generation. They inhibit the mevalonat pathway, resulting in an impaired cell function and eventually apoptosis [149]. It has also been shown that bisphosphonates are able to stimulate osteoblasts to produce an osteoclast inhibitory factor [150]. Side effects after oral administration are nausea, diarrhea and it may even cause esophageal cancer. But also more severe effects, like osteonecrosis of the jaw or atypical subtrochanteric and diaphyseal femoral fractures are associated with bisphosphonate treatment [32, 33]. Sometimes hypocalcaemia can be seen due to complexation with calcium ions in the gut.

It is known that bisphosphonates decrease bone remodeling. Therefore, some authors [151-153] were arguing if this could also affect the adaptation to mechanical loading negatively. For example Feher et al. tested the effect of different bisphosphonates on the load induced bone formation in the rat ulna [154]. In vivo loading was performed every other day for one week after bisphosphonate injection. Calcein was injected on day one and the second time 9 days after the last loading bout to label actively forming periosteal surfaces. Five days after

the last calcein injection animals were killed. In non-loaded animals, no significant differences were found in periosteal bone formation rates between bisphosphonate treated and control animals. However, loading in bisphosphonate treated animals increased bone formation compared to non-loaded bisphosphonate treated animals. Vehicle treated animals were loaded as well, however the effect of loading in bisphosphonate treated animals was significantly higher than in vehicle treated ones. This proves that mechanical loading still exerts stimulatory effects on bones, no matter which bisphosphonate was injected. As bisphosphonates decrease bone remodeling it is interesting to see whether the effects of early or late start of bisphosphonate treatment are the same. In one study, performed in ovariectomized rats, bisphosphonate was injected either right after ovariectomy or eight weeks after ovariectomy [37]. In the early treatment group no microstructural changes could be seen compared to sham operated animals. With late injection of bisphosphonates the microstructural parameters were still better than without any treatment, but not as good as with early onset of treatment. These findings support the thesis that with the reduction in bone remodeling adverse effects of estrogen deficiency can be inhibited best at an early time point after ovariectomy. Therefore bisphosphonates counteract directly the effects of loss of estrogen. These findings were endorsed by another study, where rats were injected with bisphosphonates two weeks after ovariectomy [155]. Already four weeks after the injection the microstructural parameters were back to baseline levels. After six weeks, an increase in bone parameters was found, values were similar to those of sham animals. This proportion was maintained until the end of the study after 12 weeks. Also the effects of different dosing were investigated in ovariectomized rats. In this study the authors could show a dose dependent improvement in bone micro architectural structure after injection of bisphosphonates. However, the bending modulus and cortical strength did also increase, but not dose dependently. Higher doses of bisphosphonates just increased the structural properties but not subsequently the tissue character [156].

Anabolics – Parathyroid hormone (PTH)

The level of free calcium in the blood is strictly regulated. As soon as it drops, PTH is secreted from parathyroid cells. PTH increases plasma calcium levels, by increasing bone resorption, calcium reabsorption in the kidneys and intestinal Ca absorption via an increase in Vitamin D levels. In bones it induces osteolysis. Osteoclasts do not have PTH receptors. However, when PTH binds to osteoblasts, RANKL is built into the plasma membrane of osteoblasts, which can then interact with RANK, located on osteoclasts. RANKL activates

RANK and therefore activates osteoclastogenesis [157, 158]. To exert these effects, PTH secretion is controlled tightly and can be adjusted to the actual need during the entire day. The secretion is regulated via a Ca-sensing receptor on parathyroid cells. Long term high PTH levels lead to increased bone remodeling and resorption. However, when PTH is administered intermittently (e.g. once daily) in a high concentration, it was found to have an anabolic effect on bone. Most bone formation with PTH treatment is occurring at sites of previous resorption in pre-existing BMU and adjacent to these BMU. In humans, an increased bone formation is manifest already 28 days after the onset of therapy and the accretion of bone mass is most rapid during the first 6 to 12 months of PTH treatment. [51, 159] This anabolic effect is caused by an increase in the osteoblast number by activation of survival signals and delaying of osteoblast apoptosis as shown in mice. [51] Also quiescent lining cells are activated. Kousteni et al. showed that PTH overrides the mechanisms that limit osteoblast number. In replicating osteoblast progenitor cells it induces the exit from the cell cycle by reducing the number of cells in S-phase and increasing the number of cells in G_0/G_1 and G_2+M phase. Thereby it sets stage for pro-differentiating and pro-survival effects [160]. An experiment performed in mice revealed an evident decline in osteoblast apoptosis after two days of daily PTH injections [161]. After four injections the prevalence of apoptotic osteoblast was reduced by 50%. However, a study performed in humans showed an increase of osteoblast apoptosis after 28 days of intermittent PTH injection, but also a positive correlation between osteoblast apoptosis and bone formation rate [28, 161]. Moreover, intermittent PTH shifts the differentiation from mesenchymal stem cells towards osteoblasts and away from adipocytes. A decrease in adipocytes in the bone marrow was found in monkeys treated with intermittent PTH [22]. PTH acts via two molecular pathways: Binding to a G-protein coupled receptor it subsequently mediates the activation of adenylate cyclase, increasing the levels of cAMP and activating the protein kinase A. The second path is the Gaq mediated activation of protein kinase C. Studies have shown, that the cAMP pathway is the important one to increase osteoblast number. An increase in cAMP also results in higher levels of IGF-1, which increases the differentiation and has positive effects on survival of osteoblasts. Also FGF-2 levels are elevated. This elevated levels enhance proliferation and reduce apoptosis of osteoblast progenitor cells [51]. Intermittent PTH also increases Runx2 mRNA, activity and protein levels. In contrast, constant PTH levels cause a sustained decrease in Runx2 levels [51, 162-164]. Osteocytes as primary mechanosensory cells in bone are involved in the anabolic actions of intermittent PTH, as well. A reduction in sclerostin mRNA has been found after administration of PTH. This explains the synergistic effects of PTH and mechanical load

bearing, because with mechanical loading, sclerostin levels decrease as well [165, 166]. In osteoclasts, intermittent PTH transiently increases RANKL levels and thus increases resorption activity. This increased resorption counterbalances the increased release of osteogenic growth factors from the bone matrix. However, at an early time point after the onset of treatment, the number of osteoblasts is increasing, but neither number nor activity of osteoclasts is elevated. Only at a later time point increased resorption can be monitored. To maximize bone formation rate and minimize bone resorption rate it is suggested to administer PTH for short periods in a cyclic fashion [51, 167, 168].

Recently a study to gain better insights into the mode of action of PTH was published [169]. The authors continuously infused PTH or soluble RANKL into female mice for 5 days. As PTH increases RANKL levels, the authors wanted to investigate which effects are due to increased RANKL levels and which are caused by other mechanisms. The number of osteoclasts and osteoblasts were increased with both infusions. However, the osteoblasts to osteoclasts ratio and bone formation rate were increased a lot more after PTH infusion. PTH also maintained cancellous bone, which was lost with RANKL infusion. Furthermore, an increase in the number of blood vessels in the bone marrow was visible only with PTH infusion. Therefore, the authors state, that besides the activation of an osteoclast dependent pathway, other mechanisms contribute to the actions of PTH. This study investigated the anabolic effect of intermittent PTH in female mice. However other studies also focused on male animals. Male rats were administered to intermittent PTH injections five weeks after orchiectomy [23]. With these injections the orchiectomy induced bone loss could be reversed. Even more bone was gained as there was a 155 % recovery after 6 weeks of PTH injections. Several studies also investigate in the combinatorial effect of intermittent PTH injection and loading. Growing mice were subjected to loading or PTH treatment for 6 weeks [170]. After these 6 weeks an increase in BMD and BMC could be seen in all groups, however, this increase was more prominent with PTH treatment. Nevertheless, the strength increased to a similar extends in both groups. These findings emphasize the theory that PTH induces bone formation everywhere in the bone, while loading induces formation only at sites where there is a mechanobiological need. Therefore, to increase the bone strength by 20 % with loading just 4 % increase in BMC was needed, whereas with PTH injection BMC had to increase by 11 % to improve bone strength by 20 %. In another study, mice were injected intermittently with PTH for 6 weeks [171]. During the last two weeks they were additionally subjected to loading 3 times a week. This study found a synergistic effect of loading and PTH injection in the trabecular and cortical bone.

2.3 Bone and biomechanics

2.3.1 Bone mechanobiology

At the end of the 19th century Julius Wolff stated that healthy bone will always adapt to the loads applied to it. If loading increases, bone remodeling changes the inner architecture. Trabeculae will become thicker or the cortex will thicken as well. In contrast, if loading decreases, more bone will be resorbed and the bone will become weaker due to increased remodeling [172]. Almost 100 years later Frost proposed the mechanostat theory. He said that bone mass always "fits the typical mechanical usage of healthy skeletons in a special sense: the mass can be over-adequate but never inadequate."[173]. This implies the need for a mechanism to control the process of gaining and loosing bone mass. Frost compared this to a thermostat, which can be turned ON and OFF, and called this control mechanism "mechanostat". Weight bearing and mechanical loading deform the bone and cause compression and tension. *In vivo* experiments showed that bones react differently to different strains. Below 100-300 micro strain remodeling is enhanced. This leads to bone loss as it can be said that one BMU resorbs 20 parts of bone and replaces 19 parts. In contrast, high mechanical loading reduces the number of BMU and the ratio of resorbed to replaced bone is shifted towards the replaced bone. If strains are between 1500-3000 micro strains or even higher, modeling occurs, which leads to increased cortical bone deposition resulting in lower peak strains. Hence, the mechanostat can be turned ON and OFF. Between 300 and 1500 micro strains there is the so called "lazy zone" where bone mass is maintained. Apart from modeling and remodeling, growth is the second biological mechanism that belongs to the mechanostat. Longitudinal growth can be enhanced by mechanical usage and is retarded by disuse, but not reversed. This mechanostat mechanism can be made over reactive or deaf by several diseases or agents, such as intake of glucocorticoids. The three main principles in mechanoregulation of bone are: transduction of the loading signal, sensing of the transduced signal and cell response to the loading impulse [174]. Mechanosensation is a multiscale process translating the mechanical signal from the organ level to smaller scales and creating a biological respond, starting at the biochemical level scaling up to the organ level. When the bone is loaded, stresses and strains are perceived at the tissue level causing pericellular mechanical changes which then present the mechanical stimuli to the cells [175]. But where are the elements in the bone sensing mechanical loading? In principle all eukaryotic cells are mechanosensitive, but osteocytes have been shown to be the main mechanosensory cells in bone [176]. Osteocytes sit in lacunae and have long slender processes that extend in small canals (canaliculi) within the matrix. They connect with each other, but also with lining cells

and osteoblasts via gap junctions, forming a complex three-dimensional network of communicating cells within the bone [177]. Osteocytes respond to the different strain fields occurring around the lacuna. In the front of the cutting cone, where low strains occur, they increase osteoclast activity, whereas around the closing cone, where strains are high, osteoblast activity is facilitated [178]. The exact pathways of how osteocytes sense mechanical loading are not fully understood, yet. However, the fluid flow in the canalicular system seems to be the main mechanism informing the cells about the level of loading [179]. Not only for mechanotransduction, but also to supply all osteocytes, especially the deeper located ones, with nutrients and to exchange waste, this fluid flow is very important [176, 180, 181]. During loading fluid shifts occur, which create shear forces and streaming potentials. These shear forces are sensed by osteocytes that have filamentous attachments from the cell membrane to the walls of the canaliculi [182]. Strains needed to induce cell response *in vitro* are about 1 - 10 % strain, which is much higher than the maximum strains seen *in vivo* with just about 0.2 - 0.3 %. Therefore, bone seems to enhance the mechanical loading signal. The fluid flow transmits the mechanical information and transduces small strains into larger signals, which then can be easily detected by the osteocytes [179, 181]. The lacunae in which osteocytes reside could also be involved in amplifying the loading signal [175]. Bone formation is more enhanced by dynamic than by static load. Therefore strain rate, rather than amplitude, is important to induce bone formation. Nevertheless, both magnitude and frequency are important parameters for bone formation. Low magnitude, high frequency strains are quite common in nature and are capable of stimulating bone growth. Vibration, also a typical high frequency low magnitude type of loading, has been shown in several animal studies to have positive effects on both cortical and cancellous bone [183]. Recently, also human trials confirmed these findings [184, 185]. High rates of loading, for example in high impact physical activity, have a great osteogenic potential. But high magnitude low frequency strain rates are osteogenic as well, although they do not occur very often in physiological activity [186, 187]. Besides the mechanical effect, the electrokinetic effect which occurs due to streaming potentials, evoked by convective transport of ions, plays an important role in activating osteocytes [188]. The fluid flow activates integrins and opens ion channels. Integrins are transmembrane proteins that bind to the extracellular matrix (ECM). Their activation leads to changes in ECM protein formation and also to stimulation of growth factor signaling in bone stromal cells. After opening of stretch activated ion channels the calcium levels in the cells increase. Intracellular calcium levels are also increased by an IP_3 mediated calcium release from internal stores [189, 190]. Increasing levels of calcium, IP_3 and

cAMP lead to the production of signaling molecules, secretion of prostaglandins and nitric oxide (NO). NO production in osteocytes increases rapidly after applying mechanical stress. In animal studies, bone resorption caused by immobilization was inhibited by treatment with indomethacin, a non-steroidal anti-inflammatory drug [191, 192].

The effect of loading on bone seems to be a local phenomenon. As shown in several studies, loading of one bone does not affect any other bone in the body [193]. Furthermore, it has been shown that there seems to be a sex related difference in the response to mechanical load. In a study performed on rats, growing male rats gained 4 to 6 times more bone with loading than female rats. Also in mature rats the male ones showed a higher response to loading than females. However, in female rats a higher bone density was observed, which could explain the reduced response to mechanical loading. These differences in loading response have already been shown in tennis players, where the load induced bone gain was a lot bigger in male players than in female [194, 195].

2.3.2 Mechanical intervention in osteoporosis

It is widely known and accepted that physical exercise is necessary to maintain bone mass and to achieve a high peak bone mass during growth. Athletes are known to have a higher BMD than people with a sedentary life style. Especially athletes engaged in high impact sports, for example jumping, showed a higher BMD than athletes not performing high impact sports [196]. However, not every exercise can be recommended in every part of the lifetime. In order to gain a peak BMD as high as possible, the International Osteoporosis Foundation (IOF) recommends children and adolescents to make a lifelong commitment for an active life and participate in weight bearing activities such as basketball, volleyball or gymnastics, which are more effective than weight supporting activities, such as swimming or cycling. Preferably, an activity that works all muscle groups should be selected. Furthermore, young people should avoid immobilization and eat a well-balanced diet, which is rich in calcium and proteins. Young adults and premenopausal women should do sports in order to maintain BMD and thus prevent osteoporosis. In postmenopausal women, maintenance of bone strength is important as well. Nevertheless, the main goal of physical therapy in these women is usually to increase muscle mass in order to reduce the risk for falls and to improve body balance and strength [197]. In patients already diagnosed with osteoporosis, the IOF recommends that the exercises should target posture, balance, gait, coordination and hip and trunk stabilization. It is important to note that dynamic abdominal exercises, such as sit ups or trunk flexions, must be avoided as they can cause vertebral crush fractures. Also exercises involving abrupt or

explosive loading or high impact loading should be avoided. Furthermore, normal daily activities like bending downwards to pick up objects can cause adverse effects like fractures. Therefore, proper instructions how to perform everyday tasks should be given.

Under a mechanobiological point of view, these recommendations are quite reasonable. Bone adapts to the mechanical load applied to it during growth and adulthood. In the adult body repeated load bearing leads to energy accumulation and therefore occurrence of micro-fractures. To remove this damage a well-balanced bone remodeling is important [44]. If bone remodeling is impaired this can lead to bone damage already at normal levels of loading. The bone can also be damaged if an overload occurs due to loading which exceeds the bone strength [198]. In elderly people often muscle atrophy, so called sarcopenia, can be seen. The reduced muscle strength disturbs the dynamic and static balance of the body thus leading to increased risk of falls [199]. To prevent the onset of osteoporosis, daily physical activity with exercises containing weight bearing and dynamic elements, such as walking, jumping, dancing, weight lifting, should be performed. But also exercises without mechanical loading to improve muscle strength, balance and general condition are recommended [44]. A study performed on postmenopausal women with established osteopenia showed that very intensive exercise with high mechanical loading could increase BMD at the lumbar vertebrae. No increase in pain was seen, which could have resulted from micro-fractures due to overloading of the bone. However, it must be said that the subjects tested in this study were quite active already before the start of the study [200]. Another study in elderly women with low bone mass investigated the effects of stretching, agility or resistance training on cortical bone density [201]. The authors saw a loss of cortical bone density in women, just doing stretching, whereas women performing agility training gained 0.5% in cortical bone density and women doing resistance training gained 1.4% in cortical bone density. Another study on postmenopausal women subjected one upper limb to exercise and used the contralateral side as control. The findings are somewhat contradictory to other studies. It was shown that high intensity, low repetition resistance exercise is effective in increasing BMD, whereas low intensity, high repetition endurance exercise does not show any effects [202]. Positive effects of high impact exercise have also been shown in several other studies performed in premenopausal women [203, 204]. However, other studies could show that dynamic strains rather than static strains are important for bone remodeling and modeling and that even at low magnitude, but high frequency an osteogenic potential can be observed. An animal experiment showed an increase in both bone quality and quantity. It was performed on sheep whose hind legs were stimulated for 20 minutes per day with extremely low level high

frequency strains [205]. A review paper about randomized trials of the effect of exercise on bone states that exercise in general reduces the rate of bone loss at the spine in postmenopausal women, and has positive effects on the bone mass of the lumbar spine in premenopausal women. However, at the femoral neck two of five studies did not find any positive effect of exercise on bone mass. In general, the magnitude of the effect of exercise on bone mass seems to be similar to that of calcium supplementation and just a little less than that of pharmacological intervention in osteoporosis [206]. However, patient compliance is a big issue. Especially when physical activity is recommended, it usually needs a lot more self-motivation and effort to perform the kind of activity suggested by the doctor. For such patients whole body vibration could be an alternative as it increases muscle strength, BMD, body balance and position without having to put too much effort onto the exercise. It is also better accepted by older people [207]. In another study bone loss in tail suspended rats was inhibited by putting these rats 10 minutes per day on a vibration plate, whereas 10 minutes of normal load bearing had no effect [208]. When postmenopausal women were assigned to 1 year treatment of low magnitude high frequency mechanical stimuli a weight dependent effect was observed. Women weighing less than 65 kg lost 3.32 % BMD in the spine without treatment, while women allocated to the treatment gained 0.18 % BMD. This indicates that the treatment although not anabolic, could at least prevent bone loss. However, women weighing more than 65 kg did not lose any bone. Therefore, no effect of the vibrational treatment could be seen. Also in this study patient compliance was a big issue. The authors calculated that the ideal subject with 100 % compliance could have an increase of up to 7 % in the lumbar spine. It was also proposed in the paper that due to sarcopenia less muscle dynamics are experienced. Usually there are dynamics of about 20-50 Hz during long term activities such as quiet standing. A decrease in this dynamics contributes to bone loss. The authors stated that reintroducing low magnitude high frequency stimulation could re-establish a regulatory stimulus to the bone tissue and prevent bone loss [209].

Taking together all the findings of these studies it is hard to give suggestions for clinical application. There are also hot debates about what kind of exercise and which amount is the best in osteoporotic patients. Due to ethical reasons there are no randomized control trials in humans that use fracture incidence as an outcome. Usually just changes in BMD are investigated. But when looking at pharmaceutical treatment where just small increases in BMD already provide a high protectoral effect for fractures, one can question if the same holds true for the effects of mechanical loading. In conclusion, it can be said that osteoporotic patients should be encouraged to be as active as possible. Daily walking as well as daily

physical activity such as housework or gardening should be promoted. However, it should be emphasized that no excessive loading or weight bearing must be performed. Low magnitude vibration seems to provide a good alternative with hardly any side effects for people lacking motivation and could be well used together with pharmacological treatment [198].

2.4 Animal models in postmenopausal osteoporosis and mechanobiology

Animal experiments are essential in many fields of research. They are required by law when new drugs for treatment and prevention of diseases are tested. But also in basic research they are a valuable tool to gain insight into signaling pathways and cellular, biochemical, molecular and biomechanical mechanisms. Such experiments often serve as models for human disorders. Of course, for many research questions, *in vitro* setups are available. However, such models are not complex enough to gain insight into whole regulation mechanisms. But also animal models have their limitations. These are due to the fact that animals are not humans and biological mechanisms in different species are similar but not the same. Therefore a careful choice of the model is essential. The animal model should replicate human conditions as close as possible. Of course, other considerations like ethical and legislative aspects, laboratory safety, handling of the animals, and the costs to maintain the animals and the necessary facility must not be neglected. [210, 211].

2.4.1 Animal models in postmenopausal osteoporosis

In opposite to humans, most animal species do not experience menopause. Therefore, to study the changes during menopause in animals, this phase has to be induced artificially. For this, the big species differences in the ovulatory cycle must be taken in consideration. Women have a menstrual cycle which lasts about 28 days. In animals, cycles occur between 5 days in mice and up to 18 weeks in dogs. Also, not all species show all phases within each cycle. For example in cats the ovulation only occurs after mating, while in mice the ovulation always occurs, but the Corpus Luteum only develops after mating.. While women maintain their cycle all over the year, many animal species show reproductive activity only during special seasons. Another factor that has to be taken into consideration is the number of offspring a species produces per year. For example, rodents can have several litters with up to 16 puppies throughout the year. Therefore, they are able to mobilize higher amounts of calcium in a shorter period of time for lactation. But of course they also must have a good anabolic capacity to replace the lost bone quickly after the end of lactation. Hence animals with a smaller litter size are closer to the human conditions. Usually large animals have less

offspring than small rodents [212]. However, the body of animals with seasonal ovulatory arrest like sheep is adapted to phases with low estrogen levels but without bone loss.
The cause for postmenopausal osteoporosis is the decrease of estrogen levels. The easiest method to stop the ovulatory cycle and stop estrogen production in animals is ovariectomy. But also chemical castration, the stop of the cycle by hormone application is possible. In opposite to ovariectomy this method is reversible.

When new drugs for osteoporosis treatment or prevention are supposed to be tested, the Food and Drug Administration (FDA) requires tests on two animal species [213]. The first species is the rat, because it is well characterized and develops after ovariectomy similar bone loss as in humans. However, rodents do not show haversian remodeling as it is typical in humans. Furthermore, some people argue that rats do not show remodeling at all but only modeling, although it has been shown that rats demonstrate a gradual transition from modeling to remodeling over the course of aging [210]. Thus a second species, is required, that shows haversian remodeling [210, 214]. Usually non-human primates are used to fulfill this requirement.
In the following section some animal models will be described briefly.
The use of the selective estrogen receptor modulator Tamoxifen and the bone anabolic effect of treatment with intermittent PTH were first identified in rats [211]. As mentioned before, the rat is a well described animal model for postmenopausal osteoporosis with a very reproducible site specific development of cancellous osteopenia. The rat is widely available, inexpensive, grows rapidly and has a short lifetime. However, there are also some disadvantages: the cancellous bone represents a smaller fraction of the total bone mass than in humans, and the whole skeleton contributes a smaller fraction of the total body mass compared to humans [211]. Furthermore, some bones show lifelong longitudinal growth, as the epiphyses do not close in all bones. In male rats, the epiphyses of long bones can be open until the age of 30 months, whereas in female rats the proximal tibia stops longitudinal growth around the age of 15 months and in the lumbar vertebra around 21 months [210]. However, if a mature rat is castrated, the effects on bone are quite similar to the ones seen in women after menopause. Cancellous and endocortical bone loss is apparent, together with an increased rate of bone remodeling and an imbalance between bone formation and resorption [214]. A significant bone loss in the proximal tibial metaphysis was observed 14 days, in the femoral neck 30 days and in the lumbar vertebra 60 days after the castration [210]. However, in long bone epiphyses and caudal vertebrae no ovariectomy induced bone loss was observed.

Nevertheless, when biomechanical testing was performed on bones from ovariectomized rats, it was obvious that these bones do loose significantly in bone strength [214].

Mice are even smaller than rats, so housing them is even cheaper. However, due to their small size, they have small bones with even smaller trabecular compartments. Therefore, mice are used less often in osteoporosis studies than rats. Nevertheless, due to the growing interest in genetically altered animals, mice are interesting and valuable animals in osteoporosis research. Well defined inbred strains and a large number of genetically modified mice are available. These inbred strains differ widely in bone parameters, such as BV/TV or trabecular number and therefore also show different reactions to loading or ovariectomy. In a study comparing the effect of ovariectomy in five different inbred strains it was shown, that all mice lost in vertebral trabecular BV/TV except for C3H/HeJ mice, which are known to have high basal values of trabecular BV/TV. However, in the proximal tibia the decline in trabecular BV/TV is even greater in C3H/HeJ than in C57BL/6J mice, which have a very low trabecular BV/TV baseline. The changes in cortical properties did not vary between mouse strains [215]. However there are important differences between mice and men: In mice, administration of estrogens induces endocortical bone formation, which eventually leads to osteosclerosis. This pathological effect cannot be observed in humans [216]. Data on administration of intermittent PTH suggests that mice seem to be resistant to the anabolic effects of PTH and that the anabolic effect that can be seen is more in the cortical than in the trabecular bone [211].

In dogs the structure of mature bone is close to human bone. Dogs also show haversian and cancellous remodeling, albeit having 25% shorter remodeling cycles and a cancellous bone turnover rate which is about 2-3 times higher than that of humans. However, 36 weeks after ovariectomy Beagles did show no significant reduction in bone mineral content or mechanical strength in the lumbar vertebra [212]. However, one has to keep in mind that dogs show a completely different reproductive cycle than humans. Ovulation takes place once or twice per year. Every ovulation follows a luteal phase of 64 days, independent of the occurrence of pregnancy. This is followed by an acyclic phase of about 3 months, until the next ovulation is prepared. Dogs do not show bone loss during the long acyclic phase, therefore, ovariectomy during this phase might be without any effect. Moreover, as the body is adapted to long phases with a lack of estrogen also ovariectomy during the cyclic phase might not show any effect.

Sheep are often used in orthopedic research for implant testing, due to the comfortable body size. Housing them is quite cheap and they can be trained to perform simple routine tasks, like

treadmill walking. There is some data suggesting bone loss after ovariectomy; however, other studies also found a rebound effect after a while. Ovariectomy in retired breeders could decrease BMD of the femur but not in the lumbar spine. Nevertheless, another study could show a progressive bone loss in the 5th lumbar vertebra 24 months after ovariectomy [217, 218]. However in another study osteoporosis could only be induced in sheep when ovariectomy was combined with a calcium and vitamin D deficient diet and steroid therapy [219].

As none of the species mentioned above can mimic human conditions in the bone during and after menopause perfectly, mostly non-human primates are used if a large animal model is required. These animals show high bone turnover after ovariectomy as in humans. Jee et al. found two years after ovariectomy a spinal osteopenia was apparent with about 11-15% lower bone mass. Also other parameters such as increased serum and urine markers for bone turnover and histological evident increased bone formation rates are similar to the conditions found in humans [214].

2.4.2 Animal models for unloading and loading

Healthy bone adapts to different loading conditions. Unloading reduces bone formation and increases bone resorption with subsequently decreasing bone volume. Animal models with unloading are used to mimic the processes that occur during disuse, immobilization and microgravity and the resulting disuse osteoporosis. The two most common models for immobilization are hind limb elevation and neurectomy. For hind limb elevation or tail suspension as it is also called, a special cage is needed to fix the tail to the top of the cage. That way that the forelimbs are still weight bearing and can serve as control, while the hind limbs remain unloaded. With this setup a cephalic fluid flow is provoked, which is similar as in bed rest or spaceflight. Unloading experiments up to 4 weeks did not show any signs of elevated stress levels in the animals [174, 220]. After two weeks, a bone mass deficit of 5-20% was obvious, the cancellous bone volume was reduced by 50%, osteoblast surface was decreased and osteoclast surface increased. In young animals, after an unloading period of two weeks bone formation rate and cell number went back to normal values, but the deficit in bone mass was maintained. When the animals were reloaded bone formation rate went up again and a slow but steady gain in bone mass was observed. However, it is not clear if a complete restoration of the bone mass can be achieved [174, 221]. Due to the cephalic fluid flow it is not easy to distinguish whether the observed effects result from the unloading or changes in blood flow. However, this model does not require any surgery and the animals do

not seem to be stressed to a large extend. Moreover, the forelimbs can serve as a control and no additional control groups are required. Therefore this is an often used unloading model in mice and rats [174]. Nevertheless, this model is forbidden in Switzerland due to ethical reasons.

Bone changes induced by neurectomy are similar to those seen in patients suffering from chronic spinal cord injury. To mimic such defects, about 1cm of the sciatic or femoral nerve or the plexus brachialis are dissected to induce a paralysis. Neurectomy reduces bone formation and cancellous bone volume. Bone resorption and blood flow within the bone are increased [222, 223].

The other methods used to immobilize animals are limb tapping or casting, tenotomy and spaceflight. In the first one, either a rear limb is tied against the abdomen, or a cast is put around the limb to prevent it from touching the ground. In both procedures the contra-lateral limb can serve as a control. However, the risk of overloading in this limb is high. Further, the animals seem to be stressed as weight gain in growing animals was reduced compared to controls [174]. This weight loss was shown in ovariectomized rats were the right hind limb was immobilized by attaching it to the abdomen and subsequently the left hind limb was loaded. After 60 days of unloading, cancellous bone mass and bone formation rate were decreased significantly compared to normal ovariectomized rats. However, in the left hind limb, which was loaded, bone loss was prevented and bone resorption rate decreased compared to castrated control rats [224]. Tenotomy is used to mimic the changes after tendon injury. However, the surgery performed to do the tenotomy can already have negative effects on the bone and sometimes a regrowth of the tendons is possible. Spaceflight is hardly ever used as it is very expensive and complicated to perform these experiments. However, it is an ideal model to study the effects of microgravity [174].

In skeletal loading, two main types of models are used: bending and compression models. Four point bending is used most often as it represents normal bone loading patterns best. In compression models, usually axial compression is applied upon the ulna, tibia or caudal vertebrae of turkeys and rodents. Strain gauges can be attached to the cortical surface to sufficiently measure the strain. The advantage of applying strain gauges is that the loading is well defined and can be adjusted. Therefore reproducibility is very high. Also multiple loading bouts over a long period of time can be performed [174]. Among the first axial compression loading models was the compression of the ulna of roosters. Two incisions were made in the proximal and distal epiphysis of the ulna and the cut ends were covered with cups, which were held by stainless steel pins. These pins penetrated the skin dorsally and

ventrally. Once per day they were connected to the loading device and a compressive force with a frequency of 0.5 Hz was applied onto the ulna. When applying 36 or more cycles per day, intracortical resorption was inhibited and periosteal and endosteal new bone was formed [225]. In a similar approach using turkeys, strain gauges were attached to the ulna. At strains of 0.001 bone was maintained. If the strains were lower, bone loss with increased remodeling, endosteal resorption and intracortical porosity was observed. Applied strains higher than 0.001 proved to be osteogenic with periosteal and endosteal bone formation but only little changes in intracortical remodeling [226]. Axial loading of the ulna is also performed in rodents. A study validating this model in the mouse showed that with loads up to 2000 με lamellar periosteal bone formation is present, but no endosteal bone formation. However, if strains exceed 3000 με, lamellar endosteal bone formation is apparent and at the periosteal site lamellar and woven bone formation occurs. To axially load a mouse ulna, the flexed carpus and elbow are placed into felt padded cups that are positioned on top of each other. The upper cup holds the carpus and is attached to an actuator. The lower cup holds the elbow and is placed on a dynamic load cell. Due to the anatomical shape of the ulna, the axial compression produces a medial to lateral bending, inducing strains that are similar to the ones during normal locomotion [227]. More recent studies investigating the combined effect of loading and pharmacological treatment have been performed. In a mouse tibia loading model the effects of the bisphosphonate zolendronate and loading have been investigated. To load the tibia, the knee and ankle were bended. The moving pad was put on the knee and the fixed pad on the ankle. Then an axial compression with loading of 18 N and a frequency of 2 Hz was applied for one minute on the tibia. Due to the anatomical curvature of the bone, this loading results in compressive and bending strains. When loading was applied without the bisphosphonate, cortical thickness and bone area increased. The combination of zolendronate and loading also had positive effects. However, at the most loaded site of the tibia, were the highest strains were present, the effect was significantly decreased compared to the sum of the effects. This lead to the hypothesis, that the combination of zolendronate and loading is not beneficial at very high levels of strain [228]. Another study investigated the combined effect of loading and intermittent PTH application. Mice were treated with PTH or vehicle for 6 weeks. In the last two weeks of treatment, the right ulna and tibia were additionally subjected to loading. In the tibia the loads were sufficient to stimulate an osteogenic effect in the vehicle treated animals, resulting in increased trabecular number, thickness, and increased cortical and trabecular bone volume. However, at the ulna the applied load itself was not sufficient to induce any osteogenic effect. In combination with intermittent PTH these loads could induce

osteogenic effects in the cortical regions [171]. This combined effect was also studied in rat caudal vertebrae. K-wires were inserted into the 7th and 9th caudal vertebra and a uniaxial load of 50 N or 100 N was applied. Loading or intermittent injection of PTH resulted in increased bone formation rate and mineral apposition rate. However, bone formation rate declined to the level of control animals after four weeks of both treatments. With the combination of loading and PTH treatment the increase in bone formation rate was sustained. In the first week the increase resulted mainly in increasing mineral apposition rate, and in the 2nd and 4th week in increasing labeled bone surface [165]. To study the effects of bending, four point bending was performed on tibiae of rats. The right foot was secured and the lower right leg positioned between four loading pads. The two upper pads were positioned at the lateral side and the lower pads at the medial side of the leg. As the distance between the upper pads was shorter than between the lower pads, loading generated tension on the medial and compression on the lateral surface. The results showed an increased formation surface at the medial periosteum of the tibia and fibula and an increased mineral apposition rate compared to the non-loaded limb [229]. In another study a loading-strain-dependency was demonstrated. Bone formation was increased and the newly formed bone appeared normal at low strains. However, if the strains exceed far beyond physiological loading levels, mainly woven bone is found [230]. When applying load to mice, the mouse strain needs to be taken into consideration when the results are interpreted. For example C57BL/6J mice have a lower BMD and therefore react a lot better to loading than C3H/HeJ mice which show much higher BMD [231]. Similar effects were found in another study where C57BL/6J and C3H/HeJ mice were submitted to four point bending tests. In the non-loaded limbs the total area and the marrow area of the tibial diaphysis were significantly bigger in C57BL/6J mice than in C3H/HeJ mice. After loading, the periosteal and endocortical formation surface were bigger in the mice having a low bone mineral density. Woven bone was found in both strains as a result to loading. New bone of mice with low bone mineral density contained 98% of woven bone, while that of C3H/HeJ mice consisted of 90% woven bone [231].

A third type of loading is vibration. In one study ovariectomized rats were put in a box on top of a vibration motor 30 minutes per day for 90 days. Vibration at 45 Hz increased periosteal bone formation and inhibited endocortical resorption and the decline in maximum bending stress. In contrast, rats that just underwent ovariectomy without any vibration showed a smaller increase in periosteal bone formation, but endocortical resorption and the decline in maximum bending stress was not inhibited [183].

Treadmill running induces loading as well. Ovariectomized and sham operated rats were subjected to slow running or fast running at the treadmill. In the sham group the exercise did not affect any of the mechanical or histomorphometric parameters. However, when comparing ovariectomized exercising to non-exercising rats trabecular bone loss was reduced significantly. Ovariectomy induced an increased bone formation rate and mineral apposition rate. This rate was decreased at the periosteum in rats exercising on the treadmill, but increased at the endosteum [232].

2.4.3 Quantitative assessment of bone remodeling

Bone remodeling happens at the microscopic level. Therefore, for a long time histology was the only method to measure parameters of bone remodeling. Until today it is a widely used method and "gold standard" for evaluation of several parameters. With the help of histomorphometry trabecular architectural parameters such as trabecular thickness, trabecular number or trabecular bone pattern factor [233] can be determined. Staining with histological or immunochemistry methods helps detecting different cell types, newly formed osteoid and different stages of cell activity. In addition to these static parameters, dynamic parameters can be evaluated as well in histomorphometry. This was done already as early as 1969 by Frost [53]. For this, the patient or experimental animal is treated with a fluorescent dye that is accumulated in bone during mineralization. A second dose of fluorescent label, like tetracyclin, calcein or alizarin is applied several days to weeks after the first dose. This results in two labels in the bone. The distance between these labels represents mineral apposition rate [234]. Further labeled surface is measured to estimate mineralizing surface. From this parameters bone formation rate can be calculated. Bone resorption cannot be measured so clearly, because there is no way to assess bone surface before resorption started. However, osteoclast number, assessed by TRAP-staining and eroded surface can be used to estimate bone resorption activity. Histology has the big disadvantage of the need of bone being extracted from the body. In patients or large animals this means that a biopsy has to be taken, an invasive and painful process. In small animals like rodents, the animal has to be sacrificed. This prevents the longitudinal monitoring of bone remodeling.

In clinical routine, bone mineral density (BMD) is used to estimate fracture risk of a patient. Repeated measurements of bone mass in the same location can be used to assess overall bone loss or bone gain, which represents net remodeling rates. However, half of the women presenting with fractures still have a high BMD. Furthermore, BMD does not reflect bone quality, such as trabecular bone architecture, cortical bone thickness or geometry, osteon and

osteocyte density and damage accumulation [235]. Moreover, it is impossible to measure bone formation or resorption.

To measure bone mass, typically radiological methods are applied, most commonly dual-energy X-ray absorptiometry (DEXA). With DEXA mineral content in a defined area is measured. This results in areal bone mineral density, also called bone mineral content (BMC). As a two dimensional method, DEXA is dependent on bone geometry and works reliably only in patients with normal anatomy.

A method to assess BMD in three dimension is quantitative computed tomography (QCT). However, with this method the patient is exposed to a high radiation dose. Peripheral QCT (pQCT) measurements are used to assess bone mineral density in the extremities, typically at the distal radius or tibia. Both CT-based methods give reliable values for BMD, cortical thickness and can distinguish between cortical and trabecular bone, but their resolution is too low, to assess more parameters like trabecular thickness or number.

Imaging techniques providing a spatial resolution of 100 µm or less represent the microscopical level of imaging. Here, mainly the architecture of trabecular structures, like trabecular thickness, trabecular separation and structure model index can be assessed using micro computed tomography (micro-CT) or magnet resonance imaging (MRI), for example [236]. Both, CT and MRI are non-destructive. A high resolution method for the three-dimensional assessment of bone parameters is micro-CT. However, it is restricted to small sample size (a few centimeters in diameter and length) and uses a high radiation dose. Therefore for a long time it was applied to specimen only, which made it a method for endpoint analysis. With the development of *in vivo* micro-CT a few years ago, longitudinal measurements of bone parameters can be conducted at least in small laboratory animals. *In vivo* micro-CT measures the same parameters as known from specimen scanners such as Full BV/TV, Trab BV/TV, Tb. Th, Tb. N, cort % BV [237]. Nowadays, resolution of *in vivo* micro-CT scanners goes up to around 10 µm. This resolution is sufficient to evaluate trabecular structures in mice, which have a trabecular thickness of about 30 to 50 µm [237]. In one study, for example, the effect of mechanical loading on bone micro-architecture was monitored weekly with *in vivo* micro-CT over a time course of four weeks [238]. As already mentioned, until recently histomorphometry was the only method to determine bone remodeling parameters and is still the gold standard. However, in 2011 Schulte et al. published a method to calculate bone formation rate, mineral apposition rate, mineralizing surface and even bone resorption rate, mineral resorption rate and eroded surface out of sequential micro-CT images taken from the same animal. The authors found good correlation

of the parameters with dynamic histomorphometric evaluation and applied the method to an *in vivo* loading model of mice [239]. Unfortunately, high resolution *in vivo* micro-CT imaging is limited to small animals like mice and rats. To achieve high resolution, the scanning time is long. Therefore, only small volumes can be scanned, also to avoid exposure to very high amounts of radiation. Therefore micro-CT imaging is not yet applicable to clinical purposes [211].

Another interesting imaging method to evaluate bone parameters is magnetic resonance imaging (MRI), as it does not use any ionizing radiation. Trabecular structures are visible as a negative contrast, because bone itself does not contain many hydrogen molecules, but the surrounding marrow does. Due to the high signal-to-noise-ratio and high number of trabeculae and surrounding fat marrow, resulting in a high contrast, most of the *in vivo* studies have been performed at sites of the peripheral skeleton [236, 240]. Possible resolution ranges up to the diameter of a single trabecula. However, imaging time takes much longer than with CT, and trabecular thickness can be easily overestimated [235]. In one study, ultra short echo time MRI was used to detect changes in phosphorous and water content in bones of ovariectomized rats. The authors showed a decrease in phosphorous content which indicates a decreased mineralization and a higher water content in the ovariectomized compared to sham operated rats. These changes were reversed with the administration of the bisphosphonate alendronate. After injecting alendronate, phosphorous content increased dose dependently and water content decreased. However, these measurements were just performed *in vitro* [241].

2.4.4 Ethical aspects of animal models

As seen in the previous paragraphs animal models are widely used. Not only in the field of imaging and bone biomechanics, also in many other fields of basic research as well as applied research animal models are very valuable. Scientists from all fields depend on animals models to answer their questions. However, performing experiments with living animals always raises ethical concerns. It is well known that animals do feel pain and anxiety. Many people argue that animals cannot decide whether they want to participate in animal experiments or not, which raises the question of the free will of animal and also the dignity of animals. Ethical questions cannot be answered entirely and it is hard to give a “right” or “wrong” decision for each single situation. Each researcher should scrutinize their own attitude towards animal experiments and the associated ethical concerns.

This paragraph will only focus on one concept, the three R concept, which is a guideline towards good animal experiments.

The three R concept was first introduced by Russel and Burch in 1959 in their book "The Principles of Humane Experimental Technique" [242]. The three Rs stand for Replacement, Reduction and Refinement and have become a widely used principle in research using animal experiments. National and international legislations and guidelines follow this concept and therefore aim to assure a good quality of animal welfare. In the Swiss Animal Welfare Act, several articles can be applied directly onto the three R concept [243]. Article 17 states that animal experiments that can induce pain, distress, damage or fear must be limited to the indispensable degree. This is followed up in article 19, saying that animal experiments are unacceptable if the information gained from this experiment stands in no relation to the pain, distress or fear induced by the experiment. Finally in article 20 it is stated that animal experiments are only to be allowed if it can be proven that the same information cannot be achieved with appropriate alternative methods.

The first R "replacement" was defined by Russel and Burch as "any scientific method employing non sentient material which (…) may replace methods which use conscious living vertebrates." [242]. They also distinguished between absolute replacement, where no sentient vertebrates are needed at all, and relative replacement, meaning to perform non-recovery experiments on intact but deeply anaesthetized living beings and the painless killing of animals to get cells and tissues. Furthermore, replacement can be divided into direct replacement, where the experiments provide the same information, and indirect replacement, where the gained information is different, but can be used for a similar purpose as that for which the animal experiment would have been used for [244]. Such alternative experiments are often welcome, as they can save money and time. However, of course not all animal experiments can be replaced by just one alternative experiment; sometimes several experiments have to be combined to get the information. Typical alternative experiments are the use of cell and tissue cultures or computational models. Probably the best known replacement model is the use of blood cells instead of rabbits for testing on pyrogenes in medicinal products. It is expected to save 200 000 rabbits per year with these new methods in the EU [245]. A new form of replacement is the use of in silico models. For example a lot of effort is put into the computational modeling of bone modeling and remodeling and its response to mechanical load. This model will be expanded to predict the outcome of pharmacological treatment and loading in human osteoporotic bone. This could in future substitute animal experiments for drug testing or understanding basic principles in bone remodeling at least to some extend [246-248]. Though, due to the very complex nature of

living beings, not all animal experiments can be replaced, as sometimes the interaction of a lot of different body functions is needed.

The second R represents "Reduction", which means to keep the number of used animals as low as possible. For this, sound experimental planning and the use of statistical tools to estimate the necessary sample number (e.g. power analysis) are essential. First of all researches should check if the same or similar experiments already have been performed in another lab. This can be done for example with databases as provided by the German Federal Ministry of Education and Research [249]. Second, when planning group sizes it needs to be taken into account that inter-individual variability between humans or animals of one species sometimes results in quite different reactions to treatments and high variances within experimental groups. Therefore, a certain group size is needed to obtain statistically evaluable results [250]. With a good standardization of the experimental procedure, the housing conditions of the animals and the animals themselves, using inbred strains, these inter-individual variations can be reduced, but not overcome. A longitudinal study design can reduce the group size a lot compared to cross sectional studies, because in longitudinal studies each animal can serve as its own control. In a study performed previously in our lab, the bone response to mechanical loading in mice was monitored over 4 weeks with *in vivo* micro-CT measurements. Lambers et al. could see a significant increase in trabecular BV/TV in the mice of the 8N loading group compared to the 0N group. This increase was not only seen in the averaged group values but also in single mice [238]. Therefore, much less animals are needed per study.

The last R stands for "Refinement". This means that the amount of stress or pain the animal is exposed to should be kept as low as possible. This implicates the use of a proper pain treatment, which is also required by the law in Switzerland. Furthermore, the handling of the animals should not cause any or as less stress as possible. Therefore, well trained personnel and continuous education of the staff is necessary. Also by offering adequate housing conditions, animal experiments can be refined. Hence, one has to know the natural habits of laboratory animals, for example that rodents are social animals and must not be kept single, or that a cage without any enrichment can provoke stereotype habits, which are a way to compensate stress [245].

In conclusion, it can be said, that the first aim should always be to replace animal experiments with other methods. If this is not possible as few as possible animals should be used and the conditions for the animals in the experiments concerning housing, handling and pain treatment should be as good as possible. When following these rules, scientists are aware that

animals have their own needs, that cannot be neglected and furthermore researchers know about the importance to find alternatives to animal experiments.

3 Materials and Methods

3.1 Experimental setup

To study the effects of mechanical loading and pharmacological treatment on the 6th caudal vertebra of ovariectomized (OVX) C57BL/6 mice, two experimental series were performed with a total of 240 animals.

In one of the experimental series, the early loading series, there was a time-lag of 5 weeks between the castration and the start of loading and treatment. The other experimental series was the late loading series, where the time-lag between ovariectomy and start of loading and treatment was 11 weeks. Each of the series includes three different studies.

In the ovariectomy study the effect of mechanical loading on the 6th caudal vertebra in ovariectomized mice was investigated to see if they react to mechanical loading the same way as sham operated mice do. Sham (SHM) operated mice served as a control group. All the mice, ovariectomized or sham operated were assigned into groups subjected to 0N or 8N loading.

Then the effects of two pharmacological treatments in addition to loading were investigated. The PTH study looked at the combinatorial effect of mechanical loading plus treatment with PTH on ovariectomized animals. In this study vehicle (VEH) treated, ovariectomized animals served as a control group and similarly to other studies all animals were assigned into 0N or 8N loading groups. Finally, in bisphosphonate study the combinatorial effects of mechanical loading and treatment with the bisphosphonate (BIS) zolendronate on ovariectomized mice were investigated. Similarly to the previous study, vehicle treated, ovariectomized animals served as a control group, and a load of either 0N or 8N was applied to all the animals.

A detailed overview over the experimental time schedule and different groups can be found in Figure 1 and Tables 1-3.

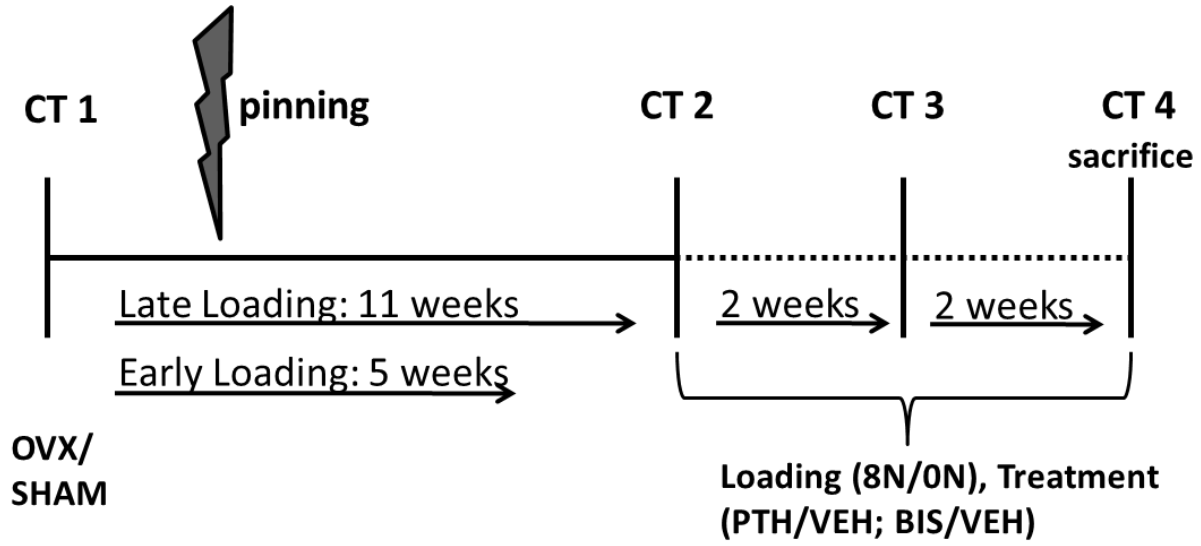

Figure 1: Experimental time schedule

OVARIECTOMY	OVX	OVX	SHM	SHM
TREATMENT	NO	NO	NO	NO
LOADING	0N	8N	0N	8N
NR OF ANIMALS	10	10	10	10

Table 1: Ovariectomy study, only loading was administered to mice

OVARIECTOMY	OVX	OVX	OVX	OVX
TREATMENT	PTH	PTH	VEH	VEH
LOADING	0N	8N	0N	8N
NR OF ANIMALS	10	10	10	10

Table 2: PTH study, both PTH treatment and loading were administered to mice

OVARIECTOMY	OVX	OVX	OVX	OVX
TREATMENT	BIS	BIS	VEH	VEH
LOADING	0N	8N	0N	8N
NR OF ANIMALS	10	10	10	10

Table 3: Bisphosphonate study, both BIS treatment and loading were administered to mice

Tables 1-3: All studies were performed in both experimental series, Early and Late Loading. Control groups are marked in grey.

3.2 Animals

The animals were purchased in groups of 20 from Harlan (Füllinsdorf, Switzerland). Due to the closure of the breeding facility in Füllinsdorf in June 2010, the mouse strain C5BL/6JRccHsd was transferred to Horst, The Netherlands. Consequently the last 40 mice which were ordered in August for the PTH study of the early loading experimental series had to be obtained from Harlan (Horst, The Netherlands).

The mice were allowed to settle at least one week before experiments started. Animals were housed in groups of 5 in cages of type II-long in Scantainers (Scantainer ^{Classic} , SCANBUR, SA) with filter tops. Room temperature in the Scantainer was 22°C, humidity 50% and the airflow at the scantainer was 25-40 x/h. The day-/night-cycle was 12 hours darkness, followed by 12 hours of light.

All mice were provided sterilized standard mouse chow ad libitum and had free access to tap water. Cages were changed once a week by a professional animal caretaker. Additionally, the weight of all animals was checked once a week and routine animal controls were performed regularly.

All experiments were approved by the local animal care and use committee (Kantonales Veterinäramt Zürich, license number 171/2008).

3.3 Ovariectomy

Ovariectomy was performed at the age of 15 weeks. The mice were shaved dorsally and laterally for about 2 cm starting at the last two ribs going caudal. Weighing of the mice was done before the surgery and on the 3 days following the surgery together with the administration of the pain medication.

Isoflurane (Attane TM Isoflurane ad us.vet, MINRAID INC. Orchard Park, New York) was used for inhalation anesthesia. For induction of anesthesia mice were placed into a transparent induction chamber, which was filled with an oxygen-isoflurane mixture. The oxygen flow was set to 400 ml/min and the isoflurane concentration was at 4 - 5 %. During the induction phase the animals were monitored constantly. After approximately 1-2 minutes, surgical tolerance stadium was reached. The mice were placed onto the operation table with the head in a facemask. Anesthesia was maintained with 2 % isoflurane. To prevent eyes from desiccation, an eye cream (Vitamin A Augensalbe, Bausch & Lomb Swiss AG, Zug, Switzerland) was applied. For pain relief 2 mg/kg Meloxicam (Metacam 5mg/ml ad us vet, Böhringer Ingelheim, Deutschland) were administered subcutaneously in the neck before the

start of the surgery. Skin disinfection was performed with an alcoholic skin disinfectant (Kodan Tinktur forte, Schülke & Mayr GmbH, Norderstedt, Germany).

A small skin incision was made at the flank. The skin was loosened by blunt preparation and redundant subcutaneous fat was removed. Internal organs seen through the thin abdominal muscles were used for orientation. An incision into the muscle layer at the area of the fat pad of the ovaries was performed with the scissors. The ipsilateral ovary was grabbed and externalized with an anatomical forceps. After blunt preparation of the Ligamentum latum uteri, preserving the Arteria and Vena uterina, a hemostat was placed to clamp the vessels and the uterus about 0.5 cm caudal of the tip of the uterine horn. The tip of the uterine horn with the attached ovary was then torn off and the hemostat remained for some time to prevent any bleeding from the big vessels. After the hemostat was removed the remaining part of the uterus horn was repositioned into the abdomen and the muscle layer was closed with an interrupted suture. Braided vicryl thread in a needle thread combination (Ethicon 6-0 13 mm, 3/8c Polyglactin, violet braided , Johnson & Johnson Intl, Brussels, Belgium) with an atraumatic needle was used for suturing. The skin was closed with staples (Precise 3M Health Care, Neuss, Germany) and a spray dressing (OPSITE permeable spray dressing, Smith & Nephew Medical Limited, Hull, England) was applied. The removal of the contra-lateral ovary was performed in the same way. 1 ml of warm saline (0.9 % Natriumchloridlösung, B. Braun Medical AG, Switzerland) was deposited into the abdomen before closing the muscle layer.

The operation procedure for mice that underwent sham surgery was the same. However, in sham operated mice the ovaries and uterus horn were not removed, but exposed and visually examined before being repositioned into the abdomen.

After surgery the mice were transferred into a pre-warmed cage. During the waking up phase the animals were monitored constantly. Once awake and walking around the mice were placed back into their home cage.

A health check was done in the evening on the day of the surgery and then daily for the following three days. If necessary, lost staples were replaced. Meloxicam was injected every 24 hours for 2 days at a dose of 2 mg/kg and on the third day 1.5 mg/kg. If necessary, the mice were checked more frequently. A health monitoring sheet was filled out on the day of surgery, and for the following three days. Weight, social behavior, body position and motion, habitus and wound condition were noted. The staples were removed 10 days after the surgery.

3.4 Pinning procedure

Pinning of the 5th and 7th caudal vertebra was performed such that there were at least 3 weeks for the mice to recover until the loading started. To prepare the operation, stainless steel pins (Austerlitz insect Pins®, stainless steel, Fine Science Tools) were cut to the appropriate length of about 2.5 cm and autoclaved. The operation itself was performed under inhalation anesthesia with isoflurane. For the pinning operation the same anesthetic protocol as for ovariectomy was used. After 1- 2 minutes in the induction chamber, surgical tolerance stadium was reached. Each mouse was then positioned on the operation table such that the head was inside the facemask and anesthesia was maintained with 2 % isoflurane. An eye cream (Vitamin A Augensalbe, Bausch & Lomb Swiss AG, Zug, Switzerland) was applied. The tail was thoroughly disinfected with alcoholic skin disinfectant (Kodan Tinktur forte, Schülke & Mayr GmbH, Norderstedt, Germany). The pins were put into the pinning device.

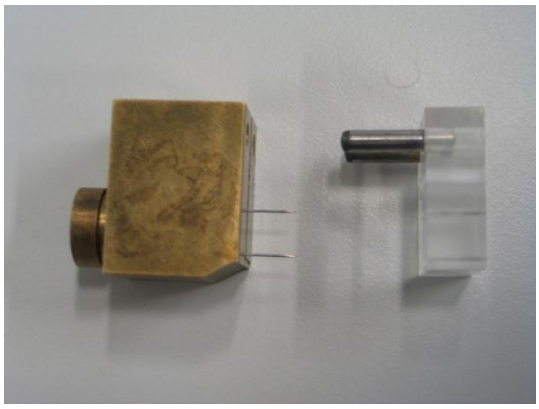

Figure 2: Pinning device with inserted Pins

As seen in Figure 2, the pinning device consists of two parts. The pins are inserted into the bronze part of the device. Their position is marked in the acrylic glass part with radio opaque markers, which are integrated at the exact same position as the holes for the pins in the bronze part. The tail is placed in between these two parts, which are then connected by two location pins to enable to press the parts together and prevent the tail from moving. To ensure that the tail is straight and not flexed, a horizontal indentation has been made on the acrylic part (see Figure 3 and 4). A more detailed description of the pinning device can be found elsewhere [251]

Figure 3: Mouse tail fixed in pinning device

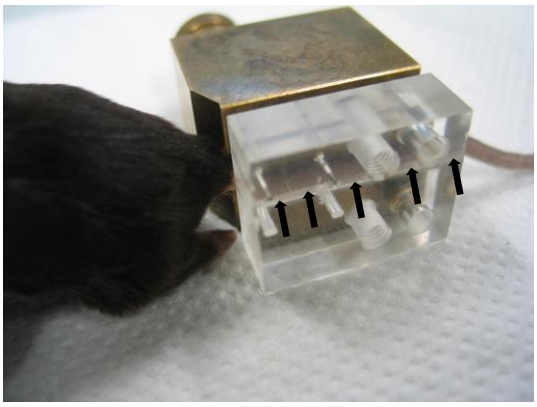

Figure 4: black arrows show indentation

With a digital mobile C-arm (OEC MiniView 6800, GE Medical Systems) the position of the pins compared to the tail vertebrae was verified and if necessary the position of the pinning device was adjusted until the markers pointed to the middle of the 5th and 7th caudal vertebra.

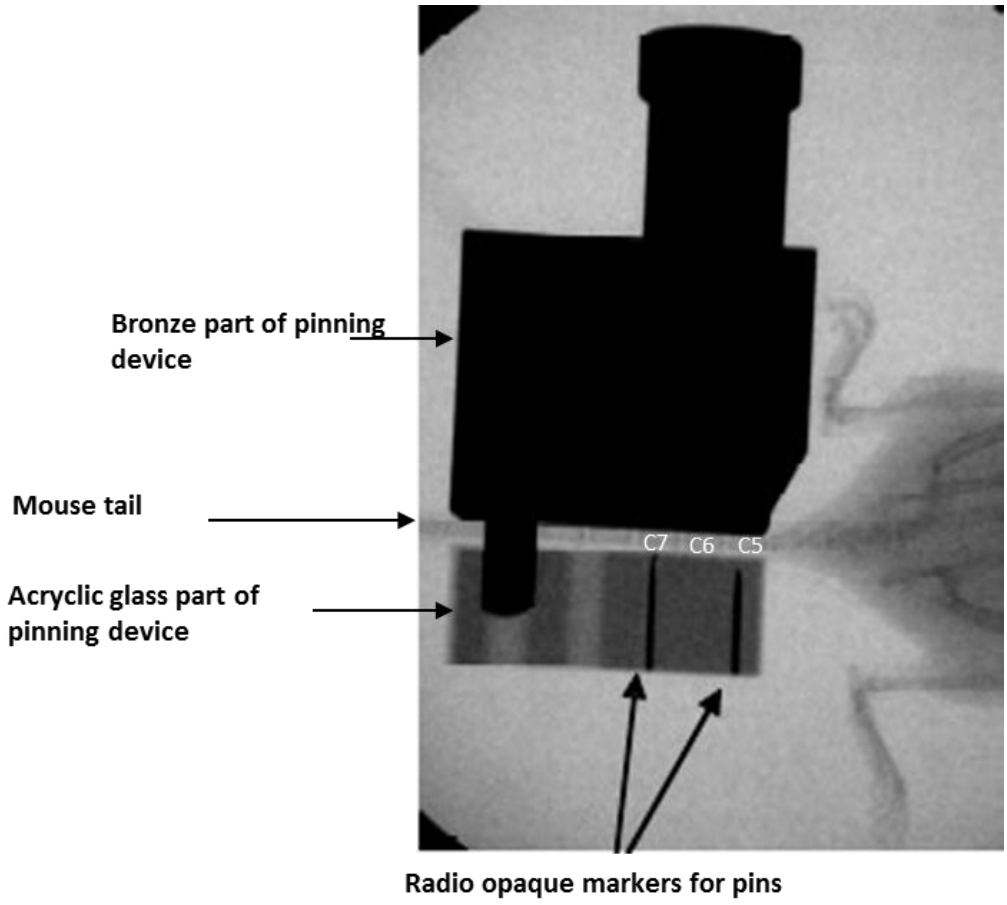

Figure 5: fluoroscopic image to determine correct position of pins

To determine the correct position of the pins the vertebrae were counted starting with the first caudal vertebra at the pelvis and going in the distal direction, as shown in Figure 5. When the pinning device was localized at the desired position, the pins were inserted into the tail by pushing them with the plug and stabilizing the transparent part of the pinning device with the

fingers. The device was then removed and a control image was taken with the C-arm to verify that the pins were inserted into the vertebra and not into the intervertebral disk.

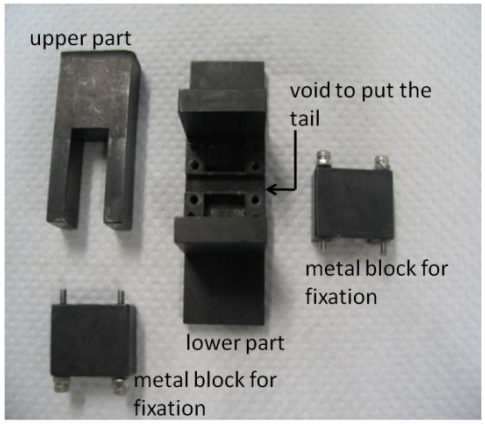

Figure 6: Bending device

The pins were then bent with the bending device, shown in Figure 6. The device itself consists of two parts, both manufactured out of metal. The lower part serves as a tail holder, while the upper part is used to bend the pins. The tail is placed into the space in the middle of the lower part. The pins are then fixed with two u-shaped metal blocks with the ends pointing into the left and right cavities of the lower part. By inserting the upper part into the cavities and hammering it, the tips of the pins are bent downwards. After bending, the pins were shortened and twisted 90°having the ends of the distal pin facing caudal and the ends of the proximal pin facing cranial as shown in Figure 7. This prevents the pins from falling out, reduces injuries of the mice and at the same time the pins are already in a correct position to put them into the loading device. The procedure of bending and cutting the pins is illustrated in Figure 7 and Figure 8.

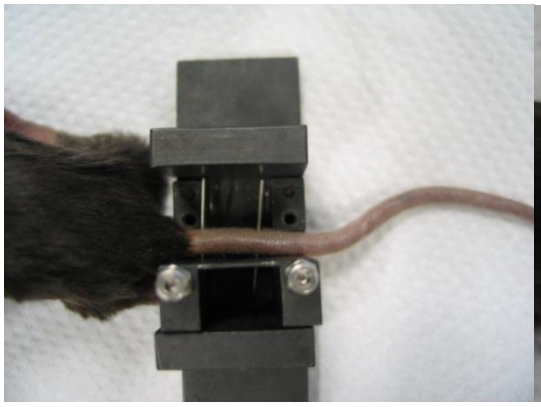

Figure 7: tail with pins in bending device

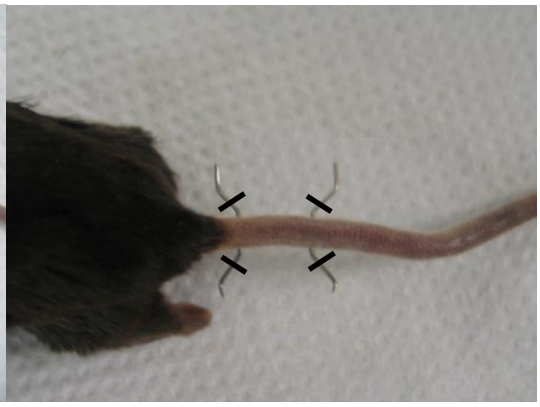

Figure 8: bended and rotated pins, black lines mark position for cutting

Finally the tail was sprayed again with Kodan and the mice were transferred to a pre-warmed cage to recover. Once fully awake the animals were placed back into their home cage. Both the pinning device and the bending device were developed at our institute [251].

The mice were checked on a daily basis for the following three days for general appearance and possible swelling around the pins. The animals were excluded from the study if severe swelling and redness around the pins was noticed. Thereafter the skin around the pins was checked for swelling and redness weekly, along with weighing of the animals. If a severe swelling occurred, such that the end of the pins were not visible anymore the animals were excluded from the study.

The animals were allowed to move freely with the pins during the whole experiment and loading was performed as it is described in section 3.5.

3.5 Loading and pharmacological treatment

After the ovariectomy a time lag of 5 or 11 weeks respectively allowed the mice to develop ovariectomy-induced osteopenia. After this time the mice were exposed to mechanical loading of the 6^{th} caudal vertebra and pharmacological treatment.

Loading

Mechanical loading was applied three times per week for 4 weeks using the Caudal Vertebrae Axial Compression Device (CVAD), developed by Webster [251]. This device was used to perform axial cyclic compression of the 6^{th} caudal vertebra. A detailed description can be found elsewhere [251]. In short, the device consists of a linear actuator (LA25-42-000A, Bei-Kimco Magnetics, Vista, USA) which is coupled to a 10N load cell (13/2443 – 16 TRANSMETRA haltec GmbH, Neuhausen, Switzerland). An applicator, into which the distal pin is inserted, connects directly to the load cell. The distal part of the tail is threaded through a screw cap and a hole into the applicator. A horizontal slot, which was cut into the front face of the applicator, secures the correct positioning of the distal pin with its ends facing in the caudal direction. By clamping the proximal pin onto a steel base plate, the load applied to the distal pin is directly transferred to the 6^{th} caudal vertebra. The loading protocol was programmed using LabView 7.0 (National Instruments). This program sends signals to the actuator. The inner core of the actuator is connected to the load cell and the applicator with the pins inserted. By the signals of the program the loading device can move forwards and backwards. To avoid damages of the tail vertebra due to sudden impulses, the force applied to the target vertebra was ramped up to $1Ns^{-1}$, before a cyclic load of 8N was applied. The force is controlled with a proportional-integral-derivative controller in a closed loop feedback. During the loading 3,000 cycles are performed with a frequency of 10 Hz, resulting in a loading duration of 5 minutes. During this time the mice were anesthetized using Isoflurane.

The mice assigned to the 0N loading group, were treated identically to the other group, namely the tail was placed into the loading device without applying loading. Anesthesia was performed for the equivalent time. After loading mice were transferred into a pre-warmed cage for waking up. Once fully awake they were placed back into their home cage.

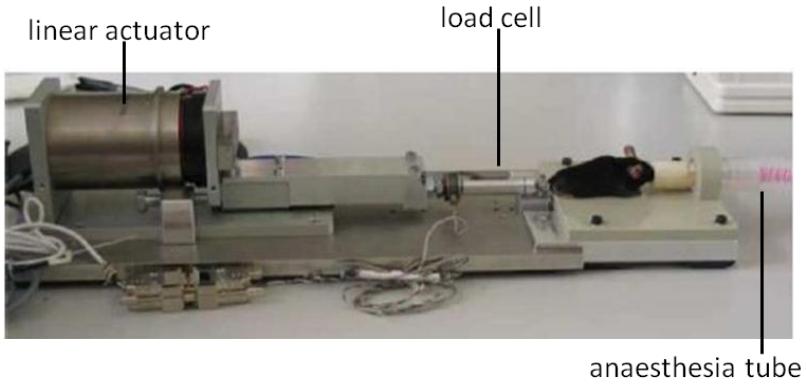

Figure 9: mouse in loading device, picture taken from [251]

Pharmacological treatment

In two studies of each experimental series pharmacological treatment was administered in combination with the mechanical loading on the 6th caudal vertebra. In one study PTH (hPTH 1-34, Bachem AG, Switzerland) or the corresponding vehicle was injected. In the other the bisphosphonate zolendronate (Zometa 4mg/5ml; Novartis Pharma Schweiz AG, Bern) was administered.

In the PTH study a dose of 80 µg/kg of PTH or vehicle was injected daily for 4 weeks, starting 5 or 11 weeks after the ovariectomy. The PTH was dissolved in 0.9 % NaCl (0.9% Natriumchloridlösung, B. Braun Medical AG, Switzerland) and 2 % heat inactivated mouse serum (Immundiagnostik AG, Bensheim, Germany). The pH was adjusted to 7.4 with 0.01N hydrochloric acid (HCl). To inactivate the mouse serum it was heated for 30 minutes in a 56°C water bath. The vehicle consisted of 0.9% NaCl, heat inactivated mouse serum and HCl to adjust the pH.

In the bisphosphonate study a zolendronate dose of 100 µg/kg or vehicle, which consisted of 0.9 % NaCl, was injected subcutaneously once 5 or 11 weeks after the ovariectomy. To be able to inject 0.01 ml/g mouse the Zolendronate was diluted with 0.9 % NaCl.

3.6 CT-measurements

During the study the loaded 6th caudal vertebra of each mouse was scanned 4 times with an *in vivo* micro-CT scanner (vivaCT 40, Scanco Medical, Brüttisellen, Switzerland). The first CT-scan was performed at the time of the castration to provide baseline values. When the loading and treatment period started (that is after 5 or 11 weeks, respectively), the mice were scanned for the second time, followed by the last two scans at a two week interval.

During CT-measurements, the animals underwent isoflurane anesthesia, which was maintained at a concentration of 2 %. The mice were placed in an in house designed mouse holder. To prevent the animals from cooling down to a critical temperature the mouse holder was heated to 35°C. As seen in Figure 10 a carbon tube is connected to the mouse holder. The tail was threaded through a small opening into this tube and clamped tightly in order to fix the tail in a straight position and to prevent it from moving and subsequently eliminate the possibility of motion artifacts appearing during the scans. An eye cream was applied before the scans started.

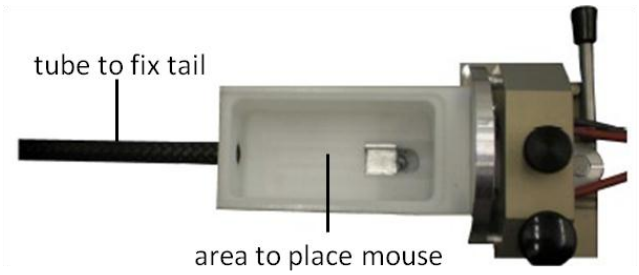

Figure 10: mouse holder

The x-ray tube was operated at 55 kVp, 145 µA, with an integration time of 200 ms. No frame averaging was applied. Scans were performed with an isotropic voxel resolution of 10.5 µm. The total scanning time for two stacks (2 x 211 slices) was 22 minutes. In a few occasions the 6th caudal vertebra was too long for two stacks, especially in the ovariectomized mice. Here 3 stacks had to be scanned, prolonging the scanning time by 10 minutes. Before the scan was started a scout view was taken to define the region of interest. In animals that have not had the pins inserted yet the 6th caudal vertebra was identified by counting the tail vertebrae starting at the pelvis. Otherwise, the vertebra in between the two pinned ones was the desired vertebra for scanning.

After the scans mice were allowed to recover in a pre-warmed cage. When they were fully awake, they were transferred back into their home cage.

To assure consistent image quality the calibration of the scanner for mineral equivalent value was checked weekly following a standard protocol with a hydroxyapatite phantom provided

by the manufacturer. Additionally, a monthly check was performed with a thin wire included in the same phantom to check the in plane spatial resolution.

3.7 Image processing and evaluation

After scanning images were processed in order to allow evaluation of the data. In the processing step first they were reconstructed with a rotation angle such that the median line was aligned to 0° in the dorso-ventral direction in all vertebrae. Thereafter, a three dimensional file with a size of 300 x 300 x 422 voxels was produced by cutting out the region of interest. To avoid stack artifacts, a stack correction was performed, where the 1st slice of the 2nd stack was registered on the last slice of the first stack and then translation was applied to complete the second stack. The images were Gaussian-filtered (sigma 1.2, support 1) and a global threshold of 220, representing 22 % of the maximum grey level-value, was applied. After the processing automatic masks were created on these binary images. The masks were programmed in-house and based on a method described elsewhere [252]. They were used to select full, trabecular and cortical regions in the bone and to calculate structural parameters of all regions. To obtain the trabecular mask, a distance transformation was applied to the outer mask leading to an inner mask. Afterwards the top and bottom 10% of the mask were removed, to exclude the growth plate from trabecular evaluation. Furthermore, the central 26% of the metaphysis were excluded in the trabecular region, which is void of trabecular bone.

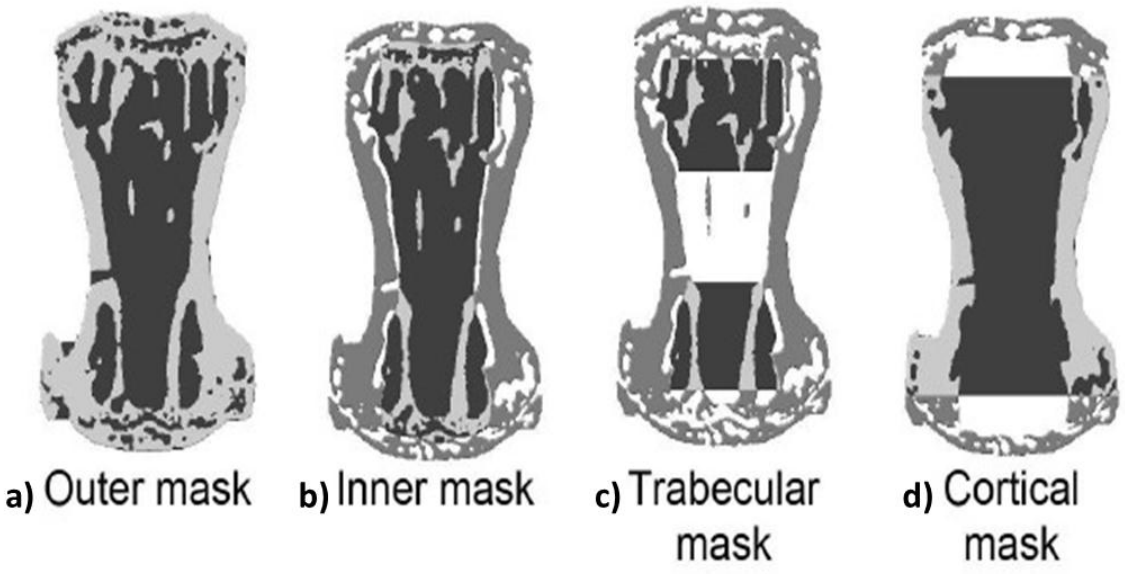

Figure 11: overview of all masks: a) outer mask includes all bone, b) inner mask after distance transformation from outer mask, c) trabecular mask with growth plates and center 26% excluded, d) cortical mask with trabecular structures removed adopted from [252]

For each scan morphometric (static) and dynamic parameters were evaluated.

The following morphometric parameters were calculated [253, 254]: For the full bone compartment, that is the bone consisting of trabecular bone, cortical bone and the growth plate, the bone volume (Full BV, [mm^3]) and total volume of interest (Full TV, [mm^3] were calculated and their ratio, the bone volume fraction (Full BV/TV, [%]) was derived. In the trabecular compartment trabecular bone volume density (Trab BV/TV, [%]) was calculated the same way as Full BV/TV. With the spheric fitting method [255] trabecular thickness (Tb.Th, [µm]) was estimated. Spheres with the largest possible diameter still completely within the trabeculae (Tb.Th), were fitted into the structures. These diameters were averaged and used to calculate the average thickness. To calculate the trabecular number (Tb.N, [1/mm]) the distance-transformation method [256] was used, where the mean distance between the mid axes of the trabeculae was measured. Tb.N is given as the inverse of this value. The cortical mask was calculated by taking the middle 75% of the inner mask and removing the trabecular structure. The cortical bone volume (Cort BV [mm^3]) and total volume of interest (Cort TV, [mm^3]) were calculated. The ratio of these two parameters is given as percent cortical bone volume (cort % BV). Using the distance-transformation method the cortical thickness (Ct.Th, [µm]) was calculated. All these parameters represent static parameters.

To calculate the dynamic parameters, two binary images from the single measurements of each mouse were added onto each other resulting in a three colored image. Voxels that were present in both images are visualized in grey, voxels that were found in only the first image, in blue, and voxels that were seen only in the last image were shown in yellow as can be seen in Figure 12.

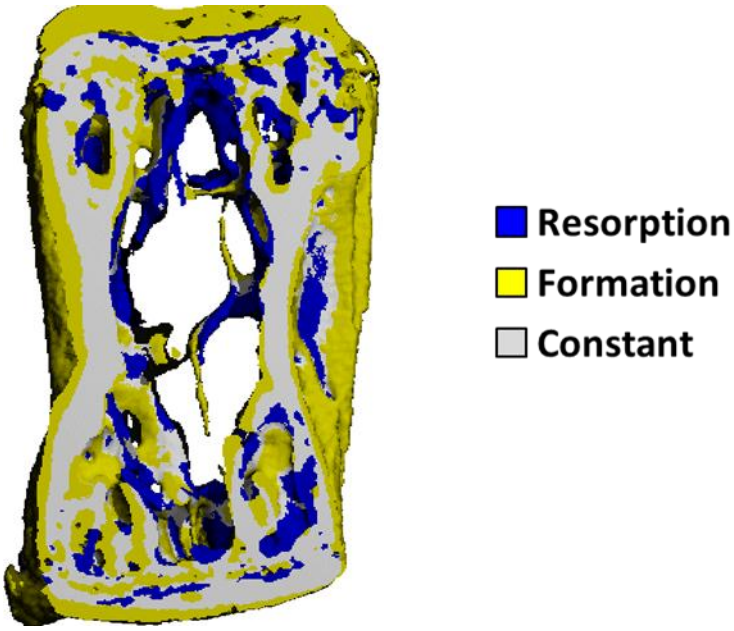

Figure 12 scans from first and last measurement from a PTH treated loaded mouse registered onto each other, blue areas represent resorbed bone, yellow areas formed bone and grey areas bone that was present in both images

With the help of these three colored volumes the direct three dimensional extraction of dynamic bone formation and bone resorption parameters was performed. A detailed description of the registration and calculation of the dynamic parameters can be found elsewhere [42]. Mineral apposition rate (MAR, [µm/d]) was calculated by applying a distance transformation algorithm to the isolated volumes of formed bone of the three colored images. It is defined as the mean thickness of formed bone divided by the days in between the measurements. Mineral resorption rate (MRR, [µm/d]) was calculated in the same fashion as MAR, using the volume of resorbed bone instead of formed bone. Mineralizing surface (MS, [%]) was calculated from the three colored image by separating the contact areas between formed and constant bone voxels. Eroded surface (ES, [%]) was calculated similarly using the area of eroded bone instead of formed bone. Bone formation rate per bone volume per day (BFR, [%/d]) was described as the amount of formed bone volume per original bone volume per day. It is determined by dividing the volume of formed bone by the initial bone volume. Using the volumes of the resorbed areas the bone resorption rate per bone volume per day (BRR, [%/d]) was calculated. With using the volumes and not surfaces to calculate bone formation and bone resorption it is possible to evaluate these parameters in a three dimensional way. This is an advantage compared to histology. In histology it is only possible to evaluate surfaces but not volumes.

3.8 Physiome map

In order to gain a better overview over the combined effects of different pharmacological treatment and loading in ovariectomized mice a physiome map was created for each static parameter.

The data of all 214 mice at the age of 15 weeks, just before ovariectomy was pooled and set to 100 % to see the effect of ovariectomy. However, to get an overview over the distribution of the original data, standard deviation of the original data was plotted at this point as well. In addition, the data of the second measurement was normalized to the first time point and the mice were pooled for ovariectomy and sham operation. Therefore, at 20 and 26 weeks of age two data points were plotted, representing the normalized pooled data with the corresponding standard deviation of all 91 ovariectomized and 16 sham operated animals respectively. After this point, lines are split up according to the different loading and treatment groups (SHM 8N and 0N, BIS 8N and 0N, PTH 8N and 0N). The ovariectomized and vehicle treated groups should show the same development during the studies, because they all represent ovariectomized mice that are not treated with pharmacologically active substances. Therefore OVX 8N mice were pooled together with the VEH 8N mice from the PTH and bisphosphonate study in the OVX/VEH 8N group, and OVX 0N mice were pooled together with the VEH 0N mice from these studies in the OVX/VEH 0N groups. This results in 8 different groups each for start of loading and treatment period at the age of 20 and 26 weeks respectively.

Because the mice had different bone mass at the age of 15 weeks and hence bone loss after ovariectomy was not identical, the data of each mouse of the measurements performed during the treatment and loading period was normalized to its second measurement. This second measurement was always executed at the beginning of the treatment and loading period at weeks 20 and 26, respectively. With this second normalization the scope of evaluation can be placed on the effects of treatment and loading without any bias due to individually different baseline values. To be able to fit this normalized values into the complete graph, the percent changes during the treatment and loading period were recalculated to represent a percent change of the value of the second measurement, which was normalized to the first measurement. To do so, the percent difference of the third and fourth measurement, in comparison to the second measurement, was calculated. Then this percent change was calculated for the value of the normalized second measurement and plotted at the third and fourth time points. Again standard deviations, referring to the normalized values were plotted.

Figure 13 is an example for such a physiome map for Trab BV/TV.

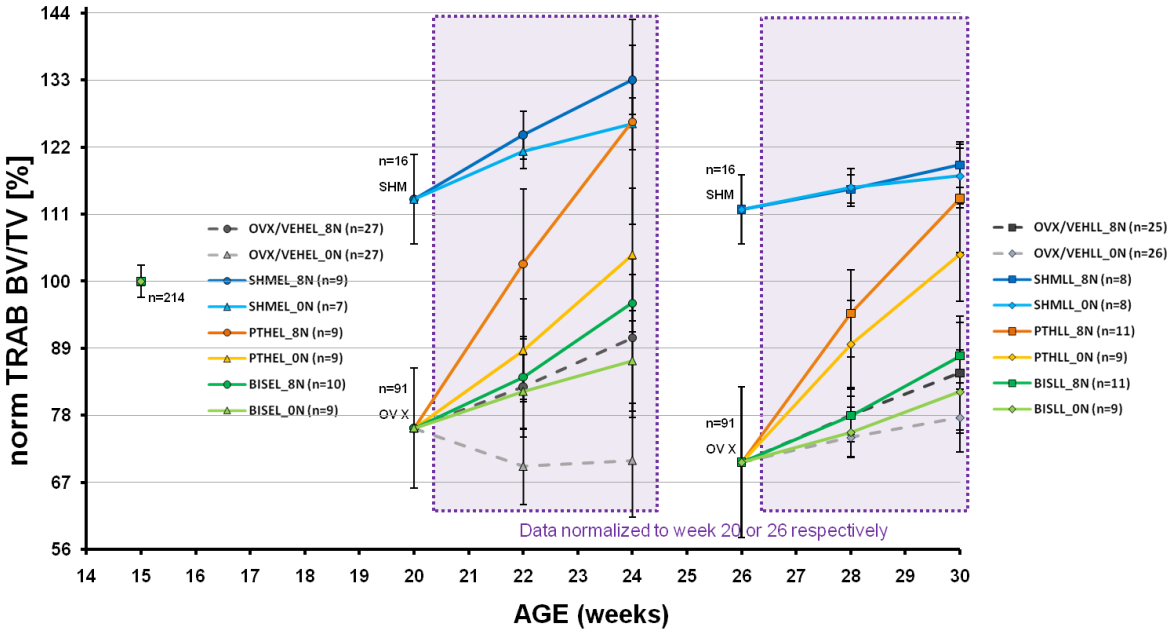

Figure 13: physiome map of Trab BV/TV

3.9 Statistical analysis

Descriptive statistics with mean and standard deviation was performed for each time point for each group of both experimental series. To compare the effects of the different loading and treatment regimens the data of the static parameters of each mouse was normalized to its second measurement, which was taken at the beginning of the loading and treatment period. Then for each study in each experimental series a univariate ANOVA with a LSD post hoc test was performed. Effects were considered significant if p-values were below 0.05. For dynamic parameters, univariate ANOVA was performed for each study with the original data. Again a LSD post hoc test was performed and p-values below 0.05 were considered to be significant. To be able to compare the course of the different groups of the static parameters during 4 weeks of loading and treatment the graphs were plotted using values normalized to the second measurement. With this normalization the different absolute values at the beginning of the loading and treatment period were all set to 100 %. For dynamic parameters the absolute values of the first two weeks and the last two weeks were compared between the groups. Therefore, the graphs for dynamic parameters were plotted using original values.

To test the combined pharmacological treatment and mechanical loading effects on the static parameters for synergistic or additive effects a one-way ANOVA was performed for each study. Therefore, the different loading and treatment combinations were assigned to groups, namely: vehicle 0N representing group 1, vehicle 8N representing group 2, pharmacological

treatment 0N representing group 3 and pharmacological treatment 8N representing group 4. Then a contrast test with the contrast vector (1, -1, -1, 1) was performed. When p-values were below 0.05 and indicating significance no additive effect was observed for this parameter. If the evaluated contrast value was negative the effect on this parameter was less than additive. If this value was positive the effect was considered to be synergistic. All p-values above 0.05 indicated an additive effect.

To analyze static parameters in the physiome map the data of the third and fourth measurement of each mouse was normalized to the second measurement. Then the values of ovariectomized loaded and vehicle treated loaded mice were pooled for each experimental series as well as the values for ovariectomized none loaded and vehicle treated non-loaded mice. For the normalized data a univariate ANOVA with LSD post hoc test was performed for each experimental series and p-values below 0.05 were considered to be significant.

All statistical analysis was performed using SPSS Statistics 17.0 (SPSS Inc, Chicago IL, USA).

4 Results

4.1 Outcome of ovariectomy and pinning operation

At the age of 15 weeks all mice underwent ovariectomy or sham operation. During the lag period of 5 or 11 weeks, pins were inserted into the 5^{th} and 7^{th} caudal vertebra.

The ovariectomy and sham operations could be performed without any complications. Five mice out of 240 that underwent surgery died during the procedure or immediately afterwards. Animals were monitored daily for 3 days after surgery, together with the administration of pain killers. According to the score sheet, monitoring included weighing, evaluation of habitus, body posture, wound and social behavior. Animals showed typically a moderate weight loss of 1-2 g after OVX. After one week, the original body weight was regained. A few mice showed a delayed cleaning of the wound, however until the second day all wounds were clean from the applied wound spray. Slight inflammations could be seen in some mice in the first three days, but the inflammation did not progress and healed within a few days. Staples lost within the first 4 days were replaced. Otherwise no signs of impaired wound healing or other adverse effects could be seen. During the lag period, until the treatment and loading started, mice were weighed weekly. A clear difference in weight gain between castrated and sham operated mice was visible. The mean weight in mice that underwent

ovariectomy in the early loading group was 21.3 g before the operation at the age of 15 weeks and 24.5 g 5 weeks after the castration at the age of 20 weeks. Corresponding values for sham operated mice are 20.1 g at the age of 15 weeks and 22.3 g at the age of 20 weeks. In the late loading groups mean weight in mice that underwent ovariectomy was 22.1 g at the age of 15 weeks, before the operation and in mice that underwent sham operation 21.8 g. After the lag period of 11 weeks the mean weight in ovariectomized mice was 26.6 g and in sham operated mice 25.1 g. The weight development early and late loading series can be seen in Table 4.

WEIGHT [gram]				
Group / age	**15 weeks**	**20 weeks**	**22 weeks**	**24 weeks**
OVX 8N	19.6 ± 1.2	23.9 ± 2.5	23.7 ± 2.1	23.9 ±2.4
OVX 0N	20.1 ± 1.3	24.9 ± 1.3	24.8 ± 1.4	24.7 ± 1.7
SHM 8N	20.4 ± 1.0	22.4 ± 0.7	22.3 ± 1.0	22.5 ± 0.7
SHM 0N	19.7 ± 0.8	19.7 ± 1.3	22.0 ± 1.4	21.9 ± 1.3
PTH 8N	21.3 ± 1.4	24.6 ± 1.5	25.0 ± 1.4	24.8 ± 1.1
PTH 0N	21.6 ± 0.9	25.2 ± 1.3	25.5 ± 1.2	25.7 ± 1.2
VEH (PTH) 8N	21.3 ± 0.9	23.9 ± 1.1	23.6 ± 1.1	23.6 ± 1.1
VEH (PTH) 0N	21.5 ± 0.8	24.7 ± 1.3	24.8 ± 1.3	24.4 ± 0.9
BIS 8N	21.0 ± 0.8	24.4 ± 1.7	24.4 ± 1.6	24.8 ± 1.7
BIS 0N	20.3 ± 1.0	23.7 ± 1.4	23.5 ± 1.1	24.0 ± 1.2
VEH (BIS) 8N	20.9 ± 1.5	24.4 ± 2.3	24.5 ± 1.9	24.7 ± 2.0
VEH (BIS) 0N	20.5 ± 1.2	23.5 ± 1.2	23.6 ± 1.0	23.9 ± 1.0

a) early loading series

WEIGHT [gram]				
Group / age	**15 weeks**	**26 weeks**	**28 weeks**	**30 weeks**
OVX 8N	22.2 ± 1.7	27.0 ± 3.7	25.9 ± 3.3	25.2 ± 3.3
OVX 0N	21.3 ± 1.0	26.6 ± 2.3	25.7 ± 2.0	25.0 ± 1.9
SHM 8N	21.8 ± 1.5	25.1 ± 2.3	25.2 ± 2.2	24.7 ± 2.0
SHM 0N	21.6 ± 0.8	25.1 ± 3.1	24.3 ± 2.3	24.4 ± 2.7
PTH 8N	22.4 ± 1.3	26.2 ± 1.9	26.1 ± 1.5	26.0 ± 1.4
PTH 0N	21.7 ± 1.2	27.0 ± 3.1	26.0 ± 2.0	25.6 ± 1.9
VEH (PTH) 8N	21.6 ± 1.6	25.5 ± 3.2	24.0 ± 2.2	24.2 ± 2.0
VEH (PTH) 0N	21.9 ± 2.0	26.2 ± 2.7	24.9 ± 2.0	24.7 ± 1.9
BIS 8N	20.9 ± 0.8	25.4 ± 1.8	24.7 ± 1.8	25.1 ± 1.6
BIS 0N	20.4 ± 2.4	25.0 ± 3.8	24.5 ± 3.9	24.8 ± 3.95
VEH (BIS) 8N	21.2 ± 1.2	25.6 ± 2.3	24.6 ± 2.4	25.2 ± 2.6
VEH (BIS) 0N	20.9 ± 0.8	26.1 ± 1.6	25.4 ± 1.7	25.5 ± 1.7

b) late loading series

Table 4: weight during experimental series; a) early loading series, b) late loading series; values are presented as mean ± standard deviation

The pinning procedure could be performed without any major difficulties. With the help of the fluoroscope the pins were positioned correctly. Just one mouse had to be sacrificed as one pin was inserted between the vertebrae by mistake. After pinning the mice were checked regularly. No inflammation or swelling was visible immediately after the pinning. However, after several weeks some mice developed a small swelling. If possible these mice were subjected to the 0N group. In total 15 out of 240 mice had to be sacrificed before the end of the experiment as the tissue around the pins was too swollen to fit them in the loading device or the pins got loose and were eventually lost completely which made it impossible to put them into the loading device.

4.2 Effect of ovariectomy

Full bone

At the age of 15 weeks mice are still growing. Therefore we saw in sham mice an increase in full bone total volume by 5.2 % five weeks and by 5.7 % 11 weeks after the surgery. Not only the total volume, but also the bone volume increased during this time. Hence full bone volume density was increased by 5.8 % in the early loading experimental series and by 7.2 % in the late loading experimental series.

Sex hormones block growth hormone production. Therefore animals castrated before growth stops, often show an additional growth spurt. Indeed, in our mice we observed an increased growth in vertebral length, which was visible already during the measurements. The axial field of view had to be increased in some mice. In the OVX mice, the total volume of the vertebrae increased 9.6 % in the early treatment groups and by 12.1 % in the late treatment groups. However, as expected, bone volume fraction decreased by about 5 % in both experimental series, resulting in a loss of full bone volume density of 13.2 % at five weeks and 15.6 % at eleven weeks after ovariectomy.

Trabecular compartment

Also in the trabecular compartment an increase in total volume and bone volume was observed in the sham operated mice. This resulted in an increase of trabecular bone volume density by 13.4 % five weeks and 11.8 % eleven weeks after surgery. However, this increase in Trab BV/TV was not due to an increased number of trabeculae. After the lag period Tb.N was decreased by around 4 %. Therefore only the thickening of trabeculae by 14.4 % in the early loading experimental series and by 11.7 % in the late loading experimental series contributed to the increased Trab BV/TV.

In OVX mice, as expected, trabecular bone volume decreased in both experimental studies resulting in a decrease of trabecular bone volume density by 24.1 % in the early experimental series and by 29.7 % in the late experimental series. This lower Trab BV/TV results out of loss of trabeculae and thinning of existing trabeculae. Interestingly, in the early experimental series the loss of 3.7 % of Tb.N is similar to that seen in sham operated mice, whereas in the late loading experimental series the decrease by 8.9 % is clearly higher in OVX than in SHM mice by 4 %.

Cortical compartment

The cortical compartment increased as well in sham operated mice. After the lag period the cortex was thickened by 4.7 % and 4.2 % respectively.

The increase of Trab BV/TV in OVX mice was also on the expense of cortical thickness. Five weeks after ovariectomy cort % BV was decreased by 3.8 % and eleven weeks after surgery by 9.6 %.

Parameter Group	Full TV [mm³]	Full BV [mm³]	Full BV/TV [%]	Ct.Th [µm]	cort % BV [%]	Tb.N [1/mm]	Tb.Th [µm]	Trab BV/TV [%]
early loading								
SHM								
15 weeks	7.7 ± 0.5	3.9 ± 0.3	50.7 ± 3.2	141.4 ± 9.1	37.4 ± 2.8	3.2 ± 0.3	67.8 ± 4.6	17.8 ± 2.1
20 weeks	8.1 ± 0.5	4.3 ± 0.3	53.7 ± 2.6	148.2 ± 8.3	39.1 ± 2.3	3.0 ± 0.3	77.7 ± 5.3	20.1 ± 2.2
OVX								
15 weeks	7.6 ± 0.5	4.0 ± 0.3	52.2 ± 2.7	143.8 ± 7.7	38.4 ± 2.4	3.0 ± 0.3	73.2 ± 5.6	18.2 ± 2.5
20 weeks	8.4 ± 0.5	3.8 ± 0.3	45.3 ± 2.7	138.2 ± 7.3	33.8 ± 2.4	2.9 ± 0.2	64.8 ± 3.9	13.7 ± 1.8
late loading								
SHM								
15 weeks	7.7 ± 0.4	3.9 ± 0.3	51.1 ± 2.6	144.6 ± 7.1	38.2 ± 1.9	3.0 ± 0.2	72.1 ± 5.1	17.2 ± 2.4
26 weeks	8.2 ± 0.4	4.5 ± 0.4	54.7 ± 2.5	150.8 ± 9.1	39.9 ± 2.1	2.9 ± 0.2	80.5 ± 6.8	19.2 ± 2.6
OVX								
15 weeks	7.7 ± 0.5	4.2 ± 0.4	54.2 ± 3.0	151.2 ± 8.6	40.4 ± 2.6	3.0 ± 0.2	75.7 ± 4.7	18.6 ± 2.7
26 weeks	8.7 ± 0.5	4.0 ± 0.3	45.7 ± 2.8	136.4 ± 8.3	33.6 ± 2.5	2.7 ± 0.2	66.3 ± 4.7	12.9 ± 1.7

Table 5: static values of ovariectomized and sham operated groups before and after ovariectomy / sham operation. Values presented as means ± standard deviation

Parameter Group	Full TV [%]	Full BV [%]	Full BV/TV [%]	Ct.Th [%]	cort % BV [%]	Tb.N [%]	Tb.Th [%]	Trab BV/TV [%]
early loading								
SHM								
15 weeks	100.0	100.0	100.0	100.0	100.0	100.0	100.0	100.00
20 weeks	105.2 ± 2.0	111.3 ± 4.7	105.8 ± 2.8	104.7 ± 2.6	104.4 ± 3.4	95.8 ± 3.9	114.4 ± 5.3	113.4 ± 7.3
OVX								
15 weeks	100.0	100.0	100.0	100.0	100.0	100.0	100.0	100.00
20 weeks	109.6 ± 2.5	95.1 ± 5.1	86.8 ± 4.6	96.2 ± 4.1	88.2 ± 5.5	96.4 ± 5.2	88.8 ± 6.1	75.9 ± 9.8
late loading								
SHM								
15 weeks	100.0	100.0	100.0	100.0	100.0	100.0	100.0	100.00
26 weeks	105.7 ± 1.7	113.3 ± 4.0	107.2 ± 2.7	104.2 ± 3.0	104.6 ± 3.5	95.9 ± 5.8	111.7 ± 6.7	111.8 ± 5.7
OVX								
15 weeks	100.0	100.0	100.0	100.0	100.0	100.0	100.0	100.00
26 weeks	112.1 ± 2.4	94.5 ± 7.0	84.4 ± 6.4	90.4 ± 5.3	83.3 ± 6.8	91.1 ± 6.7	87.9 ± 7.7	70.3 ± 12.4

Table 6: static values of ovariectomized and sham operated groups before and after ovariectomy / sham operation. Values presented as means ± standard deviation

4.3 Loading in ovariectomized mice

In the following experiments, we tested whether bones of OVX mice are mechanosensitive and can adapt to increased mechanical load. Mechanical loading started 5 or 11 weeks after surgery. Age matched sham operated animals served as controls.

Early loading – static parameters

Figure 14 shows overlaid CT images representing the loading period for each group. It can be seen, that with loading bone formation is higher than without. Furthermore in the OVX 0N group a lot of bone resorption can be observed which represents the on-going bone loss after ovariectomy.

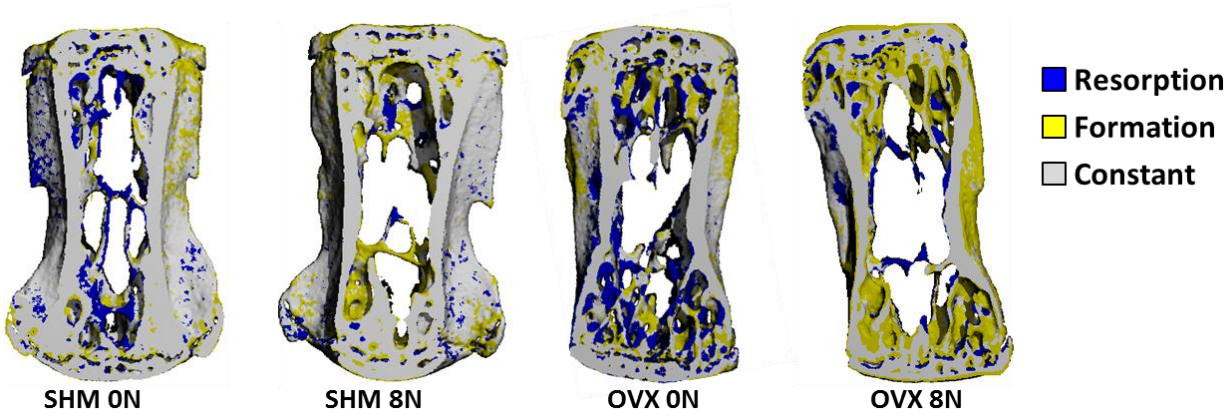

Figure 14: Visualization of bone development during 4 weeks of loading period. CT images of week 20 and 24 are overlaid and registered. Blue represents resorbed bone, yellow newly formed bone and grey constant bone.

Sham 0N (n=7)

At the age of 15 weeks mice are not fully grown yet. Therefore intact non-loaded mice represent normal growing mice. Hence, an increase in Full TV of 1.8 % from 8.1 ± 0.6 mm³ to 8.3 ± 0.7 mm³ was observed in the investigated bone (Figure 15a). Full bone volume increased even more by 6.8 % from 4.7 mm³ to 4.9 mm³ which resulted in an increase in full bone volume fraction by 4.9 % (Figure 15c). This increase was caused by thickening of the cortical and trabecular bone. Cortical thickening was 2.7 % from 144.7 ± 6.2 µm to 148.6 ± 7.1 µm (Figure 15d), resulting in an increase in cortical %BV by of 3.6 % (Figure 15 e). Trabecular number remained stable over the time (Fig15f). Due to trabecular thickening of 7.2 %, trabecular bone volume fraction increased by 10.9 % from 20.1 ± 3.1 % to 22.3 ± 3.1 % (Figure 15h).

Sham 8N (n=9)

Mechanical loading of 8N increased bone growth only slightly. Intact loaded mice showed an increase in Full TV of 2.4 % during the 4 weeks loading period (Figure 15a). The increase in full bone volume by 9.9 % from 4.4± 0.2 mm³ to 4.7 ± 0.2 mm³ was higher than in SHM 0N

animals, although not significantly (Figure 15b). Also the cortical compartment was not affected significantly by mechanical loading. In the trabecular compartment, 8N loading thickened trabeculae by 14.4 %, which is significantly more than in the control group (
g). However, trabecular number was not changed during the loading period. Loading induced an increase in trabecular bone volume fraction by 17.3 % (Figure 15h), which is a visible trend compared to the increase in non-loaded mice.

Ovariectomized 0N (n=10)

Due to estrogen depletion in ovariectomized animals growth hormones are not blocked anymore. Therefore OVX 0N mice showed a higher total volume than sham operated mice already at the age of 20 weeks. With a 2.7 % increase from 8.5 ± 0.4 mm³ to 8.7 ± 0.4 mm³ in Full TV the development over time was similar to sham operated mice, although a trend was visible towards a larger rise (Figure 15a). Full bone volume and hence Full BV/TV were increased only slightly, by 5.1 % and 2.3%, respectively (Figure 15b, c). Cortical thickness and cortical %BV remained stable and so did trabecular BV/TV. However, trabecular number was reduced by 9.1 % (Figure 15f), which is compensated by trabecular thickening of 5.0% (Figure 15g).

Ovariectomized 8N (n=10)

Loading increased all parameters significantly more compared to non-loaded ovariectomized animals, except for trabecular number.

With an increase in TV by 3.9 % from 8.3± 0.7 mm³ to 8.6 ± 0.7 mm³ bone growth was even significantly higher than in intact mice (Figure 15a). Also bone volume was increasing significantly more than in sham operated mice as Full BV was increasing by 1.4 % from 3.8± 0.4 mm³ to 4.5 ± 0.4 mm³ (Figure 15b). Hence full bone volume density was significantly increased in ovariectomized loaded mice as well. The cortex was thickened by 5.0 % and cort % BV increased by 8.6 % (Figure 15d). However, the strongest impact of loading was seen in the trabecular compartment, where bone volume fraction was increased by 28.1 % from 13.8 ± 1.7 % to 17.6 ± 2.1 % (Figure 15h). This was caused by a thickening of the trabeculae by 27.3 % (Figure 15g). That is an increase from 63.3 ± 4.5 µm to 80.4 ± 5.0 µm. The loss of trabecular number could not be prevented by loading. It was with 10.5 % not significantly different from the 0N group (Figure 15f).

The absolute values of all static parameters of the early loading study are shown in Table 7. Normalized values can be seen in Table 8.

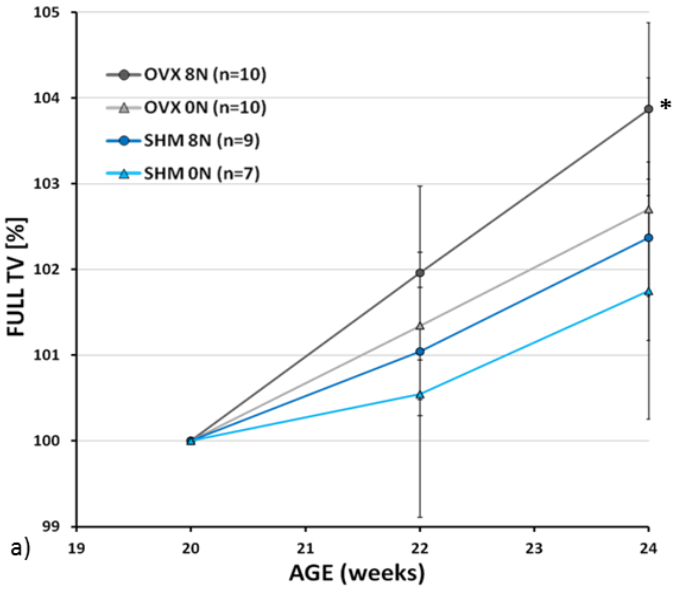
OVX 8N (n=10)
OVX 0N (n=10)
SHM 8N (n=9)
SHM 0N (n=7)
FULL TV [%]
AGE (weeks)
a)
*

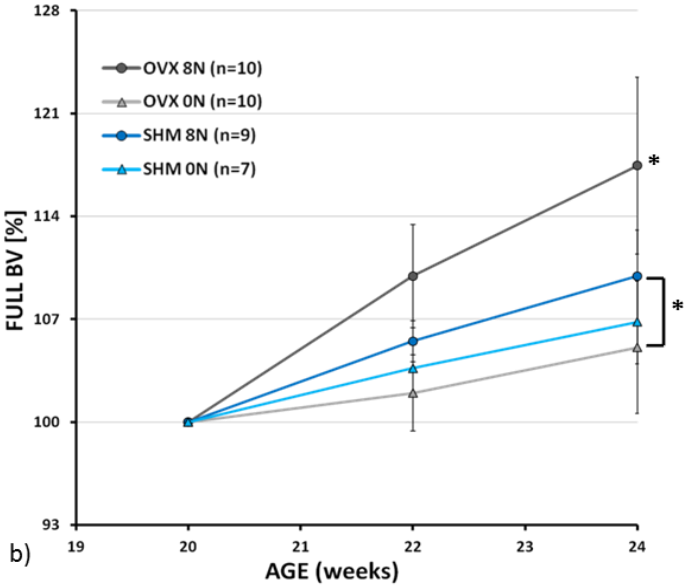
OVX 8N (n=10)
OVX 0N (n=10)
SHM 8N (n=9)
SHM 0N (n=7)
FULL BV [%]
AGE (weeks)
b)
*
*

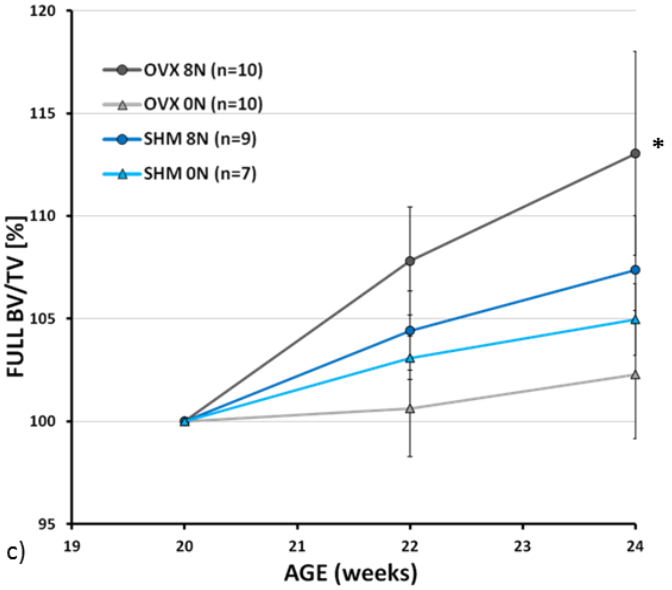
OVX 8N (n=10)
OVX 0N (n=10)
SHM 8N (n=9)
SHM 0N (n=7)
FULL BV/TV [%]
AGE (weeks)
c)
*

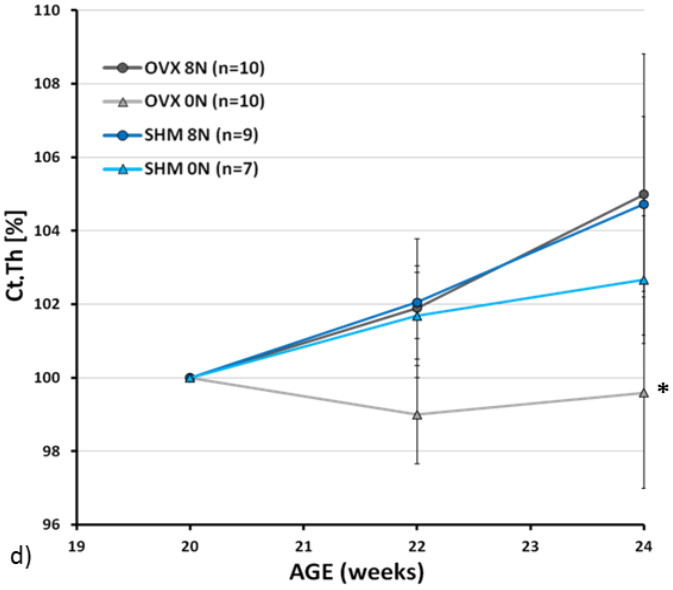
OVX 8N (n=10)
OVX 0N (n=10)
SHM 8N (n=9)
SHM 0N (n=7)
Ct.Th [%]
AGE (weeks)
d)
*

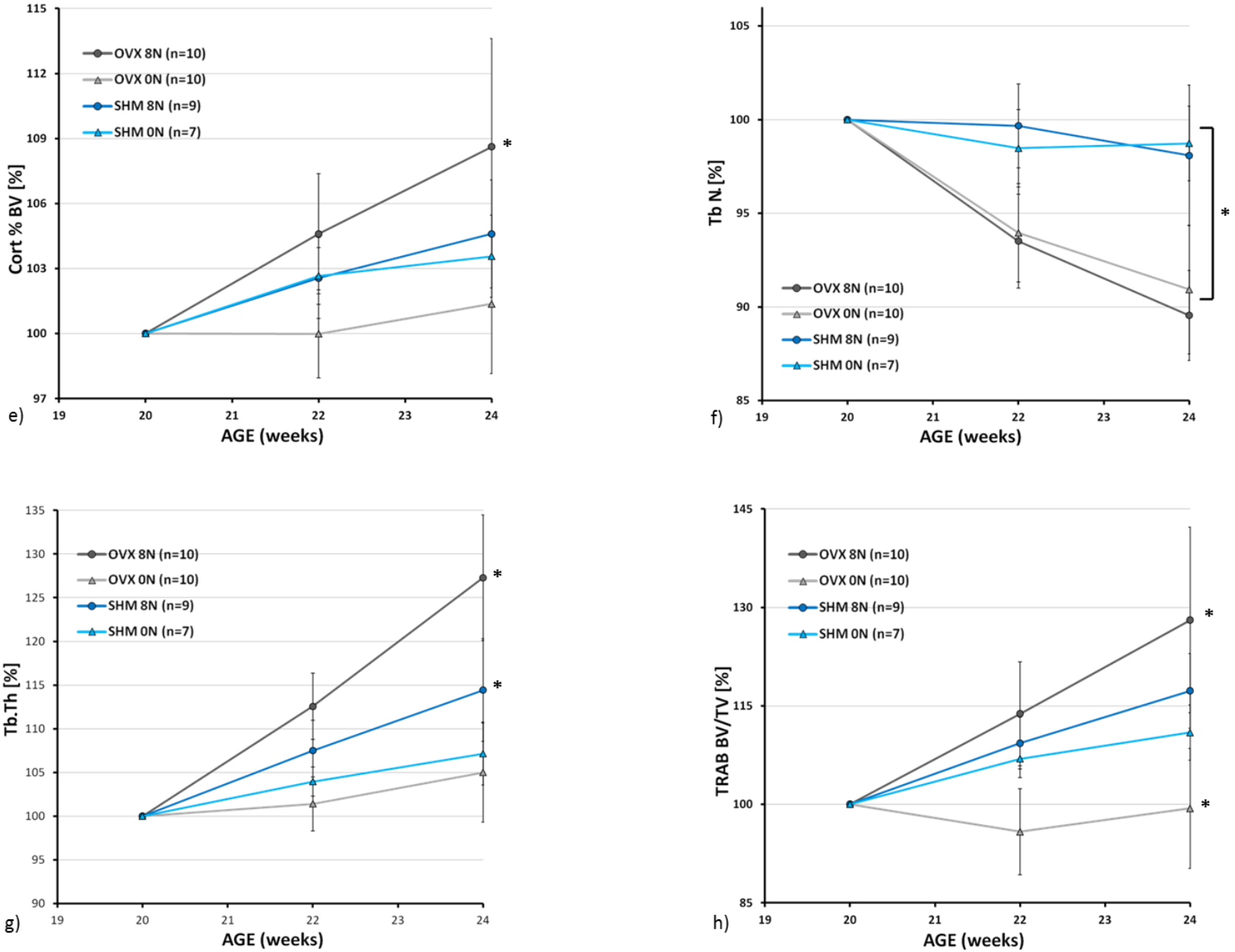

Figure 15: static parameters of ovariectomy study from early loading experimental series. Measurements normalized to first measurement at beginning of loading period. a), b) parameters from full bone; c)-g) parameters from trabecular compartment; h), I) cortical parameters

Early loading – dynamic parameters

Bone formation parameters

Intact non-loaded mice showed a BFR of 1.1 ± 0.3 %/d during the first two weeks of the observations. Loading did not increase this rate (1.2 ± 0.2 %/d) significantly. During the last two weeks of the loading period, a drop in BFR was observed in both groups. As expected, ovariectomy increased BFR significantly to 1.5 ± 0.4 %/d in OVX 0N. The highest BFR was observed in the loaded OVX group with 2.1 ± 0.5 %/d, which is significantly higher than in any other group of this study. In the second half of the observation period, BFR also dropped in the OVX groups. (Figure 16a)

Mineral apposition rate was at 1.3 µm/d in both sham operated groups during the first two weeks of the study. Due to a drop in the non-loaded group during the last two weeks, SHM 0N animals showed the significantly lowest rate at this time. Ovariectomy increased MAR during the first two weeks to 1.4 ± 0.2 µm/d in non-loaded and to 1.5 ± 0.1 µm/d in loaded animals. During the last two weeks a drop in both groups was observed. (Figure 16b)

Mineralizing surface in intact non-loaded animals was at 47.7 ± 8.4 % during the first two weeks. This was increased significantly in loaded animals (54.0 ± 5.9 %). A drop in both groups was observed during the last two weeks of the observation period. Ovariectomy decreased MS significantly. With 38.0 ± 4.5 % during the first two weeks, OVX 0N showed the lowest MS of all groups in this study. Loading in ovariectomized mice increased mineralizing surface significantly to similar values as in sham operated loaded mice (52.5 ± 4.1 %). In contrast to the two intact groups, MS increased during the last two weeks in the ovariectomized animals resulting in almost similar values for sham operated and ovariectomized non-loaded animals and significantly higher values for ovariectomized loaded animals. (Figure 16c)

Bone resorption parameters

The bone resorption rate in intact non-loaded mice was 1.0 ± 0.7 %/d during the first two weeks of the experiment. In loaded animals a clear trend towards a decreased BRR was observed (0.7 ± 0.1 %/d in SHM 8N). During the last two weeks a drop could be noticed for non-loaded animals. However, in SHM 8N mice BRR remained stable during the entire experiment. As ovariectomy induces a high turnover osteoporosis, not only bone formation but also bone resorption was increased in ovariectomized animals. With a rate of 2.1 ± 0.4 %/d during the first two weeks, OVX 0N animals showed the highest BRR of the entire study. Loading reduced bone resorption significantly in ovariectomized animals. The

OVX 8N group had a BRR of 1.1 ± 0.2 %/d during the first two weeks. In both OVX groups a drop could be observed during the last two weeks of the study. (Figure 16d)
A similar pattern was observed for mineral resorption rate. During the first two weeks SHM 0N mice showed a MRR of 1.8 ± 0.5 µm/d. This was reduced to 1.7 ± 0.2 µm/d in the loaded group. During the last two weeks a drop was observed in both groups. With 1.3 ± 0.3 µm/d SHM 0N mice had the lowest MRR of all groups in this study. Ovariectomy increased MRR significantly (2.1 ± 0.2 µm/d). Loading reduced MRR in ovariectomized animals as well. During the last two weeks a drop in both groups was observed and no differences between loaded and non-loaded ovariectomized animals was detected anymore. (Figure 16e)
Intact non- loaded animals showed an eroded surface of 32.1 ± 6.7 % during the first two weeks of the observation. Loading reduced the amount of surface significantly to 27.2 ± 5.3 %. While ES dropped in SHM 0N it increased in SHM 8N animals during the last two weeks, resulting in an eroded surface of about 29 % in both groups. Interestingly, ovariectomy did not change the percentage of eroded surface. OVX 0N animals show similar values as SHM 0N (30.2 ± 3.8 % and 28.4 ± 2.5 %, respectively). The effect of loading was intensified in ovariectomized animals, compared to intact mice. With an eroded surface of about 22 % at both time points OVX 8N mice had the smallest ES of all groups at any time point in this study. (Figure 16f)

The absolute values for the dynamic parameters can be seen in Table 12.

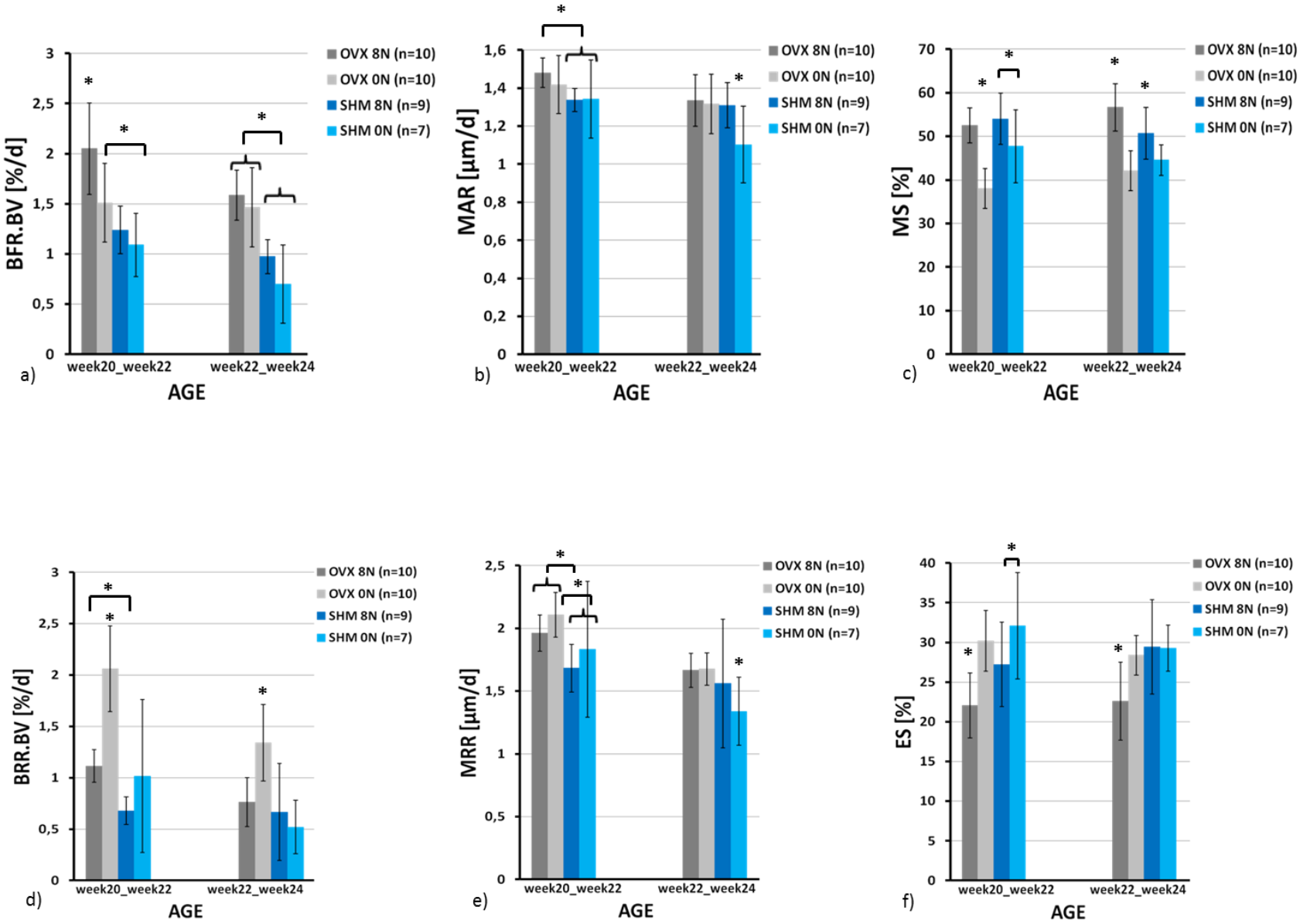

Figure 16: dynamic parameters of ovariectomy study in early loading experimental series. Upper row shows bone formation parameters, lower row shows bone resorption parameters

Late loading – static parameters

Figure 17 shows overlaid CT images representing the loading period for each group. The advanced bone loss can be observed in the OVX 0N group, as hardly any trabecular structure is remaining. However loading improves trabecular structure in both, sham operated and OVX groups.

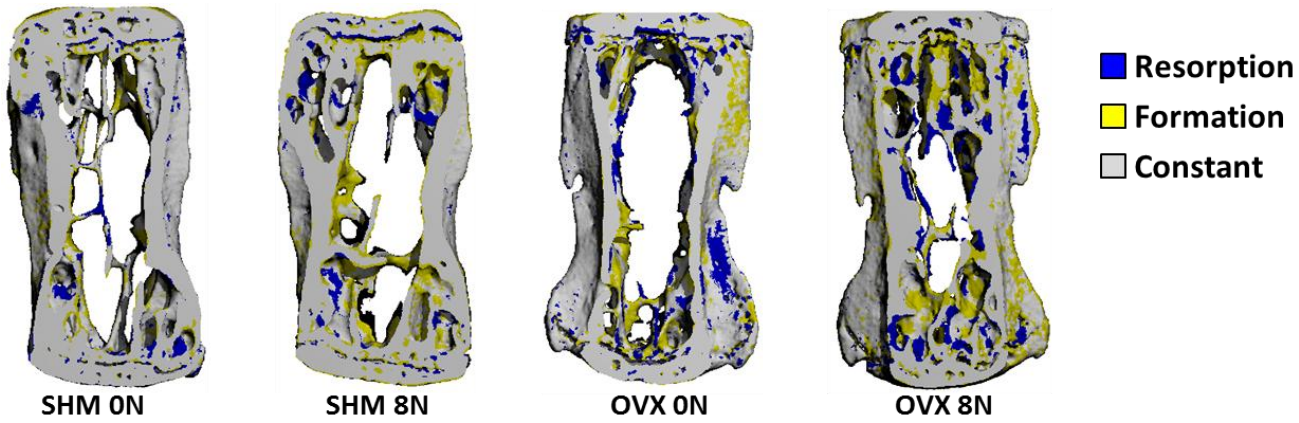

Figure 17: Visualization of bone development during 4 weeks of loading period. CT images of week 26 and 30 are overlaid and registered. Blue represents resorbed bone, yellow newly formed bone and grey constant bone.

Sham 0N (n=8)

At the age of 26 weeks, mice are fully mature and hence grow only very slowly. Therefore Full TV was stable during the 4 weeks observation period and ranged from 8.3 ± 0.2 mm³ at the age of 26 weeks to 8.4 ± 0.2 mm³ at the age of 30 weeks (Figure 18a). Bone volume did not change as well and so did full bone volume fraction. Cortical thickness and %BV were not changed during the course of the experiment. Also in the trabecular compartment no changes were observed. (Figure 18b-h)

Sham 8N (n=8)

Loading did not have an effect on the size of the bone. Full TV remained stable at similar values as in the SHM 0N group (Figure 18a). However, bone volume was increased by 4.9 % from 4.3 ± 0.4 mm³ to 4.6 ± 0.5 mm³ (Figure 18b). Hence also full bone volume density was increased by loading by 3.7 % (Figure 18c). The effect on the cortex was very small as well. The cortex was thickened by 2.2 % from 146.2 ± 7.6 µm to 149.3 ± 8.8 µm (Fig 3d). This resulted in an increase of %BV by 2.2 % (Figure 18e). Trabecular number was not changed in loaded mice throughout the experiment. Nevertheless, loading induced a thickening by 4.6 % from 78.25 ± 7.0 µm to 81.9 ± 8.0 µm (Figure 18g). This resulted in a 6.5 % increase in Trab BV/TV (Figure 18h). It has to be admitted, that although trends in loaded animals towards increased values are visible they are only small and none of them is significant.

Ovariectomized 0N (n=10)

Eleven weeks after ovariectomy bone loss had reached a plateau. Also intense bone growth, due to the lack of estrogens, which used to block growth hormones, was not visible any more. Therefore, Full TV was stable at 8.6 ± 0.4 mm³ to 8.7 ± 0.4 mm³ (Figure 18a). No changes were observed as well for bone volume and bone volume density. However, in the cortical compartment some effect of ovariectomy could still be assessed. The cortex thinned by 1.8 % from 133.2 ± 4.7 µm to 130.9 ± 7.6 µm (Figure 18d). This did not influence %BV as it remained stable during the experiment. Loss of trabecular number proceeded as well as this value was diminished by 2.1 % (Figure 18f). However, trabecular thickness was not affected and eventually Trab BV/TV increased by 9.0 % during the course of the observation period (Figure 18h).

Ovariectomized 8N (n=6)

Loading in ovariectomized animals did not influence the total volume of the vertebra. However, bone volume fraction was increased by 7.8 % from 4.1 ± 0.4 mm³ to 4.4 ± 0.4 mm³ (Figure 18b). This resulted in an increase of full bone volume density of 6.3 % (Figure 18c). In the cortical part loading counteracted on the effects of estrogen depletion and thickened the cortex by 1.6 % (Figure 18d) and increased %BV by 2.5 % (Figure 18e). The loss of trabeculae could not be stopped by loading as Tb.N was decreased by 2.6 %. Although trabeculae got less, the remaining trabeculae were thickened due to loading by 11.1 % from 65.2 ± 5.0 µm to 72.3 ± 3.0 µm (Figure 18g). This resulted in an increase of Trab BV/TV by 16.2 % (Figure 18h).

The original values of all static parameters of the late loading experimental series can be seen in Table 7. The values of the data normalized to the second measurement at week 26 can be seen in Table 8.

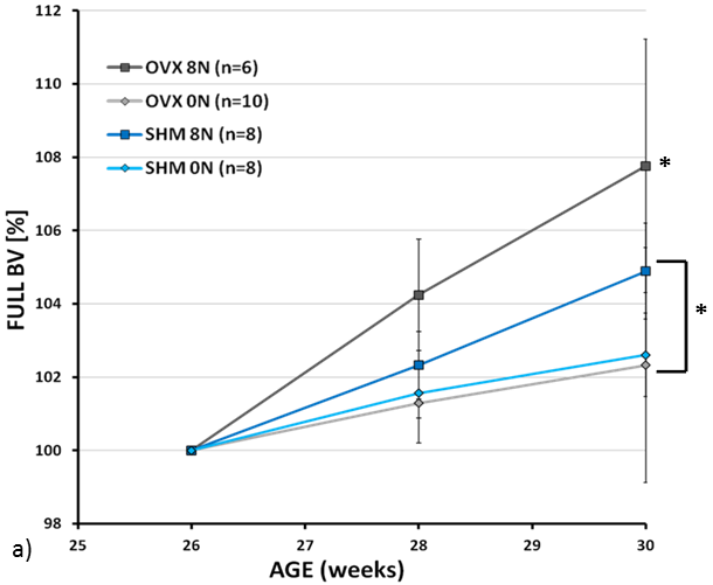
OVX 8N (n=6)
OVX 0N (n=10)
SHM 8N (n=8)
SHM 0N (n=8)
FULL BV [%]
AGE (weeks)
a)
*
*

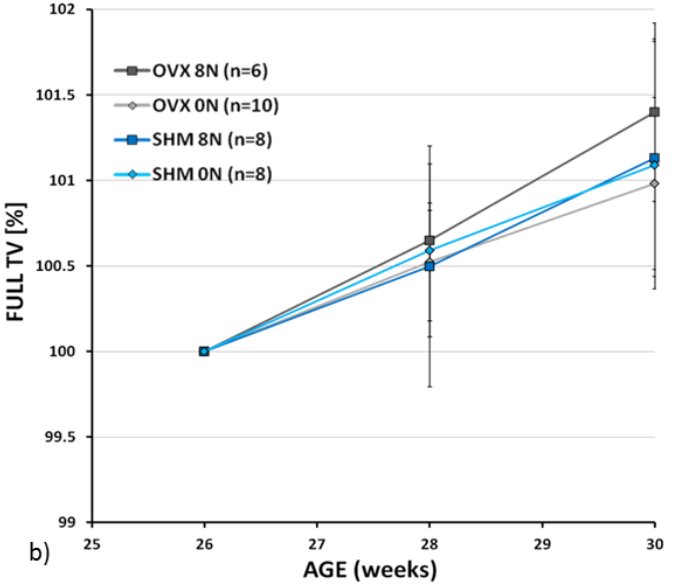
OVX 8N (n=6)
OVX 0N (n=10)
SHM 8N (n=8)
SHM 0N (n=8)
FULL TV [%]
AGE (weeks)
b)

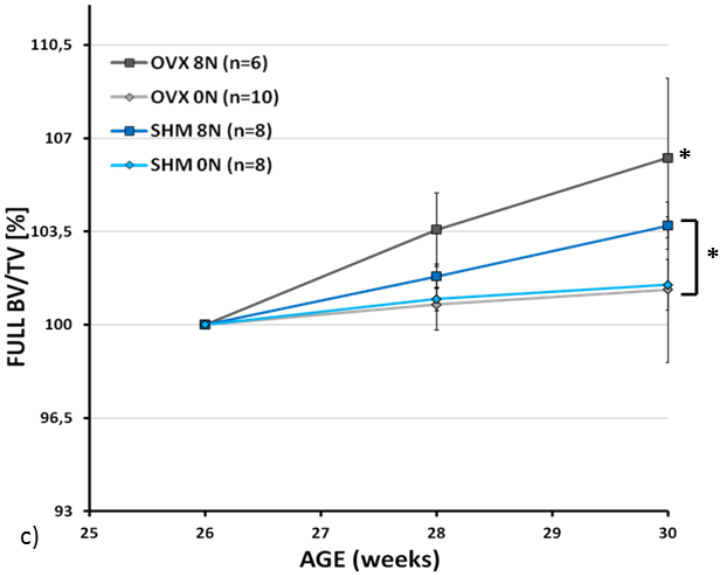
OVX 8N (n=6)
OVX 0N (n=10)
SHM 8N (n=8)
SHM 0N (n=8)
FULL BV/TV [%]
AGE (weeks)
c)
*
*

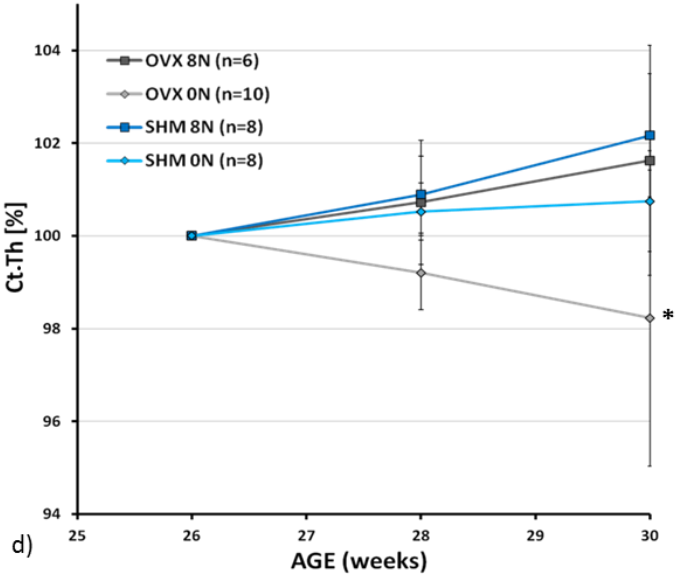
OVX 8N (n=6)
OVX 0N (n=10)
SHM 8N (n=8)
SHM 0N (n=8)
Ct.Th [%]
AGE (weeks)
d)
*

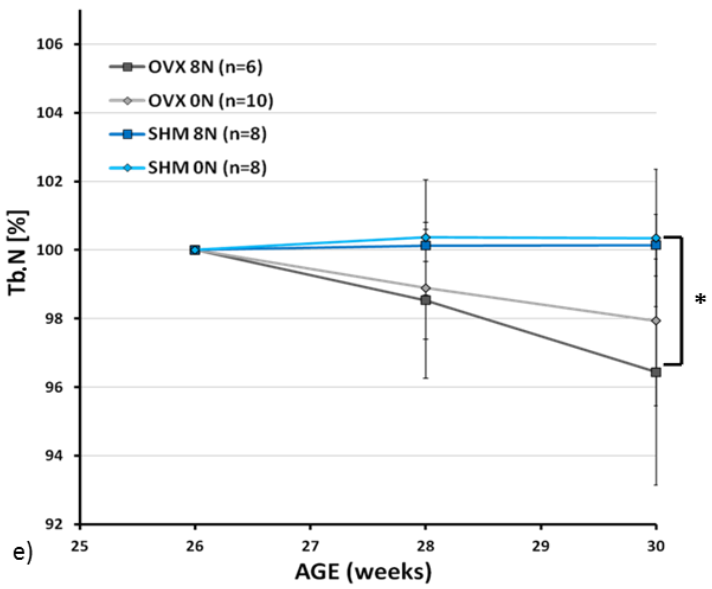

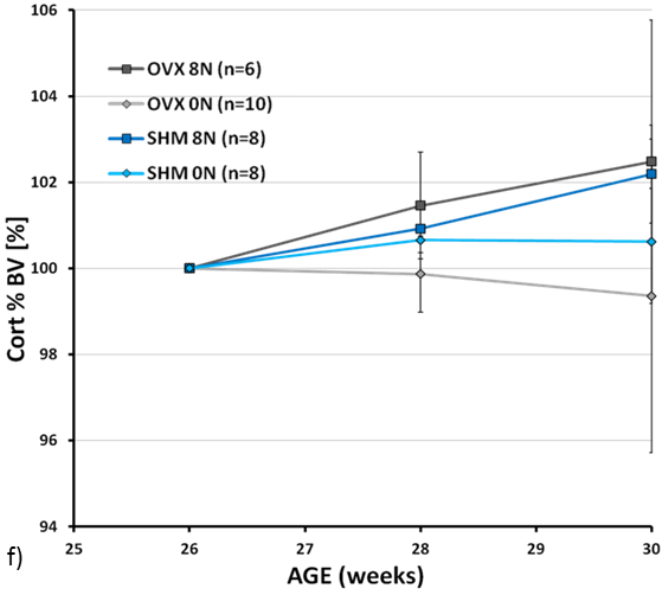

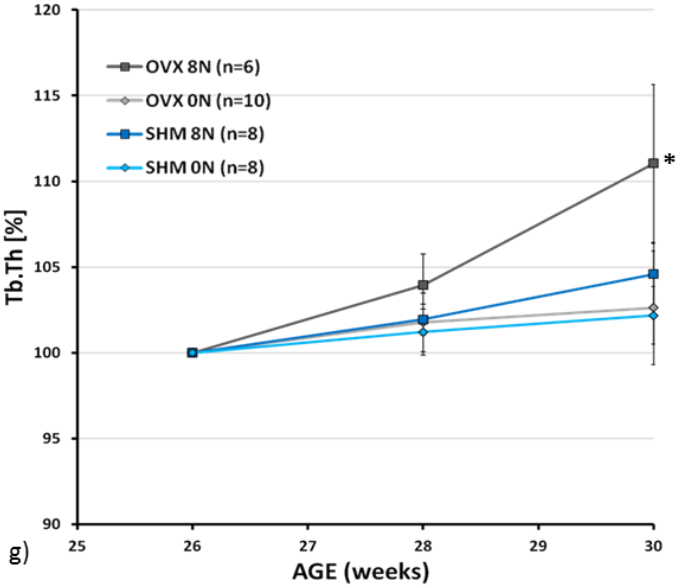

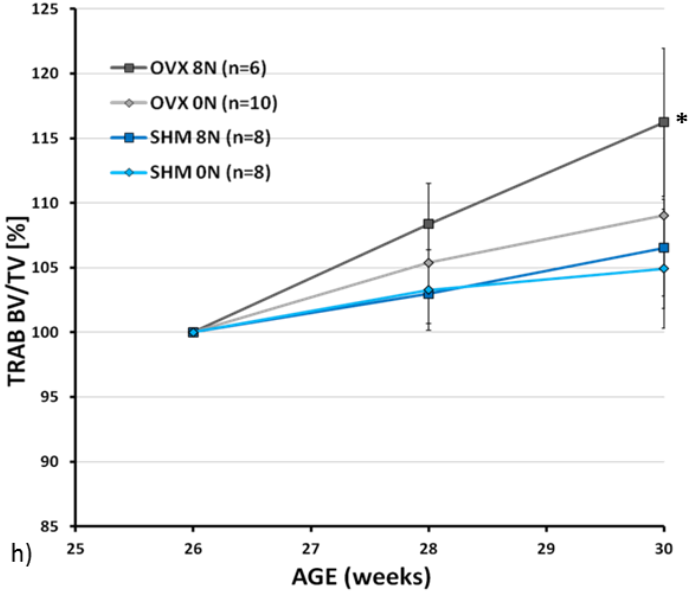

Figure 18: static parameters of ovariectomy study from late loading experimental series. Measurements normalized to first measurement at beginning of loading period. a), b) parameters from full bone; c)-g) parameters from trabecular compartment; h), I) cortical parameters

Late loading – dynamic parameters

Bone formation parameters

In the first two weeks of the late loading study SHM 0N animals had a BFR of 0.54 ± 0.12 %/d. Interestingly loading did not increase BFR. During the first two weeks SHM 8N mice had a BFR of 0.49 ± 0.17 %/d. In the last two weeks a drop in BFR was seen in both groups. Ovariectomy increased bone formation to 0.84 ± 0.15 %/d. In ovariectomized animals loading induced a clear trend to increase BFR, as it is 1.01 ± 0.33 %/d in OVX 8N animals during the first two weeks of loading. A drop during the last two weeks of the observation period was observed in these groups as well. However, both ovariectomized groups showed a significant higher BFR than sham operated groups. (Figure 19a)

Mineral apposition rate was similar in both intact groups at both time points. Ovariectomy increased MAR, however not significantly. With loading a small trend was observed towards an increased MAR at both time points. (Figure 19b)

Mineralizing surface covered 45.51 ± 3.52 % in intact non-loaded mice. A similar value was observed in the loaded group with 42.10 ± 5.76 %. Ovariectomy did not influence the percentage of mineralizing surface. With 42.95 ± 3.19 % OVX 0N mice showed similar values as sham operated animals. However, in ovariectomized animals loading increased MS surface significantly to 48.74 ± 4.53 % during the first two weeks of loading. While MS surface was decreased in the non-loaded mice during the last two weeks of the experiment it was increased in OVX 8N animals to 51.18 ± 5.16 %. (Figure 19c)

Bone resorption parameters

Bone resorption rate in SHM 0N animals was at 0.41 ± 0.16 %/d during the first two weeks of the study. In the loaded group a trend towards a decreased BRR could be observed (0.32 ± 0.08 %/d). During the last two weeks of the experiment BRR dropped in both groups. As ovariectomy induces a high bone turnover osteoporosis it increased BRR significantly to 0.64 ± 0.23 %/d during the first two weeks of the study. Again a trend was observed in the loaded group towards a decreased BRR (0.53 ± 0.23 %/d). During the last two weeks of the study a drop of BRR was observed in both ovariectomized groups as well. (Figure 19d)

Mineral resorption rate in intact non-loaded mice was 1.33 ± 0.30 µm/d at the beginning of the study. Loading reduced this rate significantly to 1.04 ± 0.20 µm/d. During the last two weeks a drop of MRR was observed in both groups. Ovariectomy did not influence mineral resorption rate. With a rate of 1.29 ± 0.20 µm/d during the first two weeks OVX 0N mice had

a similar value as SHM 0N mice. At this time point no difference could be observed between loaded and non-loaded ovariectomized animals. However, during the last two weeks, loading increased MRR in these animals, while in non-loaded mice even a drop in mineral resorption rate could be observed. (Figure 19e)

Eroded surface was similar in both sham operated groups during the first two weeks of the study. However during the last two weeks a trend for a decrease of the eroded surface due to loading was observed. At this time point SHM 0N mice had an ES of 28.67 ± 2.37 %, while it covered 25.27 ± 2.97 % in the loaded group. In the ovariectomized group a trend towards a reduced ES was observed. Loading lessened the amount to 22.54 ± 3.32 %. (Figure 19f)

The values for all dynamic parameters of the early and the late loading experimental series can be seen in Table 9.

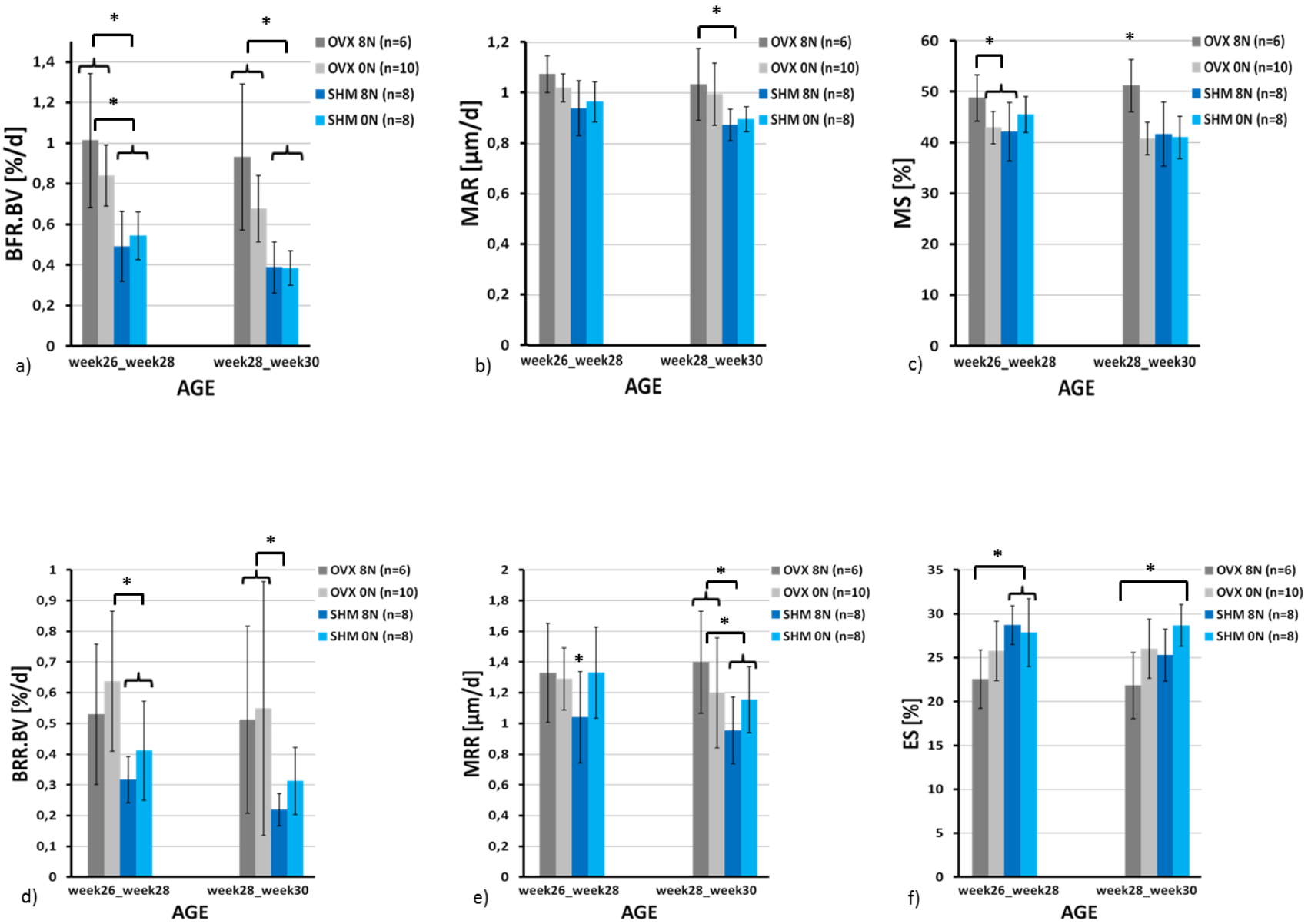

Figure 19: dynamic parameters of ovariectomy study in early loading experimental series. Upper row shows bone formation parameters, lower row shows bone resorption parameters

Parameter group	Full TV [mm³]	Full BV [mm³]	Full BV/TV [%]	Ct.Th [µm]	cort % BV [%]	Tb.N [1/mm]	Tb.Th [µm]	Trab BV/TV [%]
early loading								
SHM 0N								
15 weeks	7.7 ± 0.6	3.8 ± 0.3	49.1 ± 3.5	137.2 ± 7.3	36.2 ± 2.8	3.2 ± 0.3	66.0 ± 4.7	17.3 ± 2.9
20 weeks	8.1 ± 0.6	4.3 ± 0.3	52.7 ± 2.9	144.7 ± 6.2	38.3 ± 2.2	3.0 ± 0.3	77.0 ± 3.7	20.1 ± 3.1
22 weeks	8.2 ± 0.7	4.4 ± 0.3	54.4 ± 3.1	147.2 ± 7.3	39.3 ± 2.3	3.0 ± 0.3	80.0 ± 4.5	21.5 ± 3.5
24 weeks	8.3 ± 0.7	4.6 ± 0.3	55.3 ± 3.1	148.6 ± 7.1	39.6 ± 2.3	3.0 ± 0.3	82.5 ± 5.3	22.3 ± 3.7
SHM 8N								
15 weeks	7.7 ± 0.4	4.0 ± 0.3	52.0 ± 2.4	144.7 ± 9.5	38.5 ± 2.6	3.1 ± 0.2	69.2 ± 4.2	18.2 ± 1.3
20 weeks	8.1 ± 0.3	4.4 ± 0.2	54.4 ± 2.2	150.9 ± 9.1	39.8 ± 2.3	3.0 ± 0.3	78.2 ± 6.4	20.2 ± 1.5
22 weeks	8.2 ± 0.3	4.6 ± 0.3	56.9 ± 2.4	154.7 ± 10.5	41 ± 2.6	3.0 ± 0.3	84.0 ± 6.4	22.0 ± 1.4
24 weeks	8.2 ± 0.3	4.7 ± 0.2	57.6 ± 2.1	155.7 ± 7.6	41.0 ± 1.8	3.0 ± 0.2	88.7 ± 6.4	23.2 ± 1.3
OVX 0N								
15 weeks	7.6 ± 0.4	4.0 ± 0.4	52.4 ± 2.7	144.8 ± 5.7	38.9 ± 1.5	3.1 ± 0.3	69.3 ± 6.1	18.1 ± 4.1
20 weeks	8.5 ± 0.4	3.7 ± 0.3	44.1 ± 3.1	136.3 ± 6.4	33.2 ± 2.3	2.9 ± 0.3	62.2 ± 4.5	12.4 ± 2.3
22 weeks	8.6 ± 0.5	3.8 ± 0.3	44.4 ± 2.8	134.9 ± 5.9	33.2 ± 2.1	2.7 ± 0.2	63.0 ± 3.8	11.8 ± 1.8
24 weeks	8.7 ± 0.4	3.9 ± 0.2	45.1 ± 2.4	135.6 ± 4.7	33.6 ± 1.8	2.6 ± 0.2	65.2 ± 4.2	12.2 ± 1.8
OVX 8N								
15 weeks	7.4 ± 0.6	4.0 ± 0.4	53.2 ± 1.9	146.4 ± 6.0	39.8 ± 1.5	3.2 ± 0.2	70.1 ± 5.0	18.8 ± 1.9
20 weeks	8.3 ± 0.7	3.8 ± 0.4	45.7 ± 2.3	139.0 ± 7.4	34.1 ± 1.9	3.0 ± 0.3	63.3 ± 4.5	13.8 ± 1.7
22 weeks	8.5 ± 0.7	4.2 ± 0.4	49.2 ± 2.0	141.5 ± 6.4	35.6 ± 1.5	2.8 ± 0.3	71.1 ± 4.1	15.6 ± 1.5
24 weeks	8.6 ± 0.7	4.5 ± 0.4	51.6 ± 2.0	145.8 ± 7.1	37.0 ± 1.4	2.7 ± 0.3	80.4 ± 5.0	17.6 ± 2.1
late loading								
SHM 0N								
15 weeks	7.9 ± 0.3	4.1 ± 0.4	51.5 ± 3.2	148.0 ± 7.2	38.8 ± 2.1	3.0 ± 0.3	72.9 ± 5.4	17.3 ± 3.0
26 weeks	8.3 ± 0.2	4.6 ± 0.4	55.1 ± 3.1	155.4 ± 8.6	40.6 ± 2.4	2.7 ± 0.2	82.7 ± 6.2	19.0 ± 3.1
28 weeks	8.4 ± 0.2	4.7 ± 0.4	55.6 ± 3.0	156.2 ± 8.9	40.9 ± 2.5	2.7 ± 0.2	83.7 ± 5.8	19.6 ± 2.8
30 weeks	8.4 ± 0.2	4.7 ± 0.4	56.0 ± 3.2	156.7 ± 9.3	41.0 ± 2.6	2.7 ± 0.2	84.7 ± 5.8	19.9 ± 2.9
SHM 8N								
15 weeks	7.5 ± 0.4	3.8 ± 0.2	50.6 ± 1.8	141.2 ± 5.3	37.5 ± 1.5	3.0 ± 0.2	71.3 ± 5.0	17.2 ± 1.9
26 weeks	8.0 ± 0.5	4.3 ± 0.4	54.3 ± 2.0	146.2 ± 7.6	39.1 ± 1.5	3.0 ± 0.2	78.3 ± 7.0	19.5 ± 2.1
28 weeks	8.0 ± 0.5	4.4 ± 0.4	55.3 ± 2.2	147.5 ± 8.3	39.5 ± 1.6	3.0 ± 0.2	79.8 ± 7.4	20.0 ± 2.4
30 weeks	8.1 ± 0.5	4.5 ± 0.5	56.3 ± 2.3	149.3 ± 8.8	40.0 ± 1.8	3.0 ± 0.2	81.9 ± 8.0	20.7 ± 2.6
OVX 0N								
15 weeks	7.8 ± 0.4	4.0 ± 0.3	52.0 ± 2.7	148.5 ± 7.5	39.1 ± 2.3	2.9 ± 0.2	74.5 ± 5.9	17.3 ± 2.4
26 weeks	8.6 ± 0.4	3.9 ± 0.3	44.9 ± 2.0	133.2 ± 4.7	33.2 ± 1.5	2.5 ± 0.3	64.4 ± 4.0	11.8 ± 1.7
28 weeks	8.7 ± 0.4	3.9 ± 0.3	45.3 ± 2.1	132.1 ±4.8	33.2 ± 1.6	2.5 ± 0.3	65.5 ± 3.9	12.5 ± 1.9
30 weeks	8.7 ± 0.4	4.0 ± 0.3	45.5 ± 2.6	130.9 ± 7.6	33.0 ± 2.2	2.5 ± 0.3	66.1 ± 4.7	12.9 ± 2.3
OVX 8N								
15 weeks	8.1 ± 0.8	4.3 ± 0.7	52.6 ± 4.0	150.7 ± 12.8	39.2 ± 3.5	3.0 ± 0.1	74.7 ± 6.3	18.2 ± 2.7
26 weeks	8.9 ± 0.8	4.1 ± 0.4	46.2 ± 2.2	137.5 ± 7.9	33.8 ± 1.6	2.7 ± 0.1	65.2 ± 5.0	13.4 ± 2.2
28 weeks	8.9 ± 0.8	4.3 ± 0.4	47.8 ± 1.8	138.4 ± 7.1	34.3 ± 1.3	2.7 ± 0.2	67.7 ± 4.1	14.5 ± 2.1
30 weeks	9.0 ± 0.8	4.4 ± 0.4	49.0 ± 2.2	139.6 ± 5.4	34.7 ± 1.5	2.7 ± 0.2	72.3 ± 3.0	15.5 ± 1.9

Table 7: absolute values of static parameters of ovariectomy studies in early and late loading experimental series. Expressed as mean ± standard deviation

Parameter Group	Full TV [%]	Full BV [%]	Full BV/TV [%]	Ct.Th [%]	cort % BV [%]	Tb.N [%]	Tb.Th [%]	Trab BV/TV [%]
early loading								
SHM 0N								
20 weeks	100.0	100.0	100.00	100.00	100.00	100.00	100.00	100.00
22 weeks	100.5 ± 1.8	103.7 ± 1.8	103.1 ± 1.1	101.7 ± 1.2	102.7 ± 1.3	98.5 ± 2.1	104.0 ± 1.7	106.9 ± 2.9
24 weeks	101.8 ± 2.8 a)	106.8 ± 2.8 a)	105.0 ± 1.7 a)	102.7 ± 1.7 b)	103.6 ± 1.9 a)	98.7 ± 2.0 a)b)	107.2 ± 3.6 a)c)	110.9 ± 4.2 a)b)
SHM 8N								
20 weeks	100.0	100.0	100.00	100.00	100.00	100.00	100.00	)100.00
22 weeks	101.0 ± 1.4	105.5 ± 1.4	104.4 ± 1.9	102.1 ± 1.0	102.6 ± 1.9	99.7 ± 2.2	107.5 ± 3.5	109.3 ± 3.9
24 weeks	102.4 ± 3.1 a)	109.9 ± 3.1 a)b)	107.4 ± 2.6 a)b)	104.7 ± 2.4 b)	104.6 ± 2.5 a)	98.1 ± 3.8 a)b)	114.4 ± 5.9 a)b)d)	117.3 ± 5.7 a)b)
OVX 0N								
20 weeks	100.0	100.0	100.00	100.00	100.00	100.00	100.00	100.00
22 weeks	101.3 ± 2.6	102.0 ± 2.6	100.6 ± 2.3	99.0 ± 1.3	100.0 ± 2.0	94.0 ± 2.6	101.4 ± 3.1	95.8 ± 6.6
24 weeks	102.7 ± 4.5 a)	105.1 ± 4.5 a)c)	102.3 ± 3.1 a)	99.6 ± 2.6 a)c)d)	101.4 ± 3.2 a)	90.9 ± 3.4 c)d)	105.0 ± 5.7 a)c)	99.4 ± 9.2 a)c)d
OVX 8N								
20 weeks	100.0	100.0	100.00	100.00	100.00	100.00	100.00	100.00
22 weeks	102.0 ± 3.5	109.9 ± 3.5	107.8 ± 2.6	101.9 ± 1.9	104.6 ± 2.8	93.5 ± 2.5	112.6 ± 3.8	113.8 ± 7.9
24 weeks	103.9 ± 6.0 b)c)d)	117.4 ± 6.0 b)c)d)	113.1 ± 5.0 b)c)d)	105.0 ± 3.8 b)	108.6 ± 45.0 b)c)d)	89.5 ± 2.4 c)d)	127.3 ± 7.2 b)c)d)	128.1 ±14.2 b)c)d)
late loading								
SHM 0N								
26 weeks	100.0	100.0	100.00	100.00	100.00	100.00	100.00	100.00
28 weeks	100.6 ± 0.7	101.6 ± 0.7	101.0 ± 0.4	100.5 ± 0.6	100.7 ± 0.8	100.4 ± 1.7	101.2 ± 1.3	103.3 ± 3.1
30 weeks	101.1 ± 1.1	102.6 ± 1.1 a)	101.5 ± 1.0 a)	100.8 ± 1.1 b)	100.6 ± 1.2	100.4 ± 2.0 a)b)	102.2 ± 1.7 a)	104.9 ± 4.6 a)
SHM 8N								
26 weeks	100.0	100.0	100.00	100.00	100.00	100.00	100.00	100.00
28 weeks	100.5 ± 0.9	102.3 ± 0.9	101.8 ± 0.5	100.9 ± 0.8	100.9 ± 0.6	100.1 ± 0.5	101.9 ± 0.9	103.0 ± 2.3
30 weeks	101.1 ± 1.3	104.9 ± 1.3 a)b)	103.7 ± 0.9 a)b)	102.2 ± 1.3 b)	102.2 ± 1.1 b)	100.1 ± 0.9 a)b)	104.6 ± 1.8 a)	106.5 ± 3.7 a)
OVX 0N								
26 weeks	100.0	100.0	100.00	100.00	100.00	100.00	100.00	100.00
28 weeks	100.5 ± 1.1	101.3 ± 1.1	100.8 ± 1.0	99.2 ± 0.8	99.9 ± 0.9	98.9 ± 1.5	101.8 ± 1.7	105.4 ± 2.7
30 weeks	101.0 ± 3.2	102.3 ± 3.2 a)c)	101.3 ± 2.7 a)c)	98.2 ± 3.2 a)c)d)	99.4 ± 3.6 a)c)	97.9 ± 2.5 c)d)	102.6 ± 3.3 a)	109.0 ± 7.2 a)
OVX 8N								
26 weeks	100.0	100.0	100.00	100.00	100.00	100.00	100.00	100.00
28 weeks	100.6 ± 1.5	104.2 ± 1.5	103.6 ± 1.4	100.7 ± 1.3	101.5 ± 1.2	98.5 ± 2.3	104.0 ± 1.8	108.4 ± 3.2
30 weeks	101.4 ± 3.5	107.8 ± 3.5 b)c)d)	106.3 ± 3.0 b)c)d)	101.6 ± 2.5 b)	102.5 ± 3.3 b)	96.4 ± 3.3 c)d)	111.1 ± 4.6 b)c)d)	116.2 ± 5.7 b)c)d)

Table 8: static parameters of ovariectomy studies of early and late loading experimental series normalized to beginning of loading period. a) Significant to OVX 8N, b) significant to OVX 0N, c) significant to SHM 8N, d) significant to SHM 0N for each study; values are presented as mean ± standard deviation

Parameter group	BFR.BV [%/d]	MAR [µm/d]	MS [%]	BRR.BV [%/d]	MRR [µm/d]	ES [%]
early loading						
SHM 0N						
wk20_wk22	1.1 ± 0.3 a)b)	1.3 ± 0.2 a)	47.7 ± 8.4 b)c)	1.0 ± 0.7 b)	1.8 ± 0.5 b)	32.1 ± 6.7 a)c)
wk22_wk24	0.7 ± 0.4 a)b)	1.1 ± 0.2 a)b)c)	44.5 ± 3.5 a)c)	0.5 ± 0.3 b)	1.3 ± 0.3 a)b)c)	29.3 ± 2.9 a)
SHM 8N						
wk20_wk22	1.2 ± 0.2 a)	1.3 ± 0.1 a)	54.0 ± 5.9 b)d)	0.7 ± 0.1 a)b)	1.7 ± 0.2 a)b)	27.2 ± 5.3 a)d)
wk22_wk24	1.0 ± 0.2 a)b)	1.3 ± 0.1 d)	50.7 ± 6.0 a)b)d)	0.7 ± 0.5 b)	1.6 ± 0.5 d)	29.4 ± 6.0 a)
OVX 0N						
wk20_wk22	1.5 ± 0.4 a)d)	1.4 ± 0.2	38.0 ± 4.5 a)c)d)	2.1 ± 0.4 a)c)d)	2.1 ± 0.2 c)d)	30.2 ± 3.8 a)
wk22_wk24	1.5 ± 0.4 c)d)	1.3 ± 0.2 d)	42.1 ± 4.5 a)c)	1.3 ± 0.4 a)c)d)	1.7 ± 0.1 d)	28.4 ± 2.5 a)
OVX 8N						
wk20_wk22	2.1 ± 0.5 b)c)d)	1.5 ± 0.1 c)d)	52.5 ± 4.1 b)	1.1 ± 0.2 b)c)	2.0 ± 0.1 c)	22.1 ± 4.1 b)c)d)
wk22_wk24	1.6 ± 0.3 c)d)	1.3 ± 0.1 d)	56.7 ± 5.4 b)c)d)	0.8 ± 0.2 b)	1.7 ± 0.1 d)	22.6 ± 4.9 b)c)d)
late loading						
SHM 0N						
wk26_wk28	0.5 ± 0.1 a)	1.0 ± 0.1	45.5 ± 3.5	0.4 ± 0.2 b)	1.3 ± 0.3 c)	27.8 ± 3.9 a)
wk28_wk30	0.4 ± 0.1 a)b)	0.9 ± 0.1	41.0 ± 4.2 a)	0.3 ± 0.1	1.2 ± 0.2 a)	28.7 ± 2.4 a)
SHM 8N						
wk26_wk28	0.5 ± 0.2 a)b)	0.9 ± 0.1	42.1 ± 5.8 a)	0.3 ± 0.1 b)	1.0 ± 0.2 a)b)d)	28.7 ± 2.2 a)
wk28_wk30	0.4 ± 0.1 a)b)	0.9 ± 0.1 a)	41.6 ± 6.3 a)	0.2 ± 0.1 a)b)	1.0 ± 0.1 a)b)	25.3 ± 3.0
OVX 0N						
wk26_wk28	0.8 ± 0.2 c)	1.0 ± 0.1	43.0 ± 3.2 a)	0.6 ± 0.2 c)d)	1.3 ± 0.2 c)	25.7 ± 3.4
wk28_wk30	0.7 ± 0.2 c)d)	1.0 ± 0.1	40.8 ± 3.2 a)	0.6 ± 0.4 c)	1.2 ± 0.4 c)	26.0 ± 3.4
OVX 8N						
wk26_wk28	1.0 ± 0.3 c)d)	1.1 ± 0.1	48.7 ± 4.5 b)c)	0.5 ± 0.2	1.3 ± 0.3 c)	22.5 ± 3.3 c)d)
wk28_wk30	0.9 ± 0.4 c)d)	1.0 ± 0.1 c)	51.2 ± 5.2 b)c)d)	0.5 ± 0.3 c)	1.4 ± 0.3 c)d)	21.8 ± 3.8 d)

Table 9: bone dynamic parameters of ovariectomy studies. a) significant to OVX 8N, b) significant to OVX 0N, c) significant to SHM 8N, d) significant to SHM 0N for each study; values are presented as mean ± standard deviation

4.4 Loading in pharmacological treated ovariectomized mice

The aim of the following experiments was to investigate the combinatory effect of mechanical loading and treatment. Loading and pharmacological treatment were started 5 weeks after ovariectomy in the early loading experimental series and 11 weeks after ovariectomy in the late loading experimental series, respectively. Mice were subjected to 8N or 0N load and additionally injected with either PTH, the bisphosphonate zolendronate or the corresponding vehicle, which was pH adjusted mouse serum in the PTH treatment study and saline in the bisphosphonate treatment study.

4.4.1 PTH studies

Mice were injected daily with PTH or the corresponding vehicle for four weeks in both experimental series. All animals were subjected to 0N or 8N loading.

Early loading – static parameters

Figure 20 shows overlaid CT images representing the loading and treatment period for each group. It can be seen that both loading and PTH treatment lead to bone formation, while in the VEH 0N group bone loss after ovariectomy continues. The strongest bone formation can be seen in the PTH 8N group.

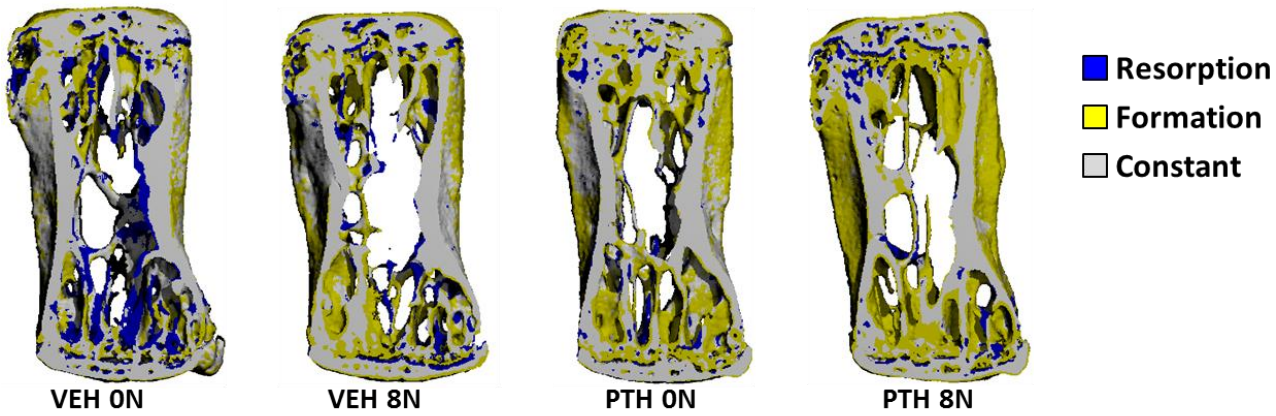

Figure 20: Visualization of bone development during 4 weeks of loading period. CT images of week 20 and 24 are overlaid and registered. Blue represents resorbed bone, yellow newly formed bone and grey constant bone.

VEH 0N (n=8)

As expected, vehicle injection did not influence the bone. Mice of the VEH 0N group were comparable to OVX 0N of the ovariectomy and loading study. The total volume remained stable and bone volume fraction showed a slight increase by 4.4 % from 3.8 ± 0.2 mm³ to 4.0 ± 0.2 mm³ (Figure 21c). No changes were observed in the cortical compartment. As was

already seen in the ovariectomy study, the loss of trabeculae continued during the observation period. Tb.N. was decreased by 6.6 % at the end of the study (Figure 21f). Because trabecular thickness remained stable, the loss in trabecular number was not compensated and resulted in a 6.7 % decreased trabecular bone volume density (Figure 21h).

VEH 8N (n=9)

Loading increased total volume only slightly by 3.1 % from 8.4 ± 0.4 mm³ to 8.6 ± 0.4 mm³ (Figure 21a). However bone volume fraction was rising by 15.1 % from 3.8 ± 0.2 mm³ to 4.4 ± 0.2 mm³ (Figure 21b), which resulted in an increase of full bone volume density by 11.5 % (Figure 21c). This increase in full bone volume fraction was hardly caused by changes in the cortical compartment. The cortex thickened by 3.3 % (Figure 21c) resulting in an increase in cortical % BV of 6.4 % (Figure 21d). The main changes were seen in the trabecular compartment as trabeculae thickened by 17.1 % from 67.2 ± 3.2 µm to 78.6 ± 2.7 µm (Figure 21g). However, the loss of trabeculae could not be stopped and Tb.N. was decreased by 6.8 % by the end of the observation period. Nevertheless, due to the thickening of the remaining trabeculae, Trab BV/TV was increased by 16.6 % (Figure 21h).

PTH 0N (n=9)

PTH is an anabolic drug, therefore an increase of 5.4 % in total volume was expected. Full bone volume fraction increased by 18.9 %, which is similar to the effect of loading (Figure 21b). Also the effect on full bone volume density is similar to loading. At the end of the observation period, Full BV/TV was increased by 12.8 % (Figure 21c). Interestingly enough, with PTH treatment the cortex lost 4.3 % in thickness during the first two weeks of treatment, but regained almost everything during the last two weeks of treatment (Figure 21d). Meanwhile, cortical % BV remained stable during the first two weeks but was increased eventually by 9.7 % by the end of the observation period (Figure 21e). The main difference of PTH treatment compared to loading was that it seems to reduce the amount of lost trabeculae. By the end of the study Tb.N. was only decreased by 3.3 %, while the thickening of trabeculae by 15.8 % was similar to the effect of loading (Figure 21f,g). However, as more trabeculae are preserved the same thickening resulted in a significantly higher increase of trabecular bone volume density compared to the one in loaded animals. After 4 weeks of PTH treatment, Trab BV/TV was increased by 37.5 % (Figure 21h).

PTH 8N (n=9)

The effects of PTH treatment and loading added on to each other, when they were combined. The full total volume was increased by 7.1 %, which was only slightly more than in PTH treated or loaded animals (Figure 21a). However, with an increase of 30.3 % the increase in bone volume fraction was significantly higher than in any other group (Figure 21b). Consequently, the increase of 21.7 % of full bone volume density was higher than in any other group (Figure 21c). These changes were due to both, changes in the cortical and in the trabecular compartment. At the end of the observation period the cortex thickened by 4.8 % from 134.6 ± 3.4 µm to 141.0 ± 3.3 µm (Figure 21d). This resulted in a 17.2 % greater cortical % BV (Figure 21e). In the trabecular compartment the changes were even more pronounced. Combined PTH treatment and loading seems to stop the continuing loss of trabeculae. Furthermore, a tremendous increase of 33.1 % in trabecular thickness was observed (Figure 21g). Trabeculae had an average thickness of 63.6 ± 2.8 µm at the beginning and of 84.5 ± 3.7 µm at the end of the observation period. As no trabeculae got lost and all trabeculae got thicker, the increase by 66.3 % in trabecular bone volume density was significantly higher than in any other group (Figure 21h).

The absolute values of all static parameters are shown in Table 10. Values normalized to the beginning of the treatment and loading period are shown in Table 11.

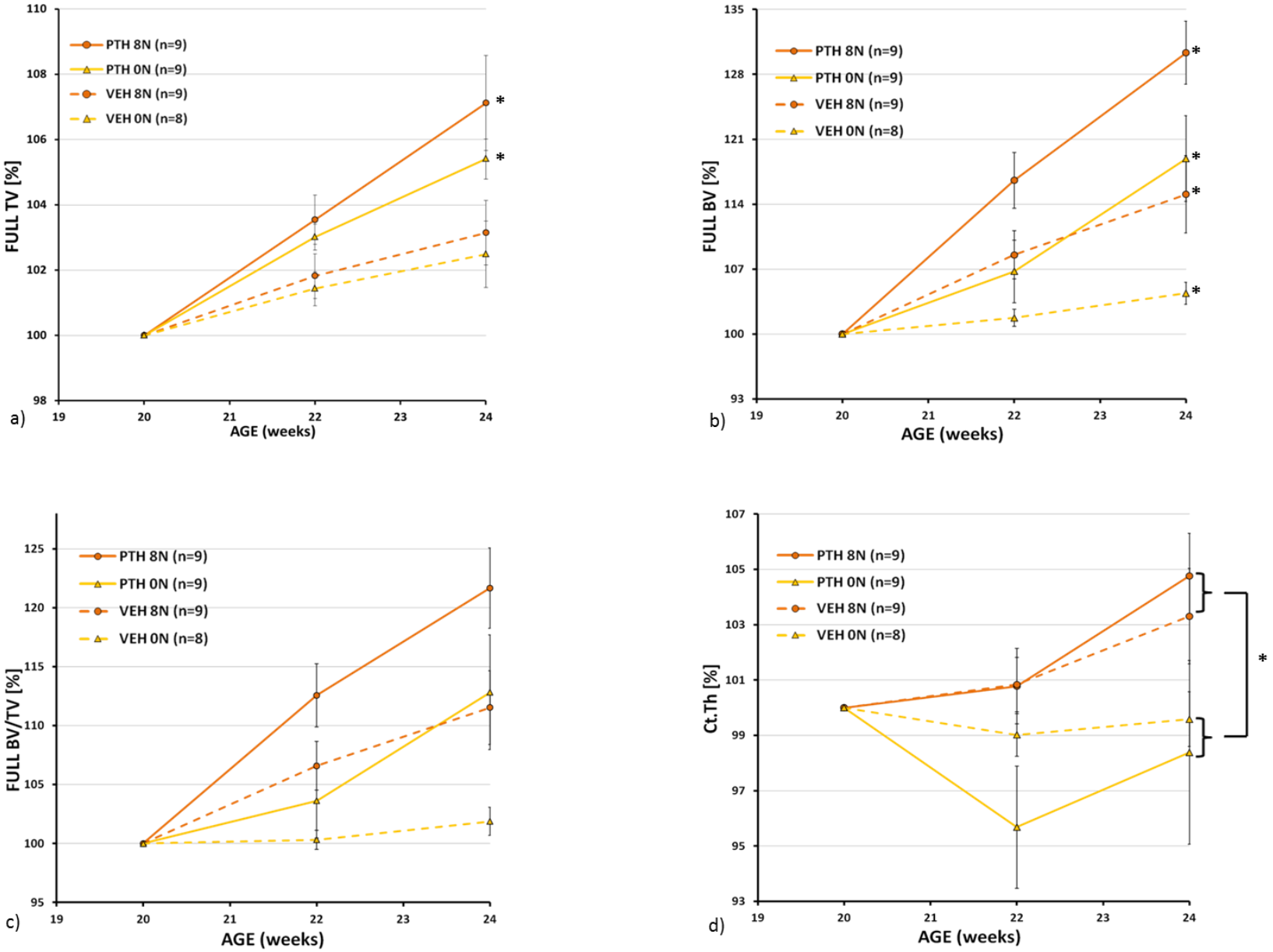
a)
FULL TV [%]
AGE (weeks)
PTH 8N (n=9)
PTH 0N (n=9)
VEH 8N (n=9)
VEH 0N (n=8)
b)
FULL BV [%]
AGE (weeks)
c)
FULL BV/TV [%]
AGE (weeks)
d)
Ct.Th [%]
AGE (weeks)

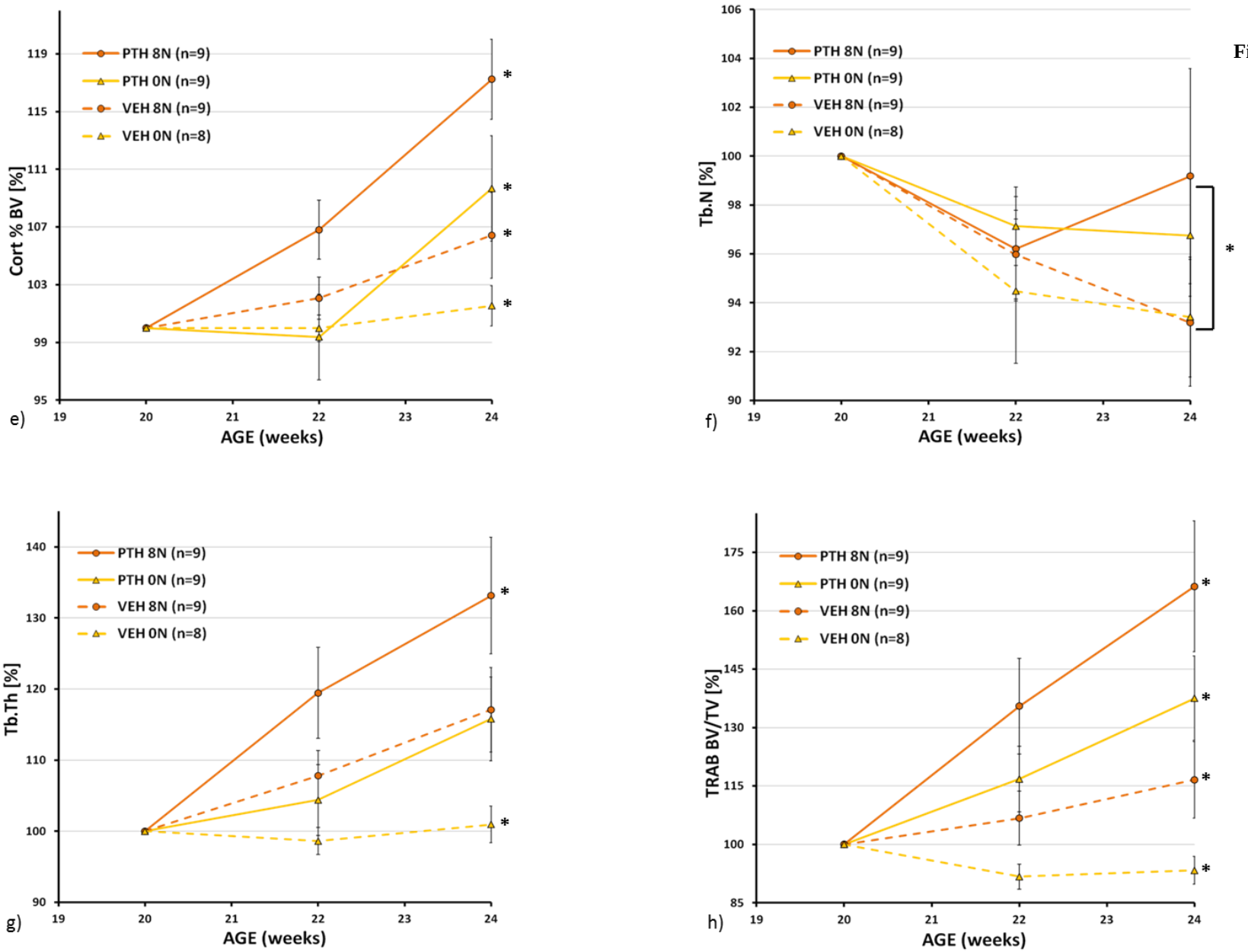

Figure 21: static parameters of PTH study from early loading experimental series. Measurements normalized to first measurement at beginning of loading period. a), b) parameters from full bone; c)-g) parameters from trabecular compartment; h), I) cortical parameters

Early loading – dynamic parameters

Bone formation

Vehicle treated non-loaded mice had a bone formation rate of 1.1 ± 0.2 %/d. Loading increased this rate significantly to 1.6 ± 0.4 %/d during the first two weeks of the observation period. A small drop of BFR during the last two weeks could be observed, however, there was still a clear trend towards a higher BFR compared to VEH 0N animals. PTH treatment increased BFR up to 2.3 ± 0.6 %/d. This is significantly higher than in loaded animals. Combination of PTH treatment and loading increased it even up to 3.6 ± 0.8 %/d during the first two weeks of the observation period, representing the highest BFR of the study. However, during the last two weeks the rate fell down to 2.0± 0.2 %/d and was at a similar level as in PTH 0N animals. (Figure 22a)

Mineral apposition rate was at 1.3 ± 0.1 µm per day in VEH 0N animals. Loading increased this rate significantly to 1.4 ± 0.1 µm per day during the first two weeks, however had no effect during the last two weeks. PTH treatment resulted in a significantly higher MAR than loading during the entire observation period. With 1.8 ± 0.1 µm per day combined loading and PTH treatment induced the significantly highest MAR of the entire study. However, the effect of loading fades away during the second half of the observation period as in the loaded vehicle treated group. Hence, similar values as for PTH 0N animals could be observed. (Figure 22b)

The mineralizing surface in VEH 0N animals covered between 38.0 ± 2.3 % and 40.6 ± 1.6%. The portion of MS was increased in the following order: loading induced the smallest increase, followed by PTH treatment. The combination of PTH treatment and loading resulted in the significantly highest MS of 68.9 ± 4.0 % of the entire study. (Figure 22c)

Hence, PTH and loading exert their effects on both MAR and MS and therefore increase bone formation rate.

Bone resorption

Bone resorption rate was highest in VEH 0N animals with 1.7 ± 0.4 %/d during the first two weeks and 1.2 ± 0.2 %/d during the last two weeks of the observation study. Loading decreased bone resorption to 1.2 ± 0.3 %/d at the beginning and 0.6 ± 0.2 %/d at the end of the study. Similar values were observed in the PTH treated group. Combining PTH treatment and loading reduced bone resorption rate significantly during the first two weeks of the study compared to any other group. However, during the last two weeks, similar values for all three

treated groups (loading, PTH treatment, PTH treatment plus loading) were observed. All values were significantly lower than in the non-treated group. (Figure 22d)

During the first two weeks, mineral resorption rate ranged between 1.8 to 1.9 µm per day for all groups. However, PTH treatment increased mineral resorption rate with a delay. This could be expected, as the physiologic function of PTH is to increase blood calcium levels by increasing bone resorption. Loading in combination with PTH treatment increased the rise in MRR significantly. (Figure 22e)

Eroded surface was highest in VEH 0N animals. It reached values of 32.1 ± 2.7 % to 33.7 ± 1.9 %. Both, loading and PTH treatment, reduced the amount of eroded surface to a similar extend (27.7 ± 5.0 % to 28.8 ± 4.6 % during the first two weeks and 23.6 ± 4.0 % to 21.6 ± 4.2 % during the last two weeks). PTH treatment in combination with loading decreased ES significantly to 17.9 ± 5.6 % during the first two weeks of the observation period. However, as observed for BRR, during the last two weeks of the study no differences were observed between loaded, PTH treated or PTH treated and loaded animals. (Figure 22f)

While BFR was influenced by both MAR and MS, the effect of PTH and loading on BRR was mainly due to the effect on the amount of eroded surface. Although PTH treatment in combination with loading even increased MRR significantly compared to vehicle treated animals, this was compensated by a significantly lower ES resulting in an overall lower bone resorption rate than in vehicle treated non-loaded animals.

The values of the dynamic parameters can be seen in Table 12.

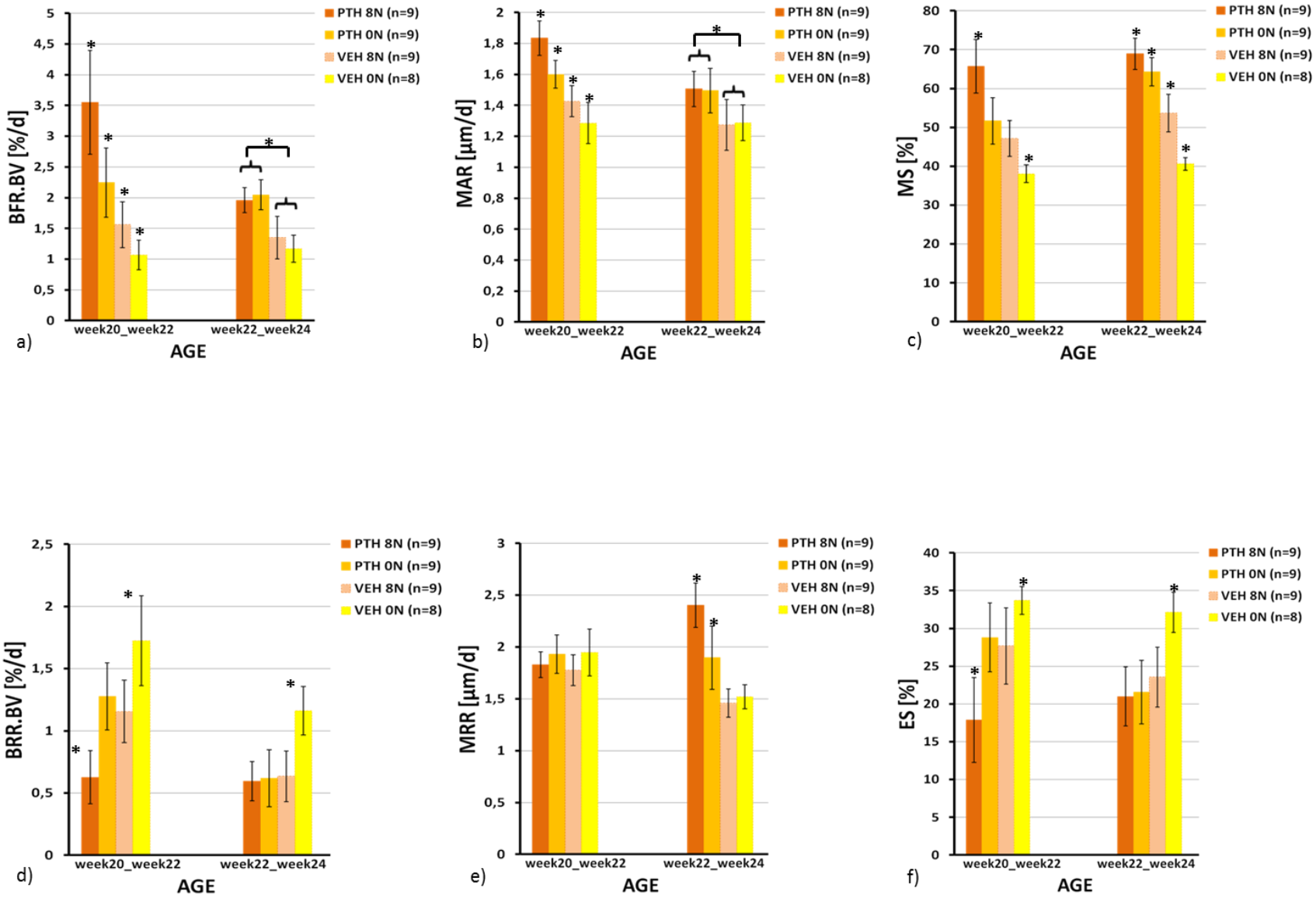

Figure 22: dynamic parameters of PTH study in early loading experimental series. Upper row shows bone formation parameters, lower row shows bone resorption parameters

Late loading – static parameters

Figure 23 shows overlaid CT images representing the loading period for each group. While a deteriorated bone structure can be observed in the VEH 0N group, it can be seen that both loading and PTH treatment improve the bone structure. The largest amount of bone formation can be found in the PTH 8N group.

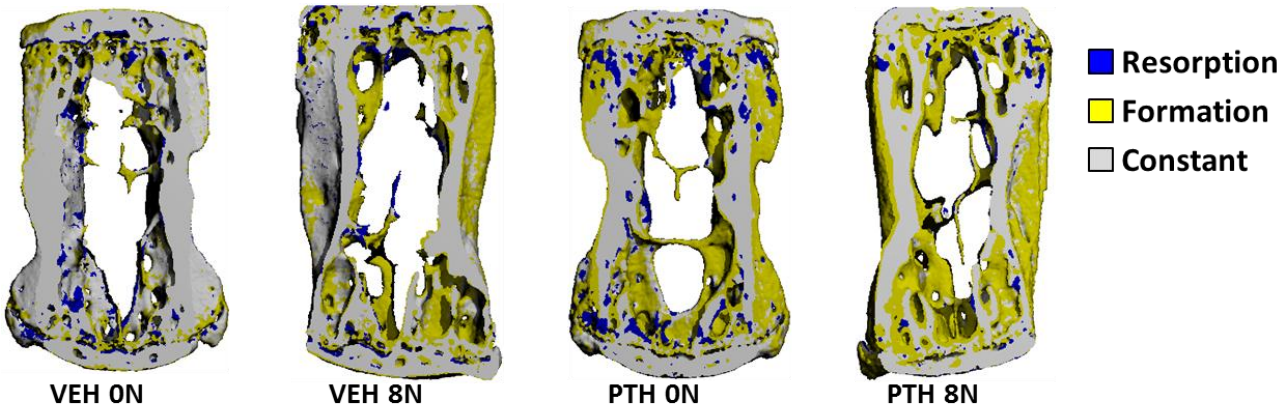

Figure 23: Visualization of bone development during 4 weeks of loading period. CT images of week 26 and 30 are overlaid and registered. Blue represents resorbed bone, yellow newly formed bone and grey constant bone.

VEH 0N (n=8)

The developments of static parameters in the VEH 0N group are comparable to those from the OVX 0N group of the ovariectomy and loading study. Total volume did not change during the observation period, while full bone volume fraction increased by 7.0 % from 3.8 ± 0.3 mm³ to 4.0 ± 0.3 mm³ (Figure 24b). This resulted in a 5.4 % greater full bone volume density at the end of the observation period (Figure 24c). Both, cortical thickness and cortical % BV did not change during the study (Figure 24d, e). As already seen in the ovariectomy study, the loss of trabeculae continues to a small extend and by the end of the study Tb.N. was reduced by 2.1 % (Figure 24f). This loss was compensated by a thickening of 4.5 % from of the remaining trabeculae (Figure 24g). Therefore trabecular bone volume density was increased, as well, by 11.2 % (Figure 24h).

VEH 8N (n=9)

Also loading did not change the total volume of the bone. Bone volume was increased by 13.4 % from 3.8 ± 0.3 mm³ to 4.3 ± 0.2 mm³ (Figure 24b). This resulted in a significantly higher increase of full bone volume fraction by 11.7 % (Figure 24c). On one hand this was due to the thickening of the cortex by 5.0 % from 130.8 ± 4.5 µm to 137.33 ± 3.8 µm (Figure 24d) and the consequently increase in cortical % BV by 8.0 % (Figure 24e). On the other hand, although loss of trabeculae could not be stopped, the thickening of trabeculae by 14.6 %

from 63.8 ± 3.1 µm to 73.1 ± 3.8 µm (Figure 24g) improved trabecular bone volume density by 24.1 % (Figure 24h), which contributed to the higher Full BV/TV as well.

PTH 0N (n=9)

PTH treatment increased total volume only slightly by 3.7 % from 8.8 ± 0.5 mm³ to 9.1 ± 0.6 mm³ (Figure 24a). The effect of PTH on full bone volume fraction was stronger than the effect of loading. After 4 weeks of treatment it was increased by 19.5 % (Figure 24b). Hence, also the rise of 15.2 % in full bone volume density was higher than in loaded animals (Figure 24c). The fact that PTH treatment has a stronger effect than loading was not observed for cortical thickness, which did not change at all during the treatment period. However, the increase of 13.3 % in cortical % BV was higher than in the loaded group (Figure 24e). As it was already observed in the early loading experimental series, PTH treatment seems to stop the on-going loss of trabeculae (Figure 24f) and enhance the thickening of all trabeculae. After 4 weeks of treatment trabecular thickness increased from 62.0 ± 2.8 µm to 74.3 ± 2.7 µm, which is an increase by 20.0 % (Figure 24g). Because no trabeculae were lost and mean thickness increased, trabecular bone volume density increased significantly by 48.4 % (Figure 24h).

PTH 8N (n=11)

Also the combination of PTH and loading increased the total volume only by 4.8 % (Figure 24a). However, bone volume was increased by 30.7 % from 3.9 ± 0.5 mm³ to 5.0 ± 0.3 mm³ (Figure 24b). This shows the synergistic effect of the combined PTH treatment and mechanical loading. The combination of both also revealed a synergistic effect on Full BV/TV, which was increased significantly by 26.67 % by the end of the study (Figure 24c). While only PTH treatment did not have an effect on cortical thickness, loading of PTH treated animals revealed synergistic effects as Ct. Th. was increased by 8.3 % from 131 ± 5.6 µm to 142 ± 5.0 µm (Figure 24d). This resulted in a 22.2 % greater cortical % BV (Figure 24e). As already observed in the early loading study, PTH treatment stops the loss of trabeculae (Figure 24f). This effect was not influenced by loading in PTH treated animals. However, the combined PTH treatment and loading displayed their synergistic effect also for trabecular thickness. After 4 weeks trabeculae were thickened by 35.1 %, which was an increase from 64.0 ± 3.0 µm to 86.4 ± 5.3 µm (Figure 24h). Since trabeculae did not vanish but got thicker, trabecular bone volume density was increasing significantly as well by 61.5 % (Figure 24h).

Absolute values of the PTH study can be seen in Table 10. Values normalized to week 26 are shown in Table 11.

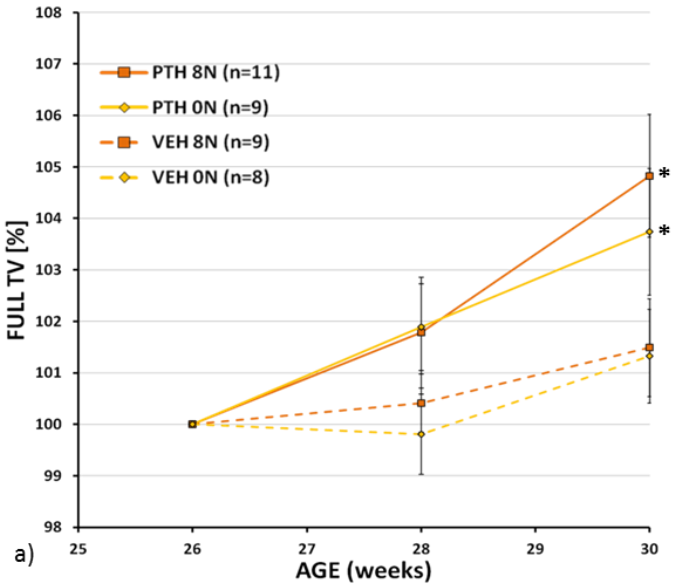
PTH 8N (n=11)
PTH 0N (n=9)
VEH 8N (n=9)
VEH 0N (n=8)
FULL TV [%]
AGE (weeks)
a)

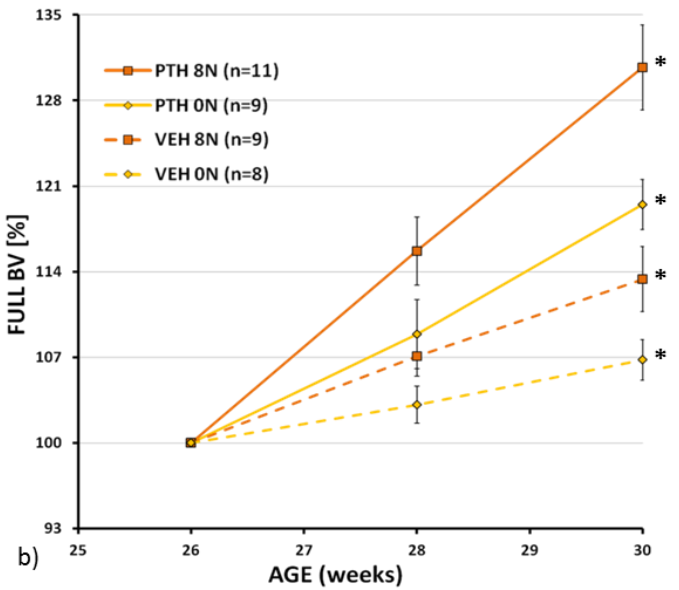
PTH 8N (n=11)
PTH 0N (n=9)
VEH 8N (n=9)
VEH 0N (n=8)
FULL BV [%]
AGE (weeks)
b)

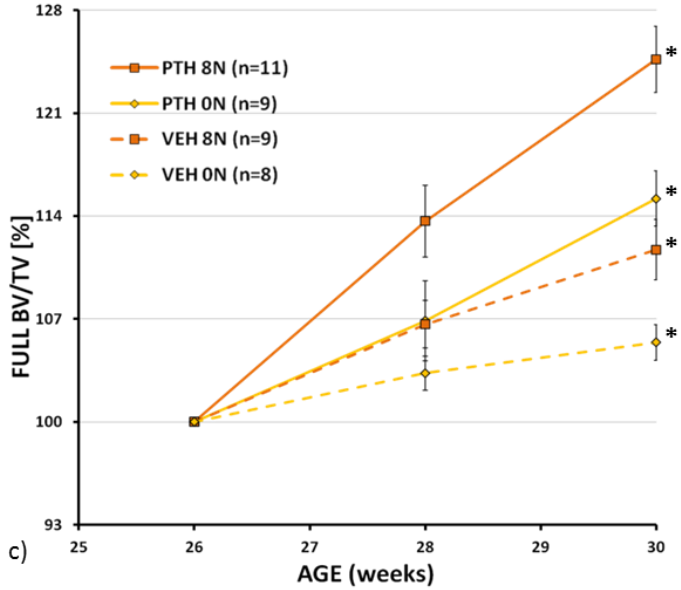
PTH 8N (n=11)
PTH 0N (n=9)
VEH 8N (n=9)
VEH 0N (n=8)
FULL BV/TV [%]
AGE (weeks)
c)

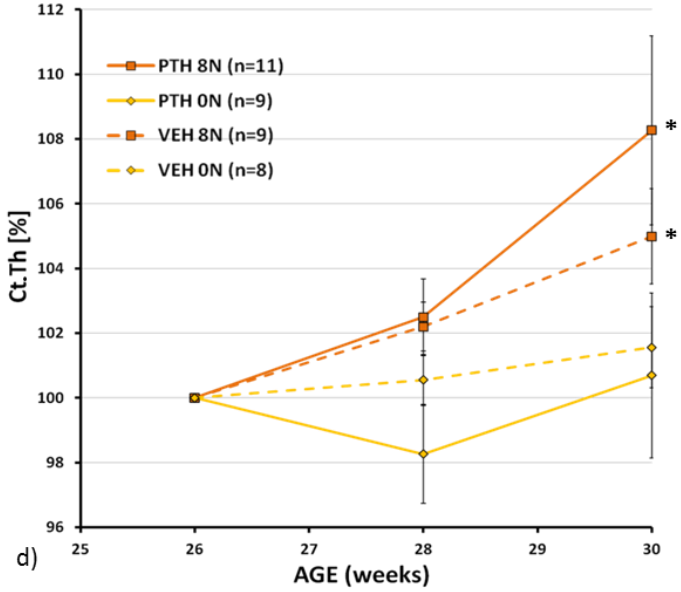
PTH 8N (n=11)
PTH 0N (n=9)
VEH 8N (n=9)
VEH 0N (n=8)
Ct.Th [%]
AGE (weeks)
d)

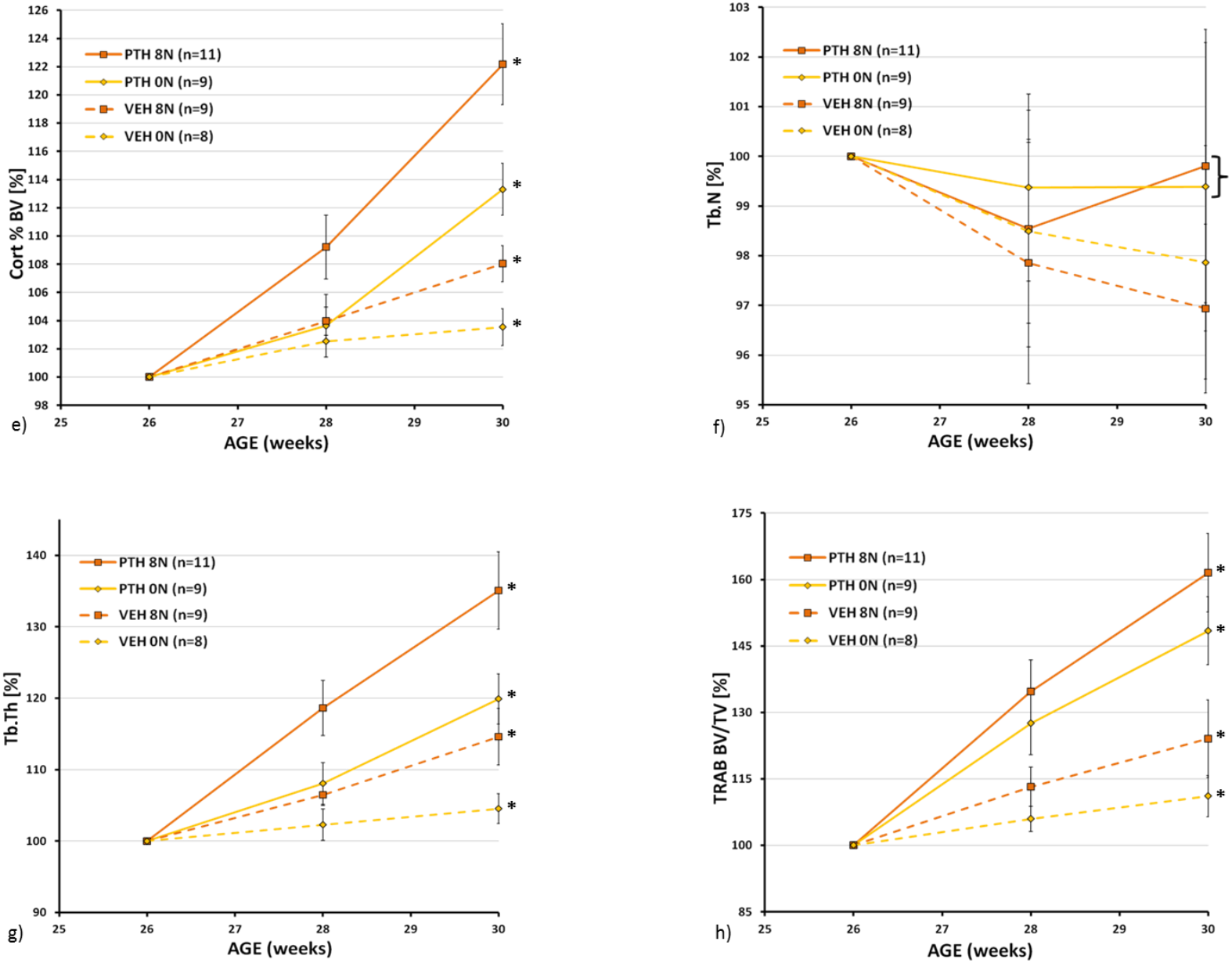

Figure 24: static parameters of PTH study from late loading experimental series. Measurements normalized to first measurement at beginning of loading period. a), b) parameters from full bone; * c)-g) parameters from trabecular compartment; h), I) cortical parameters

Late loading – dynamic parameters

Bone formation

Vehicle treated non-loaded animals showed the significantly lowest bone formation rate during the entire study. It was 1.8 ± 0.2 %/d during the first two weeks and dropped to 1.0 ± 0.4 %/d during the last two weeks of the observation period. Loading increased bone formation rate to 2.7 ± 0.5 %/d during the first two weeks. Again a drop was observed in the last two weeks of the observation period resulting in a similar bone formation rate as VEH 0N animals. Treating animals with PTH significantly increased bone formation rate to 4.9 ± 0.5 %/d and when loading was added it even reached 6.1 ± 0.6 %/d at the beginning of the study. Again in both groups a drop during the last two weeks was observed and the PTH 0N and PTH 8N group were not significantly different anymore. (Figure 25a)

With 1.4 ± 0.1 µm/d MAR was lowest in VEH 0N mice and with 2.3 ± 0.1 µm/d highest in PTH 8N animals. Again a drop was observed in all groups during the last two weeks and while there were tendencies towards a higher MAR in the loaded groups compared to the non-loaded, no significant differences were observed between the two vehicle treated groups and the PTH treated groups, respectively. (Figure 25b)

The mineralizing surface ranged in the first two weeks between 49.7 ± 2.4 % in the VEH 0N group and 77.4 ± 4.7 % in the PTH 8N group. Again a drop was observed for all groups during the last two weeks. However, mineralizing surface was significantly higher in the loaded groups throughout the entire study. (Figure 25c)

Hence, while PTH seems to have influenced both MAR and MS, loading only exerted the strongest effect on MS.

Bone resorption

Bone resorption rate was highest in VEH 0N animals. It reached 1.0 ± 0.2 %/d during the first two weeks and dropped to 0.8 ± 0.3 %/d during the last two weeks of the study. Loading decreased the rate significantly to 0.7 ± 0.2 %/d at the beginning and 0.5 ± 0.3 %/d at the end of the study. Interestingly, PTH treatment alone did not influence bone resorption significantly with 0.9 ± 0.2 %/d and 0.6 ± 0.2 %/d bone resorption rate was comparable to the VEH 0N group. Again loading induced a significant decrease. PTH treated, loaded animals had a bone resorption rate of 0.6 ± 0.2 %/d which dropped to 0.4 ± 0.1 %/d at the end of the study. (Figure 25d)

Mineral resorption rate was at 1.8 ± 0.3 µm/d and dropped to 1.3 ± 0.2 µm/d in the VEH 0N group. Loading decreased MRR only marginally to 1.7 ± 0.2 µm/d during the first two weeks of the study. A drop during the last two weeks was observed in the VEH 8N group as well. Interestingly PTH treatment increased MRR to 2.4 ± 0.3 µm/d and 2.1 ± 0.3 µm/d, respectively. This is expected when the physiological function of PTH is taken into consideration, which is to increase the calcium levels in the blood. To do so, bone has to be resorbed and calcium is released from the storages within the bone. Loading in combination with PTH treatment even enhanced MRR to a small extend. PTH 8N mice had a MRR of 2.5 ± 0.3 µm/d and 2.2 ± 0.4 µm/d, respectively. (Figure 25e)

Eroded surface showed a similar pattern as bone resorption rate. The largest amount of eroded surface could be found in VEH 0N animals. It was 24.6 ± 1.9 % during the first two weeks of the observation period and covered 30.3 ± 4.9 % by the end of the observation period. Loading reduced the amount covered by eroded surface significantly to 19.1 ± 3.9 % and 23.1 ± 6.0 %, respectively. In contrast to bone resorption rate, PTH treatment did reduce eroded surface to similar values as in loaded animals. When loading was combined with PTH treatment significantly less bone was covered by eroded surface. The amount was 12.5 ± 3.2 % at the beginning of the observation period and 17.5 ± 2.8 % at the end. (Figure 25f)

Hence the reduction of eroded surface compensated for the increased mineral resorption rate and still resulted in a reduced bone resorption rate when mice were loaded or treated with PTH or the combination of both.

The values of the dynamic parameters for the late loading experimental series are shown in Table 12.

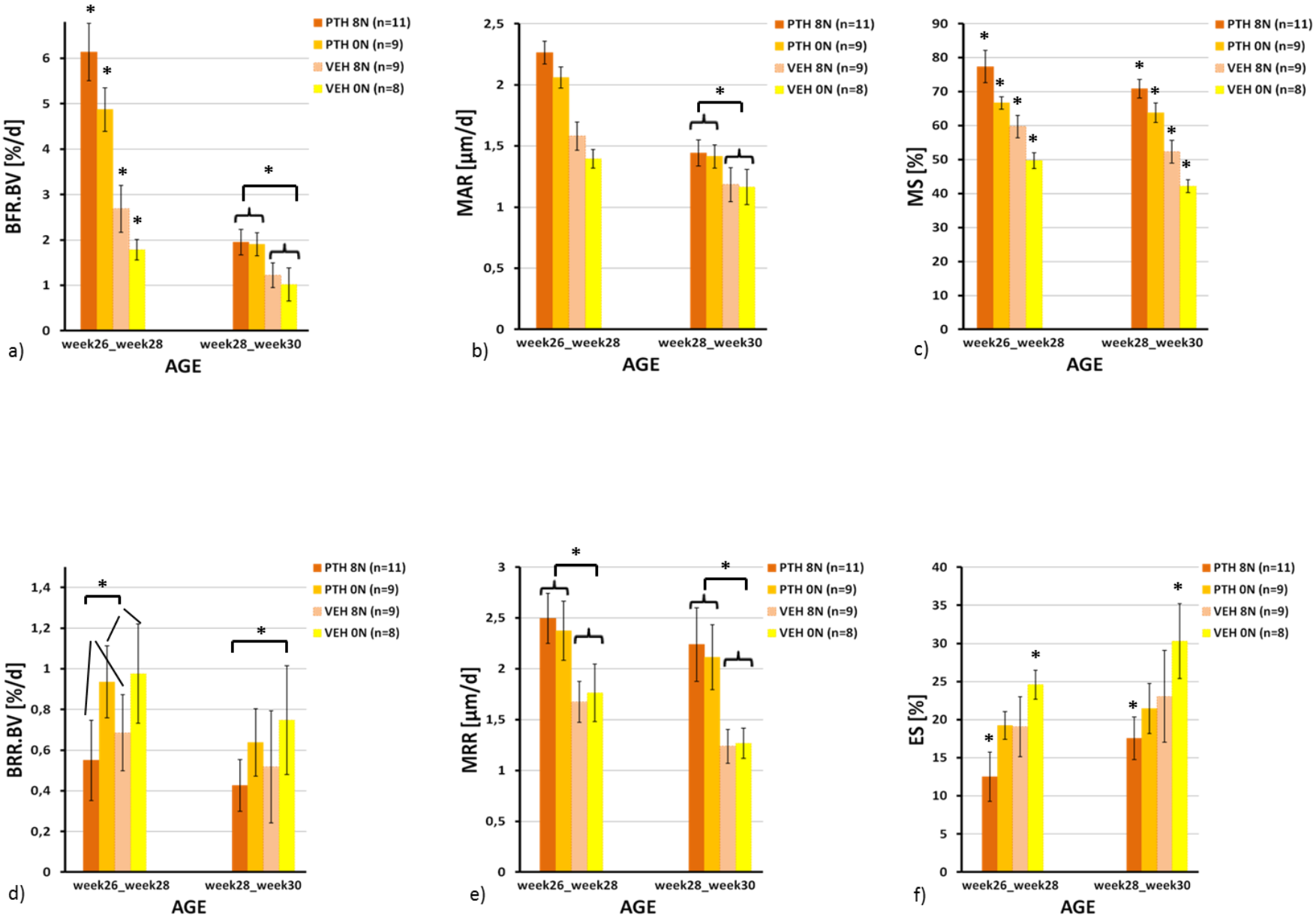

Figure 25: dynamic parameters of PTH study in late loading experimental series. Upper row shows bone formation parameters, lower row shows bone resorption parameters

Parameter group	Full TV [mm³]	Full BV [mm³]	Full BV/TV [%]	Ct.Th [µm]	cort % BV [%]	Tb.N [1/mm]	Tb.Th [µm]	Trab BV/TV [%]
early loading								
VEH 0N								
15 weeks	7.5 ± 0.2	3.9 ± 0.2	52.6 ± 2.5	144.5 ± 8.0	38.8 ± 2.5	2.9 ± 0.1	77.7 ± 3.3	18.5 ± 1.7
20 weeks	8.2 ± 0.4	3.8 ± 0.2	45.8 ± 2.1	139.8 ± 5.3	34.2 ± 2.2	2.9 ± 0.2	66.8 ± 2.5	14.0 ± 1.0
22 weeks	8.3 ± 0.4	3.8 ± 0.2	45.9 ± 2.2	138.4 ± 5.6	34.2 ± 2.3	2.7 ± 0.2	65.9 ± 2.5	12.8 ± 0.8
24 weeks	8.4 ± 0.3	3.9 ± 0.2	46.6 ± 2.2	139.2 ± 5.2	34.8 ± 2.1	2.7 ± 0.2	67.4 ± 2.9	13.0 ± 0.6
VEH 8N								
15 weeks	7.5 ± 0.4	3.8 ± 0.2	50.7 ± 2.1	137.5 ± 5.9	36.4 ± 2.1	3.1 ± 0.2	77.6 ± 4.1	19.1 ± 2.5
20 weeks	8.4 ± 0.4	3.8 ± 0.2	45.4 ± 1.6	135.9 ± 4.4	33.5 ± 1.3	3.0 ± 0.2	67.3 ± 3.2	14.8 ± 1.8
22 weeks	8.5 ± 0.4	4.1 ± 0.2	48.4 ± 1.0	137.0 ± 3.8	34.2 ± 1.1	2.9 ± 0.2	72.4 ± 2.7	15.7 ± 1.5
24 weeks	8.6 ± 0.4	4.4 ± 0.2	50.6 ± 0.9	140.4 ± 3.4	35.6 ± 1.0	2.8 ± 0.2	78.6 ± 2.7	17.1 ± 1.3
PTH 0N								
15 weeks	7.5 ± 0.4	3.9 ± 0.3	52.0 ± 4.3	143.5 ± 9.6	38.0 ± 3.3	3.0 ± 0.2	77.8 ± 6.4	18.9 ± 2.9
20 weeks	8.2 ± 0.5	3.7 ± 0.3	45.8 ± 3.2	139.5 ± 9.0	34.4 ± 3.0	2.9 ± 0.2	65.4 ± 3.4	14.0 ± 1.6
22 weeks	8.4 ± 0.5	4.0 ± 0.3	47.4 ± 3.1	133.4 ± 7.6	34.2 ± 2.8	2.8± 0.2	68.2 ± 4.2	16.3 ± 1.7
24 weeks	8.6 ± 0.5	4.4 ± 0.3	51.6 ± 3.6	137.0 ± 6.4	37.7 ± 3.0	2.8 ± 0.2	75.7 ± 4.9	19.2 ± 2.4
PTH 8N								
15 weeks	7.5 ± 0.5	3.8 ± 0.2	51.2 ± 2.6	136.8 ± 5.0	36.6 ± 2.0	3.1 ± 0.2	75.1 ± 4.2	19.3 ± 2.3
20 weeks	8.2 ± 0.5	3.7 ± 0.2	45.0 ± 2.0	134.6 ±3.4	33.2 ± 1.4	3.0 ± 0.2	63.6 ± 2.8	14.2 ± 1.8
22 weeks	8.5 ± 0.4	4.3 ± 0.1	50.7 ± 1.9	135.6 ± 3.8	35.4 ± 1.7	2.9 ± 0.2	75.9 ± 3.2	19.1 ± 1.4
24 weeks	8.8 ± 0.4	4.8 ± 0.2	54.7 ± 1.3	141.0 ± 3.3	38.9 ± 1.4	3.0 ± 0.3	84.5 ± 3.7	23.4 ± 2.0
late loading								
VEH 0N								
15 weeks	7.7 ± 0.4	4.2 ± 0.2	54.6 ± 2.5	149.1 ± 8.7	40.4 ± 2.9	3.0 ±0.2	76.2 ± 4.0	18.9 ± 1.8
26 weeks	8.6 ± 0.4	3.8 ± 0.3	43.9 ± 1.8	130.7 ± 7.3	32.2 ± 2.0	2.8 ± 0.2	63.3 ± 2.8	12.0 ± 1.2
28 weeks	8.6 ± 0.3	3.9 ± 0.3	45.3 ± 2.0	131.4 ± 7.6	33.0 ± 2.1	2.7 ± 0.2	64.7 ± 3.5	12.8 ± 1.3
30 weeks	8.7 ± 0.3	4.0 ± 0.3	46.2 ± 1.6	132.7 ± 7.4	33.3 ± 1.8	2.7 ± 0.2	66.1 ± 3.0	13.3 ± 1.0
VEH 8N								
15 weeks	7.6 ± 0.6	4.1 ± 0.5	53.8 ± 3.5	147.1 ± 10.4	39.7 ± 2.9	3.0 ± 0.2	74.7 ± 6.3	18.7 ± 3.1
26 weeks	8.6 ± 0.6	3.8 ± 0.3	44.2 ± 1.7	130.8 ± 4.5	32.3 ± 1.4	2.7 ± 0.3	63.8 ± 3.1	12.5 ± 1.1
28 weeks	8.6 ± 0.6	4.1 ± 0.2	47.1 ± 1.6	133.7 ± 4.4	33.6 ± 1.4	2.7 ± 0.3	67.9 ± 3.2	14.2 ± 1.2
30 weeks	8.7 ± 0.6	4.3 ± 0.2	49.4 ± 1.4	137.3 ± 3.8	34.9 ± 1.5	2.6 ± 0.3	73.1 ± 3.8	15.5 ± 1.2
PTH 0N								
15 weeks	7.8 ± 0.4	4.4 ± 0.3	57.1 ± 3.6	154.5 ± 11.7	41.9 ± 3.7	3.1 ± 0.2	79.0 ± 5.1	21.8 ± 3.0
26 weeks	8.8 ± 0.5	3.8 ± 0.3	43.7 ± 2.0	131.3 ± 4.3	31.5 ± 1.7	2.8 ± 0.2	62.0 ± 2.8	12.6 ± 1.5
28 weeks	8.9 ± 0.5	4.2 ± 0.2	46.7 ± 1.8	129.0 ± 3.8	32.7 ± 1.5	2.8 ± 0.2	67.0 ± 2.8	16.0 ± 2.0
30 weeks	9.1 ± 0.6	4.6 ± 0.3	50.3 ± 1.8	132.2 ± 3.7	35.7 ± 1.7	2.8 ± 0.2	74.3 ± 2.7	18.6 ± 1.9
PTH 8N								
15 weeks	7.8 ± 0.5	4.2 ± 0.3	54.2 ± 1.9	147.2 ± 5.3	39.7 ± 1.4	3.0 ± 0.3	76.6 ± 3.7	19.6 ± 2.2
20 weeks	8.8 ± 0.5	3.9 ± 0.3	43.7 ± 1.7	131.0 ± 5.6	31.6 ± 1.6	2.8 ± 0.2	64.0 ± 2.9	13.2 ± 1.5
22 weeks	9.0 ± 0.5	4.5 ± 0.3	49.7 ± 1.7	134.2 ± 5.0	34.5 ± 1.8	2.7 ± 0.2	75.9 ± 4.6	17.7 ± 1.5
24 weeks	9.2 ± 0.5	5.0 ± 0.3	54.5 ± 1.8	141.7 ± 5.0	38.6 ± 1.7	2.8 ± 0.2	86.4 ± 5.3	21.2 ± 1.9

Table 10: absolute values of static parameters of PTH studies in early and late loading experimental series. Expressed as mean ± standard deviation

Parameter group	Full TV [%]	Full BV [%]	Full BV/TV [%]	Ct.Th [%]	cort % BV [%]	Tb.N [%]	Tb.Th [%]	Trab BV/TV [%]
early loading								
VEH 0N								
20 weeks	100.0	100.0	100.00	100.00	100.00	100.00	100.00	100.00
22 weeks	101.4 ± 0.5	101.8 ± 0.9	100.3 ± 0.8	99.0 ± 0.8	100.0 ± 0.9	94.5 ± 3.0	98.6 ± 1.9	91.7 ± 3.2
24 weeks	102.5 ± 1.0 a)b)	104.4 ± 1.2 a)b)c)	101.9 ± 1.2 a)b)c)	99.6 ± 1.0 a)c)	101.5 ± 1.4 a)b)c)	93.4 ± 2.5 a)b)	101.0 ± 2.6 a)b)c)	93.3 ± 3.6 a)b)c)
VEH 8N								
20 weeks	100.0	100.0	100.00	100.00	100.00	100.00	100.00	100.00
22 weeks	101.8 ± 0.7	108.5 ± 2.6	106.6 ± 2.1	100.8 ± 1.0	102.1 ± 1.5	96.0 ± 1.8	107.8 ± 3.6	106.7 ± 6.9
24 weeks	103.1 ± 1.0 a)b)	115.1 ± 4.2 a)b)d)	111.5 ± 3.1 a)d)	103.3 ± 1.7 b)d)	106.4 ± 3.0 a)b)d)	93.2 ± 2.6 a)b)	117.1 ± 6.0 a)d)	116.6 ± 9.8 a)b)d)
PTH 0N								
20 weeks	100.0	100.0	100.00	100.00	100.00	100.00	100.00	100.00
22 weeks	103.0 ± 0.4	106.7 ± 3.4	103.6 ± 3.2	95.7 ± 2.2	99.4 ± 3.0	97.1 ± 1.6	104.4 ± 5.0	116.8 ± 8.4
24 weeks	105.4 ± 0.6 a)c)d)	118.9 ± 4.6 a)c)d)	112.8 ± 4.9 a)d)	98.4 ± 3.3 a)c)	109.7 ± 3.7 a)c)d)	96.8 ± 2.5 c)d)	115.8 ± 5.9 a)d)	137.5 ±10.9 a)c)d)
PTH 8N								
20 weeks	100.0	100.0	100.00	100.00	100.00	100.00	100.00	100.00
22 weeks	103.5 ± 0.8	116.6 ± 3.0	112.6 ± 2.7	100.8 ± 1.4	106.8 ± 2.0	96.2 ± 2.1	119.5 ± 6.4	135.5 ± 12.3
24 weeks	107.1 ± 1.5 b)c)d)+)	130.3 ± 3.4 b)c)d)+)	121.7 ± 3.0 b)c)d)+)	104.8 ± 1.5 b)d)+)	117.2 ± 2.8 b)c)d)+)	99.2 ± 4.4 c)d)+)	133.1 ± 8.2 b)c)d)+)	166.3 ±16.8 b)c)d)+)
late loading								
VEH 0N								
26 weeks	100.0	100.0	100.00	100.00	100.00	100.00	100.00	100.00
28 weeks	99.8 ± 0.8	103.1 ± 1.5	103.3 ± 1.2	100.6 ± 0.8	102.5 ± 1.1	98.5 ± 1.9	102.3 ± 2.2	106.0 ± 2.8
30 weeks	101.3 ± 0.9 a)b)	106.8 ± 1.6 a)b)c)	105.4 ± 1.2 a)b)c)	101.6 ± 1.3 a)c)	103.5 ± 1.3 a)b)c)	97.9 ± 2.4	104.5 ± 2.1 a)b)c)	111.2 ± 4.7 a)b)c)
VEH 8N								
26 weeks	100.0	100.0	100.00	100.00	100.00	100.00	100.00	100.00
28 weeks	100.4 ± 0.6	107.1 ± 1.6	106.6 ± 1.6	102.2 ± 0.8	104.0 ± 1.0	97.9 ± 2.4	106.5 ± 1.5	113.2 ± 4.4
30 weeks	101.5 ± 1.0 a)b)	113.4 ± 2.7 a)b)d)	111.7 ± 2.0 a)b)d)	105.0 ± 1.5 a)b)d)	108.0 ± 1.3 a)b)d)	96.9 ± 1.7 a)b)	114.6 ± 4.0 a)b)d)	124.1 ± 8.8 a)b)d)
PTH 0N								
26 weeks	100.0	100.0	100.00	100.00	100.00	100.00	100.00	100.00
28 weeks	101.9 ± 0.8	108.9 ± 2.8	106.9 ± 2.7	98.3 ± 1.5	103.7 ± 2.2	99.4 ± 1.9	108.1 ± 2.9	127.6 ± 7.1
30 weeks	103.7 ± 1.2 a)c)d)	119.5 ± 2.1 a)c)d)	115.2 ± 1.9 a)c)d)	100.7 ± 2.6 a)c)	113.3 ± 1.8 a)c)d)	99.4 ± 2.9 c)	119.9 ± 3.5 a)c)d)	148.4 ± 7.7 a)c)d)
PTH 8N								
26 weeks	100.0	100.0	100.00	100.00	100.00	100.00	100.00	100.00
28 weeks	101.8 ± 1.1	115.7 ± 2.8	113.7 ± 2.4	102.5 ± 1.2	109.2 ± 2.3	98.5 ± 2.4	118.6 ± 3.9	134.8 ± 7.1
30 weeks	104.8 ± 1.2 b)c)d)+)	130.7 ± 3.5 b)c)d)#)	124.7 ± 2.2 b)c)d)#)	108.3 ± 2.9 b)c)d)#)	122.2 ± 2.9 b)c)d)#)	99.8 ± 2.8 c)+)	135.1 ± 5.4 b)c)d)#)	161.5 ± 8.9 b)c)d)+)

Table 11: static parameters of PTH studies of early and late loading experimental series normalized to beginning of loading period. a) Significant to PTH 8N, b) significant to PTH 0N, c) significant to VEH 8N, d) significant to VEH 0N for each study, +) combined effect of PTH and loading is additive, #) combined effect of PTH and loading is synergistic; values are presented as mean ± standard deviation

Parameter group	BFR.BV [%/d]	MAR [µm/d]	MS [%]	BRR.BV [%/d]	MRR [µm/d]	ES [%]
early loading						
VEH 0N						
wk20_wk22	1.1 ± 0.2 a)b)c)	1.3 ± 0.1 a)b)c)	38.1 ± 2.3 a)b)c)	1.7 ± 0.4 a)b)c)	2.0 ± 0.2	33.7 ± 1.9 a)b)c)
wk22_wk24	1.2 ± 0.2 a)b)	1.3 ± 0.1 a)b)	40.6 ± 1.6 a)b)c)	1.2 ± 0.2 a)b)c)	1.5 ± 0.1 a)b)	32.1 ± 2.7 a)b)c)
VEH 8N						
wk20_wk22	1.6 ± 0.4 a)b)d)	1.4 ± 0.1 a)b)d)	47.1 ± 4.6 a)d)	1.2 ± 0.3 a)d)	1.8 ± 0.2	27.7 ± 5.0 a)d)
wk22_wk24	1.4 ± 0.4 a)b)	1.3 ± 0.2 a)b)	53.7 ± 4.8 a)b)d)	0.6 ± 0.2 d)	1.5 ± 0.1 a)b)	23.6 ± 4.0 d)
PTH 0N						
wk20_wk22	2.3 ± 0.6 a)c)d)	1.6 ± 0.1 a)c)d)	51.7 ± 6.0 a)d)	1.3 ± 0.3 a)d)	1.9 ± 0.2	28.8 ± 4.6 a)d)
wk22_wk24	2.1 ± 0.2 c)d)	1.5 ± 0.1 c)d)	64.3 ± 3.6 a)c)d)	0.6 ± 0.2 d)	1.9 ± 0.3 a)c)d)	21.6 ± 4.2 d)
PTH 8N						
wk20_wk22	3.6 ± 0.8 b)c)d)	1.8 ± 0.1 b)c)d)	65.7 ± 6.9 b)c)d)	0.6 ± 0.2 b)c)d)	1.8 ± 0.1	17.9 ± 5.6 b)c)d)
wk22_wk24	2.0 ± 0.2 c)d)	1.5 ± 0.1 c)d)	68.9 ± 4.0 b)c)d)	0.6 ± 0.2 d)	2.4 ± 0.2 b)c)d)	21.0 ± 3.9 d)
late loading						
VEH 0N						
wk26_wk28	1.8± 0.2 a)b)c)	1.4± 0.1	49.7 ± 2.4 a)b)c)	1.0 ± 0.2 a)c)	1.8 ± 0.3 a)b)	24.6 ± 1.9 a)b)c)
wk28_wk30	1.0 ± 0.4 a)b)	1.2 ± 0.1 a)b)	42.1 ± 1.9 a)b)c)	0.8 ± 0.3 a)	1.3 ± 0.2 a)b)	30.3 ± 4.9 a)b)c)
VEH 8N						
wk26_wk28	2.7 ± 0.5 a)b)d)	1.6 ± 0.1	59.7 ± 3.3 a)b)d)	0.7 ± 0.2 b)d)	1.7 ±0.2 a)b)	19.1 ± 3.9 a)d)
wk28_wk30	1.2 ± 0.3 a)b)	1.2 ± 0.1 a)b)	52.3 ± 3.4 a)b)d)	0.5 ± 0.3	1.2 ± 0.2 a)b)	23.1 ± 6.0 a)d)
PTH 0N						
wk26_wk28	4.9 ± 0.5 a)c)d)	2.1 ± 0.1	66.7 ± 1.8 a)c)d)	0.9 ± 0.2 a)c)	2.4 ± 0.3 c)d)	19.2 ± 1.8 a)d)
wk28_wk30	1.9 ± 0.3 c)d)	1.4 ± 0.1 c)d)	63.8 ± 2.9 a)c)d)	0.6 ± 0.2	2.1 ± 0.3 c)d)	21.5 ± 3.3 a)d)
PTH8N						
wk26_wk28	6.1 ± 0.6 b)c)d)	2.3 ± 0.1	77.4 ± 4.7 b)c)d)	0.6 ± 0.2 b)d)	2.5 ± 0.3 c)d)	12.5 ± 3.2 b)c)d)
wk28_wk30	2.0 ± 0.3 c)d)	1.4 ± 0.1 c)d)	70.8 ± 2.7 b)c)d)	0.4 ± 0.1 d)	2.2 ± 0.4 c)d)	17.5 ± 2.8 b)c)d)

Table 12: bone dynamic parameters of PTH studies. a) significant to PTH 8N, b) significant to PTH 0N, c) significant to VEH 8N, d) significant to VEH 0N for each study; values are presented as mean ± standard deviation

4.4.2 Bisphosphonate study

At the beginning of the treatment period mice were injected once with the bisphosphonate zolendronate or 0.9 % NaCl, which served as a vehicle in these studies. Additionally all animals were subjected to 8N or 0N loading.

Early loading – static parameters

Figure 26 shows overlaid CT images representing the loading period for each group. While in the VEH 0N group bone loss continues, the amount of resorbed bone is reduced with bisphosphonate treatment. Loading increases bone formation in vehicle treated and bisphosphonate treated animals.

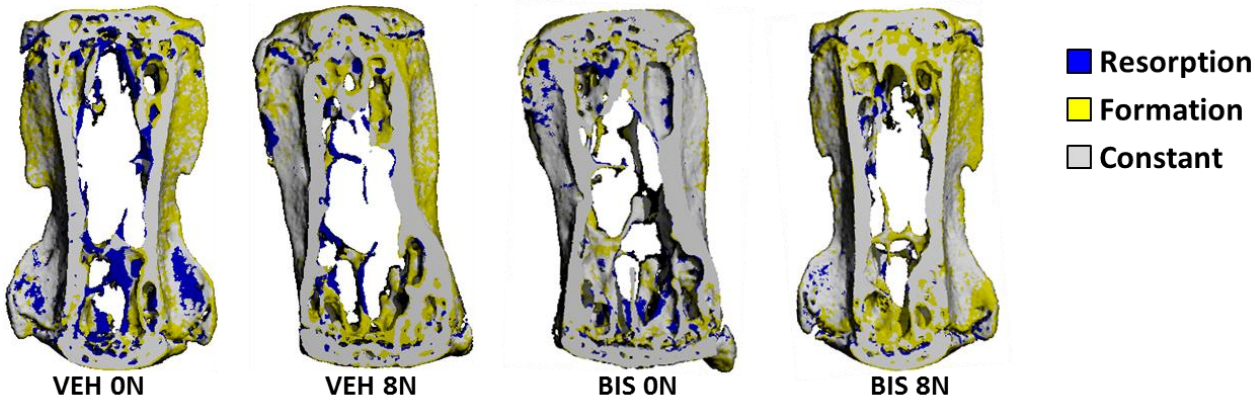

Figure 26: Visualization of bone development during 4 weeks of loading period. CT images of week 20 and 24 are overlaid and registered. Blue represents resorbed bone, yellow newly formed bone and grey constant bone.

VEH 0N (n=9)

In non-loaded vehicle treated mice a marginal increase of the total volume by 3.1 % from 8.3 ±0.4 mm³ to 8.6 ±0.4 mm³ was observed after 4 weeks (Figure 27a). However, bone volume fraction remained stable. The marginal bone growth together with a stable bone volume resulted in a negligible reduction of Full BV/TV by 1.3 % (Figure 27c). Both cortical parameters, Ct. Th and cortical % BV were as well slightly reduced by 2.9 % and 2.5 %, respectively (Figure 27d,e). While the on-going effect of estrogen depletion reduced trabecular number by 10.2 % (Figure 27f), thickness of the remaining trabeculae stayed stable (Figure 27g). Nevertheless, due to fewer trabeculae, trabecular bone volume density was decreased by 14.2 % (Figure 27h).

VEH 8N (n=8)

Total volume of loaded bones increased as well marginally by 3.0 % as it was observed in non-loaded animals (Figure 27a). However, loading increased bone volume fraction by 11.8 % from 4.0 ± 0.4 mm³ to 4.5 ± 0.3 mm³ (Figure 27b). Thus an 8.5 % greater bone volume density was observed after 4 weeks of loading (Figure 27c). The effect of loading on the cortical compartment was only small. The cortex thickened by 2.8 % from 143.4 ± 8.4 µm to 147.8 ± 5.4 µm (Figure 27d) and cortical % BV was increased by 4.2 % (Figure 27e). However, as already observed in the vehicle groups of the PTH study and the OVX 8N groups of the ovariectomy study, loading had a greater impact on the trabecular compartment. Although the loss of trabeculae could not be stopped, four weeks of loading increased the thickness of the remaining ones by 18.0 % from 67.5 ± 3.2 µm to 79.6 ± 2.8 µm (Figure 27g). This thickening resulted in a 12.1 % greater trabecular bone volume density (Figure 27h).

BIS 0N (n=9)

Similarly to the vehicle treated groups, a marginal increase by 2.3 % of the total volume was observed in the bisphosphonate treated group (Figure 27a). Both, the effect of bisphosphonate treatment on full bone volume fraction and full bone volume density were comparable to the effect of loading. Full BV is increased by 11.5 % and Full BV/TV is 9.0 % greater after 4 weeks of bisphosphonate treatment (Figure 27b,c). In the cortical compartment the impact of the antiresorptive drug was analogous to loading. The antiresorptive action could be observed nicely in the trabecular compartment. While in both vehicle groups loss of trabeculae continued, this was stopped with bisphosphonate treatment. The number of trabeculae remained stable at 2 per mm throughout the entire study (Figure 27f). Thickness of trabeculae is increased by only 5 % (Figure 27g). Although it is increased less than in loaded animals, as the quantity of trabeculae was preserved, bisphosphonate treatment resulted in a 14 % greater trabecular bone volume density than at the beginning of the study (Figure 27h).

BIS 8N (n=10)

Also combined loading and bisphosphonate treatment did not result in a higher total volume than in the other groups. However, both types of treatment had additive effects on bone volume fraction and full bone volume density. Full BV was increased by 18.8 % from 4.0 ± 0.2 mm³ to 4.7 ± 0.3 mm³ and Full BV/TV by 14.8 % (Figure 27b,c). Loading of bisphosphonate treated animals thickened the cortex similarly as loading of vehicle treated animals (by 3.3 %). However, both effects added onto each other for cortical % BV, which

was increased by 7.5 % (Figure 27e). Again bisphosphonate treatment preserved trabeculae and with the combined loading trabecular thickness was increased by 18.8 % (Figure 27f,g). Thus, thickening of trabeculae was comparable to loaded animals; however, as trabecular number was preserved it applied to a larger amount of trabeculae. Therefore the increase in trabecular bone volume of 27.0 % was significantly higher than in any other group of the study (Figure 27h).

Absolute values are shown in Table 13 and normalized values in Table 14.

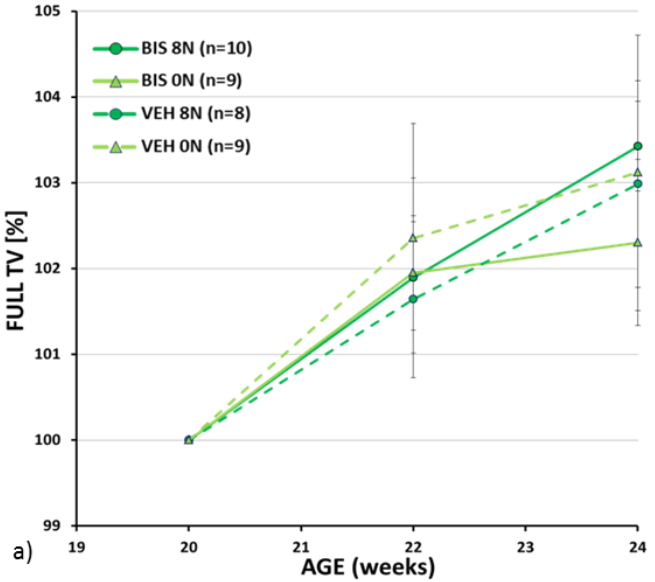
BIS 8N (n=10)
BIS 0N (n=9)
VEH 8N (n=8)
VEH 0N (n=9)
FULL TV [%]
AGE (weeks)
a)

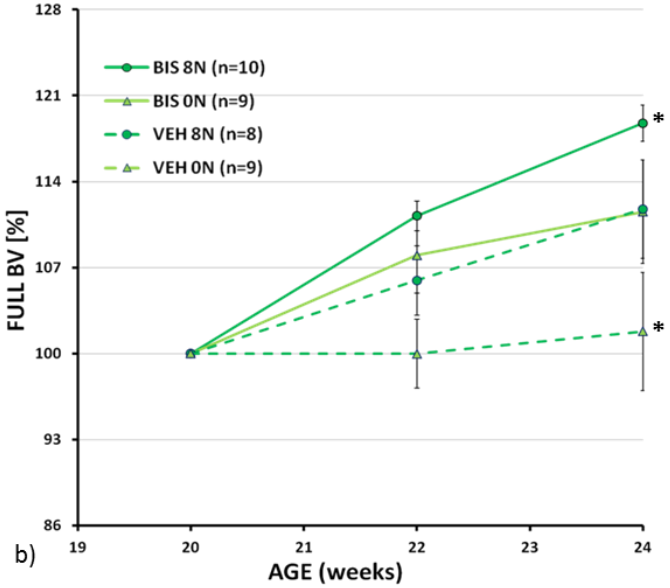
BIS 8N (n=10)
BIS 0N (n=9)
VEH 8N (n=8)
VEH 0N (n=9)
FULL BV [%]
AGE (weeks)
b)
*
*

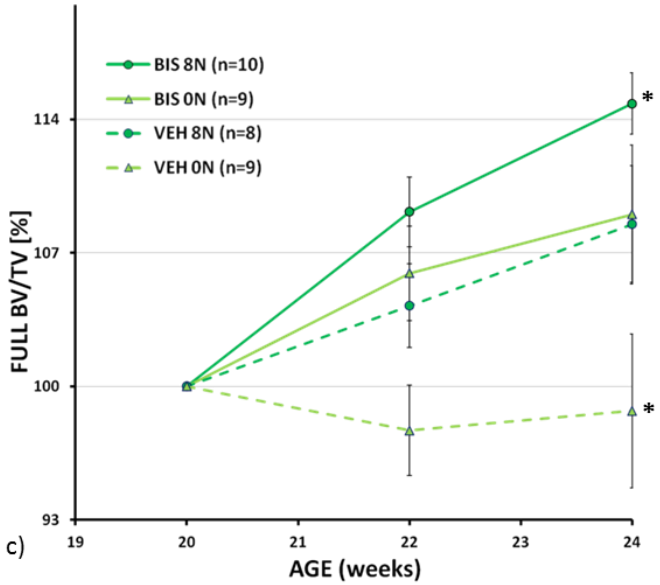
BIS 8N (n=10)
BIS 0N (n=9)
VEH 8N (n=8)
VEH 0N (n=9)
FULL BV/TV [%]
AGE (weeks)
c)
*
*

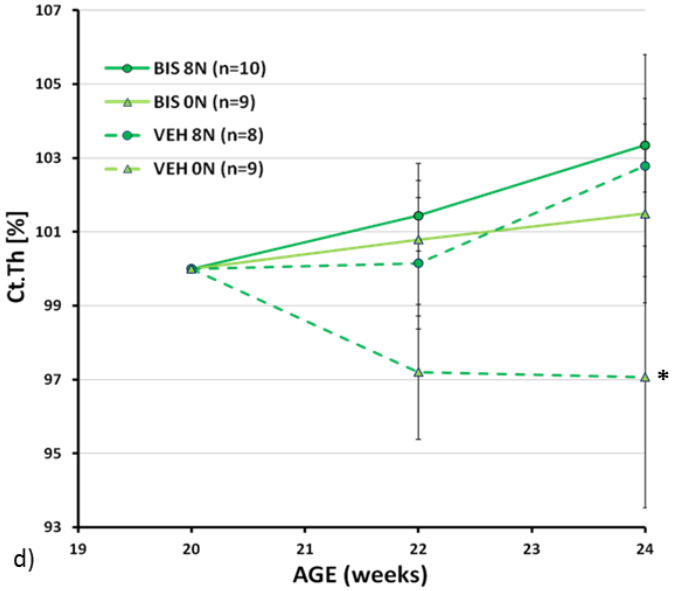
BIS 8N (n=10)
BIS 0N (n=9)
VEH 8N (n=8)
VEH 0N (n=9)
Ct.Th [%]
AGE (weeks)
d)
*

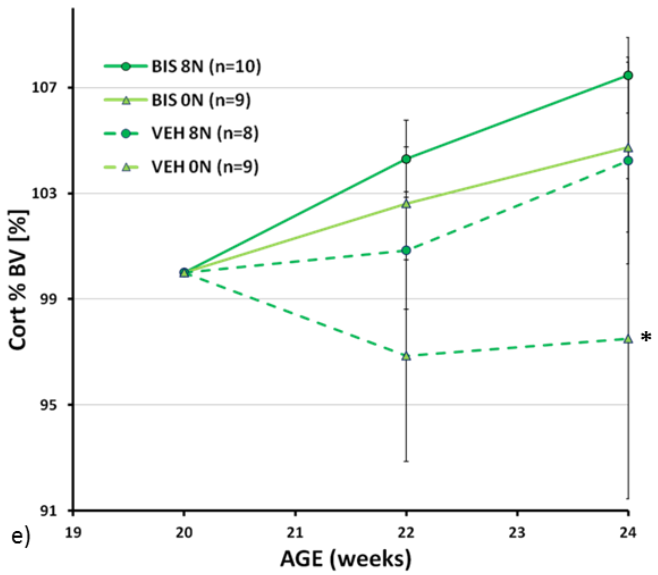

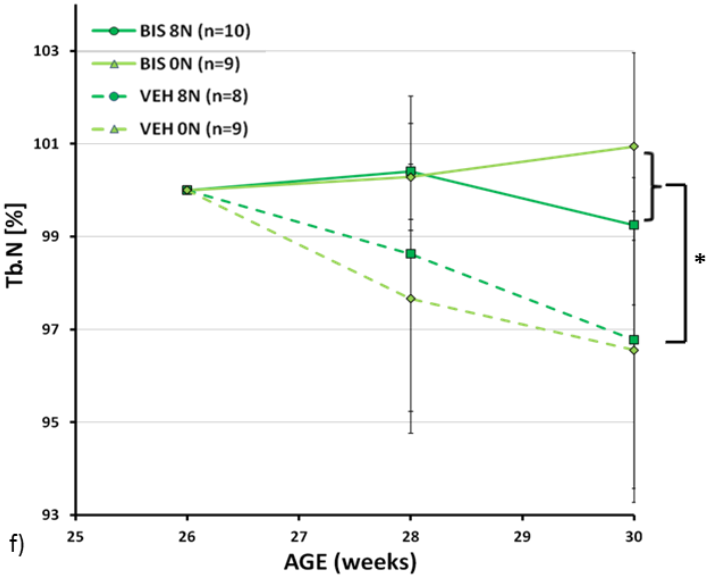

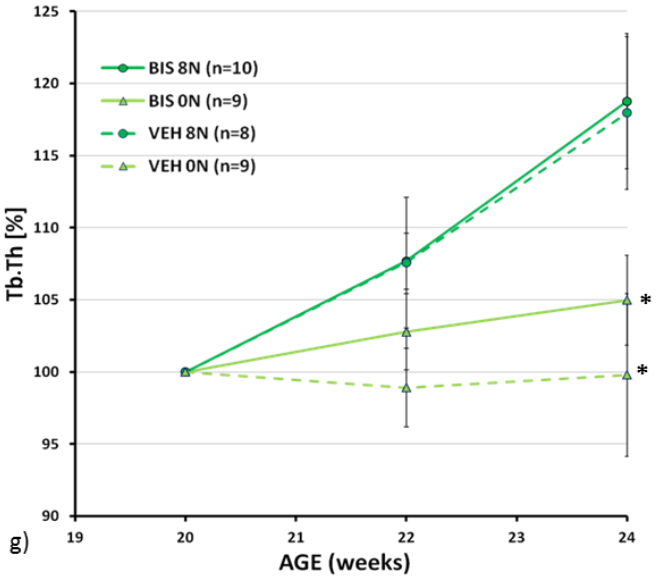

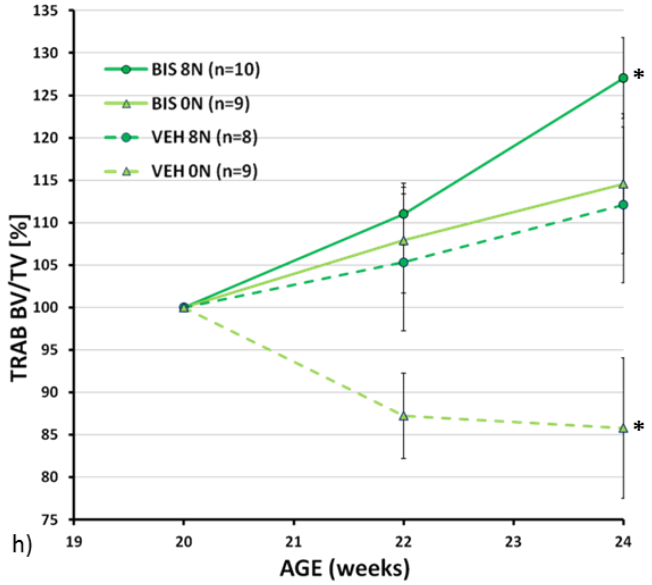

Figure 27: static parameters of bisphosphonate study from early loading experimental series. Measurements normalized to first measurement at beginning of loading period. a), b) parameters from full bone; c)-g) parameters from trabecular compartment; h), I) cortical parameters

Early loading – dynamic parameters

Bone formation

Vehicle treated non-loaded animals showed with a rate of 1.3 ± 0.4 %/d the lowest bone formation rate during the first two weeks of the study. However, during the last two weeks bone formation rate rose to 1.4 ± 0.2 %/d. When loading was applied, bone formation rate was at 1.5 ± 0.3 %/d at the beginning but dropped to similar values as in non-loaded animals at the end of the study. While the bone formation rate of 1.4 ± 0.2 %/d during the first two weeks in bisphosphonate treated animals was higher as in vehicle treated animals it dropped to a significantly lower rate of 1.0 ± 0.2 %/d during the last two weeks of the study. Loading in combination with bisphosphonate treatment increased bone formation significantly to 1.7 ± 0.4 %/d during the first two weeks. However, again a drop was observed towards the end of the study, resulting in a similar bone formation rate as in vehicle treated loaded animals, but still significantly higher as in bisphosphonate treated non-loaded animals. (Figure 28a)

Mineral apposition rate was similar in vehicle treated non-loaded and loaded animals during the entire study. It was at around 1.4 µm/d at the beginning and at around 1.3 µm/d at the end of the study. Bisphosphonate treatment reduced MAR to 1.3 ± 0.1 µm/d and 1.2 ± 0.1 µm/d, respectively. However, when loading was added to bisphosphonate treatment, it increased MAR to similar values as in vehicle treated animals. (Figure 28b)

Mineralizing surface covered the smallest amount in VEH 0N animals with 33.2 ± 3.3 % and 38.7 ± 2.8 %, respectively. In bones of loaded animals MS was increased significantly to 46.3± 5.7 % during the first two weeks and reached even 53.0± 5.2 % at the end of the study. Bisphosphonate treatment increased MS surface significantly compared to vehicle treatment during the first two weeks of the study. However during the last two weeks it covered a similar amount as in VEH 0N animals and significantly less as in VEH 8N animals. Bisphosphonate treatment in combination with loading resulted in a similar amount of MS as vehicle treatment with loading at both time points. Hence, loading always increased MS no matter if treated with vehicle or with bisphosphonates. (Figure 28c)

As the effect of loading or bisphosphonate treatment on mineral apposition rate was very small, bone formation rate seemed to be influenced mainly by mineralizing surface in this study.

Bone resorption

The significantly highest bone resorption rate was observed in vehicle treated non-loaded animals with 2.5 ± 0.4 %/d and 1.6 ± 0.3 %/d, respectively. Loading reduced the rate to 1.3 ± 0.3 %/d and 0.9 ± 0.2 %/d. With bisphosphonate treatment bone resorption went down to 0.9 ± 0.4 %/d at the beginning and 0.6 ± 0.2 %/d at the end of the study. This was a significantly lower rate than in any vehicle treated group. However, loading in bisphosphonate treated animals did not reduce the rate any further than bisphosphonate treatment alone. (Figure 28d)

A similar pattern was observed for mineral resorption rate. The highest mineral resorption rates were observed for the vehicle treated groups, where MRR ranged between 1.7 µm/d and 2.3 µm/d. Bisphosphonate treatment reduced MRR significantly to values between 1.1 µm/d and 1.3 µm/d. Again, no difference was observed between loaded and non-loaded bisphosphonate treated animals. (Figure 28e)

With 32.5 ± 4.6 % and 31.3 ± 1.8 % eroded surface covered the largest amount in VEH 0N animals. Loading reduced ES to 26.7 ± 4.7 % and 23.9 ± 3.5 %, respectively. However, with 31.0 ± 5.8 % at the beginning and 29.0 ± 3.8 % during the last two weeks eroded surface covered a similar amount in bisphosphonate treated animals as in vehicle treated animals. Again, when loading was applied to the bisphosphonate treated animals, ES was reduced, however, not significantly. (Figure 28f)

Hence, bisphosphonate treatment reduced bone resorption mainly by reducing mineral resorption rate and not by influencing eroded surfaces while loading affected ES and not MRR.

The values of the dynamic parameters can be seen in Table 15.

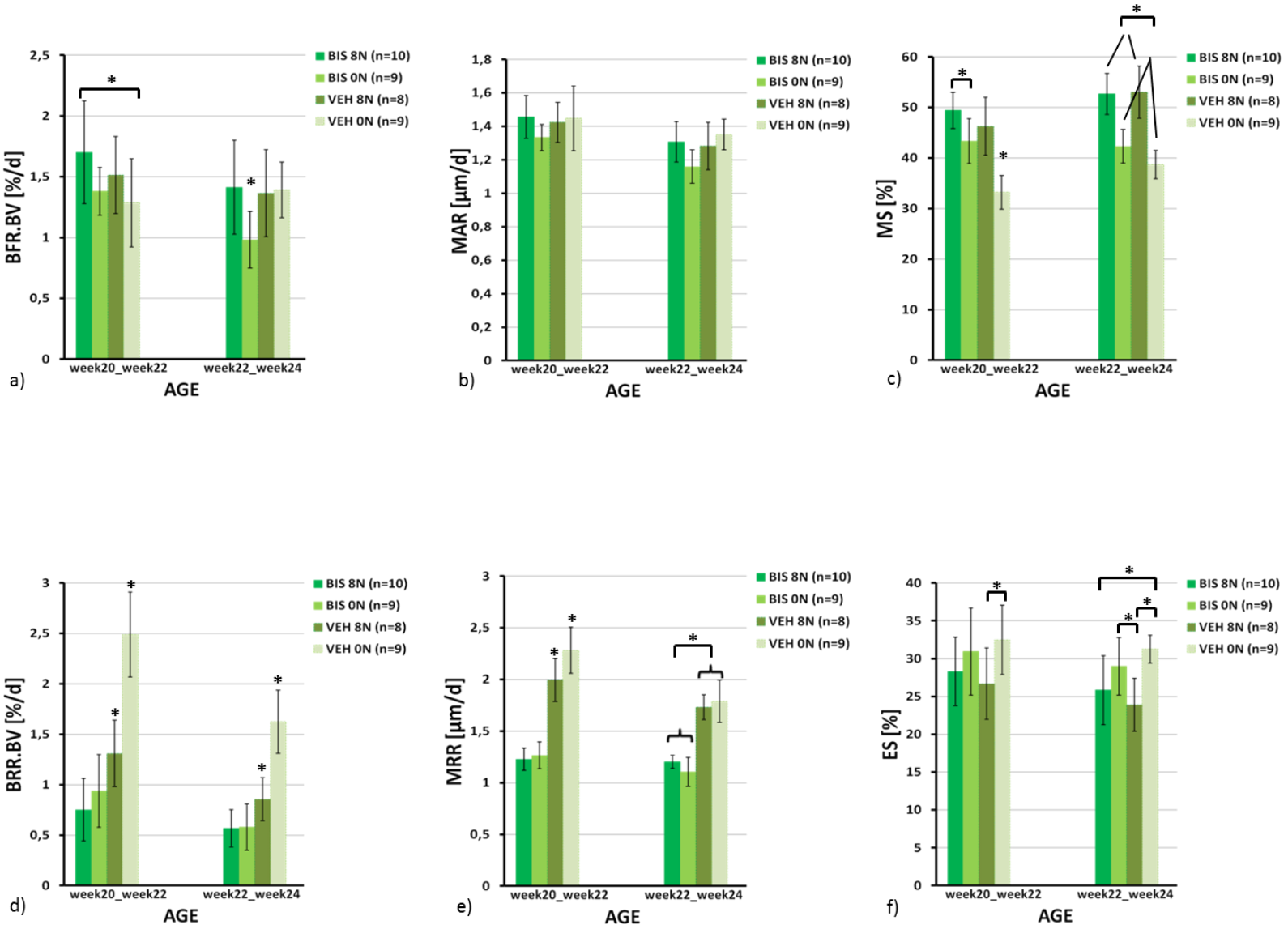

Figure 28: dynamic parameters of bisphosphonate study in early loading experimental series. Upper row shows bone formation parameters, lower row shows bone resorption parameters

Late loading – static parameters

Figure 29 shows overlaid CT images representing the loading period for each group. Loading increases bone formation, while merely bisphosphonate treatment reduces bone resorption.

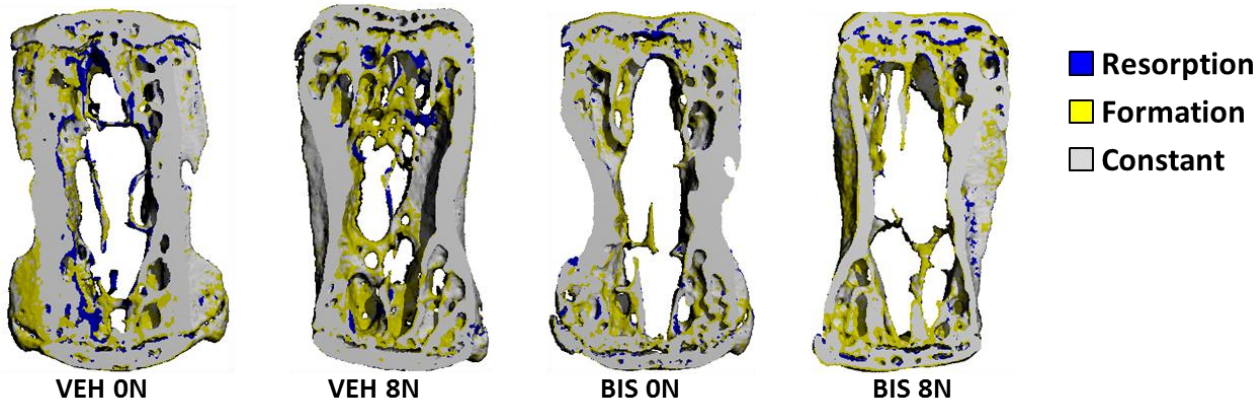

Figure 29: Visualization of bone development during 4 weeks of loading period. CT images of week 26 and 30 are overlaid and registered. Blue represents resorbed bone, yellow newly formed bone and grey constant bone.

VEH 0N (n=8)

Total volume was not changed and also bone volume fraction was only increased slightly by 5.9 % from 4.3 ± 0.2 mm³ to 4.5 ± 0.3 mm³ (Figure 30a,b). This resulted in a 4.3 % greater bone volume density at the end of the observation period (Figure 30c). No changes could be noticed in the cortical compartment. As it was already seen in other vehicle groups, loss of trabeculae due to the effect of estrogen depletion continued. However, trabeculae got thicker by 7.3 % from 72.8 ± 3.7 µm to 78.2 ± 5.8 µm (Figure 30g). This is most likely a physiologic mechanism to maintain mechanical stability of the bone. Due to increased trabecular thickness, trabecular bone volume density was increased by 11.4 % by the end of the observation period (Figure 30h).

VEH 8N (n=10)

Loading had no effect on the total volume of the bone. However, bone volume was increased by 10.0 % from 4.1 ± 0.3 mm³ to 4.5 ± 0.3 mm³, which resulted in a 8.0 % greater bone volume density after four weeks of loading (Figure 30b,c). The impact on the cortical compartment was only marginally. Cortical thickness was increased by 2.8 % and cortical % BV by 4.3 % (Figure 30d,e). As already noticed in other studies, loading did not stop loss of trabeculae. However, it increased the thickness of the remaining ones in this group. Tb.Th was increased by 10.7 % from 71.3 ± 4.2 µm to 78.8 ± 4.3 µm (Figure 30g). Nevertheless, it has to be admitted that this was only slightly and not significantly more compared to the non-loaded group of this study. Yet, the greater thickening resulted in a significantly greater

increase of trabecular bone volume density, compared to VEH 0N. After four weeks of loading Trab BV/TV was 20.6 % greater (Figure 30h).

BIS 0N (n 9)

Total volume was not changed and the increase of 7.5 % in full bone volume density was slightly more than in VEH 0N animals, but less than in loaded ones (Figure 30a,b). Hence, also the effect on Full BV/TV was less than in loaded animals. Cortical thickness remained stable and only a small increase by 3.2 % was observed for cortical % BV (Figure 30d,e). As already seen in the early loading study, the antiresorptive action of bisphosphonates could be monitored best in the trabecular compartment. It preserved trabecular structure as trabecular number remained at 2.7 per mm throughout the study (Figure 30f). Even a small thickening of 6.1 % of the trabeculae was observed (Figure 30g). However, as in the late loading study compared to the early loading study more trabeculae were already lost before treatment started, preservation of trabeculae together with thickening did increase Trab BV/TV by 16.4 % (Figure 30h). Nevertheless this is not as much as it was observed in the loaded group.

BIS 8N (n= 11)

Again Full TV was not changed throughout the observation period. The effect on full bone volume fraction was an additive effect of both, bisphosphonates and loading (Figure 30b). It was increased by 13.0 % from 4.1 ± 0.2 mm³ to 4.6 ± 0.2 mm³. This resulted in the significantly greatest increase of Full BV/TV in this study (10.8 %) (Figure 30c). The effect on the cortical compartment was significantly greater than for only bisphosphonate treated animals and also a trend towards a greater increase compared to only loaded animals was observed. Cortical thickness was increased by 3.4 %, while 4 weeks of loading and bisphosphonate treatment resulted in a 6.1 % greater cortical % BV (Figure 30d,e). Again bisphosphonate treatment preserved trabecular number. Together with a trabecular thickening by 12.5 % trabecular bone volume density was increased by 24.8 % by the end of the observation period (Figure 30f-h).

Absolute values of all static parameters are shown in Table 13. Values normalized to week 26 are shown in Table 14.

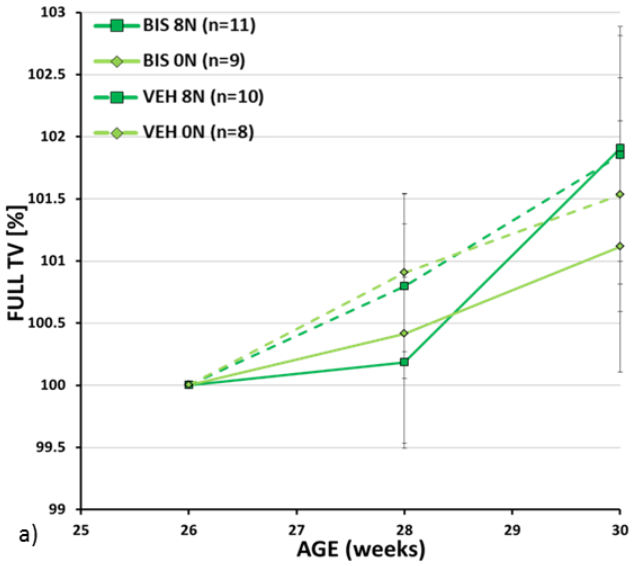
BIS 8N (n=11)
BIS 0N (n=9)
VEH 8N (n=10)
VEH 0N (n=8)
FULL TV [%]
AGE (weeks)
a)

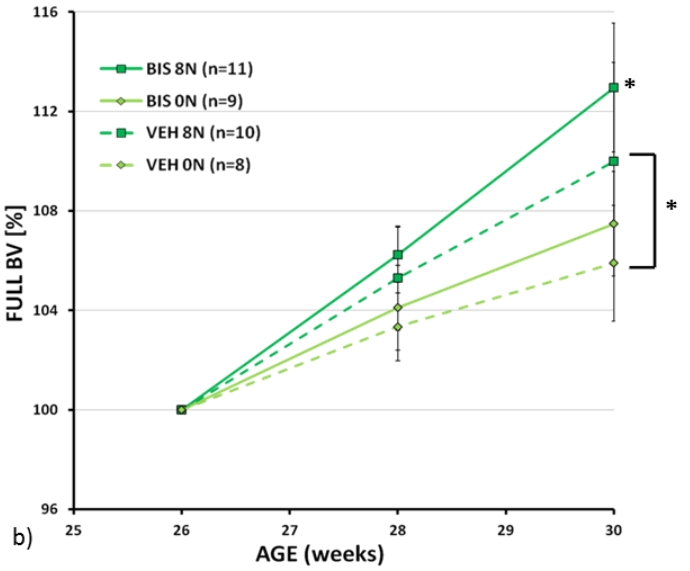
BIS 8N (n=11)
BIS 0N (n=9)
VEH 8N (n=10)
VEH 0N (n=8)
FULL BV [%]
AGE (weeks)
b)
*
*

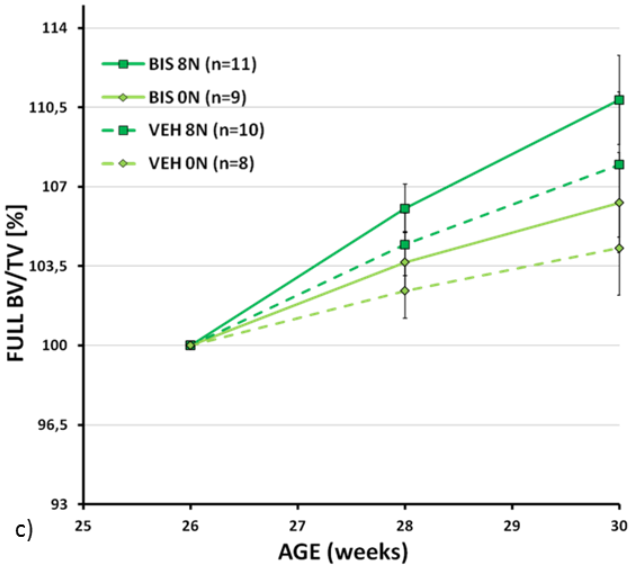
BIS 8N (n=11)
BIS 0N (n=9)
VEH 8N (n=10)
VEH 0N (n=8)
FULL BV/TV [%]
AGE (weeks)
c)

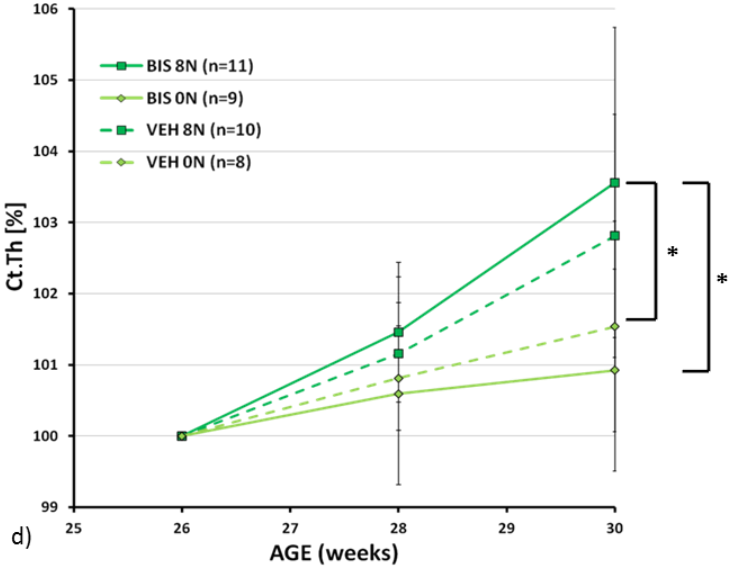
BIS 8N (n=11)
BIS 0N (n=9)
VEH 8N (n=10)
VEH 0N (n=8)
Ct.Th [%]
AGE (weeks)
d)
*
*

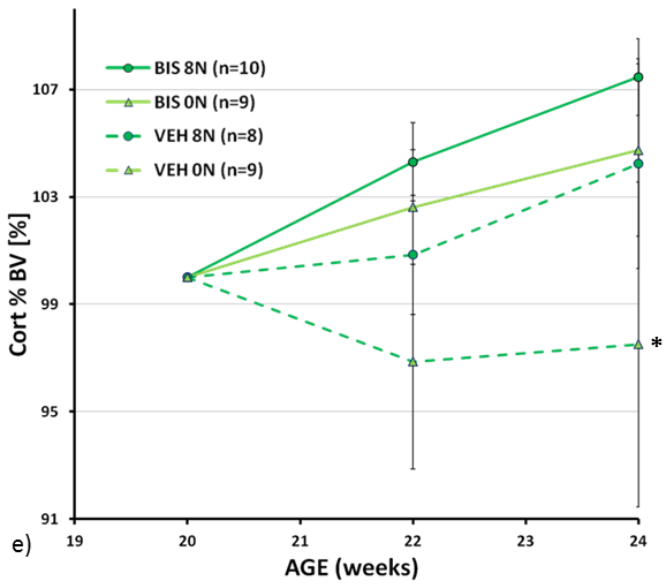

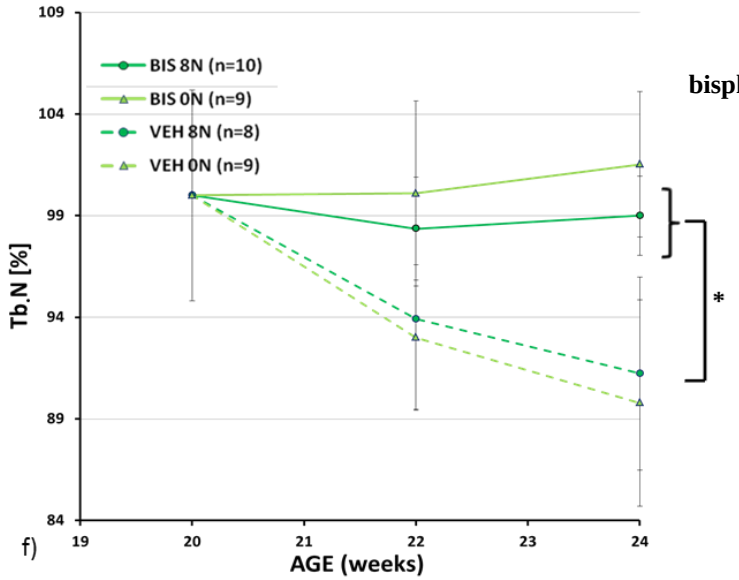

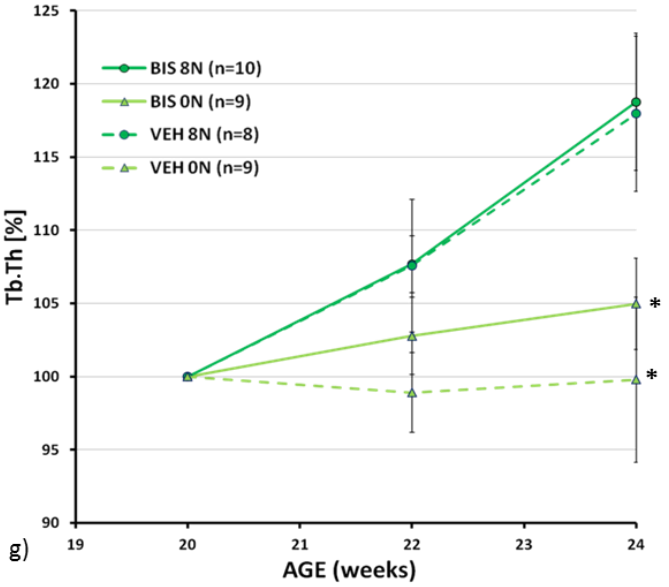

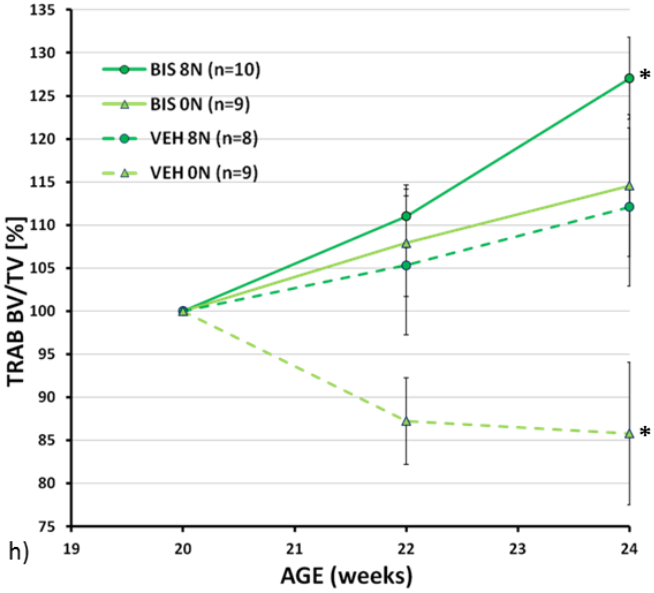

Figure 30: static parameters of bisphosphonate study from late loading experimental series. Measurements normalized to first measurement at beginning of loading period. a), b) parameters from full bone; c)-g) parameters from trabecular compartment; h), I) cortical parameters

Late loading – dynamic parameters

Bone formation

The bone formation rate of VEH 0N mice was at 1.1 ± 0.2 %/d during the first two weeks and at 1.0 ± 0.5 %/d during the last two weeks of the study. Loading increased bone formation only marginally and also bisphosphonate treatment did not influence bone formation. When bisphosphonate treatment was combined with loading a trend towards a higher bone formation rate could be observed as it was 1.3 ± 0.3 %/d during the first two weeks and 1.3 ± 0.2 %/d during the last two weeks of the study. (Figure 31a)

Mineral apposition rate was neither influenced by loading, nor by bisphosphonate treatment as it ranged between 1.2 µm/d and 1.3 µm/d for all groups during the entire study. (Figure 31b)

Mineralizing surface covered 46.7 ± 5.0 % during the first two weeks and 45.4 ± 4.8 % during the last two weeks in VEH 0N animals. Again loading increased it only marginally, while bisphosphonate treatment did not influence the amount covered by mineralizing surface at all. When bisphosphonate treatment and loading were combined a slight trend towards a larger mineralizing surface was observed. (Figure 31c)

Bone resorption

The highest bone resorption rate was observed in vehicle treated non-loaded animals. It was at 0.8 ± 0.3 %/d at the beginning and at 0.7 ± 0.3 %/d at the end of the observation period. Loading reduced the rate significantly to 0.6 ± 0.3 %/d throughout the entire study. During the first two weeks bisphosphonate treatment reduced BRR even further to 0.5 ± 0.2 %/d. However the rate increased again to 0.7 ± 0.3 %/d at the end of the study. The lowest bone resorption rate was observed when bisphosphonate treatment and loading were combined. (Figure 31d)

A similar pattern was observed for mineral resorption rate. In vehicle treated non-loaded animals this rate was at 1.5 ± 0.2 µm/d at the beginning and at 1.4 ± 0.2 µm/d at the end of the study. Loading reduced mineral resorption rate significantly during the first two weeks, while no differences were observed during the last two weeks of the study. Bisphosphonate treatment reduced MRR to rates between 1.1 µm/d and 1.2 µm/d regardless if the loading was applied. (Figure 31e)

Eroded surface covered 27.5 ± 4.4 % and 29.0 ± 4.6 %, respectively in vehicle treated non-loaded animals. Applying loading reduced the amount to around 25 %, while bisphosphonate treatment did not change ES. However, combining bisphosphonate treatment and loading

reduced ES to similar values as only loading. In BIS 8N animals it covered 24.1 ± 5.3 % during the first two weeks and 24.5 ± 5.7 % during the last two weeks. (Figure 31f)

Hence while bisphosphonate treatment reduced mineral resorption rate the effect on eroded surface was only mediated by loading. Both effects influenced bone resorption rate to similar extends, although in the first two weeks the effect of bisphosphonate treatment seemed to be stronger, while during the last two weeks the effect of loading seemed to be more pronounced. Values of dynamic parameters are shown in Table 15.

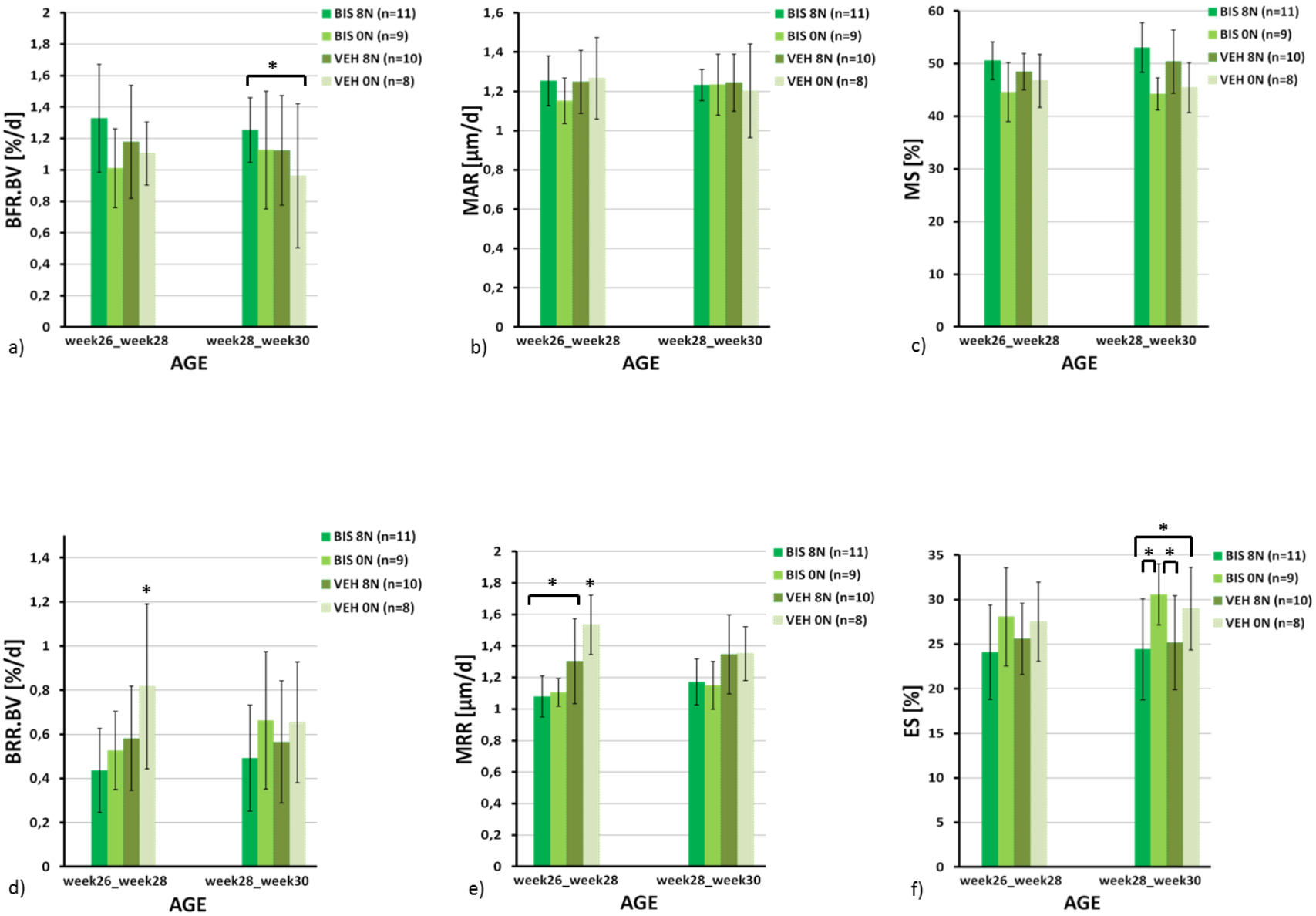

Figure 31: dynamic parameters of bisphosphonate study in late loading experimental series. Upper row shows bone formation parameters, lower row shows bone resorption parameters

Parameter group	Full TV [mm³]	Full BV [mm³]	Full BV/TV [%]	Ct.Th [µm]	cort % BV [%]	Tb.N [1/mm]	Tb.Th [µm]	Trab BV/TV [%]
early loading								
VEH 0N								
15 weeks	7.8 ± 0.3	4.1 ± 0.3	53.3 ± 2.4	149.1 ± 6.4	39.6 ± 2.0	2.9 ± 0.2	73.2 ± 4.3	17.4 ± 1.6
20 weeks	8.3 ± 0.4	3.7 ± 0.4	44.5 ± 4.5	138.2 ± 11.7	33.2 ± 3.9	2.8 ± 0.2	64.3 ± 4.1	13.1 ± 2.4
22 weeks	8.5 ± 0.4	3.7 ± 0.4	43.3 ± 3.5	134.2 ± 9.7	32.0 ± 2.8	2.6 ± 0.2	63.6 ± 3.4	11.4 ± 1.8
24 weeks	8.6 ± 0.4	3.8 ± 0.3	43.7 ± 3.1	133.8 ± 7.7	32.2 ± 2.4	2.5 ± 0.2	64.1 ± 3.5	11.1 ± 1.6
VEH 8N								
15 weeks	7.9 ± 0.7	4.2 ± 0.4	52.7 ± 2.2	148.1 ± 6.8	39.3 ± 1.7	2.9 ± 0.3	71.9 ± 3.8	17.2 ± 2.3
20 weeks	8.5 ± 0.8	4.0 ± 0.4	46.9 ± 3.0	143.9 ± 8.4	35.5 ± 2.9	2.8 ± 0.2	67.5 ± 3.2	13.9 ± 1.8
22 weeks	8.7 ± 0.7	4.2 ± 0.3	48.8 ± 2.5	144.1 ± 7.0	35.8 ± 2.4	2.7 ± 0.2	72.6 ± 2.3	14.6 ± 1.7
24 weeks	8.8 ± 0.7	4.5 ± 0.3	50.8 ± 2.2	147.8 ± 5.4	36.9 ± 2.0	2.6 ± 0.2	79.6 ± 2.8	15.5 ± 1.6
BIS 0N								
15 weeks	7.6 ± 0.5	3.9 ± 0.5	51.2 ± 2.8	140.5 ± 6.9	37.6 ± 2.1	3.1 ± 0.3	68.9 ± 4.6	17.3 ± 2.5
20 weeks	8.3 ± 0.5	3.7 ± 0.4	44.2 ± 2.7	135.1 ± 6.8	33.1 ± 2.3	2.9 ± 0.3	63.2 ± 2.2	13.0 ± 1.2
22 weeks	8.4 ± 0.5	3.9 ± 0.3	46.8 ± 1.9	136.1 ± 4.4	34.0 ± 1.8	2.9 ± 0.3	64.9 ± 2.5	14.0 ± 0.7
24 weeks	8.4 ± 0.5	4.1 ± 0.3	48.1 ± 1.7	137.0 ± 4.5	34.6 ± 1.6	2.9 ± 0.2	66.3 ± 3.0	14.9 ± 0.7
BIS 8N								
15 weeks	7.9 ± 0.2	4.2 ± 0.3	52.6 ± 2.9	146.6 ± 8.5	38.9 ± 2.6	3.0 ± 0.3	72.1 ± 4.6	17.5 ± 2.5
20 weeks	8.6 ± 0.3	3.9 ± 0.2	45.6 ± 1.9	140.6 ± 5.3	34.0 ± 2.0	2.9 ± 0.2	65.9 ± 4.3	14.2 ± 1.8
22 weeks	8.8 ± 0.3	4.4 ± 0.2	49.7 ± 1.9	142.6 ± 5.8	35.5 ± 2.1	2.9 ± 0.2	70.9 ± 4.5	15.7 ± 1.7
24 weeks	8.9 ± 0.3	4.7 ± 0.3	52.3 ± 2.1	145.3 ± 6.5	36.5 ± 2.0	2.9 ± 0.2	78.2 ± 6.1	18.0 ± 2.1
late loading								
VEH 0N								
15 weeks	7.8 ± 0.2	4.3 ± 0.2	55.4 ± 3.3	157.0 ± 9.0	41.4 ± 2.7	2.9 ± 0.3	77.5 ± 4.2	19.0 ± 2.7
26 weeks	8.7 ± 0.4	4.3 ± 0.2	49.1 ± 2.3	147.8 ± 5.9	36.6 ± 2.3	2.7 ± 0.3	72.8 ± 3.7	14.2 ± 2.2
28 weeks	8.8 ± 0.4	4.4 ± 0.3	50.3 ± 2.5	149.0 ± 6.5	37.1 ± 2.3	2.6 ± 0.3	75.6 ± 5.0	15.1 ± 2.7
30 weeks	8.8 ± 0.4	4.5 ± 0.3	51.2 ± 2.7	150.1 ± 6.7	37.5 ± 2.3	2.6 ± 0.3	78.2 ± 5.8	15.8 ± 2.8
VEH 8N								
15 weeks	7.6 ± 0.3	4.0 ± 0.3	52.9 ±2.0	151.0 ± 5.4	40.2 ± 1.7	2.8 ± 0.3	73.6 ± 2.9	16.1 ± 2.9
26 weeks	8.5 ± 0.4	4.1 ± 0.3	48.0 ± 3.6	142.8 ± 8.8	35.8 ± 3.4	2.6 ± 0.2	71.3 ± 4.2	13.3 ± 2.1
28 weeks	8.5 ± 0.5	4.3 ± 0.3	50.1 ± 3.5	144.8 ± 9.5	36.8 ± 3.4	2.6 ± 0.3	74.8 ± 4.1	14.6 ± 2.2
30 weeks	8.6 ± 0.5	4.5 ± 0.3	51.9 ± 2.9	147.2 ± 8.0	37.6 ± 2.7	2.6 ± 0.3	78.8 ± 4.3	16.0 ± 2.2
BIS 0N								
15 weeks	7.6 ± 0.8	4.1 ± 0.5	53.8 ± 2.4	151.1 ± 7.6	40.0 ± 1.8	3.0 ± 0.2	73.9 ± 3.8	18.0 ± 2.0
26 weeks	8.5 ± 0.9	3.9 ± 0.4	45.9 ± 2.1	137.4 ± 4.5	33.5 ± 1.3	2.6 ± 0.1	67.3 ± 3.1	12.8 ± 1.3
28 weeks	8.5 ± 0.9	4.1 ± 0.5	47.6 ± 2.2	138.3 ± 6.0	34.1 ± 1.5	2.7 ± 0.1	69.0 ± 3.8	13.7 ± 1.5
30 weeks	8.6 ± 0.9	4.2 ± 0.5	48.8 ± 2.3	138.7 ± 6.1	34.5 ± 1.6	2.7 ± 0.1	71.4 ± 4.0	14.9 ± 1.6
BIS 8N								
15 weeks	7.6 ± 0.3	4.2 ± 0.2	55.3 ± 2.2	155.4 ± 6.3	41.8 ± 2.0	2.9 ± 0.2	75.5 ± 3.5	18.0 ± 1.8
20 weeks	8.6 ± 0.3	4.1 ± 0.2	47.4 ± 2.4	141.8 ± 7.4	35.2 ± 2.0	2.7 ± 0.3	68.6 ± 1.7	13.1 ± 1.8
22 weeks	8.6 ± 0.3	4.3 ± 0.2	50.2 ± 2.4	143.9 ± 6.6	36.4 ± 1.8	2.7 ± 0.3	71.8 ± 1.8	14.5 ± 2.0
24 weeks	8.7 ± 0.3	4.6 ± 0.2	52.5 ± 2.3	146.8 ± 5.8	37.3 ± 1.6	2.7 ± 0.3	77.2 ± 2.2	16.3 ± 1.9

Table 13: absolute values of static parameters of bisphosphonate studies in early and late loading experimental series. Expressed as mean ± standard deviation

Parameter group	Full TV [%]	Full BV [%]	Full BV/TV [%]	Ct.Th [%]	cort % BV [%]	Tb.N [%]	Tb.Th [%]	Trab BV/TV [%]
early loading								
VEH 0N								
20 weeks	100.0	100.0	100.00	100.00	100.00	100.00	100.00	100.00
22 weeks	102.4 ± 1.3	100.0 ± 2.8	97.7 ± 2.4	97.2 ± 1.8	96.9 ± 4.0	93.0 ± 3.6	98.9 ± 2.7	87.2 ± 5.0
24 weeks	103.1 ± 1.6	101.8 ± 4.8 a)b)c)	98.7 ± 4.0 a)b)c)	97.1± 3.6 a)b)c)	97.5 ± 6.1 a)b)c)	89.8 ± 5.1 a)b)	99.8 ± 5.6 a)b)c)	85.8 ± 8.3 a)b)c)
VEH 8N								
20 weeks	100.0	100.0	100.00	100.00	100.00	100.00	100.00	100.00
22 weeks	101.6 ± 0.9	105.9 ± 2.8	104.2 ± 2.2	100.2 ± 1.8	100.9 ± 2.2	93.9 ± 4.4	107.6 ± 4.5	105.3 ± 8.0
24 weeks	103.0 ± 1.2	111.8 ± 4.0 a)d)	108.5 ± 3.1 a)d)	102.8 ± 3.0 d)	104.2 ± 3.9 d)	91.2 ± 4.8 a)b)	118.0 ± 5.3 b)d)	112.1 ± 9.2 a)d)
BIS 0N								
20 weeks	100.0	100.0	100.00	100.00	100.00	100.00	100.00	100.00
22 weeks	101.9 ± 0.7	108.0 ± 3.1	105.9 ± 2.5	100.8 ± 2.1	102.6 ± 2.1	100.1 ± 4.6	102.8 ± 2.6	107.9 ± 6.2
24 weeks	102.3 ± 1.0	111.5 ± 4.2 a)d)	109.0 ± 3.6 a)d)	101.5 ± 2.4 d)	104.7 ± 3.2 d)	101.5 ± 3.6 c)d)	105.0 ± 3.1 a)c)d)	114.6 ± 8.2 a)d)
BIS 8N								
20 weeks	100.0	100.0	100.00	100.00	100.00	100.00	100.00	100.00
22 weeks	101.9 ± 1.2	111.2 ± 1.2	109.1 ± 1.8	101.4 ± 1.0	104.3 ± 1.5	98.4 ± 2.5	107.7 ± 1.9	111.0 ± 3.6
24 weeks	103.4 ± 0.5 +)	118.8 ± 1.5 b)c)d)+)	114.8 ± 1.6 b)c)d)+)	103.3 ± 1.3 d)	107.5 ± 1.4 d)+)	99.0 ± 2.0 c)d)+)	118.8 ± 4.7 b)d)+)	127.0 ± 4.7 b)c)d)
late loading								
VEH 0N								
26 weeks	100.0	100.0	100.00	100.00	100.00	100.00	100.00	100.00
28 weeks	100.9 ± 0.6	103.3 ± 1.4	102.4 ± 1.2	100.8 ± 0.7	101.5 ± 1.0	97.7 ± 2.9	103.8 ± 1.9	106.1 ± 4.3
30 weeks	101.5 ± 0.9	105.9 ± 2.3 a)c)	104.3 ± 2.1 a)c)	101.5 ± 1.5 a)	102.6 ± 2.0 a)	96.6 ± 3.0 a)b)	107.3 ± 3.8 a)	111.4 ± 4.8 a)c)
VEH 8N								
26 weeks	100.0	100.0	100.00	100.00	100.00	100.00	100.00	100.00
28 weeks	100.8 ± 0.7	105.3 ± 2.1	104.5 ± 1.4	101.2 ± 1.1	102.1 ± 0.9	98.6 ± 3.4	104.9 ± 2.6	110.3 ± 4.1
30 weeks	101.9 ± 1.0	110.0 ± 4.0 a)d)	108.0 ± 3.2 a)d)	102.8 ± 1.7 b)	104.3 ± 2.6	96.8 ± 3.5 a)b)	110.7 ± 5.7 b)	120.6 ± 11.1 d)
BIS 0N								
26 weeks	100.0	100.0	100.00	100.00	100.00	100.00	100.00	100.00
28 weeks	100.4 ± 0.9	104.1 ± 1.7	103.7 ± 1.4	100.6 ± 1.3	101.9 ± 1.4	100.3 ± 1.2	102.4 ± 1.9	107.0 ± 4.1
30 weeks	101.1 ± 1.0	107.5 ± 2.1 a)	106.3 ± 2.2 a)	100.9 ± 1.4 a)c)	103.2 ± 2.3 a)	100.9 ± 2.0 c)d	106.2 ± 3.3 a)c)	116.4 ± 6.8 a)
BIS 8N								
20 weeks	100.0	100.0	100.00	100.00	100.00	100.00	100.00	100.00
22 weeks	100.2 ± 0.7	106.2 ± 1.1	106.0 ± 1.1	101.5 ± 1.0	103.4 ± 1.2	100.4 ± 1.0	104.6 ± 2.0	110.9 ± 3.2
24 weeks	101.9 ± 0.9 +)	113.0 ± 2.6 b)c)d)+)	110.8 ± 2.0 b)c)d)+)	103.6 ± 2.2 b)d)+)	106.1 ± 2.0 b)d)+)	99.3 ± 1.7 c)d)+)	112.5 ± 3.9 b)d)+)	124.8 ± 5.5 b)d)+)

Table 14 static parameters of bisphosphonate studies of early and late loading experimental series normalized to beginning of loading period. a) Significant to BIS 8N, b) significant to BIS 0N, c) significant to VEH 8N, d) significant to VEH 0N for each study, +) combined effect of BIS and loading is additive; values are presented as mean ± standard deviation

Parameter group	BFR.BV [%/d]	MAR [µm/d]	MS [%]	BRR.BV [%/d]	MRR [µm/d]	ES [%]
early loading						
VEH 0N						
wk20_wk22	1.3 ± 0.4 a)	1.5 ± 0.2	33.2 ± 3.3 a)b)c)	2.5 ± 0.4 a)b)c)	2.3 ± 0.2 a)b)c)	32.5 ± 4.6 c)
wk22_wk24	1.4 ± 0.2 b)	1.4 ± 0.1 b)	38.7 ± 2.8 a)c)	1.6 ±0.3 a)b)c)	1.8 ±0.2 a)b)	31.3 ± 1.8 a)c)
VEH 8N						
wk20_wk22	1.5 ± 0.3	1.4 ± 0.1	46.3 ± 5.7 d)	1.3 ± 0.3 a)b)d)	2.0 ± 0.2 a)b)d)	26.7 ± 4.7 d)
wk22_wk24	1.4 ± 0.4 b)	1.3 ± 0.1	53.0 ± 5.2 b)d)	0.9 ± 0.2 a)b)d)	1.7 ± 0.1 a)b)	23.9 ± 3.5 b)d)
BIS 0N						
wk20_wk22	1.4 ± 0.2	1.3 ± 0.1 a)	43.3 ± 4.4 a)d)	0.9 ± 0.4 c)d)	1.3 ± 0.1 c)d)	30.9 ± 5.8
wk22_wk24	1.0 ± 0.2 a)c)d)	1.2 ± 0.1 a)d)	42.3 ± 3.3 a)c)	0.6 ± 0.2 c)d)	1.1 ± 0.1 c)d)	29.0 ± 3.8 c)
BIS 8N						
wk20_wk22	1.7 ± 0.4 d)	1.5 ± 0.1 b)	49.4 ± 3.6 b)d)	0.8 ± 0.3 c)d)	1.2 ± 0.1 c)d)	28.3 ± 4.5
wk22_wk24	1.4 ± 0.4 b)	1.3 ± 0.1 b)	52.7 ± 4.1 b)d)	0.6 ± 0.2 c)d)	1.2 ± 0.1 c)d)	25.8 ± 4.6 d)
late loading						
VEH 0N						
wk26_wk28	1.1 ± 0.2	1.3 ± 0.2	46.7 ± 5.0 a)	0.8 ± 0.4 a)b)c)	1.5 ± 0.2 a)b)c)	27.5 ± 4.4
wk28_wk30	1.0 ± 0.5 a)	1.2 ± 0.2	45.4 ± 4.8 a)c)	0.7 ± 0.3	1.4 ± 0.2	29.0 ± 4.6 a)
VEH 8N						
wk26_wk28	1.2 ± 0.4	1.3 ± 0.2	48.5 ± 3.5 b)	0.6 ± 0.2 d)	1.3 ± 0.3 a)d)	25.6 ± 4.0
wk28_wk30	1.1 ± 0.4	1.2 ± 0.2	50.4 ± 6.0 b)d)	0.6 ± 0.3	1.4 ± 0.3	25.2 ± 5.3 b)
BIS 0N						
wk26_wk28	1.0± 0.3	1.2 ± 0.1	44.6 ± 5.6 a)c)	0.5 ± 0.2 d)	1.1 ± 0.1 d)	28.1 ± 5.5 a)
wk28_wk30	1.1 ± 0.4	1.2 ± 0.2	44.2 ± 3.1 a)c)	0.7 ± 0.3	1.2 ± 0.2	30.6 ± 3.4 a)c)
BIS 8N						
wk26_wk28	1.3 ± 0.3	1.3 ± 0.1	50.6 ± 3.6 b)	0.4 ± 0.2 d)	1.1 ± 0.1 c)d)	24.1 ± 5.3 b)
wk28_wk30	1.3 ± 0.2 d)	1.2 ± 0.1	53.1 ± 4.7 b)d)	0.5 ± 0.2	1.2 ± 0.2	24.5 ± 5.7 b)d)

Table 15: bone dynamic parameters of bisphosphonate studies. a) significant to BIS 8N, b) significant to BIS 0N, c) significant to VEH 8N, d) significant to VEH 0N for each study; values are presented as mean ± standard deviation

4.5 Physiome map

The physiome map provides a good tool to directly compare the effects of the different treatment and loading regimens at both starting points. To get a better overview, the vehicle groups from the PTH and bisphosphonate studies were pooled with respective ovariectomized groups from the ovariectomy study for each experimental series.

In general, it can be noticed that for all parameters a higher effect can be seen in the loaded groups compared to their non-loaded controls. What is also striking is that PTH exerts the most prominent effect in almost all parameters at both starting points 5 and 11 weeks after ovariectomy. Except for Full TV sham operated mice start at a higher level when the loading period begins, no matter if it is 5 or 11 weeks after ovariectomy. The number of all animals in all groups can be seen in Table 16.

group	SHM 0N	SHM 8N	OVX/VEH 0N	OVX/VEH 8N	PTH 0N	PTH 8N	BIS 0N	BIS 8N
# of animals in early loading study	7	9	27	27	9	9	9	10
# of animals in late loading study	8	8	26	25	9	11	9	11

Table 16 number of animals during all studies per group

Static parameters

Full bone

The physiome maps of full bone parameters demonstrate the different effects of ovariectomy. Due to the lack of estrogen longitudinal growth of the bone is increased while bone volume fraction and subsequently bone volume density are decreased in ovariectomized animals.

During the treatment period total volume was increased most significantly when PTH and loading were combined. This is followed by the effect from merely PTH treatment. However, while during the late loading experimental series the effects of all other treatments (BIS 0N, BIS 8N, VEH 8N) did not differ significantly from each other, loading increased the total volume in the early loading experimental series, both in combination with bisphosphonate and vehicle

injection. In contrast loading did not show any significant effects on sham operated animals at any time point. The physiome map of Full TV can be seen in Figure 32

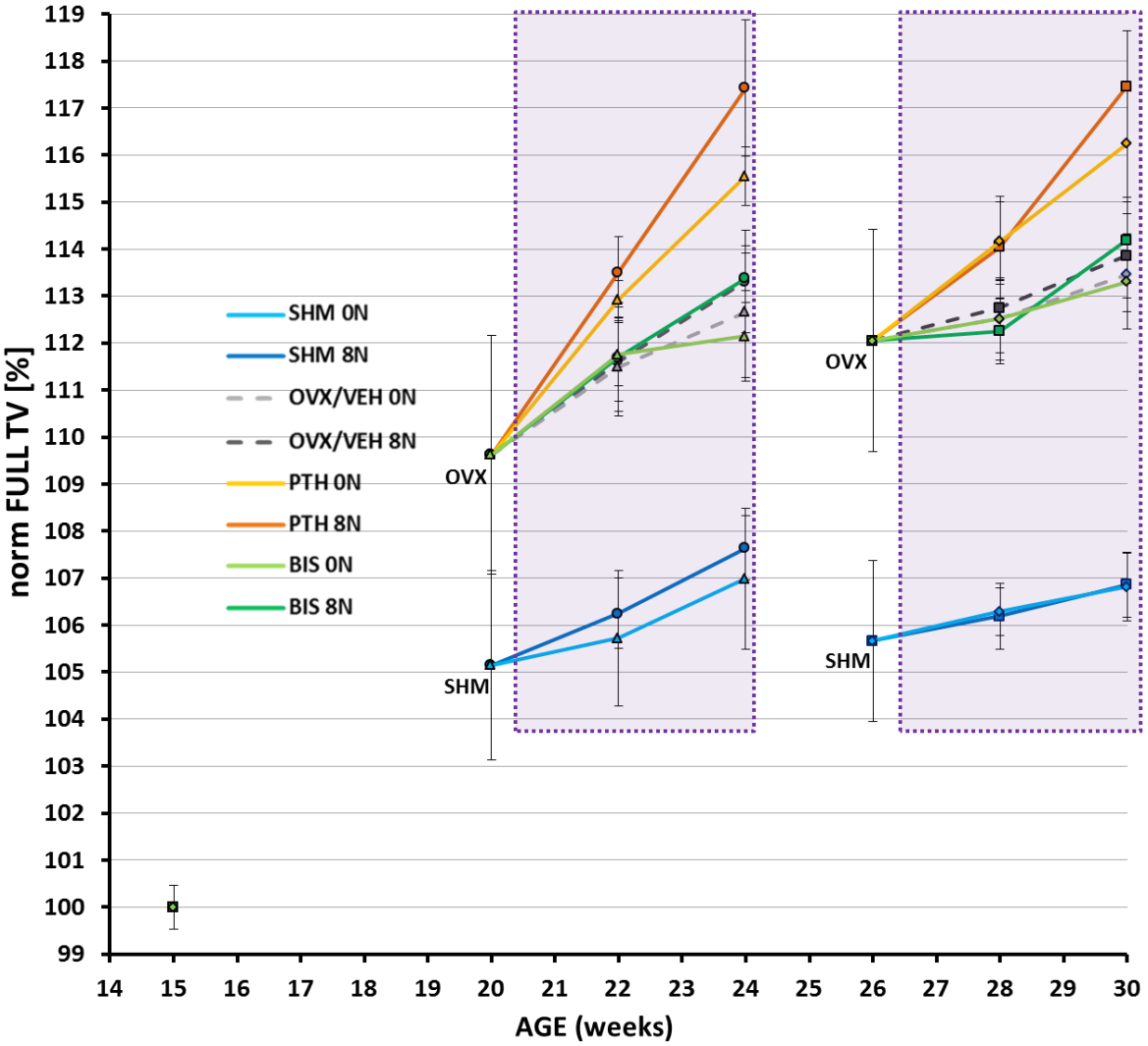

Figure 32: physiome map of Full TV. Early loading studies are represented with ○ and Δ, while late loading studies are represented with □ and ◊. Grey boxes mark data normalized to treatment start at week 20 and 26, respectively. For n per group see **Table 16**.

While the effects of treatment on total volume were more restrained, a large impact of all treatments was observed for the bone volume. Again the significantly strongest effect in both experimental series was observed, when PTH and loading were combined. During the early loading experimental series merely PTH treatment increased FULL BV to the same extend as the combination of bisphosphonate treatment and loading. This is in contrast to the late loading experimental series, where the effect of BIS 8N was significantly less than the effect of PTH treatment. In both experimental series loading showed a stronger effect than bisphosphonate

treatment alone. However, also merely bisphosphonate treatment could still significantly improve full bone volume fraction. Compared to sham operated animals, any treatment in ovariectomized animals had a significantly stronger effect than loading of sham animals in the early loading experimental series. This was also found in the late loading experimental series, however not for bisphosphonate treatment. The physiome map of Full BV can be seen in Figure 33

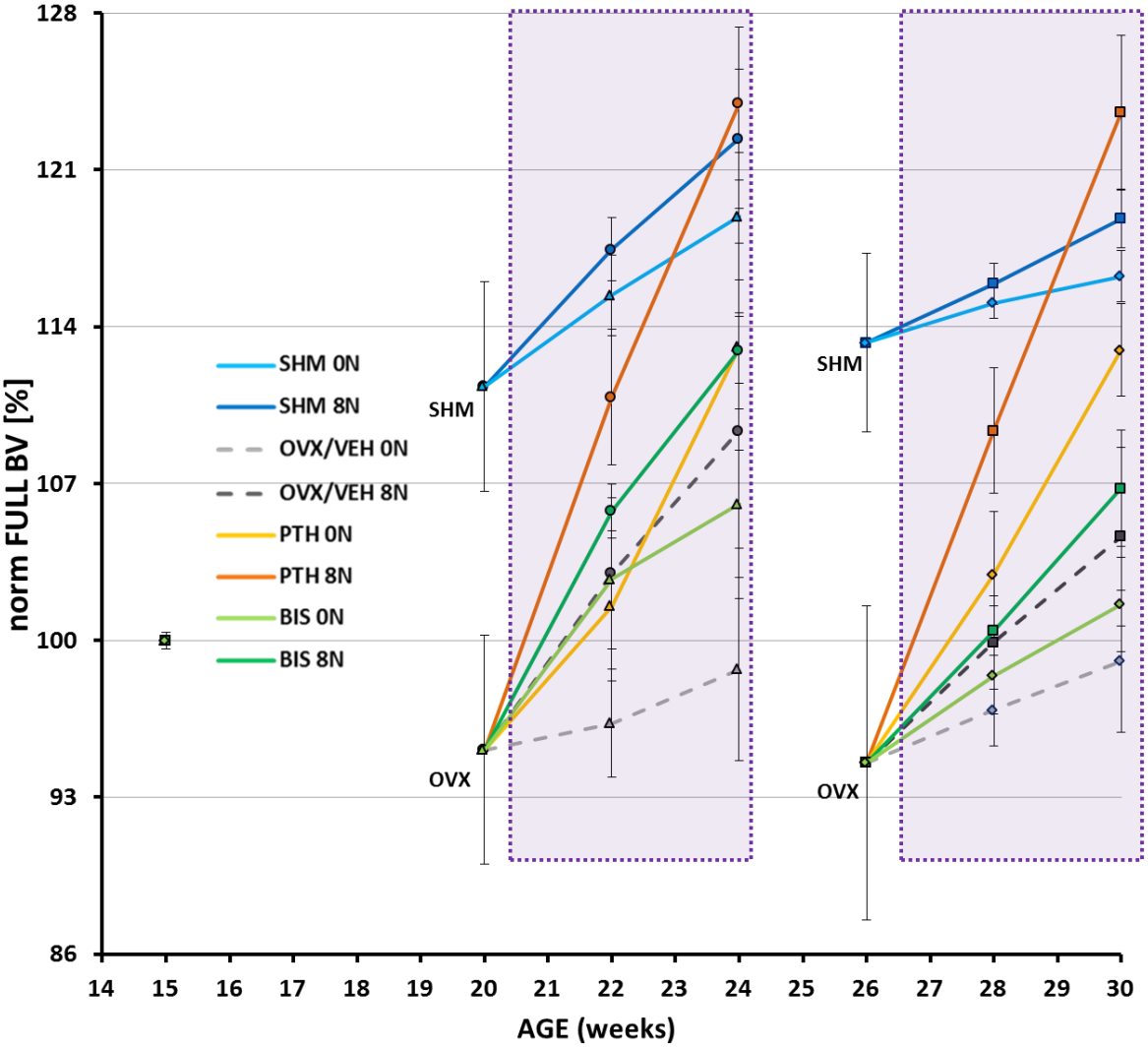

Figure 33: Physiome map of Full BV. Early loading studies are represented with ○ and Δ, while late loading studies are represented with □ and ◊. Grey boxes mark data normalized to treatment start at week 20 and 26, respectively. For n per group see **Table 16**.

The physiome map of full bone volume fraction illustrates the bone loss after OVX. While the SHM groups show a time-dependent increase in Full BV/TV, it is severely decreased in the OVX groups at the time-points when the treatment starts.

As mentioned before, combined PTH treatment and loading exerted the significantly strongest effect on Full BV/TV, no matter when treatment and loading were started. Both groups reached BV/TV values above their basal levels; however they could not reach the time matched SHM 0N values. While in the early loading series all other treatments (PTH 0N, BIS 8N and BIS 0N) caused an intermediate increase in Full BV/TV, PTH 0N exceeded the effects of BIS 8N and BIS 0N in the late loading groups. This was caused by the apparently higher efficacy of early bisphosphonate treatment (with and without loading) compared to the late treatment start. However, at both time-points loading added additive to bisphosphonate treatment. Loading alone was more effective than bisphosphonate without loading in both experimental series. The physiome map of Full BV/TV is shown in Figure 34.

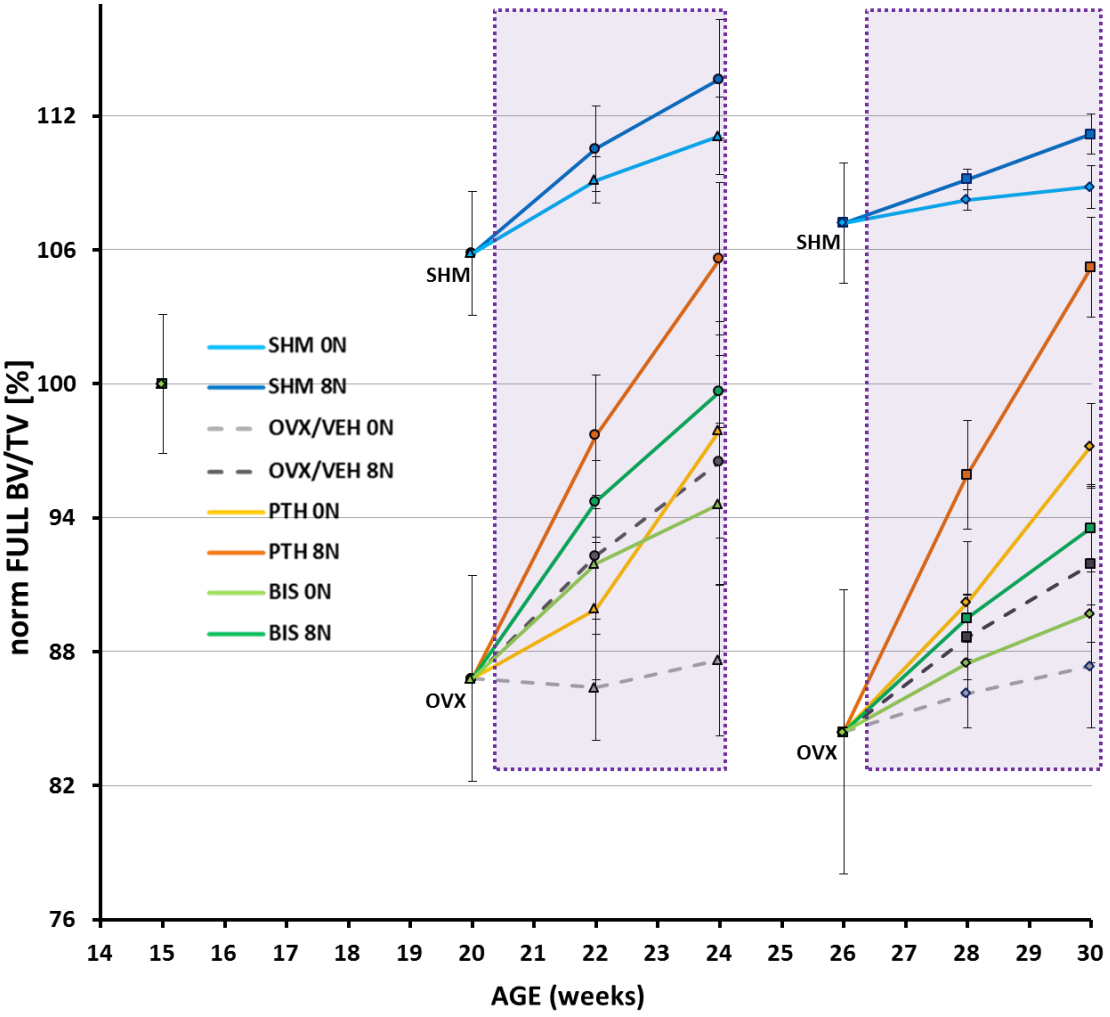

Figure 34: Physiome map of Full BV/TV. Early loading studies are represented with ○ and Δ, while late loading studies are represented with □ and ◊. Grey boxes mark data normalized to treatment start at week 20 and 26, respectively. For n per group see **Table 16**.

Cortical compartment

Also in the cortical compartment the effect of ovariectomy was visible. While at both time-points, 5 and 11 weeks after OVX, the cortex was getting thinner, thickness was increased in sham operated animals.

Cortical thickening throughout the loading and treatment period was mainly influenced by loading and not by pharmacological treatment. Loading increased Ct. Th by the same extend in all loaded groups of the early loading series. When loading was started after 11 weeks, cortical thickening apparently was susceptible to a second stimulus as the cortex thickened significantly more in PTH treated mice than in bisphosphonate treated or vehicle injected mice.

During the early loading experimental series the cortical thinning continued in untreated animals. This could be stopped with bisphosphonate injection. However, as Ct. Th had reached a minimum value in the late loading experimental series before treatment started, the preserving effect of bisphosphonate treatment did not result in an improvement compared to non-treated animals. When only PTH was injected, cortical thickness dropped in the first two weeks even more than in non-treated mice in both experimental series. This loss was compensated in the last two weeks and after 4 weeks of treatment values reached the same level as non-treated mice.

Cortical thickness can be seen in Figure 35.

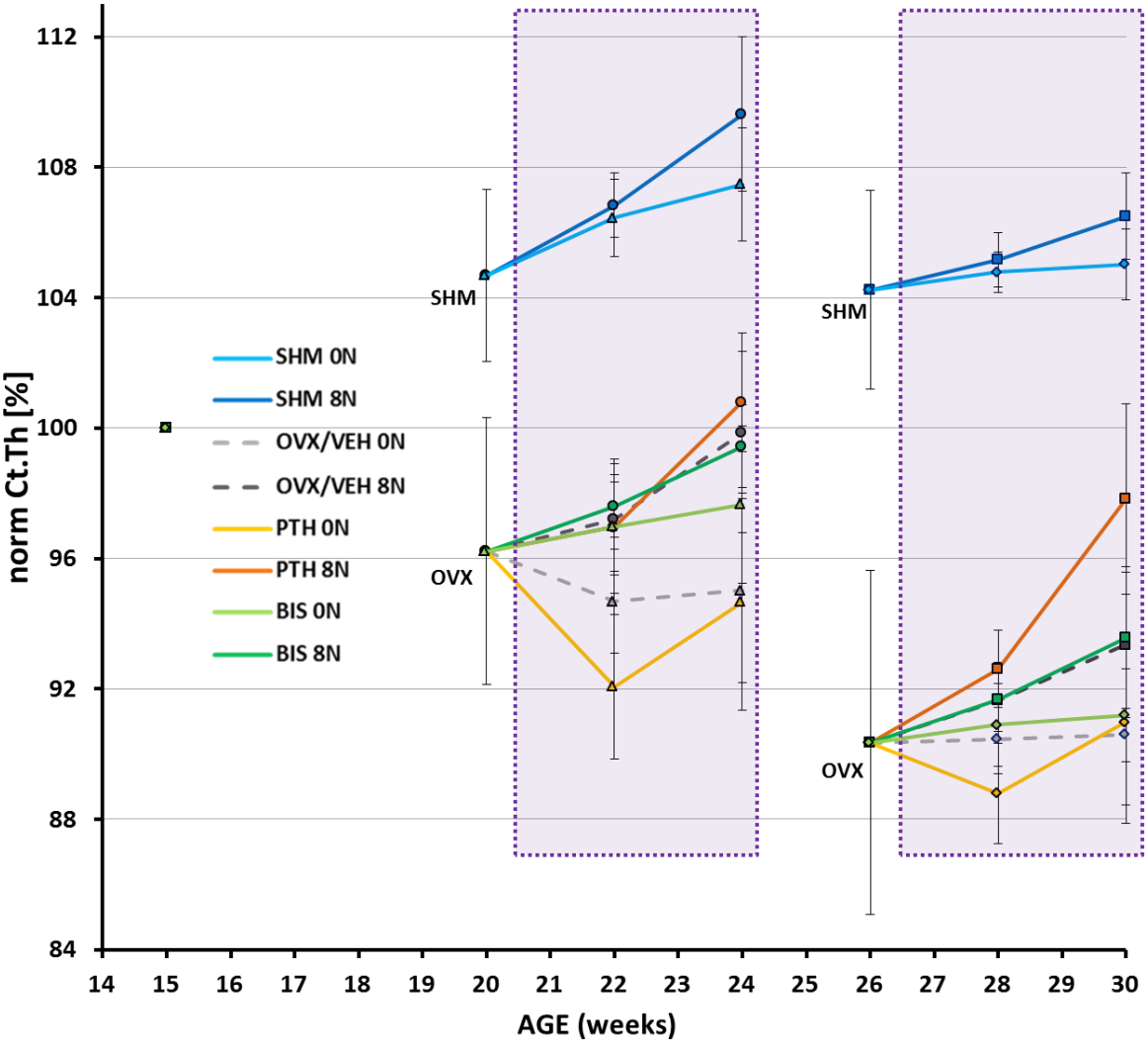

Figure 35 Physiome map of Ct. Th. Early loading studies are represented with ○ and Δ, while late loading studies are represented with □ and ◊. Grey boxes mark data normalized to treatment start at week 20 and 26, respectively. For n per group see **Table 16**.

In ovariectomized animals cortical % BV was reduced at both time points, 5 and 11 weeks after ovariectomy, while it stayed almost stable in sham operated animals.

PTH treatment in combination with loading induced the most prominent increase in cortical % BV in both series. In the early loading series all other treatments (PTH 0N, BIS 8N, BIS 0N, VEH 8N) induced similar effects and improved cort % BV in comparison to non-treated animals. In contrast in the late loading experimental series, only PTH treatment or loading could increase this value (with the highest effect seen in PTH treated animals). However merely bisphosphonate treatment did not induce significant changes compared to non-treated animals. Interestingly, after

the first two weeks in the early loading series PTH 0N animals even lost as much cortical % BV as VEH 0N mice and just showed a noticeably increase in this parameter during the last two weeks of treatment.

Cortical % BV is shown in Figure 36.

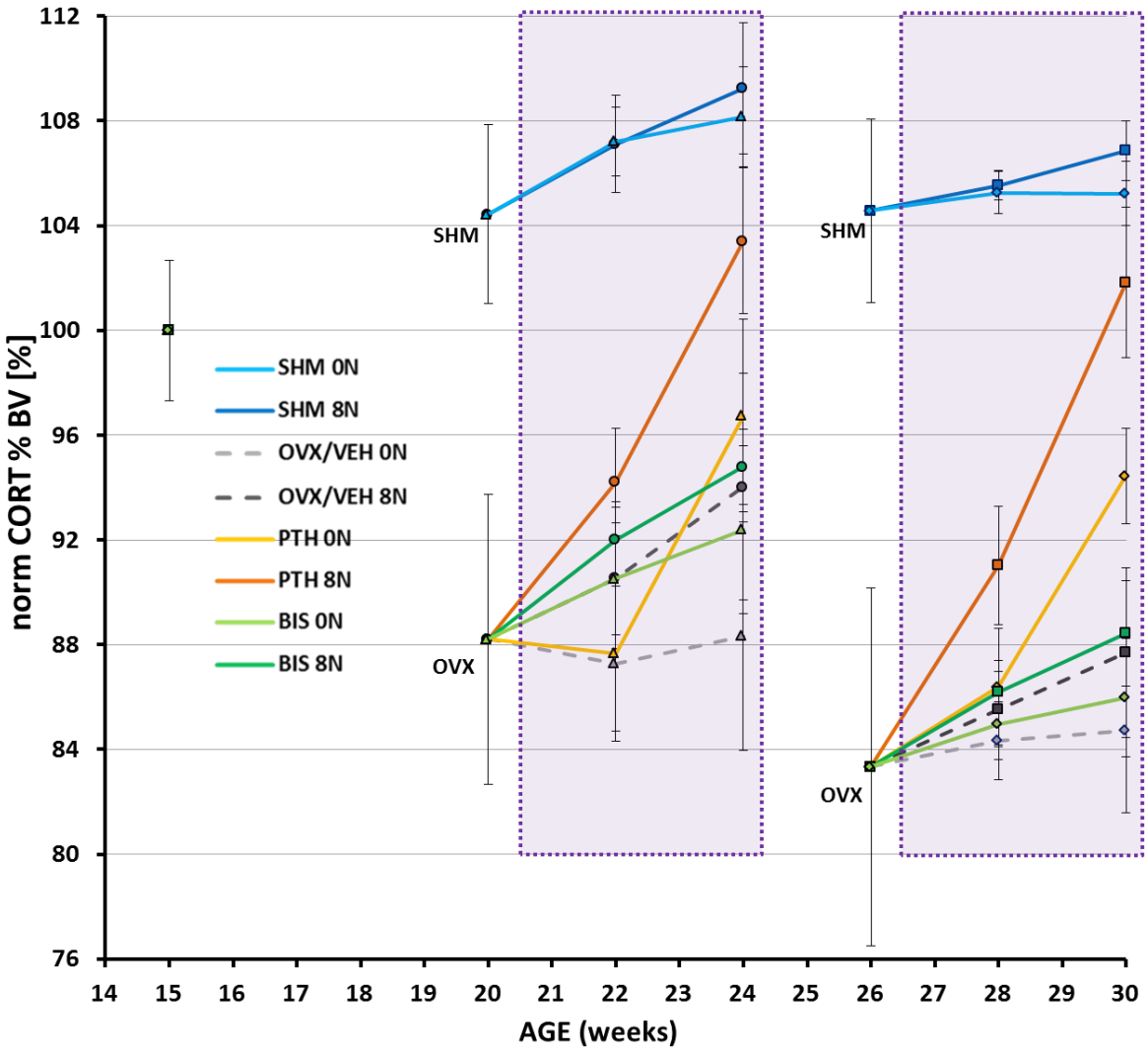

Figure 36: Physiome map of cortical % BV. Early loading studies are represented with ○ and Δ, while late loading studies are represented with □ and ◊. Grey boxes mark data normalized to treatment start at week 20 and 26, respectively. For n per group see **Table 16**.

Trabecular compartment

While at the age of 20 weeks no difference in Tb.N was observed between ovariectomized and sham operated animals, OVX mice at the age of 26 weeks had significantly less trabeculae than SHM mice.

Vehicle treated animals constantly lost trabeculae during both experimental series. This loss could be reduced with PTH treatment or almost stopped with bisphosphonate treatment. In the early experimental series bisphosphonate treatment slightly increased Tb.N. The on-going loss in vehicle treated animals is clearly a continuing effect of ovariectomy, as in sham operated animals Tb.N was not changed during the course of the experiment.

Trabecular number can be seen in Figure 37

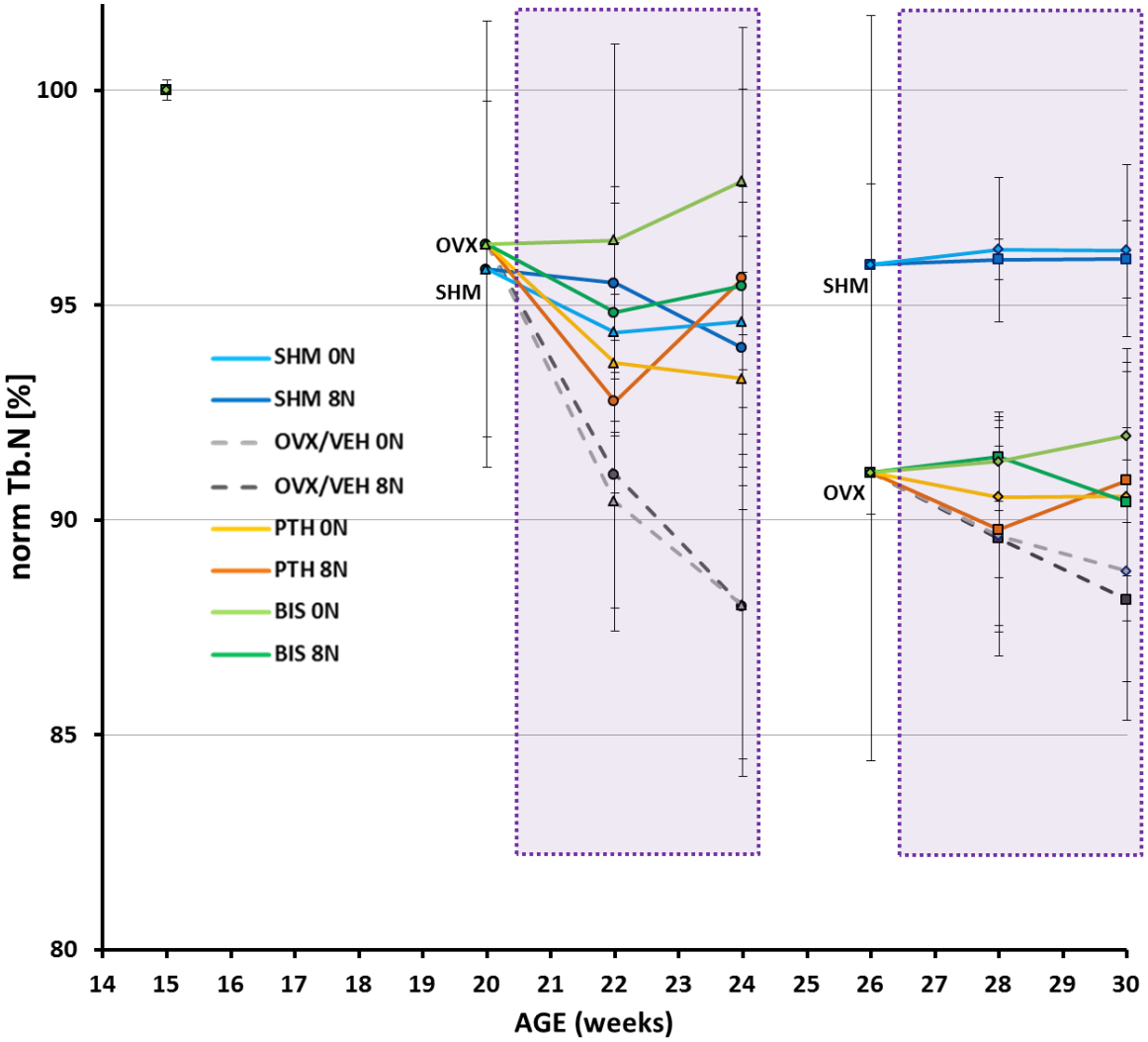

Figure 37: Physiome map of Tb.N. Early loading studies are represented with ○ and Δ, while late loading studies are represented with □ and ◊. Grey boxes mark data normalized to treatment start at week 20 and 26, respectively. For n per group see **Table 16**.

After ovariectomy trabeculae were thinned, while a thickening of trabeculae was observed in sham operated animals at the start of the treatment.

PTH treatment in combination with loading had the strongest effect in both experimental series. In the early experimental series, loading thickened trabeculae significantly more than PTH treatment. The opposite effect was observed in the late experimental series, where PTH treatment induced a greater thickness than 4 weeks of loading or combined bisphosphonate treatment and loading. Only bisphosphonate treatment did not result in thicker trabeculae in any of the studies. In general it can be said, that the effect of loading on Tb. Th was higher in the early loading series than in the late loading series. This was also true for sham operated mice.

Trabecular thickness is shown in Figure 38.

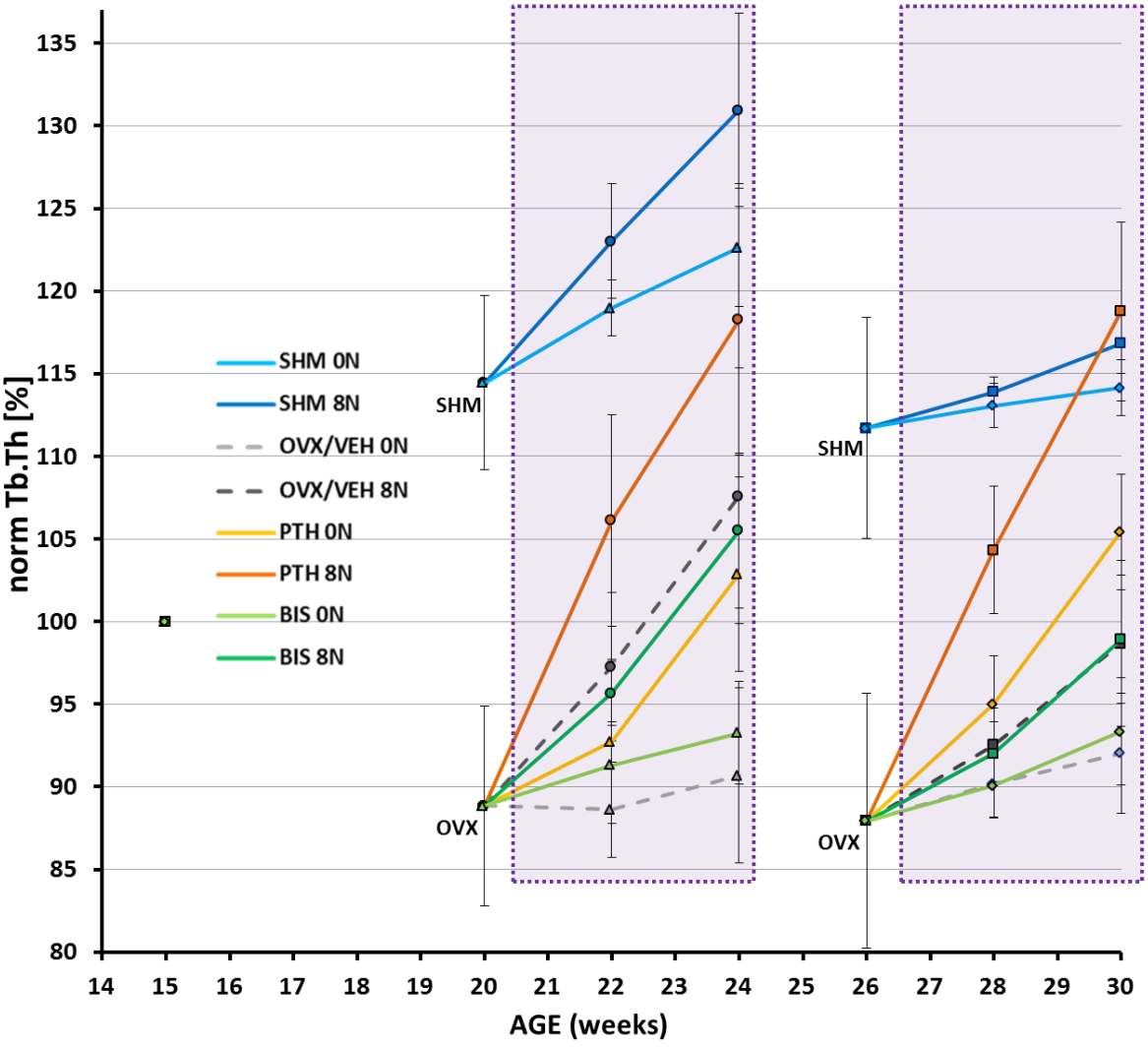

Figure 38: Physiome map of. Early loading studies are represented with ○ and Δ, while late loading studies are represented with □ and ◊. Grey boxes mark data normalized to treatment start at week 20 and 26, respectively. For n per group see **Table 16**.

As trabeculae were getting thinner and Tb.N was reduced after OVX, also Trab BV/TV was reduced 5 and 11 weeks after ovariectomy, while the increased in Tb.Th resulted in an increase in Trab BV/TV in sham operated animals.

Within one treatment period, the effects of treatments on Trab BV/TV where highest in PTH 8N, followed by PTH 0N, BIS 8N, VEH 8N, and BIS 0N. Despite for the sham operated groups, loading always significantly increased trabecular bone volume density compared to the corresponding non-loaded groups. As Trab BV/TV was still declining in non-treated animals during the early experimental series, it has to be admitted that the overall effect of any treatment was stronger in the early experimental series than in the late experimental series.

Trab BV/TV is shown in Figure 39.

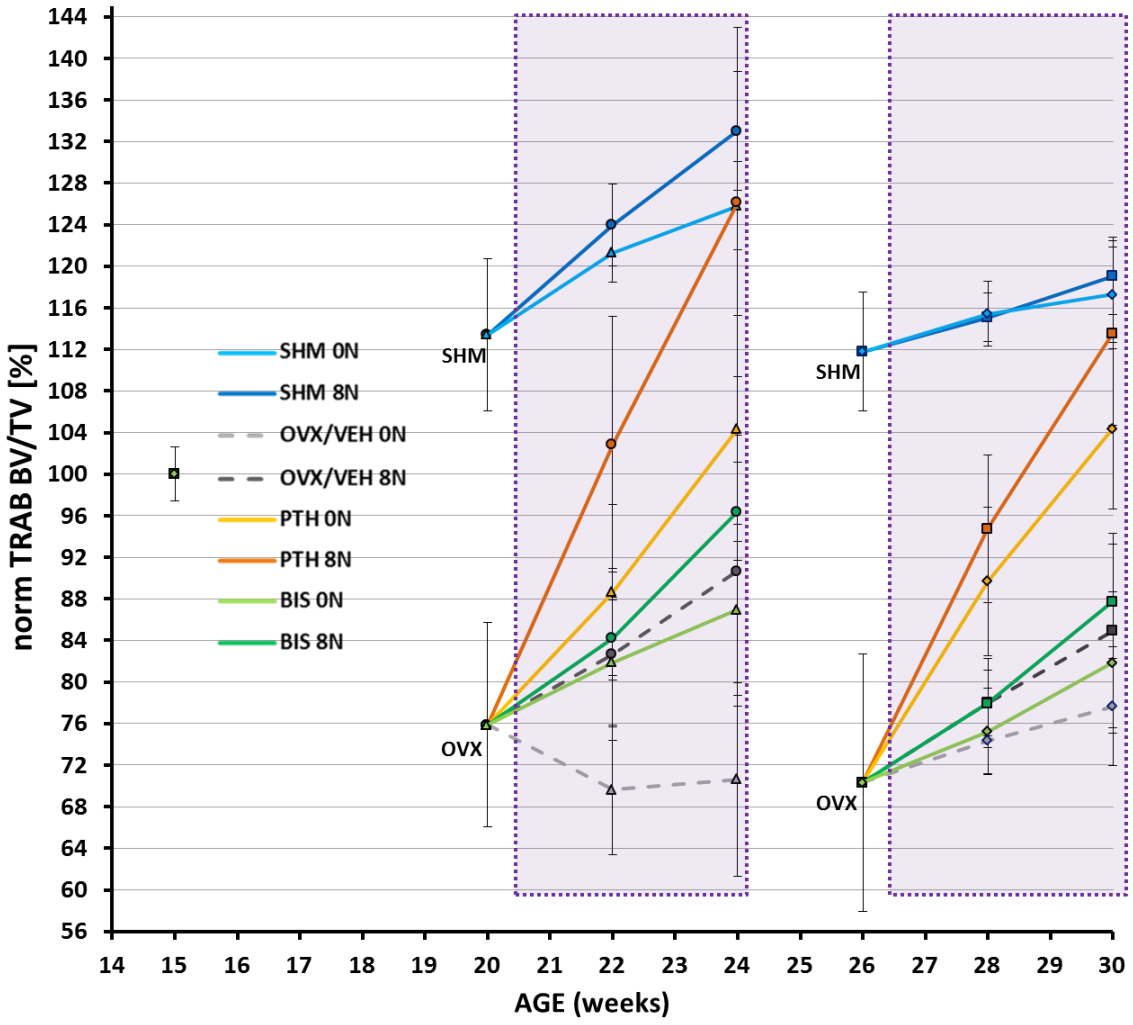

Figure 39: Physiome map of Full TV. Early loading studies are represented with ○ and Δ, while late loading studies are represented with □ and ◊. Grey boxes mark data normalized to treatment start at week 20 and 26, respectively. For n per group see **Table 16**.

Dynamic parameters

The following chapter will provide a summary and comparison of the dynamic parameters of all studies in both experimental series.

Bone formation

Bone formation rate was lowest in sham operated mice and increased in all OVX animals, showing that the estrogen depletion increased bone turnover rates. The highest values were found in PTH treated mice. Bisphosphonate treated and vehicle treated mice showed about the same BFR in both experimental series. When loading was combined with pharmacological treatment, it increased the effect of bisphosphonate treatment at all-time points. However, in combination with PTH treatment a significantly higher BFR could only be seen during the first two weeks but not during the last two weeks of both experimental series. While in the late experimental series both sham operated groups had a significantly lower bone formation rate than any other group, BFR of SHM 8N mice in the early experimental series did not differ significantly from the VEH 0N group.

Mineral apposition rate was significantly elevated in the PTH treated groups at all-time points. However, a decline was observed from the first two weeks to the last two weeks. While in the first two weeks loading significantly increased MAR in PTH treated animals, no significant differences could be observed during the last two weeks of both experimental series. Bisphosphonate treatment resulted in similar MAR as in sham operated animals in the early experimental series. However, during the late experimental series SHM mice showed a significantly lower MAR than any other group of this series. Loading increased mineral apposition rate in bisphosphonate, vehicle treated animals and sham operated animals during the last two weeks of the early experimental series.

Mineralizing surface was significantly higher in all loaded ovariectomized animals than in their non-loaded control groups. However, in sham operated mice no differences were seen in the late experimental series. The largest MS at all-time points was found in PTH treated mice subjected to loading. While in vehicle and PTH treated animals of the early experimental series an increase in MS over time could be observed, a decrease was found for the same groups in the late loading experimental series. However, PTH treated animals showed the largest MS at both time points in

the late experimental series and during the last two weeks of the early experimental series. All bone formation parameters can be seen in Figure 40.

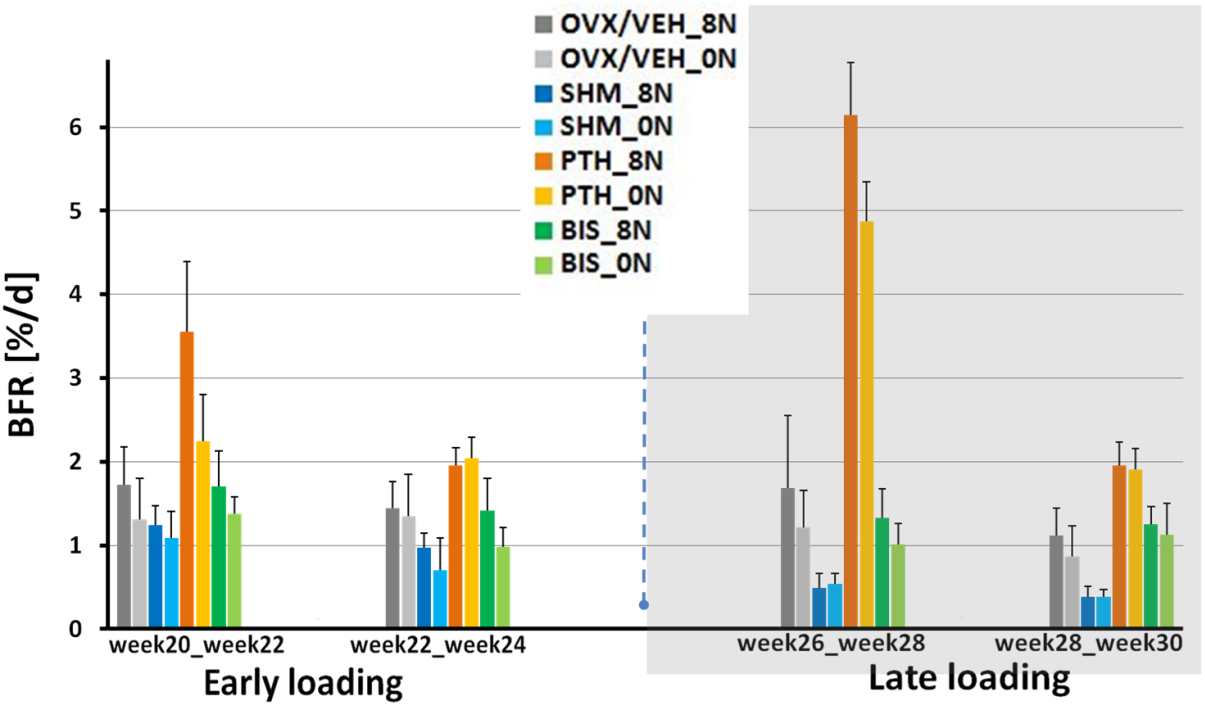

a)

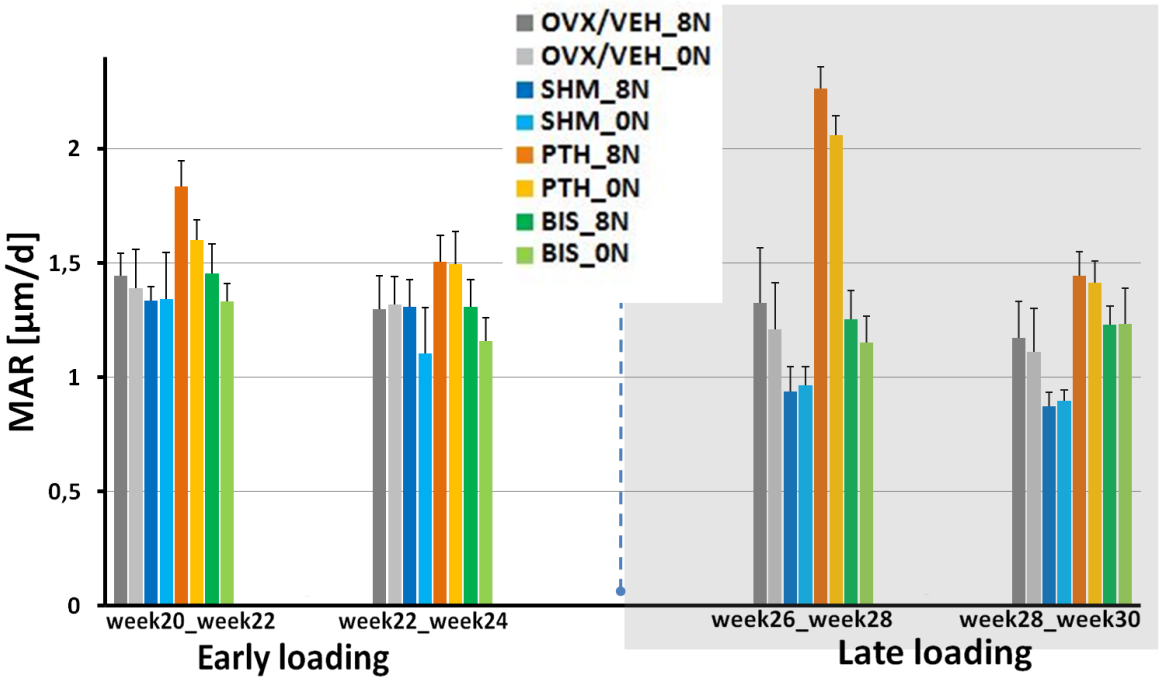

b)

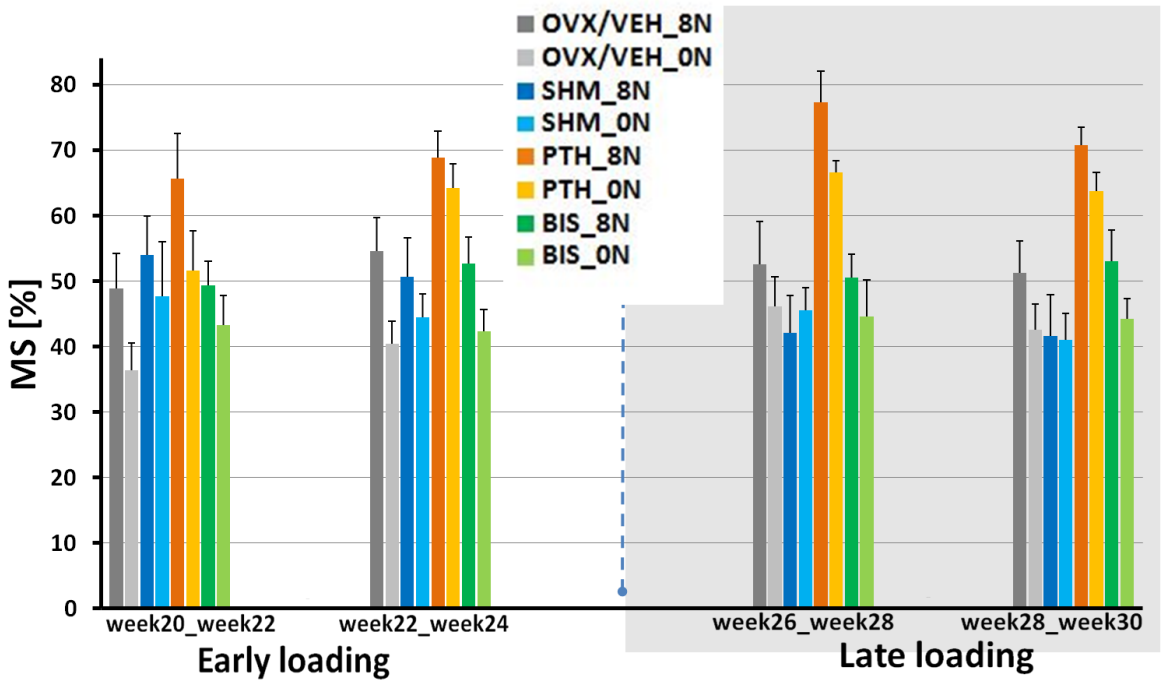

c)

Figure 40: bone formation parameters a) bone formation rate (BFR), b) mineral apposition rate (MAR), c) mineralizing surface (MS). The early loading study is presented with a white background while the late loading study is presented with a grey background

Bone resorption

In the early experimental series bone resorption rate was reduced by at least 20% compared to the corresponding vehicle treated non-loaded group, when loading or pharmacological treatment was applied. In bisphosphonate treated loaded mice it was even reduced by 70% during the first two weeks of treatment. During this time BRR in bisphosphonate treated mice was significantly lower than in PTH 0N or vehicle treated mice, while PTH 8N animals showed the lowest BRR. At all-time points vehicle treated non-loaded mice had a highly significant increased bone resorption rate compared to any other group in the early loading series. This difference was not as prominent in the late loading series. Sham operated loaded mice showed the lowest bone resorption during the whole late experimental series. While tendencies towards a reduced bone resorption rate in the loaded group were found when bisphosphonate treatment was combined with loading, significant differences can be found in PTH treated mice. Mineral resorption rate in the early experimental series was lowest in bisphosphonate treated mice and also in the late experimental series only SHM 8N mice had a lower MRR. Treatment with PTH increased MRR significantly. This effect was even enhanced, when loading was added to the PTH treatment.

Loading reduced eroded surface in all groups. PTH treatment reduced the amount of ES at almost all time points. This effect was enhanced when loading was added, as PTH 8Nmice showed the lowest ES at any time point in both experimental series. Bisphosphonate treated animals showed similar ES as vehicle treated or sham operated groups. When loading was combined with bisphosphonate treatment, eroded surface was reduced significantly. Bone resorption parameters are shown in Figure 41.

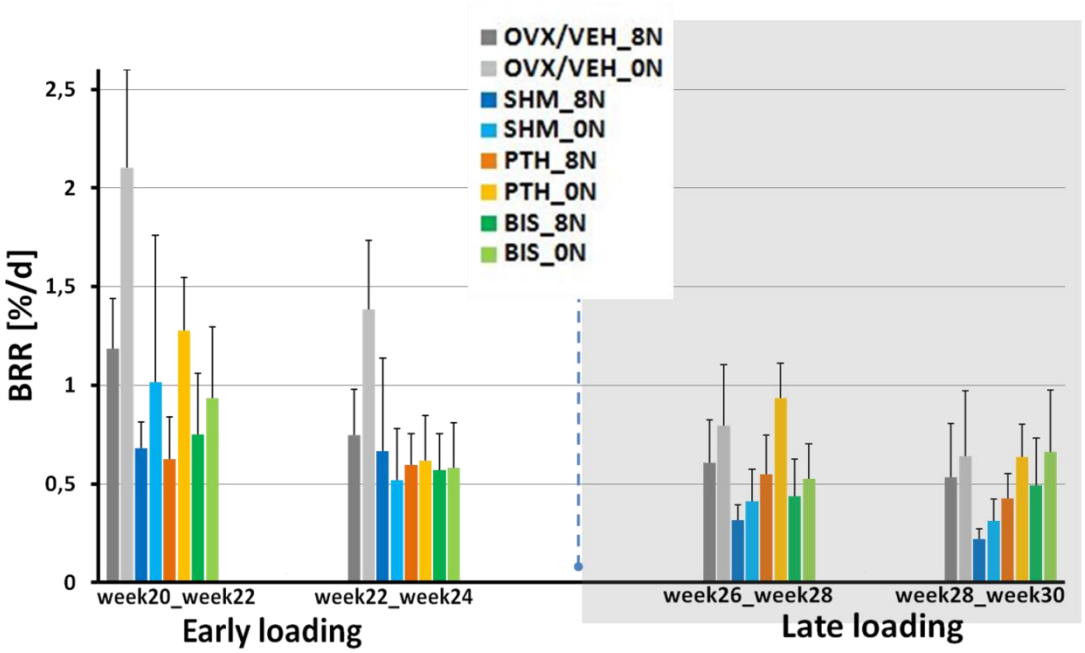

a)

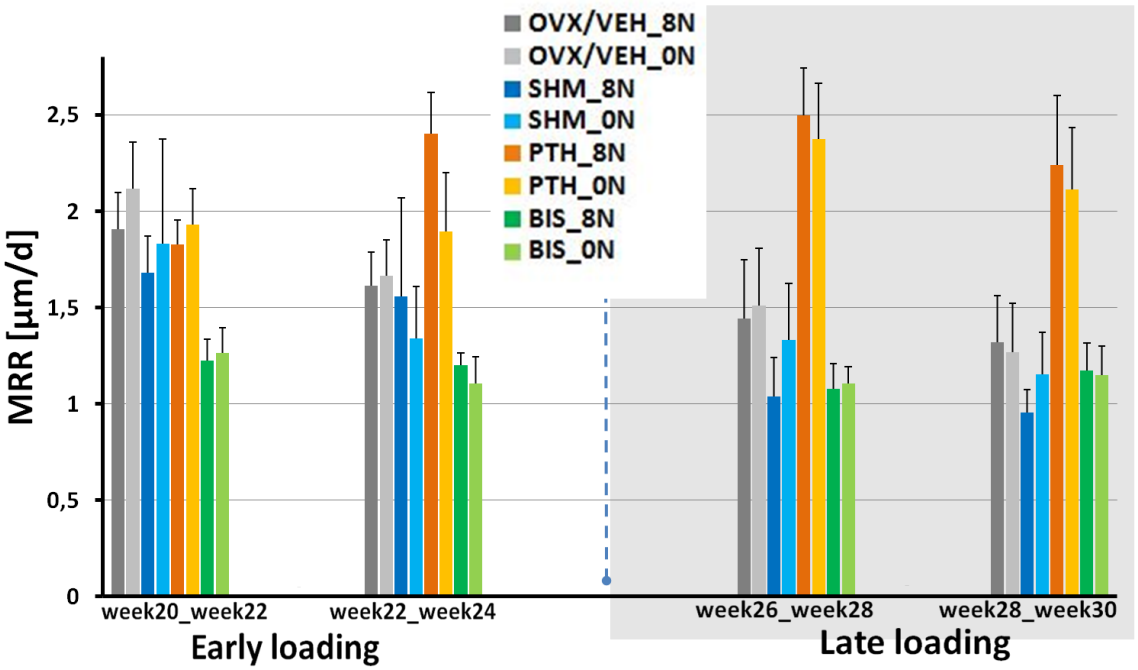

b)

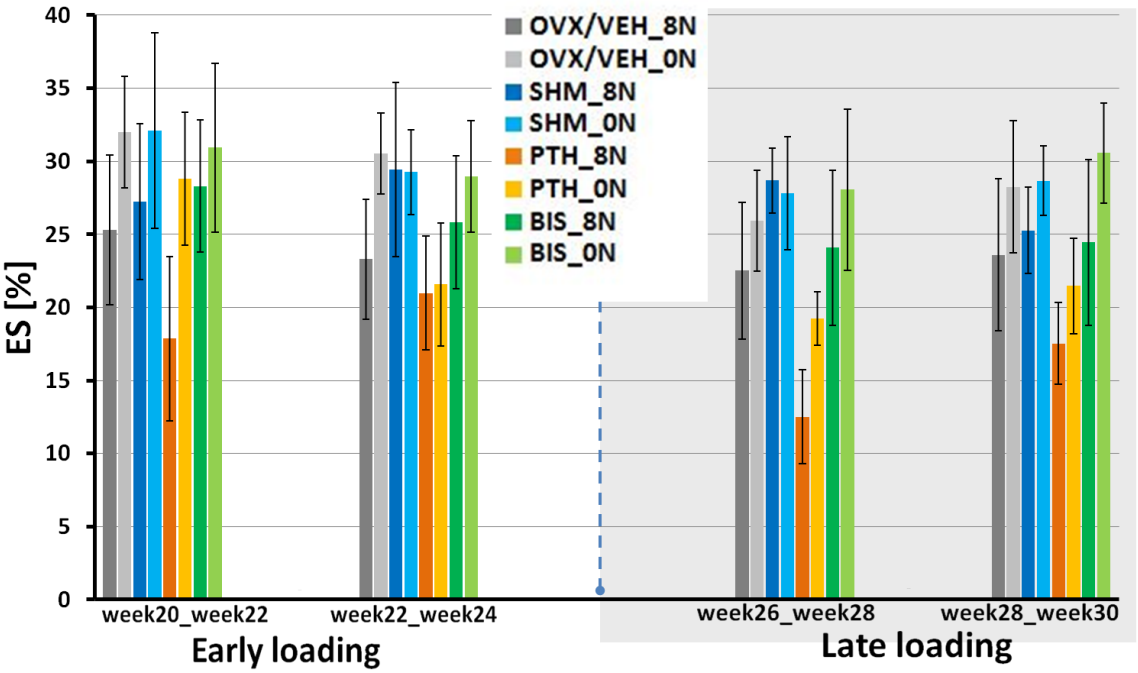

c)

Figure 41: bone resorption parameters a) bone resorption rate (BRR.BV), b) mineral apposition rate (MRR), c) mineralizing surface (ES). The early loading study is presented with a white background while the late loading study is presented with a grey background

5 Discussion

5.1 Model, Methods and experimental design

We used the mouse tail model, developed at the Institute for Biomechanics, to study the interaction of mechanical loading with osteoporosis treatment. Mice are well suited for experimental research. Not only because they are small, cheap and easy to handle, but also most biological mechanisms are similar to those in humans. Another advantage is that the genome of the mouse has been mapped and therefore a wide range of genetically modified strains are available to specifically study certain genetic effects. The use of standardized inbred mouse strains reduces the required number of animals per experiment remarkably. Standardization of experiments can be enhanced by standardized housing conditions, which can be achieved much easier in small animals than in large ones. It has to be admitted, that growth plates of bones in mice, in contrast to human bone, never close. Therefore murine bones continuously grow during the entire lifetime. Another difference compared to human bone, is that the cortex of mouse bone does not show a structure of haversian canals and osteons. However, the main focus of the studies presented in this thesis was to investigate trabecular remodeling. Therefore the mouse bone was well suited.

The ovariectomized mouse as model for postmenopausal osteoporosis

In humans, the most common form of osteoporosis is postmenopausal osteoporosis which is caused by cessation of estrogen production. Estrogens are necessary to maintain the balance between bone resorption and formation. When the production of these hormones is not sufficient anymore, bone remodeling is shifted towards higher resorption, resulting in deteriorated bone mass and bone morphologic parameters [257, 258]. Therefore human postmenopausal osteoporosis is characterized by increased bone turnover with a negative balance between formation and resorption resulting in bone loss.

We used ovariectomy to induce estrogen depletion in our mice. Ovariectomy resulted in significant loss of bone mass and increased bone formation and resorption rates. These effects are similar to those described in studies performed in human bones [257, 258]. In our studies almost all static parameters decreased after ovariectomy. Full and trabecular BV/TV were decreasing significantly, as well as cortical % BV. However, while trabeculae got thinner in

ovariectomized animals, their number was not reduced much compared to intact animals. The cortex was getting thinner as well when estrogens were lacking. This deteriorated bone structure also reduces mechanical bone stability, as has been shown recently in a study performed at our institute [259]. Similar changes can be found in humans after menopause and the reduced mechanical stability of bones increases fracture risk in humans significantly [3, 14].

However, sex hormones are known to not only balance bone formation and resorption, but also have different effects on bone [95]. Sex hormones for example influence the levels of growth hormones. Indeed we found an accelerated longitudinal growth in the OVX animals compared to the controls. The investigated tail vertebra was longer and bone volume as well as trabecular volume increased significantly more during the course of our experiments. Moreover, castrated animals were found to be heavier than the control animals at the age of 20 and 26 weeks, respectively. On the one hand this was due to an increased growth resulting out of the lack of sex hormones. On the other hand, Gloy et al. described that ovariectomized animals have an increased body fat content [260], which might also be a reason for the weight gain in our OVX mice.

In general it can be said that ovariectomy in the mouse is a suitable model to mimic postmenopausal osteoporosis. The animals show a high turnover bone loss, but no fractures. However, as we investigated bone remodeling, fractures were not necessary for our research and therefore would not be tolerable from an ethical point of view.

The mouse tail – a loading model with yellow bone marrow

To investigate the effect of loading in bone, mimicking the situation in human osteoporotic bone, the bone of interest has to fulfill certain requirements:

The bone should be preferably small and accessible for micro-CT measurements. Furthermore it has to be accessible to apply loading and the bone has to represent the human condition during postmenopausal osteoporosis.

As humans get older, the red bone marrow, which used to be the source for hematopoietic stem cells, slowly turns into yellow fatty bone marrow at many sites [261, 262]. It was also shown that in osteoporotic patients the content of bone marrow fat is higher than in age matched controls [262]. Other studies have shown an inverse relation between lipid concentration of HDL and BMD [263]. A possible link between the fat and the bone metabolism was found just recently by

Kim et al. [264], who investigated the levels of monocyte chemo attractant protein-1 (MCP-1) production in ovariectomized rats. Fat tissue of OVX rats expressed higher values of MCP-1 than that of sham operated animals. Furthermore, the study showed that cell culture medium extracted from fat tissue from ovariectomized rats stimulated osteoclastogenesis to a higher extend than medium from control animals. This led to the conclusion that elevated MCP-1 levels in ovariectomized animals contribute at least in part to the increased bone loss. As in ovariectomized mice the weight gain is higher than in sham operated mice it can be assumed that similar mechanisms apply for these animals. The tail vertebrae in mice do contain yellow bone marrow [265]. Furthermore it has been shown that the content of yellow marrow fat increases after ovariectomy. Furthermore, Gimble et al. could show in the same study in rats that there is a negative correlation between yellow bone marrow and bone mineral density [266]. In contrast to our findings, another study, also performed in rats, could not detect any bone loss after ovariectomy at sites of yellow bone marrow. Even though a high bone turnover was apparent, no difference in bone mineral density was observed between ovariectomized and sham operated rats after 6 months [267]. Li et al. state that an imbalance between bone formation and resorption can only be found at sites of red marrow. One of the reasons could be the fact that yellow bone marrow is less vascularized than red bone marrow. Therefore, osteoclast precursors, nutrients and hormones which are all delivered via the vascular system cannot reach the bone as well as in red bone marrow. Consequently, this difference in vascularization leads to a more favorable environment for bone resorption at sites of red bone marrow. These findings are not only contradictory to our studies but also to the clinical situation found in humans. Ovariectomized mice in our studies showed a clear loss in Trab BV/TV already 5 weeks after ovariectomy. Bouxsein et al. discovered a loss of vertebral trabecular bone volume after ovariectomy for all tested mouse strains, except for C3H/HeJ mice [215]. Furthermore, a study performed at the institute recently could show, that ovariectomy increases both bone formation rate and bone resorption rate, compared to sham operated mice [268].

Another advantage of using the mouse tail vertebra is that it contains more trabecular bone than mouse tibia or ulna, which are often used in other osteoporosis studies . Ulna and tibia belong to the long bones which do not contain many trabeculae. However, osteoporosis in humans appears mainly in trabecular bone.

One disadvantage of the tail vertebra is, that in order to load the vertebra pins have to be inserted into the adjacent vertebrae. However, the pinning procedure and loading were tolerated well. Unfortunately, some mice had to be excluded from the study due to tissue swelling around the pins, which sometimes worsened during the loading period. No distinct underlying cause was found, but one reason could be adverse effects due to the pin-material or accidentally destruction of certain structures, such as muscles, tendons and vessels during the pinning procedure. This can result in an impaired healing process. Of course this problem could have been avoided by loading model which does not need pins.

In contrast to many other loading models, where load is applied to the tibia or ulna and the contra lateral side is used as a control, the studies presented in this thesis used non-loaded animals as controls, which could be seen as a disadvantage. However, loading of tibia or ulna and the therefore necessary flexing of the adjacent joints can cause pain or unpleasant sensations even after loading. Hence the contra lateral side might be used more for walking resulting in a non-physiologic overload of this side and an avoidance of loading at the ipsilateral side during normal walking. This unbalanced use of both legs could falsify the results. As the caudal vertebrae are not directly used during walking none of these effects can be observed in the tail model. Moreover, climbing behavior, where the tail is used for, did not seem to be reduced in loaded animals compared to non-loaded controls.

In conclusion the mouse tail vertebra is very well suited to study the effects of loading on postmenopausal osteoporosis. It is a small, easy accessible bone that mimics human conditions well. Furthermore the use of the tail vertebra has no adverse effects on the animals.

In vivo micro-CT and longitudinal design

Our studies were designed as longitudinal studies, which helps to reduce the number of animals per experiment and is in accordance with the 3R concept. With *in vivo* micro-CT measurement the effect of ovariectomy, loading and pharmacological treatment on mouse bone could be monitored over a long period of time and morphological parameters could be calculated at a three-dimensional level. This is a great advantage over cross-sectional studies and histomorphometry. In cross-sectional studies just one time point can be evaluated and inter-individual differences can overlay treatment effects. Furthermore, bone is a three-dimensional construct. Therefore, evaluating just two- dimensional histological slides will never result in the

same exact and deep insight into the structure as a three-dimensional evaluation. As bones of mice are relatively small, a very high resolution can be achieved in an appropriate scanning time. This is another advantage of using small animals, such as mice.

Until recently, histology used to be the standard method to evaluate dynamic parameters. Although bone formation parameters can be evaluated easily with this method, it is hard to specify bone resorption parameters as, of course, resorbed bone cannot be evaluated any more. A standard technique is TRAP staining, which stains for active osteoclasts and therefore gives an estimation of the current number of osteoclasts and the amount of surface they are covering. However, a new method was developed at our institute recently. This allows to register images from longitudinal *in vivo* micro-CT measurements and evaluate bone formation and bone resorption parameters at a three dimensional level [42]. As *in vivo* scans are used, follow up measurements are possible and bone remodeling can be followed over a longer time. This is in contrast to histology, where just one measurement per animal is possible.

Physiome map

Often it is difficult to compare the results of different studies due to differences in study design, treatment periods and differing basal values between groups. In our project we used the same time course and experimental setup for all experimental series. This allows the comparison of different treatment groups.

To overcome inter-individual differences of the absolute values we normalized the results to a certain time point. This normalization was used to create a physiome map. The physiome map is, to our knowledge a unique tool to plot the bone morphologic parameters of different studies together in one diagram. This overview makes it possible to directly compare the effects of each treatment and to evaluate and compare the development of bone parameters in intact and ovariectomized animals. Of course, results from other studies can be added as well, which increases the information value of the physiome map.

5.2 Results

5.2.1 Loading in ovariectomized mice

The effect of loading the 6th caudal vertebra in ovariectomized and sham operated mice was studied. Depending on the experimental series, the studies started 5 or 11 weeks after

ovariectomy. This time points were chosen accordingly to a study performed recently, in our laboratory [43]. In this study 15 week old mice were ovariectomized or sham operated and measured with *in vivo* micro-CT every second week for the next 12 weeks. It was shown that bone loss after ovariectomy proceeds in two phases. The first phase with fast bone loss lasts until about week 8 followed by the second phase of slow bone loss, where a plateau is reached. These results support the findings by Boyd et al., who studied the effects of ovariectomy in rats and found the bone loss to occur in two phases as well. However, because the remodeling in rats takes much longer the first fast phase was in the first three months after ovariectomy, followed by the slower phase [269]. Boyd also proposed that any treatment should be started in the first three months, as in that time bone response to treatment is much better than in the later slower phase. According to the findings of the previous study from our institute we chose the two different time points for the starting of the loading and treatment period. Five weeks after ovariectomy bone loss is still in the fast phase, while eleven weeks after ovariectomy it has reached its plateau.

In general, it can be said that loading had much bigger effects in ovariectomized mice than in sham operated animals. However, in both groups, an early start of loading induced a larger increase in bone mass than a late loading start. Mice seem to grow more during the early phase than in the late experimental series. Sham operated non-loaded mice (SHM 0N) have a stronger increase in full, trabecular and cortical bone mass as well as in trabecular and cortical thickness when the treatment is started early compared to a late treatment. Apparently, if the growing rate is faster, also loading seems to have a stronger effect on the bones. The effect difference between SHM 0N and SHM 8N mice is much bigger in the early loading study for Trab BV/TV, Tb.Th and Ct.Th than in the late loading study. Similar findings are known from human medicine. In children physical activity contributes to gain a high bone mass, whereas in adults, which are not growing anymore, physical activity rather helps maintaining the peak bone mass achieved in adulthood than increasing bone mass [270-272]. However, mice do not close the growth plates and therefore continue growing throughout their whole life time. Nevertheless, a higher growth rate seems to increase the effect of loading. Another possible explanation for the lack of response in late loading sham operated mice could be that due to growing these mice already have a high bone mass and loading of 8N is not sufficient anymore to induce osteogenic signals. Several studies, using mice of different strains differing in bone mass have shown that the effect of

loading but also ovariectomy is dependent on the basal bone mass [215, 251, 273]. A former study performed at the Institute for Biomechanics showed that C3H/HeJ mice, which have a high bone mass do not react as well to loading as C57BL/6J mice of the same age, which have a much lower bone mass.

The effect difference in our studies between loaded and non-loaded ovariectomized mice is much bigger in the early loading study. As non-loaded ovariectomized mice in the early loading study still decrease in Trab BV/TV, OVX 8N mice also have to counteract on this loss, whereas OVX 0N mice of the late loading study already increase Trab BV/TV. Therefore, the increase from OVX 8N compared to OVX 0N mice in the late loading study is even less. The reason for this difference could be that as the mice in the early loading study did not lose so much bone it is easier for them to regain more bone mass after loading. Maybe also the BMU are more active in these mice, so that the shift towards an increasing bone mass caused by mechanical loading has a greater effect.

Ovariectomy and the resulting estrogen depletion are known to increase bone remodeling rates. This has been shown in many previous studies [183, 232, 274] and the findings were confirmed by our results. Bone formation rate was increased in both experimental series with OVX compared to SHM mice. Also mineral apposition rate was elevated in the ovariectomized mice in both experimental series. While in the early loading experimental series there was only a trend towards an elevated MAR in OVX mice compared to sham operated animals, in the late loading experimental series OVX 8N mice showed a significantly higher MAR. Mineralizing surface was not affected by ovariectomy, but by loading. This leads to the conclusion that osteoblasts deposit more osteoid in a certain time but at fewer places in loaded ovariectomized animals. When comparing the absolute values of the formation parameters of all groups it can be noticed that in the early loading experimental series not only mineral apposition rate but also bone formation rate have higher values than in the late loading experimental series. One of the reasons, especially in the sham operated mice, could be that mice reach skeletal maturity at the age of about 20 weeks [275]. At this age they have reached their peak bone mass, however, the cross sectional geometry increases up to the age of about 24 weeks. This period of reaching skeletal maturity corresponds to the age that mice have during the loading period in the early loading experimental series. Therefore, as they are still growing and reaching skeletal maturity

bone formation parameters might be enhanced compared to mice of the late loading experimental series, which already have reached their peak bone mass and have reached full skeletal maturity. When load is applied to fully mature bones at peak bone mass, the resulting strains are less than in younger animals. Therefore, the applied load of 8N probably was not appropriate to induce a sufficient mechanical loading signal. This could also explain, why sham operated mice of the early loading study show some reaction to the loading while sham operated mice of the late loading study are hardly affected by loading. Furthermore, ovariectomized mice are still in the fast bone loosing period during the early loading experimental series. Maybe, when the bone loss reaches a steady state in the late loading experimental series also bone remodeling slows down and the turnover is not as high as it was at the beginning anymore. The strains induced by 8N loading are different in ovariectomized and sham operated animals. As it is well known that strain rates do influence the outcome of mechanical loading [226, 251], it could be helpful if in further studies the strains are determined and the amount of load is adjusted induce the same strain in all groups.

In a high turnover remodeling state not only bone formation but also bone resorption parameters are elevated. The results from our studies show that mineral resorption rate has higher absolute values in the early loading experimental series than in the late loading experimental series. The same factors as for mineral apposition rate could be the reason for the differences between early and late loading experimental series. (On one hand skeletal maturity, which is not yet reached in the early loading study but in the late study. On the other hand mice in the early study are still in the fast bone loosing period after ovariectomy, while bone loss in the late study has reached the slower phase.) In both experimental series at least a trend towards an elevated MRR in ovariectomized mice could be observed. Eroded surface was reduced by loading in both series. In the late loading experimental series OVX 8N mice even showed the lowest eroded surface of all groups, which is in accordance with previous studies from our institute [276]. Furthermore, the biggest difference between loaded and non-loaded mice was observed in the early loading experimental series. This again supports the idea, that younger mice or animals in the fast bone loosing period are more susceptible to mechanical loading than at an older age and in the plateau phase. Bone resorption rate, although reduced by loading as well was highest in ovariectomized animals in both experimental series.

These findings show, that mechanical loading has a beneficial effect on ovariectomized mice. It increases bone formation parameters and decreases bone resorption. Due to hormone depletion after ovariectomy, bone remodeling is elevated. Both bone formation and resorption are increased, however, the balance is shifted towards a higher bone resorption. When this increased bone resorption can be alleviated, for example with antiresorptive treatment, bone loss can be stopped or slowed down and eventually bone formation can exceed bone resorption.
The positive effects of mechanical loading in ovariectomized mice on bone remodeling have been shown previously in mice and rats as well as in humans [183, 206, 224, 232, 274, 277].

5.2.2 Loading in pharmacological treated ovariectomized mice

To treat mice with pharmacological substances, the two most often applied medications from human medicine were used. As an anticatabolic treatment served the bisphosphonate zolendronate and as an anabolic treatment the hormone PTH. Again two different starting points for the treatment were chosen. The early point was during the phase of fast bone loss 5 weeks after the ovariectomy and with the second time point treatment started when the osteopenia was already established and bone loss was progressing slower. For each medication own vehicle control groups were studied as well. Additionally, half of the mice were subjected to 8N loading, while the other half served as a control at 0N load. The aim was to investigate not only the effect of pharmacological treatment or mechanical loading on ovariectomized mice, but also to gain insight into the combinatorial effect of these two and to investigate this in a longitudinal study approach.

5.2.2.1 PTH studies

The physiological function of PTH is to increase blood Ca^{2+} levels if needed. Therefore, it increases osteoclast activity and the release of calcium, as bones function as internal Ca^{2+} storages. However, if PTH is given in an intermittent fashion, it increases bone formation and enhances bone quality. PTH is so far the only EMEA approved anabolic drug to treat osteoporosis. It enhances bone remodeling and shifts the remodeling balance from net resorption back to net bone formation. These effects have been observed in studies on humans for many years [25, 29, 278, 279]. Injection of PTH alone already had a big impact on bone parameters. However, the combination of PTH injection and loading has been found to be additive or

synergistic in several studies [190, 280, 281]. In the studies presented in this thesis the combination of PTH and loading induced the biggest changes in almost all parameters. Only Tb.N was not changed with combined treatment, however a decline was observed in the other groups. For most parameters, PTH alone has a bigger effect than loading alone. However, Ct.Th first decreased in both PTH 0N groups and returns back to basal values towards the end of the treatment period. In contrast, in all other groups of both experimental series Ct.Th increases during the whole study. An additive effect was found for all static parameters in the early loading experimental series and for most of the static parameters in the late loading experimental series. However, the combinatorial effect on Full BV/TV, Ct.Th and Cort % BV was synergistically and almost synergistically on Tb.Th in the late loading experimental series.

An explanation for this synergistic effects could be that both, PTH and mechanical loading, stimulate the same or interacting biochemical pathways. For example, it was found, that PTH as well as loading increase IGF-1 levels [165]. Furthermore, a study performed by Carvalho et al. showed that intracellular signals like cAMP, IP_3 and protein kinase C increase with mechanical strain. However, their levels are increased even more when PTH was added to the cells [190]. PTH not only increases the stimulation of the same biochemical pathways as mechanical loading, but it is important for sensitizing osteoblasts for osteogenic signals. This is done probably by enhancing the mobilization of intracellular calcium via the aforementioned intracellular signals [282]. Chow et al. subjected rats to thyroidparathyroidectomy (TPTX) [281]. These rats were lacking hormones produced by the thyroid and parathyroid gland, namely Thyroxin, Calcitonin and PTH. Applying mechanical stimulation to these rats did not increase bone formation rate, while a significant increase was observed in intact animals. When hormone deficient rats received PTH prior to the loading, bone formation rate increased significantly. However, when PTH was injected after the loading, dynamic parameters did not change. This proofs that physiological levels of PTH are important for osteoblasts to be able to react to mechanical stimuli.

While in our studies PTH injections alone exert a greater effect on many parameters than loading alone as it was also found in another study [283], there is at least one study that did not find a more positive effect of only PTH injection [281]. However, this difference is probably due to the fact that this study used rats instead of mice.

It is well known that mechanical loading induces bone formation at sites of high stresses and strains resulting in improved biomechanical parameters and higher bone strength. The question is whether the bone gain induced by PTH treatment results in similar improvements of biomechanical parameters. McAteer et al. compared the amount of bone gain after PTH treatment or mechanical loading with the resulting increase in bone strength [283]. With both treatment regimens bone strength was increased by 20%. However, bone mineral content was only increased by 4% with mechanical loading while an increase of 11% was observed after PTH treatment. This implies that loading ads bone at biomechanical important sites, whereas PTH treatment leads to bone gain at all sites, no matter if stresses or strains are high or low. When combining loading with PTH treatment Roberts et al. found a trend towards a more localized bone formation at biomechanical relevant sites [284]. Therefore, it would be interesting in further studies to do a strain energy density analysis of treated bones and perform biomechanical tests. One study supporting the idea that PTH might override the local mechanical control of the bone has recently been performed at our institute [285]. The authors did not see any differences in strain energy density (SED) between quiescent and resorption sites in PTH treated animals, whereas in vehicle treated animals SED values were higher at resorption sites than at quiescent sites.

While in our studies in the trabecular compartment PTH exerted a positive effect on most statical parameters, cortical thickness was not increased by PTH treatment. Moreover, in the first two weeks, in both experimental series, a loss in cortical thickness was observed, which was compensated in the last two weeks. These findings are consistent with a study by Zhou et al., who evaluated the effect of PTH on cortical and cancellous bone at different skeletal sites [280]. While a strong increase in the cancellous compartment was observed, PTH treatment added only a little bone at the tibia but did not influence cortical width significantly in the vertebra. In this study 3 or 7 weeks of PTH treatment were sufficient to restore basal values, when the treatment was started 4 weeks after the ovariectomy. This is consistent with our findings. In the early loading experiment, where PTH treatment started 5 weeks after ovariectomy, basal values were restored after 4 weeks of treatment. However, in the late loading experimental series, with treatment starting 11 weeks after ovariectomy, bone loss was probably too progressed, as in this study PTH treatment alone could not restore basal values. When loading was added to the

pharmacological treatment, however, basal values were also reached in the late loading experimental series.

In the dynamic parameters mineral apposition rate was increased by PTH treatment in both experimental series. However, while during the first two weeks a significant difference between loaded and non-loaded PTH treated animals was observed, there was no difference between the two groups during the last two weeks in either of the experimental series. Especially in the last two weeks of the late loading study a drop in MAR was observed in PTH treated animals. Similar findings were also discovered in bone formation rate. It is increased by PTH treatment and loading, however in the last two weeks no difference between PTH treated loaded and non-loaded mice was observed. Furthermore, a drop in absolute values was found for PTH treated mice. Comparable results were found in other studies performed in mice as well [165, 286]. In the study of Childress et al., bone formation rate started to decline after 7 weeks of PTH treatment because the response to PTH started to plateau [286]. Solely PTH treatment has been found to induce a uniform formation throughout the entire bone [284]. However, in combination with loading the localized formation, due to the mechanical loading is augmented by PTH treatment. This study found a high correlation for the apposition pattern between the bones of rats that received bending and vehicle treatment and those receiving bending and PTH treatment. Therefore, the authors draw the conclusion that PTH enhances the mechanical induced bone formation. However, it is well known that a minimum strain is needed to induce bone formation. Maybe after two weeks of intensive bone formation the strains produced by the loading with 8N in our studies were not sufficient anymore to induce bone formation and hence no differences were observed between loaded and non-loaded PTH treated mice. Nevertheless, mineralizing surface showed a clear load dependent response throughout the entire study in both experimental series, however still elevated by PTH treatment. Therefore, the amount of surface covered by osteoblasts did not change during the study, only the mineral apposition rate. That might be due to single osteoblasts that are more active and produce more osteoid.

Our data for resorption parameters is somewhat inconsistent. While in the early loading experiment mineral resorption rate was elevated in PTH treated mice only in the last two weeks, it was increased in the entire treatment period in the late loading experimental series. Bone resorption rate was decreased in both studies and eroded surface was mainly reduced by loading, but also to some extend by PTH treatment. While an effect of loading in combination with PTH

treatment on eroded surface was observed only during the first two weeks but not during the last two weeks in the early loading it was the other way in the late loading study. The decreased eroded surface could simply be due to the fact that bone formation is occurring at so many sites, that there are fewer possibilities for osteoclasts to resorb bone. Only mineral resorption rate is increased with PTH treatment compared to vehicle treatment. However, other studies have shown that bone resorption is increasing after administration of PTH. As the hormone initiates new BMUs, first it has to promote the differentiation of osteoclasts from hematopoietic progenitors. However, due to the fact that bone formation and resorption are coupled and osteoclasts prepare the bone for osteoblasts, one would expect the bone resorption parameters to increase to the same extend and to the same time or even earlier, as formation parameters. However, this was not the case in our studies, as in the early loading experimental series mineral resorption rate only increased during the last two weeks, when mineral apposition rate already started to decline. This supports the idea that PTH exerts osteoclast independent stimulatory effects on bone formation.

One study, performed by Dognig et al., showed that after PTH infusion the number of osteoblasts increased, without requiring the proliferation of progenitors [30]. Therefore, the authors suggested that PTH also activates bone lining cells. Another study could proof that osteoclast independent mechanisms contribute to the increase in bone formation [26]. In this study PTH or RANKL was infused in mice. With both types of treatment osteoclast number increased, however, to a higher extend in RANKL treated animals. Osteoblast numbers on the other hand increased to the same extend in both treatments. Hence, the increase of osteoblasts per osteoclast was higher in PTH treated animals than in RANKL treated animals and also osteoblast activity was higher in those animals. Activation of lining cells and other osteoclast independent pathways could explain the initial strong response to PTH treatment followed by a decline of mineral apposition rate in the last two weeks and an increase in mineral resorption rate at the same time.

In general the findings of our experiments imply that PTH treatment in combination with loading is beneficial at all times of treatment start and even though solely PTH injection already exerts a more distinctive effect on many parameters than loading alone, combining both treatments contributes to an even higher effect.

5.2.2.2 Bisphosphonate studies

Bisphosphonates are probably the best known anticatabolics. They inhibit resorption by decreasing osteoclast activity and increasing osteoclast apoptosis. Therefore, bisphosphonates prevent further bone loss after menopause and eventually increase bone mass. Questions arouse if the reduced remodeling also impairs the positive effect of mechanical loading in bisphosphonate treated animals and humans. In the studies presented here, an additive effect of the combination of loading and pharmacological treatment was found for many parameters in both experimental series. Only for Trab BV/TV and Ct.Th in the early loading experimental series no additive effects were observed. As VEH 0N mice still lose in Trab BV/TV and Ct.Th in the early loading study, while they gain bone mass in the late loading study, the effect difference between loaded and non-loaded vehicle treated mice was much bigger in the early loading study. However, the effect of bisphosphonate injection or loading on these parameters is almost the same in both experimental series. There are several other studies supporting our findings, which showed additive effects of mechanical loading and bisphosphonate treatment as well [287-289]. Sugiyama et al. investigated the effect of dynamic load on mouse tibiae in combination with daily risendronate injection. In this study an additive effect on Trab BV/TV was found [287]. However, Stadelmann et al. did not find an additive effect of bisphosphonate treatment and mechanical loading. When evaluating mechanical loaded tibias the outcome was similar as with bisphosphonate treatment alone. However, at the area of highest strain in the tibia they could show that the combined effect on bone parameters was significantly smaller than the sum of the single effects. This lead to the suggestion that there might be a negative effect of bisphosphonate treatment and loading at very high levels of strain [290].

The anticatabolic action of bisphosphonates can be seen very nice in our mice in Tb.N. In both bisphosphonate treated groups of both studies Tb.N remained stable, while it was decreasing in vehicle treated animals. Loading did not influence Tb.N but Tb.Th as trabeculae became thicker in loaded groups compared to non-loaded groups.

An anticatabolic mode of action implies that bone resorption is reduced. As bone formation and bone resorption are coupled during bone remodeling one would expect also bone formation to be reduced. In our studies in the non-loaded bisphosphonate treated animals mineral apposition rate and bone formation rate were similar as in vehicle treated non-loaded animals and only in a few reduced compared to vehicle treated controls. Mineral apposition rate of bisphosphonate treated

animals in the early loading experimental series was even lower than in vehicle treated non-loaded animals. The same was found during the last two weeks of the early loading series in bone formation rate as well as for mineral apposition rate during the first two weeks of the late loading experimental series. However, when loading was applied on the bones no reduced bone formation was found and both mineral apposition rate and bone formation rate were similar to vehicle treated loaded animals in both experimental series. This shows that the effect of loading is not blocked by bisphosphonate treatment. Similar results were obtained also in other studies. In one study, Jagger et al. loaded the caudal vertebra of rats that were subjected to bisphosphonate treatment [289]. Bisphosphonate treatment did not inhibit the increase of dynamic and static bone formation parameters in these bones. However, Jagger et al. also evaluated dynamic parameters of the tibias, which did receive bisphosphonate treatment but were not affected by loading. In these bones a reduction of mineral apposition rate was found [289]. However, in the loaded vertebrae no differences in bone formation parameters were observed compared to non-treated animals. In another study, bisphosphonates were injected for three weeks, followed by a short period of loading [288]. Non-loaded bisphosphonate treated animals showed a significantly lower trabecular mineralizing surface than vehicle treated animals but no differences between treatment groups could be observed for the loaded animals. Moreover, significant higher bone formation parameters were observed in the bisphosphonate treated loaded group compared to the treated non-loaded group.

Resorption parameters are reduced significantly in our studies in both experimental series. While in the early loading experimental series the effect of loading on bisphosphonate treated mice is not as strong as in vehicle treated mice, significant differences between the loaded and non-loaded bisphosphonate treated animals can be observed in the late loading study. This could be due to different basal levels in the two experimental series. While vehicle treated mice of the early loading series show a significantly higher mineral resorption rate and bone resorption rate than in the late loading experimental series, no differences can be observed in the absolute values of the bisphosphonate treated mice of these two series. Therefore, the absolute reduction in resorption parameters is higher in the early loading series, already without loading and probably cannot be reduced any further by loading.

Studies performed on humans showed that the activation frequency is reduced with bisphosphonate treatment [39]. However, it would be interesting to know if it is only the

initiation of new BMUs that is reduced or also the amount of resorbed bone per osteoclast. To investigate this Allen et al. assessed parameters of the resorption cavities in bisphosphonate treated dogs [291]. They could show that bisphosphonate treatment significantly reduces resorption area and resorption width. However, only a trend towards a reduced resorption depth compared to vehicle treated animals was observed. According to these findings they conclude that not osteoclast activity but osteoclast number per BMU is reduced. In our studies bone resorption rate and mineral resorption rate of both experimental series are significantly lower in bisphosphonate treated mice than in vehicle treated animals. However, no effect of pharmacological treatment in eroded surface was observed. This is somewhat in contradiction to the findings of Allen et al., as these results would rather suggest a reduction in osteoclast activity and not the spots where bone is resorbed. However, as with our method not the single osteoclasts but their effects on the bone structure at a three dimensional level are observed, a reduced number of osteoclasts per resorption pit could result in a reduced mineral resorption rate as well.

5.2.3 Comparison PTH and Bisphosphonates

To allow an easy comparison of all experimental series, we normalized the data for each animal and created a physiome map.

It can be noted that PTH treated animals show the highest values at the endpoint of the studies for all parameters, except for Tb.N. Often loaded groups have higher values than their corresponding non-loaded groups. The fact that PTH treatment increases not only static but also dynamic parameters stronger than bisphosphonate treatment was also discovered in humans. Keaveny et al. investigated the effects of teriparatide and alendronate on vertebral strength in osteoporotic women [292]. They could clearly show that vertebral compressive strength is increased by both kinds of treatments. However, the increase with PTH is markedly higher than with bisphosphonate treatment. Furthermore, while vertebral strength remained stable between 6 and 18 months of alendronate treatment, it almost doubled with PTH treatment in the same time. Finkelstein et al. investigated the effect of PTH treatment and bisphosphonate treatment in osteoporotic men [279]. They measured bone mineral density of the spine and the femur and could show that it increases significantly more in men treated with PTH than in those treated with alendronate or the combination of PTH and alendronate.

The findings that PTH apparently exerts more beneficial effects on bone than bisphosphonate treatment lead to the question why bisphosphonates are still the most often prescribed pharmacological treatment and not PTH. Also in a sequential therapy antiresorptives, such as bisphosphonates are often used in first place followed by a sequence of PTH treatment [21]. Recently, Cusano and Bilezikian discussed this problem and stated some reasons why PTH is not used more often [293]. PTH has to be administered daily with a subcutaneous injection which is more time consuming and unpleasant for the patient than the oral administration of bisphosphonates. Furthermore, PTH is expensive and antiresorptive therapy has proofed to be efficacious as well. In addition, so far there was no head to head study favoring PTH against bisphosphonate treatment when fractures are a study endpoint. Also bisphosphonates are in use for osteoporosis treatment already since middle of 1990s while teriparatide was approved by the EMEA for use in osteoporotic patients in 2003. The duration of the treatment period with PTH must not be longer than two years and it should only be administered once in a lifetime. This period is consistent with the findings that PTH loses its efficacy after some time. Bilezikian calls this time, when PTH is maximal anabolic the "anabolic window" [21]. As PTH initially stimulates bone formation and just after a while increases bone resorption, as well it is most beneficial up to a period of about two years in humans. After this period, however, all bone turnover parameter go back to their baseline levels and no beneficial effect can be observed anymore. Some tendencies that support this were already to be seen in our experiments. Bone formation rate and mineral resorption rate decreased during the last two weeks; however both of them are still significantly higher than in any other group. Bone resorption parameters would have been expected to be elevated as well with PTH treatment. However, at no time point bone resorption rate of PTH treated animals exceeds the rate of ovariectomized vehicle treated animals. During the entire loading and treatment period bone resorption rate is always in the range of sham operated or bisphosphonate treated animals. However, in the late loading experimental series mineral resorption rate is elevated above the values of any other group. Probably in this group PTH already started to increase bone resorption parameters. The two-year time frame that was stated for humans cannot be transferred to mice one by one. This is simply due to the fact that the metabolism in mice is faster as in humans. For example while the life span of an osteoblast is 10-12 days in a mouse it is about 150 days in humans. Also average bone

formation rate with 0.150 $\mu m^2/\mu m/d$ is much higher in mice than in humans with just 0.038 $\mu m^2/\mu m/d$ [51].

When in a sequential therapy antiresorptive drugs are used before anabolics are administered, a drug dependent time delay was observed until bone mineral density started to increase with PTH treatment. This time delay was up to 6 months after bisphosphonate treatment [21, 293]. However, following other antiresorptive drugs such as raloxifene, bone mineral density increased immediately, as soon as PTH was administered. Nevertheless, a study performed by Bilezikian, with different baseline bone turnover markers found a good and immediate response to PTH treatment after bisphosphonate treatment [21]. Therefore, Bilezikian stated that not specifically the antiresorptive drug but the baseline bone turnover rate is important for the efficacy of the PTH treatment.

Some studies also investigated the effect of administering PTH and bisphosphonates at the same time and not in a sequential fashion. As PTH is increasing the bone formation and bisphosphonates are decreasing bone resorption one could expect beneficial effects of this combination compared to a monotherapy. However, the results from these studies are somewhat conflicting. Some studies report that the anabolic action of PTH is blunted when both PTH and bisphosphonates are given at the same time [279, 294]. Other studies, mainly in animals, did not find any negative effects for the combination of these two drugs [295-297]. One study also investigated the effect of combined PTH and alendronate in mice. They distinguished between the effects on the primary spongiosa, representing non-remodeling bone, and secondary spongiosa, representing remodeling bone [298]. While an additive effect of the combination of these two drugs was found in the primary spongiosa, which is consistent with most animal data, no additive effect was found for the secondary spongiosa which is consistent with most human data. The authors state that one reason for this difference could be that in non-remodeling bone no coupling of osteoblasts and osteoclasts can be found and therefore bone formation can increase without a necessarily increase in bone resorption. However, in remodeling bone, bone formation and bone resorption are coupled and the impeding action of bisphosphonates on bone remodeling is blunting the anabolic action of PTH.

When looking at the previous findings, it could be beneficial to start a sequential treatment with injection of PTH and after withdrawal to continue with bisphosphonate treatment. Thereby the anabolic action of PTH treatment could exert the full beneficial effect at the beginning of the

treatment and once PTH has to be stopped, resorption of the newly formed bone can be prevented with bisphosphonate treatment. Studies performed on humans support this idea and show very promising results. After PTH treatment is ceased, therapy was continued with bisphosphonate medication. With this treatment bone gain was continued compared to bone loss in patients receiving placebo after PTH treatment [299-301]. Also as PTH treatment exerts more positive effects on the bone structure than bisphosphonate treatment in our studies, it seems beneficial to start with a course of PTH treatment followed by bisphosphonates to preserve the new bone structure.

In our studies loading was always added to the pharmacological treatment. In all groups the loaded animals showed a higher gain in bone parameters than the non-loaded mice. However, as can be seen in Table 17, only bisphosphonate treatment does not seem to have many beneficial effects compared to only loading in ovariectomized mice. This is in contrast to PTH treatment. The effects of solely PTH administration can be compared to those of bisphosphonates in combination with loading. Combined loading and PTH treatment have the strongest effects in both experimental series. In the late loading experimental series even synergistic effects were found for some static parameters when these two are combined. Therefore, although data from animal experiments always has to be handled carefully when it is going to be applied in human conditions, but if one wants to give recommendations out of the presented data they would be the following:

Pharmacological treatment should always be combined with mechanical loading as the effect of the combination of both is more beneficial than a monotherapy. PTH treatment in combination with loading has the most positive effects. Taken into consideration that the time of these beneficial effects is limited and usually bone loss is severe when patients are diagnosed with osteoporosis for the first time it is worth considering PTH as the first line drug, followed by bisphosphonates, again in combination with loading.

	PTH				BIS			
	8N		0N		8N		0N	
	Early	Late	Early	Late	Early	Late	Early	Late
Increase similar or higher than VEH 8N								
TRAB BV/TV	YES	YES	YES	YES	YES	YES	NO	NO
Tb.Th	YES	YES	NO	YES	NO	NO	NO	NO
Cort % BV	YES	YES	YES	YES	YES	YES	NO	NO
Ct.Th	YES	YES	NO	NO	YES	YES	NO	NO
Synergistic effects								
Tb.Th	NO	YES	NO	NO	NO	NO	NO	NO
Cort % BV	NO	YES	NO	NO	NO	NO	NO	NO
Ct.Th	NO	YES	NO	NO	NO	NO	NO	NO
Dynamic parameters (compared to VEH 8N)								
Increased BFR	YES	YES	YES	YES	NO	NO	NO	NO
Increased MAR	YES	YES	YES	YES	NO	NO	NO	NO
Increased MS	YES	YES	YES	YES	NO	NO	NO	NO
Decreased BRR	YES	NO	NO	NO	YES	YES	NO	NO
Decreased MRR	NO	NO	NO	NO	YES	YES	YES	YES
Decreased ES	YES	YES	NO	YES	NO	NO	NO	NO
SUMMARY	**YES**	**YES**	YES	YES	YES	YES	YES	YES
	NO	NO	NO	NO	NO	NO	**NO**	**NO**

Table 17: comparison between PTH treatment and bisphosphonate treatment. Effects of both pharmacological treatments were compared to effects of only mechanical loading as this would be the easiest way to improve bone mass. If pharmacological treatment is given it should improve bone parameters more than mechanical loading.

6 Outlook

In the presented studies the effect on ovariectomized mice of PTH as an anabolic pharmacological treatment and the bisphosphonate zolendronate, as an antiresorptive pharmacological treatment in combination with mechanical loading was investigated. The acquired data was put together in a physiome map. This allowed a direct comparison of all treatment options. However, this physiome map is not exhaustive. It could be interesting to compare the results of the present studies to other types of pharmacological treatments, such as selective estrogen receptor modulators, like raloxifene, or RANKL antibodies like denosumab. As both of them are rather antiresorptive drugs it would be interesting to see if their effect is more in the range of bisphosphonates or of PTH.

All experiments have been performed in mice. Since there are many genetically altered mouse strains available, it is possible to use different mouse strains and therefore simulate different bone conditions. For example SAMP 6 mice are a model for senile osteoporosis. Signs that are typical in human senile bone appear in these mice already at an early age [120]. Therefore, they are an interesting model to investigate the effect of pharmacological treatment on this bone. While postmenopausal osteoporosis is a high turnover osteoporosis with a high bone remodeling rate, senile osteoporosis is a low turnover osteoporosis with a lower bone remodeling rate. Hence it could be appealing to not only compare the effects on the static parameters, but also the absolute values of the dynamic parameters. If the entire bone remodeling rate is reduced it would be interesting to see whether PTH increases bone formation parameters to the same level as it does in ovariectomized mice or at least to the same percentage or if this increase is smaller. Also it would be interesting to know if bisphosphonate treatment can reduce the bone dynamic parameters even more or if it does not affect them at all. Other potentially attractive mouse strains are SOST knock out and SOST over expressing mice. SOST is a gene highly expressed in osteocytes and with its product sclerostin it has been found to inhibit bone formation. Moreover, it has been discovered that PTH inhibits the expression of SOST and therefore increases bone formation and exerts its anabolic effects [302]. Kramer et al. could show that in mice over expressing SOST, anabolic action of PTH is blunted. SOST k.o. mice, already had a high bone mass, before treatment was started. However, the anabolic action of PTH was blunted in these animals as well, as BMD in treated and non-treated animals did not differ significantly [303]. It

would be worth investigating if these SOST k.o. mice react to mechanical loading the same way as ovariectomized mice did or if higher loads are needed to induce a reaction or if no reaction at all can be induced anymore as the bone mass is already quite high. Furthermore, it could be worth to study the effects of other pharmacological treatment over a longer time. For example, if bisphosphonates, although they only reduced bone resorption rate to a certain extend in ovariectomized mice, are able to reduce bone resorption rate as well in these mice. In addition if bisphosphonates are given for a longer period of time, if they could potentially inhibit the increased bone formation due to the lack of SOST. There are also many other knock out mouse strains that show a different bone physiology than wild-type mice. The following section will just briefly describe some of the strains.

In 2002 Hoff et al. published a study about the CT/CGRP k.o. mouse. In these animals the calcitonin (CT)/ calcitonin gene related peptide alpha (CGRP) was knocked out. The mice were found to have a higher trabecular bone volume and a higher bone formation rate at the age of 1 and 3 months, compared to wild type animals. Furthermore, they did not lose bone after ovariectomy and showed a higher response to PTH treatment than control mice. This was shown by increased levels of serum calcium concentration and urine deoxypyridinoline crosslinks [304]. Other mice that have been shown to be resistant against bone loss after ovariectomy are osteopontin k.o. mice [305]. Another genetically modified mouse strain are GDF8 knockout mice. As a member of the transforming growth factor beta (TGF-β) super family, GDF8 (myostatin) regulates skeletal muscle growth in a negative way. The k.o. mice have been found to have twice the muscle mass as wild-type mice. But also BMD and BMC were affected. DEXA and pQCT measurements revealed that these mice have about 20 % higher cortical BMC at the metaphysis of the femur. Furthermore, cortical thickness at the femur was increased by 10 % [306]. Manipulation at the hypothalamic level also effects bone mass. Neuropeptide Y (NPY) is expressed in the hypothalamus in increasing levels during fasting. Mice lacking this factor have been shown to have a significant increase in bone mass. Mice over expressing NPY have been shown to significantly reduce bone mass. Therefore, NPY was identified for being very important to maintain bone homeostatic signals. It induces an increased bone mass in times of obesity, when NPY levels are low, and decreases bone mass under starving conditions, when NPY levels are high to save energy [307]. Kong et al. reported in 1999 about mice lacking

osteoprotegerin ligand (OPGL). Osteoblasts are not able to support osteoclastogenesis anymore. Therefore, these mice severe osteopetrosis due to the complete lack of osteoclasts [308].

But not only new data could be acquired and added to the physiome map. It is also worth investigating further into the data that is presented here. Recently, the local strains of bones from ovariectomized mice were compared in 3D with bone formation and resorption sites at our institute [309]. According to the mechanostat theory, bone formation would be expected to occur at sites of high strains, while bone resorption occurs at sites of low strains. However, with pharmacological treatment bone formation and resorption does not necessarily have to follow these rules. It has been shown for example that solely PTH treatment induces a uniform bone formation while in combination with mechanical load it increases the local bone formation [284]. Nevertheless, the bones in that study were only analyzed with means of histology. Comparing local strains and bone formation and resorption sites at a three dimensional level at different time points of a longitudinal study would give a better insight where and how new bone is deposited or old bone resorbed. Furthermore, not only the effect of two different pharmacological treatments on the distribution of bone formation and resorption can be evaluated, but also the combination of these with loading. Biomechanical tests also provide a good possibility to evaluate the bone quality and biomechanical quality of the newly formed bone from the different loading and treatment regimes. Therefore, it could be interesting to perform mechanical tests on the loaded and treated bones, but also on non-loaded but treated bones.

Another future experiment could also investigate the development of static and dynamic bone parameters once treatment is stopped. As bisphosphonates have a longer half time it would be expected that they exert a longer positive effect on bone than PTH. However, with PTH bone parameters increased to a much higher extend than with bisphosphonates. Therefore, even if some bone is lost after a certain time, bone mass could still be the same as in bisphosphonate treated mice.

Ovariectomized mice are a good model to mimic postmenopausal osteoporosis. Also the treatment effects were similar to those observed in humans. Therefore, the data suits very well to be implemented into a computer simulation model. With the help of such a model, build upon *in vivo* data and verified with this data the change in static and dynamic parameters of human bones can be predicted well. In the future this could give clinicians chances to not only predict the

efficacy of a treatment but also to choose the appropriate treatment for the patients based on solid data.

7 List of references

1. *Who are candidates for prevention and treatment for osteoporosis?* Osteoporos Int, 1997. **7**(1): p. 1-6.
2. Cooper, C., G. Campion, and L.J. Melton, *Hip fractures in the elderly: A world-wide projection.* Osteoporosis International, 1992. **2**(6): p. 285-289.
3. *Assessment of fracture risk and its application to screening for postmenopausal osteoporosis. Report of a WHO Study Group.* World Health Organ Tech Rep Ser, 1994. **843**: p. 1-129.
4. Kanis, J., *WHO SCIENTIFIC GROUP ON THE ASSESSMENT OF OSTEOPOROSIS AT PRIMARY HEALTH CARE LEVEL*, in *WHO Osteoporosis Meeting, May 5-7, 2004*2007: Brussels, Belgium.
5. Cummings, S.R. and L.J. Melton, *Epidemiology and outcomes of osteoporotic fractures.* The Lancet, 2002. **359**(9319): p. 1761-1767.
6. Kanis, J.A., et al., *Guidelines for diagnosis and management of osteoporosis.* Osteoporosis International, 1997. **7**(4): p. 390-406.
7. Lippuner, K., M. Golder, and R. Greiner, *Epidemiology and direct medical costs of osteoporotic fractures in men and women in Switzerland.* Osteoporosis International, 2005. **16**(0): p. S8-S17.
8. Kanis, J.A. and O. Johnell, *Requirements for DXA for the management of osteoporosis in Europe.* Osteoporosis International, 2005. **16**(3): p. 229-238.
9. Johnell, O. and J. Kanis, *An estimate of the worldwide prevalence and disability associated with osteoporotic fractures.* Osteoporosis International, 2006. **17**(12): p. 1726-1733.
10. Cooper, C., et al., *Population-Based Study of Survival after Osteoporotic Fractures.* American Journal of Epidemiology, 1993. **137**(9): p. 1001-1005.
11. Leibson, C.L., et al., *Mortality, Disability, and Nursing Home Use for Persons with and without Hip Fracture: A Population-Based Study.* Journal of the American Geriatrics Society, 2002. **50**(10): p. 1644-1650.
12. Magaziner, J., et al., *Predictors of Functional Recovery One Year Following Hospital Discharge for Hip Fracture: A Prospective Study.* Journal of Gerontology, 1990. **45**(3): p. M101-M107.
13. Kroger, H., et al., *Development of bone mass and bone density of the spine and femoral neck--a prospective study of 65 children and adolescents.* Bone Miner, 1993. **23**(3): p. 171-82.
14. Van Der Linden, J.C., et al., *Mechanical Consequences of Bone Loss in Cancellous Bone.* Journal of Bone and Mineral Research, 2001. **16**(3): p. 457-465.
15. Bass, S.L., et al., *The Effect of Mechanical Loading on the Size and Shape of Bone in Pre-, Peri-, and Postpubertal Girls: A Study in Tennis Players.* Journal of Bone and Mineral Research, 2002. **17**(12): p. 2274-2280.
16. Khan, K., et al., *Does childhood and adolescence provide a unique opportunity for exercise to strengthen the skeleton?* Journal of Science and Medicine in Sport, 2000. **3**(2): p. 150-164.
17. Brooke-Wavell, K., et al., *Commencing, Continuing and Stopping Brisk Walking: Effects on Bone Mineral Density, Quantitative Ultrasound of Bone and Markers of Bone*

Metabolism in Postmenopausal Women. Osteoporosis International, 2001. **12**(7): p. 581-587.
18. Karlsson, M., *Has exercise an antifracture efficacy in women?* Scandinavian Journal of Medicine & Science in Sports, 2004. **14**(1): p. 2-15.
19. Hartard, M., et al., *SYSTEMATIC STRENGTH TRAINING AS A MODEL OF THERAPEUTIC INTERVENTION: A Controlled Trial in Postmenopausal Women with Osteopenia1.* American Journal of Physical Medicine & Rehabilitation, 1996. **75**(1): p. 21-28.
20. Hauer, K., et al., *Intensive physical training in geriatric patients after severe falls and hip surgery.* Age and Ageing, 2002. **31**(1): p. 49-57.
21. Bilezikian, J., *Combination anabolic and antiresorptive therapy for osteoporosis: Opening the anabolic window.* Current Osteoporosis Reports, 2008. **6**(1): p. 24-30.
22. Sato, M., et al., *Teriparatide [PTH(1–34)] Strengthens the Proximal Femur of Ovariectomized Nonhuman Primates Despite Increasing Porosity.* Journal of Bone and Mineral Research, 2004. **19**(4): p. 623-629.
23. Gabet, Y., et al., *Intermittently administered parathyroid hormone 1-34 reverses bone loss and structural impairment in orchiectomized adult rats.* Osteoporos Int, 2005. **16**(11): p. 1436-43.
24. DEMPSTER, D.W., et al., *Anabolic Actions of Parathyroid Hormone on Bone.* Endocr Rev, 1993. **14**(6): p. 690-709.
25. Reeve, J., et al., *Anabolic effect of human parathyroid hormone fragment on trabecular bone in involutional osteoporosis: a multicentre trial.* Br Med J, 1980. **280**(6228): p. 1340-4.
26. Jilka, R.L., et al., *Continuous elevation of PTH increases the number of osteoblasts via both osteoclast-dependent and -independent mechanisms.* J Bone Miner Res.
27. Zhang, Q., et al., *Dramatic increase in cortical thickness induced by femoral marrow ablation followed by a 3-month treatment with PTH in rats.* J Bone Miner Res. **25**(6): p. 1350-9.
28. Lindsay, R., et al., *Effects Of a One-Month Treatment With PTH(1–34) on Bone Formation on Cancellous, Endocortical, and Periosteal Surfaces of the Human Ilium.* Journal of Bone and Mineral Research, 2007. **22**(4): p. 495-502.
29. Dempster, D.W., et al., *Effects of daily treatment with parathyroid hormone on bone microarchitecture and turnover in patients with osteoporosis: a paired biopsy study.* J Bone Miner Res, 2001. **16**(10): p. 1846-53.
30. Dobnig, H. and R.T. Turner, *Evidence that intermittent treatment with parathyroid hormone increases bone formation in adult rats by activation of bone lining cells.* Endocrinology, 1995. **136**(8): p. 3632-8.
31. Alexander, J.M., et al., *Human parathyroid hormone 1-34 reverses bone loss in ovariectomized mice.* J Bone Miner Res, 2001. **16**(9): p. 1665-73.
32. Woo, S.-B., J.W. Hellstein, and J.R. Kalmar, *Systematic Review: Bisphosphonates and Osteonecrosis of the Jaws.* Annals of Internal Medicine, 2006. **144**(10): p. 753-761.
33. Shane, E., et al., *Atypical subtrochanteric and diaphyseal femoral fractures: Report of a task force of the American Society for Bone and Mineral Research.* Journal of Bone and Mineral Research: p. n/a-n/a.

34. Glatt, M., *The bisphosphonate zoledronate prevents vertebral bone loss in mature estrogen-deficient rats as assessed by micro-computed tomography.* Eur Cell Mater, 2001. **1**: p. 18-26.
35. Ohnishi, H., et al., *Bisphosphonate tiludronate increases bone strength by improving mass and structure in established osteopenia after ovariectomy in rats.* Bone, 1997. **21**(4): p. 335-43.
36. Bell, N.H. and R.H. Johnson, *Bisphosphonates in the treatment of osteoporosis.* Endocrine, 1997. **6**(2): p. 203-6.
37. Brouwers, J.E., et al., *Bone degeneration and recovery after early and late bisphosphonate treatment of ovariectomized wistar rats assessed by in vivo micro-computed tomography.* Calcif Tissue Int, 2008. **82**(3): p. 202-11.
38. De La Piedra, C., et al., *Daily or monthly ibandronate prevents or restores deteriorations of bone mass, architecture, biomechanical properties and markers of bone turnover in androgen-deficient aged rats.* Aging Male.
39. Recker, R.R., et al., *Effects of intravenous zoledronic acid once yearly on bone remodeling and bone structure.* J Bone Miner Res, 2008. **23**(1): p. 6-16.
40. Gasser, J.A., et al., *Long-term protective effects of zoledronic acid on cancellous and cortical bone in the ovariectomized rat.* J Bone Miner Res, 2008. **23**(4): p. 544-51.
41. Kanis, J., et al., *European guidance for the diagnosis and management of osteoporosis in postmenopausal women.* Osteoporosis International, 2008. **19**(4): p. 399-428.
42. Schulte, F.A., et al., *In vivo micro-computed tomography allows direct three-dimensional quantification of both bone formation and bone resorption parameters using time-lapsed imaging.* Bone.
43. G. Kuhn, F.M.L., F. A. Schulte, K. Koch, C. Weigt and R. Müller, *Mimicking postmenopausal bone loss in tail vertebrae of mice.* Abstracts 11th FELASA and 40th Scand-LAS Joint Meeting "New Paradigms in Laboratory Animal Science", Helsinki, Finland2010, June 14-17: p. 35.
44. Ksiezopolska-Orlowska, K., *Changes in bone mechanical strength in response to physical therapy.* Pol Arch Med Wewn, 2010. **120**(9): p. 368-73.
45. Aguirre, J.I., et al., *Osteocyte Apoptosis Is Induced by Weightlessness in Mice and Precedes Osteoclast Recruitment and Bone Loss.* Journal of Bone and Mineral Research, 2006. **21**(4): p. 605-615.
46. Miller, S.C., et al., *Bone lining cells: structure and function.* Scanning Microsc, 1989. **3**(3): p. 953-60; discussion 960-1.
47. Lyritis, G.P., T. Georgoulas, and C.P. Zafeiris, *Bone anabolic versus bone anticatabolic treatment of postmenopausal osteoporosis.* Ann N Y Acad Sci, 2010. **1205**: p. 277-83.
48. Martin, T.J. and E. Seeman, *Bone remodelling: its local regulation and the emergence of bone fragility.* Best Practice & Research Clinical Endocrinology & Metabolism, 2008. **22**(5): p. 701-722.
49. Elefteriou, F., et al., *Leptin regulation of bone resorption by the sympathetic nervous system and CART.* Nature, 2005. **434**(7032): p. 514-20.
50. Takahashi, N., et al., *Cells of Bone: Osteoclast Generation*, in *Principles of Bone Biology (Second Edition)*2002, Academic Press: San Diego. p. 109-126.
51. Jilka, R.L., *Molecular and cellular mechanisms of the anabolic effect of intermittent PTH.* Bone, 2007. **40**(6): p. 1434-46.

52. van Bezooijen, R.L., et al., *Sclerostin Is an Osteocyte-expressed Negative Regulator of Bone Formation, But Not a Classical BMP Antagonist.* The Journal of Experimental Medicine, 2004. **199**(6): p. 805-814.
53. Frost, H.M., *Tetracycline-based histological analysis of bone remodeling.* Calcif Tissue Res, 1969. **3**(3): p. 211-37.
54. Hollinger, J.O., J.R. Lieberman, and G.E. Friedlaender, *Bone Dynamics, Bone Regeneration and Repair*, 2005, Humana Press. p. 1-19.
55. Parfitt, A.M., *Osteonal and hemi-osteonal remodeling: the spatial and temporal framework for signal traffic in adult human bone.* J Cell Biochem, 1994. **55**(3): p. 273-86.
56. Mosekilde, L., *Consequences of the remodelling process for vertebral trabecular bone structure: a scanning electron microscopy study (uncoupling of unloaded structures).* Bone Miner, 1990. **10**(1): p. 13-35.
57. Chan, G.K. and G. Duque, *Age-Related Bone Loss: Old Bone, New Facts.* Gerontology, 2002. **48**(2): p. 62-71.
58. Frost, H.M., *Bone dynamics in metabolic bone disease.* J Bone Joint Surg Am, 1966. **48**(6): p. 1192-203.
59. Parfitt, A., *Quantum concept of bone remodeling and turnover: Implications for the pathogenesis of osteoporosis.* Calcified Tissue International, 1979. **28**(1): p. 1-5.
60. Szulc, P. and E. Seeman, *Thinking inside and outside the envelopes of bone.* Osteoporosis International, 2009. **20**(8): p. 1281-1288.
61. Kornak, U. and S. Mundlos, *Genetic Disorders of the Skeleton: A Developmental Approach.* The American Journal of Human Genetics, 2003. **73**(3): p. 447-474.
62. Wergedal, J.E., et al., *Patients with Van Buchem Disease, an Osteosclerotic Genetic Disease, Have Elevated Bone Formation Markers, Higher Bone Density, and Greater Derived Polar Moment of Inertia than Normal.* Journal of Clinical Endocrinology & Metabolism, 2003. **88**(12): p. 5778-5783.
63. Balemans, W., et al., *Increased bone density in sclerosteosis is due to the deficiency of a novel secreted protein (SOST).* Human Molecular Genetics, 2001. **10**(5): p. 537-543.
64. Rauch, F. and F.H. Glorieux, *Osteogenesis imperfecta.* The Lancet, 2004. **363**(9418): p. 1377-1385.
65. OIF, ***Fast Facts on Osteogenesis Imperfecta***. Osteogenesis Imperfecta Foundation, 2011. **http://www.oif.org/site/PageServer?pagename=FastFacts**.
66. Friedrichs, W.E., et al., *Sequence Analysis of Measles Virus Nucleocapsid Transcripts in Patients with Paget's Disease.* Journal of Bone and Mineral Research, 2002. **17**(1): p. 145-151.
67. Burr, D.B. and R.B. Martin, *Errors in bone remodeling: Toward a unified theory of metabolic bone disease.* American Journal of Anatomy, 1989. **186**(2): p. 186-216.
68. Marcus, R., *Normal and Abnormal Bone Remodelling in Man.* Annual Review of Medicine, 1987. **38**(1): p. 129-141.
69. WHO, *Assessment of fracture risk and its application to screening for postmenopausal osteoporosis. Report of a WHO Study Group.* World Health Organ Tech Rep Ser, 1994. **843**: p. 1-129.
70. Melton, L.J., et al., *How Many Women Have Osteoporosis?* Journal of Bone and Mineral Research, 2005. **20**(5): p. 886-892.

71. Center, J.R., et al., *Mortality after all major types of osteoporotic fracture in men and women: an observational study.* The Lancet, 1999. **353**(9156): p. 878-882.
72. *Osteoporosis in Men: New Insights into Aetiology, Pathogenesis, Prevention and Management.* Drugs & Aging, 1998. **13**: p. 421-434.
73. Siris, E. and P. Delmas, *Assessment of 10-year absolute fracture risk: a new paradigm with worldwide application.* Osteoporosis International, 2008. **19**(4): p. 383-384.
74. Kanis, J., et al., *FRAX™ and the assessment of fracture probability in men and women from the UK.* Osteoporosis International, 2008. **19**(4): p. 385-397.
75. Fujiwara, S., et al., *Development and application of a Japanese model of the WHO fracture risk assessment tool (FRAX™).* Osteoporosis International, 2008. **19**(4): p. 429-435.
76. Dawson-Hughes, B., et al., *Implications of absolute fracture risk assessment for osteoporosis practice guidelines in the USA.* Osteoporosis International, 2008. **19**(4): p. 449-458.
77. Leslie, W., *Absolute fracture risk reporting in clinical practice: A physician-centered survey.* Osteoporosis International, 2008. **19**(4): p. 459-463.
78. Riggs, B.L., et al., *Changes in bone mineral density of the proximal femur and spine with aging. Differences between the postmenopausal and senile osteoporosis syndromes.* J Clin Invest, 1982. **70**(4): p. 716-23.
79. Nguyen, T.V., P.N. Sambrook, and J.A. Eisman, *Bone Loss, Physical Activity, and Weight Change in Elderly Women: The Dubbo Osteoporosis Epidemiology Study.* Journal of Bone and Mineral Research, 1998. **13**(9): p. 1458-1467.
80. Pasco, J., et al., *The population burden of fractures originates in women with osteopenia, not osteoporosis.* Osteoporosis International, 2006. **17**(9): p. 1404-1409.
81. Kanis, J.A., et al., *Alcohol intake as a risk factor for fracture.* Osteoporos Int, 2005. **16**(7): p. 737-42.
82. De Laet, C., et al., *Body mass index as a predictor of fracture risk: a meta-analysis.* Osteoporos Int, 2005. **16**(11): p. 1330-8.
83. Kanis, J.A., et al., *A family history of fracture and fracture risk: a meta-analysis.* Bone, 2004. **35**(5): p. 1029-37.
84. Kanis, J.A., et al., *A meta-analysis of previous fracture and subsequent fracture risk.* Bone, 2004. **35**(2): p. 375-82.
85. Kanis, J.A., et al., *Smoking and fracture risk: a meta-analysis.* Osteoporos Int, 2005. **16**(2): p. 155-62.
86. ALBRIGHT, F., P.H. SMITH, and A.M. RICHARDSON, *POSTMENOPAUSAL OSTEOPOROSIS.* Journal of the American Medical Association, 1941. **116**(22): p. 2465-2474.
87. Riggs, B.L. and L.J. Melton Iii, *Evidence for two distinct syndromes of involutional osteoporosis.* The American Journal of Medicine, 1983. **75**(6): p. 899-901.
88. Greendale, G.A. and H.L. Judd, *The menopause: health implications and clinical management.* J Am Geriatr Soc, 1993. **41**(4): p. 426-36.
89. Chang, R.J. and H.L. Judd, *The ovary after menopause.* Clin Obstet Gynecol, 1981. **24**(1): p. 181-91.
90. Zallone, A., *Direct and indirect estrogen actions on osteoblasts and osteoclasts.* Ann N Y Acad Sci, 2006. **1068**: p. 173-9.

91. Nakamura, T., et al., *Estrogen Prevents Bone Loss via Estrogen Receptor [alpha] and Induction of Fas Ligand in Osteoclasts.* Cell, 2007. **130**(5): p. 811-823.
92. Kousteni, S., et al., *Kinase-mediated regulation of common transcription factors accounts for the bone-protective effects of sex steroids.* The Journal of Clinical Investigation, 2003. **111**(11): p. 1651-1664.
93. Manolagas, S.C., S. Kousteni, and R.L. Jilka, *Sex Steroids and Bone.* Recent Prog Horm Res, 2002. **57**(1): p. 385-409.
94. Khosla, S., *Minireview: The OPG/RANKL/RANK System.* Endocrinology, 2001. **142**(12): p. 5050-5055.
95. Pacifici, R., et al., *Postmenopausal Osteoporosis: How the Hormonal Changes of Menopause Cause Bone Loss*, in *Osteoporosis (Third Edition)*2008, Academic Press: San Diego. p. 1041-1054.
96. Hofbauer, L.C., et al., *Estrogen Stimulates Gene Expression and Protein Production of Osteoprotegerin in Human Osteoblastic Cells.* Endocrinology, 1999. **140**(9): p. 4367-4370.
97. Cenci, S., et al., *Estrogen deficiency induces bone loss by enhancing T-cell production of TNF-Î±.* The Journal of Clinical Investigation, 2000. **106**(10): p. 1229-1237.
98. Nanes, M.S., *Tumor necrosis factor-[alpha]: molecular and cellular mechanisms in skeletal pathology.* Gene, 2003. **321**: p. 1-15.
99. Roggia, C., et al., *Up-regulation of TNF-producing T cells in the bone marrow: A key mechanism by which estrogen deficiency induces bone loss in vivo.* Proceedings of the National Academy of Sciences of the United States of America, 2001. **98**(24): p. 13960-13965.
100. Ammann, P., et al., *Transgenic mice expressing soluble tumor necrosis factor-receptor are protected against bone loss caused by estrogen deficiency.* J Clin Invest, 1997. **99**(7): p. 1699-703.
101. Srivastava, S., et al., *Estrogen blocks M-CSF gene expression and osteoclast formation by regulating phosphorylation of Egr-1 and its interaction with Sp-1.* J Clin Invest, 1998. **102**(10): p. 1850-9.
102. Srivastava, S., et al., *Estrogen decreases TNF gene expression by blocking JNK activity and the resulting production of c-Jun and JunD.* J Clin Invest, 1999. **104**(4): p. 503-13.
103. Wei, S., et al., *IL-1 mediates TNF-induced osteoclastogenesis.* J Clin Invest, 2005. **115**(2): p. 282-90.
104. Kimble, R.B., et al., *Simultaneous block of interleukin-1 and tumor necrosis factor is required to completely prevent bone loss in the early postovariectomy period.* Endocrinology, 1995. **136**(7): p. 3054-61.
105. Weitzmann, M.N., et al., *Increased production of IL-7 uncouples bone formation from bone resorption during estrogen deficiency.* The Journal of Clinical Investigation, 2002. **110**(11): p. 1643-1650.
106. McNamara, L.M., et al., *Strength of cancellous bone trabecular tissue from normal, ovariectomized and drug-treated rats over the course of ageing.* Bone, 2006. **39**(2): p. 392-400.
107. Ederveen, A.G.H., et al., *Effect of 16 Months of Treatment with Tibolone on Bone Mass, Turnover, and Biomechanical Quality in Mature Ovariectomized Rats.* Journal of Bone and Mineral Research, 2001. **16**(9): p. 1674-1681.

108. Li, B. and R.M. Aspden, *Material Properties of Bone from the Femoral Neck and Calcar Femorale of Patients with Osteoporosis or Osteoarthritis.* Osteoporosis International, 1997. **7**(5): p. 450-456.
109. Bailey, A.J., et al., *Biochemical changes in the collagen of human osteoporotic bone matrix.* Connective Tissue Research, 1993. **29**(2): p. 119-132.
110. Ciarelli, T.E., D.P. Fyhrie, and A.M. Parfitt, *Effects of vertebral bone fragility and bone formation rate on the mineralization levels of cancellous bone from white females.* Bone, 2003. **32**(3): p. 311-315.
111. Gadeleta, S.J., et al., *A physical, chemical, and mechanical study of lumbar vertebrae from normal, ovariectomized, and nandrolone decanoate-treated cynomolgus monkeys (macaca fascicularis).* Bone, 2000. **27**(4): p. 541-550.
112. van der Linden, J.C., et al., *Altered tissue properties induce changes in cancellous bone architecture in aging and diseases.* J Biomech, 2004. **37**(3): p. 367-74.
113. FUJISAWA, Y., K. KIDA, and H. MATSUDA, *Role of Change in Vitamin D Metabolism with Age in Calcium and Phosphorus Metabolism in Normal Human Subjects.* J Clin Endocrinol Metab, 1984. **59**(4): p. 719-726.
114. Gallagher, J.C., et al., *Intestinal calcium absorption and serum vitamin D metabolites in normal subjects and osteoporotic patients: effect of age and dietary calcium.* J Clin Invest, 1979. **64**(3): p. 729-36.
115. Clemens, T.L., et al., *Serum Vitamin D2 and Vitamin D3 Metabolite Concentrations and Absorption of Vitamin D2 in Elderly Subjects.* J Clin Endocrinol Metab, 1986. **63**(3): p. 656-660.
116. Lund, B., et al., *Serum 1,25-Dihydroxyvitamin D in Normal Subjects and in Patients with Postmenopausal Osteopenia. Influence of Age, Renal Function and Oestrogen Therapy.* Horm Metab Res, 1982. **14**(05): p. 271,274.
117. Bullamore, J.R., et al., *EFFECT OF AGE ON CALCIUM ABSORPTION.* The Lancet, 1970. **296**(7672): p. 535-537.
118. Francis, R.M., et al., *Calcium malabsorption in elderly women with vertebral fractures: evidence for resistance to the action of vitamin D metabolites on the bowel.* Clin Sci (Lond), 1984. **66**(1): p. 103-7.
119. Eastell, R., et al., *Interrelationship among vitamin D metabolism, true calcium absorption, parathyroid function, and age in women: Evidence of an age-related intestinal resistance to 1,25-dihydroxyvitamin D action.* Journal of Bone and Mineral Research, 1991. **6**(2): p. 125-132.
120. Chen, H., et al., *Site-specific bone loss in senescence-accelerated mouse (SAMP6): a murine model for senile osteoporosis.* Exp Gerontol, 2009. **44**(12): p. 792-8.
121. McCalden, R.W., et al., *Age-related changes in the tensile properties of cortical bone. The relative importance of changes in porosity, mineralization, and microstructure.* J Bone Joint Surg Am, 1993. **75**(8): p. 1193-205.
122. Tsuboyama, T., et al., *Decreased endosteal formation during cortical bone modelling in SAM-P/6 mice with a low peak bone mass.* Bone Miner, 1989. **7**(1): p. 1-12.
123. Parfitt, A.M., *Age-related structural changes in trabecular and cortical bone: cellular mechanisms and biomechanical consequences.* Calcif Tissue Int, 1984. **36 Suppl 1**: p. S123-8.

124. Riggs, B.L., et al., *A Population-Based Assessment of Rates of Bone Loss at Multiple Skeletal Sites: Evidence for Substantial Trabecular Bone Loss in Young Adult Women and Men.* Journal of Bone and Mineral Research, 2008. **23**(2): p. 205-214.
125. Rozman, C., et al., *Age-related variations of fat tissue fraction in normal human bone marrow depend both on size and number of adipocytes: a stereological study.* Exp Hematol, 1989. **17**(1): p. 34-7.
126. Park, S.R., R.O. Oreffo, and J.T. Triffitt, *Interconversion potential of cloned human marrow adipocytes in vitro.* Bone, 1999. **24**(6): p. 549-54.
127. Parfitt, A.M., et al., *Relationships between surface, volume, and thickness of iliac trabecular bone in aging and in osteoporosis. Implications for the microanatomic and cellular mechanisms of bone loss.* J Clin Invest, 1983. **72**(4): p. 1396-409.
128. Mosekilde, L., *Age-related changes in vertebral trabecular bone architecture--assessed by a new method.* Bone, 1988. **9**(4): p. 247-50.
129. Thomsen, J.S., E.N. Ebbesen, and L.I. Mosekilde, *Age-related differences between thinning of horizontal and vertical trabeculae in human lumbar bone as assessed by a new computerized method.* Bone, 2002. **31**(1): p. 136-42.
130. Mosekilde, L., *Sex differences in age-related loss of vertebral trabecular bone mass and structure--biomechanical consequences.* Bone, 1989. **10**(6): p. 425-32.
131. Wakamatsu, E. and H.A. Sissons, *The cancellous bone of the iliac crest.* Calcif Tissue Res, 1969. **4**(2): p. 147-61.
132. Weinstein, R.S. and M.S. Hutson, *Decreased trabecular width and increased trabecular spacing contribute to bone loss with aging.* Bone, 1987. **8**(3): p. 137-42.
133. Stauber, M. and R. Muller, *Age-related changes in trabecular bone microstructures: global and local morphometry.* Osteoporos Int, 2006. **17**(4): p. 616-26.
134. Jilka, R.L., et al., *Linkage of decreased bone mass with impaired osteoblastogenesis in a murine model of accelerated senescence.* J Clin Invest, 1996. **97**(7): p. 1732-40.
135. Cao, J.J., et al., *Aging Increases Stromal/Osteoblastic Cell-Induced Osteoclastogenesis and Alters the Osteoclast Precursor Pool in the Mouse.* Journal of Bone and Mineral Research, 2005. **20**(9): p. 1659-1668.
136. Dent, C.E. and M. Friedman, *Idiopathic Juvenile Osteoporosis.* Q J Med, 1965. **34**: p. 177-210.
137. Ward, L., et al., *Osteoporosis in Childhood and Adolescence*, in *Osteoporosis (Third Edition)*2008, Academic Press: San Diego. p. 1095-1133.
138. Krassas, G.E., *Idiopathic juvenile osteoporosis.* Ann N Y Acad Sci, 2000. **900**: p. 409-12.
139. Villaverde, V., et al., *Difficulty walking. A presentation of idiopathic juvenile osteoporosis.* J Rheumatol, 1998. **25**(1): p. 173-6.
140. Smith, R., *Idiopathic osteoporosis in the young.* J Bone Joint Surg Br, 1980. **62-B**(4): p. 417-27.
141. Rauch, F., et al., *Deficient bone formation in idiopathic juvenile osteoporosis: a histomorphometric study of cancellous iliac bone.* J Bone Miner Res, 2000. **15**(5): p. 957-63.
142. Kelepouris, N., et al., *Severe Osteoporosis in Men.* Annals of Internal Medicine, 1995. **123**(6): p. 452-460.
143. Fitzpatrick, L.A., *Secondary Causes of Osteoporosis.* Mayo Clinic Proceedings, 2002. **77**(5): p. 453-468.

144. Gallacher, S.J. and T. Dixon, *Impact of treatments for postmenopausal osteoporosis (bisphosphonates, parathyroid hormone, strontium ranelate, and denosumab) on bone quality: a systematic review.* Calcif Tissue Int, 2010. **87**(6): p. 469-84.
145. Cummings, S.R., et al., *Denosumab for Prevention of Fractures in Postmenopausal Women with Osteoporosis.* New England Journal of Medicine, 2009. **361**(8): p. 756-765.
146. Fonseca, J.E., *Rebalancing bone turnover in favour of formation with strontium ranelate: implications for bone strength.* Rheumatology, 2008. **47**(suppl 4): p. iv17-iv19.
147. Fleisch, H., *[Introduction to bisphosphonates. History and functional mechanisms]*. Orthopade, 2007. **36**(2): p. 103-4, 106-9.
148. Hughes, D.E., et al., *Bisphosphonates promote apoptosis in murine osteoclasts in vitro and in vivo.* Journal of Bone and Mineral Research, 1995. **10**(10): p. 1478-1487.
149. Widler, L., et al., *Highly potent geminal bisphosphonates. From pamidronate disodium (Aredia) to zoledronic acid (Zometa).* J Med Chem, 2002. **45**(17): p. 3721-38.
150. Vitte, C., H. Fleisch, and H. Guenther, *Bisphosphonates induce osteoblasts to secrete an inhibitor of osteoclast-mediated resorption.* Endocrinology, 1996. **137**(6): p. 2324-2333.
151. Iwata, K., et al., *Bisphosphonates suppress periosteal osteoblast activity independently of resorption in rat femur and tibia.* Bone, 2006. **39**(5): p. 1053-8.
152. Allen, M.R., et al., *Antiremodeling agents influence osteoblast activity differently in modeling and remodeling sites of canine rib.* Calcif Tissue Int, 2006. **79**(4): p. 255-61.
153. Bikle, D.D., et al., *Alendronate increases skeletal mass of growing rats during unloading by inhibiting resorption of calcified cartilage.* J Bone Miner Res, 1994. **9**(11): p. 1777-87.
154. Feher, A., et al., *Bisphosphonates do not inhibit periosteal bone formation in estrogen deficient animals and allow enhanced bone modeling in response to mechanical loading.* Bone, 2009. **46**(1): p. 203-7.
155. Perilli, E., et al., *Detecting early bone changes using in vivo micro-CT in ovariectomized, zoledronic acid-treated, and sham-operated rats.* Osteoporos Int, 2009.
156. Shahnazari, M., et al., *Higher doses of bisphosphonates further improve bone mass, architecture, and strength but not the tissue material properties in aged rats.* Bone, 2009. **46**(5): p. 1267-74.
157. Hanley, D.A., et al., *Pharmacological Mechanisms of Therapeutics: Parathyroid Hormone*, in *Principles of Bone Biology (Third Edition)*2008, Academic Press: San Diego. p. 1659-1695.
158. Wikipedia, *http://de.wikipedia.org/wiki/Parathormon*. 2011.
159. Lindsay, R., et al., *A Novel Tetracycline Labeling Schedule for Longitudinal Evaluation of the Short-Term Effects of Anabolic Therapy With a Single Iliac Crest Bone Biopsy: Early Actions of Teriparatide.* Journal of Bone and Mineral Research, 2006. **21**(3): p. 366-373.
160. Kousteni, S. and J.P. Bilezikian, *The cell biology of parathyroid hormone in osteoblasts.* Curr Osteoporos Rep, 2008. **6**(2): p. 72-6.
161. Bellido, T., et al., *Proteasomal Degradation of Runx2 Shortens Parathyroid Hormone-induced Anti-apoptotic Signaling in Osteoblasts: A PUTATIVE EXPLANATION FOR WHY INTERMITTENT ADMINISTRATION IS NEEDED FOR BONE ANABOLISM.* J. Biol. Chem., 2003. **278**(50): p. 50259-50272.
162. Whitfield, J., et al., *Stimulation of the growth of femoral trabecular bone in ovariectomized rats by the novel parathyroid hormone fragment, hPTH-(1–*

31)NH₂ (Ostabolin). Calcified Tissue International, 1996. **58**(2): p. 81-87.
163. Armamento-Villareal, R., et al., *An Intact N Terminus Is Required for the Anabolic Action of Parathyroid Hormone on Adult Female Rats.* Journal of Bone and Mineral Research, 1997. **12**(3): p. 384-392.
164. Krishnan, V., et al., *Parathyroid Hormone Bone Anabolic Action Requires Cbfa1/Runx2-Dependent Signaling.* Mol Endocrinol, 2003. **17**(3): p. 423-435.
165. Kim, C.H., et al., *Trabecular bone response to mechanical and parathyroid hormone stimulation: the role of mechanical microenvironment.* J Bone Miner Res, 2003. **18**(12): p. 2116-25.
166. A.G. Robling, T.M.B.a.C.H.T., *Mechanical loading reduces osteocyte expression of sclerostin protein.* J Bone Miner Res 2006. **21**(Suppl 1): p. S72 (abs 1275).
167. Iida-Klein, A., et al., *Effects of cyclic vs. daily treatment with human parathyroid hormone (1-34) on murine bone structure and cellular activity.* Bone, 2007. **40**(2): p. 391-398.
168. Cosman, F., et al., *Treatment with PTH Peptides*, in *Osteoporosis (Third Edition)*2008, Academic Press: San Diego. p. 1793-1808.
169. Jilka, R.L., et al., *Continuous elevation of PTH increases the number of osteoblasts via both osteoclast-dependent and -independent mechanisms.* J Bone Miner Res, 2010.
170. McAteer, M.E., et al., *Mechanical stimulation and intermittent parathyroid hormone treatment induce disproportional osteogenic, geometric, and biomechanical effects in growing mouse bone.* Calcif Tissue Int, 2010. **86**(5): p. 389-96.
171. Sugiyama, T., et al., *Mechanical loading enhances the anabolic effects of intermittent parathyroid hormone (1-34) on trabecular and cortical bone in mice.* Bone, 2008. **43**(2): p. 238-48.
172. Wolff, J., *Das Gesetz der Transformation der Knochen.* Dtsch Med Wochenschr, 1893. **19**(47): p. 1222,1224.
173. Frost, H.M., *Bone "mass" and the "mechanostat": a proposal.* Anat Rec, 1987. **219**(1): p. 1-9.
174. Halloran, B., et al., *Mechanisms of Immobilization-Induced Bone Loss*, in *Osteoporosis (Third Edition)*2008, Academic Press: San Diego. p. 1177-1185.
175. Jacobs, C.R., S. Temiyasathit, and A.B. Castillo, *Osteocyte mechanobiology and pericellular mechanics.* Annu Rev Biomed Eng, 2010. **12**: p. 369-400.
176. Klein-Nulend, J., et al., *The Osteocyte*, in *Principles of Bone Biology (Third Edition)*2008, Academic Press: San Diego. p. 153-174.
177. Donahue, H.J., et al., *Cell-to-cell communication in osteoblastic networks: Cell line–dependent hormonal regulation of gap junction function.* Journal of Bone and Mineral Research, 1995. **10**(6): p. 881-889.
178. Klein-Nulend, J., R.G. Bacabac, and M.G. Mullender, *Mechanobiology of bone tissue.* Pathologie Biologie, 2005. **53**(10): p. 576-580.
179. Knothe Tate, M., et al., *In vivo demonstration of load-induced fluid flow in the rat tibia and its potential implications for processes associated with functional adaptation.* J Exp Biol, 2000. **203**(18): p. 2737-2745.
180. Kufahl, R.H. and S. Saha, *A theoretical model for stress-generated fluid flow in the canaliculi-lacunae network in bone tissue.* Journal of Biomechanics, 1990. **23**(2): p. 171-180.

181. Burr, D.B., et al., *In vivo measurement of human tibial strains during vigorous activity.* Bone, 1996. **18**(5): p. 405-410.
182. Burger, E.H. and J. Klein-Nulend, *Mechanotransduction in bone—role of the lacuno-canalicular network.* The FASEB Journal, 1999. **13**(9001): p. 101-112.
183. Oxlund, B.S., et al., *Low-intensity, high-frequency vibration appears to prevent the decrease in strength of the femur and tibia associated with ovariectomy of adult rats.* Bone, 2003. **32**(1): p. 69-77.
184. Judex, S., et al., *Low-magnitude mechanical signals that stimulate bone formation in the ovariectomized rat are dependent on the applied frequency but not on the strain magnitude.* Journal of Biomechanics, 2007. **40**(6): p. 1333-1339.
185. Rittweger, J., et al., *Prevention of bone loss during 56 days of strict bed rest by side-alternating resistive vibration exercise.* Bone. **46**(1): p. 137-147.
186. Mosley, J.R. and L.E. Lanyon, *Strain rate as a controlling influence on adaptive modeling in response to dynamic loading of the ulna in growing male rats.* Bone, 1998. **23**(4): p. 313-318.
187. Rubin, C.T., et al., *Inhibition of osteopenia by low magnitude, high-frequency mechanical stimuli.* Drug Discovery Today, 2001. **6**(16): p. 848-858.
188. Salzstein, R.A. and S.R. Pollack, *Electromechanical potentials in cortical bone--II. Experimental analysis.* Journal of Biomechanics, 1987. **20**(3): p. 271-280.
189. Giancotti, F.G. and E. Ruoslahti, *Integrin Signaling.* Science, 1999. **285**(5430): p. 1028-1033.
190. Carvalho, R.S., et al., *Stimulation of signal transduction pathways in osteoblasts by mechanical strain potentiated by parathyroid hormone.* Journal of Bone and Mineral Research, 1994. **9**(7): p. 999-1011.
191. Thompson, D.D. and G.A. Rodan, *Indomethacin inhibition of tenotomy-induced bone resorption in rats.* Journal of Bone and Mineral Research, 1988. **3**(4): p. 409-414.
192. Kleinnulend, J., et al., *Pulsating Fluid Flow Increases Nitric Oxide (NO) Synthesis by Osteocytes but Not Periosteal Fibroblasts - Correlation with Prostaglandin Upregulation.* Biochemical and Biophysical Research Communications, 1995. **217**(2): p. 640-648.
193. Sugiyama, T., J.S. Price, and L.E. Lanyon, *Functional adaptation to mechanical loading in both cortical and cancellous bone is controlled locally and is confined to the loaded bones.* Bone, 2009. **46**(2): p. 314-21.
194. Järvinen, T.L.N., et al., *Estrogen deposits extra mineral into bones of female rats in puberty, but simultaneously seems to suppress the responsiveness of female skeleton to mechanical loading.* Bone, 2003. **32**(6): p. 642-651.
195. Haapasalo, H., et al., *Dimensions and estimated mechanical characteristics of the humerus after long-term tennis loading.* Journal of Bone and Mineral Research, 1996. **11**(6): p. 864-872.
196. Warburton, D.E., N. Glendhill, and A. Quinney, *The effects of changes in musculoskeletal fitness on health.* Can J Appl Physiol, 2001. **26**(2): p. 161-216.
197. Michael Pfeifer, H.W.M., *Bone Loading Exercise Recommendations for Prevention and Treatment of Osteoporosis.* http://www.iofbonehealth.org/health-professionals/special-topics/exercise-recommendations.html, 2011.
198. Shipp, K., *Exercise for people with osteoporosis: Translating the science into clinical practice.* Current Osteoporosis Reports, 2006. **4**(4): p. 129-133.

199. Szulc, P., et al., *Low Skeletal Muscle Mass Is Associated With Poor Structural Parameters of Bone and Impaired Balance in Elderly Men—The MINOS Study.* Journal of Bone and Mineral Research, 2005. **20**(5): p. 721-729.
200. Stengel, S.V., et al., *Power training is more effective than strength training for maintaining bone mineral density in postmenopausal women.* Journal of Applied Physiology, 2005. **99**(1): p. 181-188.
201. Liu-Ambrose, T.Y., et al., *Both resistance and agility training increase cortical bone density in 75- to 85-year-old women with low bone mass: a 6-month randomized controlled trial.* J Clin Densitom, 2004. **7**(4): p. 390-8.
202. Kerr, D., et al., *Exercise effects on bone mass in postmenopausal women are site-specific and load-dependent.* Journal of Bone and Mineral Research, 1996. **11**(2): p. 218-225.
203. Niu, K., et al., *Effect of office-based brief high-impact exercise on bone mineral density in healthy premenopausal women: the Sendai Bone Health Concept Study.* J Bone Miner Metab, 2010. **28**(5): p. 568-77.
204. Martyn-St James, M. and S. Carroll, *Effects of different impact exercise modalities on bone mineral density in premenopausal women: a meta-analysis.* J Bone Miner Metab, 2009. **28**(3): p. 251-67.
205. Rubin, C., et al., *Quantity and Quality of Trabecular Bone in the Femur Are Enhanced by a Strongly Anabolic, Noninvasive Mechanical Intervention.* Journal of Bone and Mineral Research, 2002. **17**(2): p. 349-357.
206. Wallace, B.A. and R.G. Cumming, *Systematic review of randomized trials of the effect of exercise on bone mass in pre- and postmenopausal women.* Calcif Tissue Int, 2000. **67**(1): p. 10-8.
207. Gusi, N., A. Raimundo, and A. Leal, *Low-frequency vibratory exercise reduces the risk of bone fracture more than walking: a randomized controlled trial.* BMC Musculoskeletal Disorders, 2006. **7**(1): p. 92.
208. Rubin, C., G. Xu, and S. Judex, *The anabolic activity of bone tissue, suppressed by disuse, is normalized by brief exposure to extremely low-magnitude mechanical stimuli.* The FASEB Journal, 2001. **15**(12): p. 2225-2229.
209. Rubin, C., et al., *Prevention of Postmenopausal Bone Loss by a Low-Magnitude, High-Frequency Mechanical Stimuli: A Clinical Trial Assessing Compliance, Efficacy, and Safety.* Journal of Bone and Mineral Research, 2004. **19**(3): p. 343-351.
210. Lelovas, P.P., et al., *The laboratory rat as an animal model for osteoporosis research.* Comp Med, 2008. **58**(5): p. 424-30.
211. Iwaniec, U.T., et al., *Animal Models for Osteoporosis*, in *Osteoporosis (Third Edition)*2008, Academic Press: San Diego. p. 985-1009.
212. Reinwald, S. and D. Burr, *Review of nonprimate, large animal models for osteoporosis research.* J Bone Miner Res, 2008. **23**(9): p. 1353-68.
213. Administration, D.o.M.a.E.D.P.F.a.D., *Guidelines for Preclinical and Clinical Evaluation of Agents used in the Prevention or Treatment of Postmenopausal Osteoporosis.* 1994.
214. Jee, W.S. and W. Yao, *Overview: animal models of osteopenia and osteoporosis.* J Musculoskelet Neuronal Interact, 2001. **1**(3): p. 193-207.
215. Bouxsein, M.L., et al., *Ovariectomy-induced bone loss varies among inbred strains of mice.* J Bone Miner Res, 2005. **20**(7): p. 1085-92.

216. Turner, R.T., *Mice, estrogen, and postmenopausal osteoporosis.* J Bone Miner Res, 1999. **14**(2): p. 187-91.
217. Borsari, V., et al., *Osteointegration of titanium and hydroxyapatite rough surfaces in healthy and compromised cortical and trabecular bone: in vivo comparative study on young, aged, and estrogen-deficient sheep.* Journal of Orthopaedic Research, 2007. **25**(9): p. 1250-1260.
218. Sigrist, I.M., et al., *The long-term effects of ovariectomy on bone metabolism in sheep.* Journal of Bone and Mineral Metabolism, 2007. **25**(1): p. 28-35.
219. Egermann, M., et al., *A sheep model for fracture treatment in osteoporosis: benefits of the model versus animal welfare.* Lab Anim, 2008. **42**(4): p. 453-64.
220. Wronski, T.J. and E.R. Morey-Holton, *Skeletal response to simulated weightlessness: a comparison of suspension techniques.* Aviat Space Environ Med, 1987. **58**(1): p. 63-8.
221. Sessions, N.D., et al., *Bone response to normal weight bearing after a period of skeletal unloading.* Am J Physiol, 1989. **257**(4 Pt 1): p. E606-10.
222. Turner, R.T. and N.H. Bell, *The effects of immobilization on bone histomorphometry in rats.* Journal of Bone and Mineral Research, 1986. **1**(5): p. 399-407.
223. Schoutens, A., et al., *Bone loss and bone blood flow in paraplegic rats treated with calcitonin, diphosphonate, and indomethacin.* Calcif Tissue Int, 1988. **42**(2): p. 136-43.
224. Lin, B.Y., et al., *Mechanical loading modifies ovariectomy-induced cancellous bone loss.* Bone Miner, 1994. **25**(3): p. 199-210.
225. Rubin, C. and L. Lanyon, *Regulation of bone formation by applied dynamic loads.* J Bone Joint Surg Am, 1984. **66**(3): p. 397-402.
226. Rubin, C.T. and L.E. Lanyon, *Regulation of bone mass by mechanical strain magnitude.* Calcif Tissue Int, 1985. **37**(4): p. 411-7.
227. Lee, K.C.L., A. Maxwell, and L.E. Lanyon, *Validation of a technique for studying functional adaptation of the mouse ulna in response to mechanical loading.* Bone, 2002. **31**(3): p. 407-412.
228. Stadelmann, V.A., N. Bonnet, and D.P. Pioletti, *Combined effects of zoledronate and mechanical stimulation on bone adaptation in an axially loaded mouse tibia.* Clin Biomech (Bristol, Avon), 2010.
229. Raab-Cullen, D.M., et al., *Bone response to alternate-day mechanical loading of the rat tibia.* Journal of Bone and Mineral Research, 1994. **9**(2): p. 203-211.
230. *Bone Adaptation Response to Sham and Bending Stimuli in Mice.* Journal of Clinical Densitometry, 2002. **5**: p. 207-216.
231. Akhter, M.P., et al., *Bone Response to In Vivo Mechanical Loading in Two Breeds of Mice.* Calcified Tissue International, 1998. **63**(5): p. 442-449.
232. Peng, Z.Q., H.K. Vaananen, and J. Tuukkanen, *Ovariectomy-induced bone loss can be affected by different intensities of treadmill running exercise in rats.* Calcif Tissue Int, 1997. **60**(5): p. 441-8.
233. Dalle Carbonare, L., et al., *Bone microarchitecture evaluated by histomorphometry.* Micron, 2005. **36**(7-8): p. 609-16.
234. Parfitt, A.M., et al., *Bone histomorphometry: standardization of nomenclature, symbols, and units. Report of the ASBMR Histomorphometry Nomenclature Committee.* J Bone Miner Res, 1987. **2**(6): p. 595-610.
235. Bauer, J.S. and T.M. Link, *Advances in osteoporosis imaging.* Eur J Radiol, 2009. **71**(3): p. 440-9.

236. Engelke, K., et al., *Macro- and Microimaging of Bone Architecture*, in *Principles of Bone Biology (Third Edition)*2008, Academic Press: San Diego. p. 1905-1942.
237. Bouxsein, M.L., et al., *Guidelines for assessment of bone microstructure in rodents using micro-computed tomography.* J Bone Miner Res, 2010. **25**(7): p. 1468-1486.
238. Lambers, F.M., et al., *In vivo micro computed tomography allows monitoring of load induced microstructural bone adaptation.* Bone, 2009. **44**(Supplement 2): p. S300-S300.
239. Schulte, F.A., et al., *In vivo micro-computed tomography allows direct three-dimensional quantification of both bone formation and bone resorption parameters using time-lapsed imaging.* Bone, 2010.
240. Ito, M., *Recent progress in bone imaging for osteoporosis research.* J Bone Miner Metab, 2011.
241. Anumula, S., et al., *Ultra-short echo-time MRI detects changes in bone mineralization and water content in OVX rat bone in response to alendronate treatment.* Bone, 2010. **46**(5): p. 1391-9.
242. Burch, W.R.a.R., *The Principles of Humane Experimental Technique.* Universities Federation for Animal Welfare: Wheathampstead, UK, 1959 (reprinted 1992).
243. TSchG, *455 Tierschutzgesetz vom 16. Dezember 2005 (TSchG), Stand am 1. Januar 2011*. 2005.
244. Balls, M., *Professor W.M.S. Russell (1925-2006): doyen of the three Rs.* Alternatives to Animal Experimentation, 2007. **14**(sup.1/4): p. 1-7.
245. 3R", S.F., *Gute Forschung mit weniger Tierversuchen.* 2007.
246. Gerhard, F.A., et al., *In silico biology of bone modelling and remodelling: adaptation.* Philosophical Transactions of the Royal Society A: Mathematical, Physical and Engineering Sciences, 2009. **367**(1895): p. 2011-2030.
247. Ruimerman, R., et al., *A 3-dimensional computer model to simulate trabecular bone metabolism.* Biorheology, 2003. **40**(1-3): p. 315-20.
248. Webster, D.J., et al., *A novel in vivo mouse model for mechanically stimulated bone adaptation--a combined experimental and computational validation study.* Comput Methods Biomech Biomed Engin, 2008. **11**(5): p. 435-41.
249. go3R, *http://www.go3r.org/*. 2011.
250. Russell, W.M.S., *The Three Rs: Past, Present and Future.* Animal Welfare, 2005. **14**: p. 279-286.
251. Webster, D.J., *<<A>> combined experimental and computational model for genetic control of micro structural bone adaptation*, 2008, ETH: Zürich. p. 1 Band.
252. Kohler, T., et al., *Automated compartmental analysis for high-throughput skeletal phenotyping in femora of genetic mouse models.* Bone, 2007. **41**(4): p. 659-67.
253. Hildebrand, T., et al., *Direct three-dimensional morphometric analysis of human cancellous bone: microstructural data from spine, femur, iliac crest, and calcaneus.* J Bone Miner Res, 1999. **14**(7): p. 1167-74.
254. Bouxsein, M.L., et al., *Guidelines for assessment of bone microstructure in rodents using micro-computed tomography.* J Bone Miner Res. **25**(7): p. 1468-1486.
255. Hildebrand, T. and P. Rüegsegger, *A new method for the model-independent assessment of thickness in three-dimensional images.* Journal of Microscopy, 1997. **185**(1): p. 67-75.
256. Danielsson, P.-E., *Euclidean distance mapping.* Computer Graphics and Image Processing, 1980. **14**(3): p. 227-248.

257. Kimmel, D.B., et al., *A comparison of iliac bone histomorphometric data in post-menopausal osteoporotic and normal subjects.* Bone and Mineral, 1990. **11**(2): p. 217-235.
258. Arlot, M.E., et al., *Trabecular and endocortical bone remodeling in postmenopausal osteoporosis: Comparison with normal postmenopausal women.* Osteoporosis International, 1990. **1**(1): p. 41-49.
259. Lambers, F.M., et al., *Longitudinal assessment of in vivo bone dynamics in a mouse tail model of postmenopausal osteoporosis.* Calcif Tissue Int, 2012. **90**(2): p. 108-19.
260. Gloy, V., et al., *Ovariectomy and overeating palatable, energy-dense food increase subcutaneous adipose tissue more than intra-abdominal adipose tissue in rats.* Biol Sex Differ. **2**: p. 6.
261. Ellis, R.E., *The distribution of active bone marrow in the adult.* Phys Med Biol, 1961. **5**: p. 255-8.
262. Rosen, C.J., et al., *Marrow fat and the bone microenvironment: developmental, functional, and pathological implications.* Crit Rev Eukaryot Gene Expr, 2009. **19**(2): p. 109-24.
263. Dennison, E.M., et al., *Lipid profile, obesity and bone mineral density: the Hertfordshire Cohort Study.* QJM, 2007. **100**(5): p. 297-303.
264. Kim, Y.Y., et al., *Increased fat due to estrogen deficiency induces bone loss by elevating monocyte chemoattractant protein-1 (MCP-1) production.* Molecules and Cells. **29**(3): p. 277-282.
265. Gimble, J.M., J.N. Beresford, and M.E. Owen, *Marrow stromal adipocytes Marrow Stromal Cell Culture*1998: Cambridge University Press.
266. Lei, Z., Z. Xiaoying, and L. Xingguo, *Ovariectomy-associated changes in bone mineral density and bone marrow haematopoiesis in rats.* Int J Exp Pathol, 2009. **90**(5): p. 512-9.
267. Li, M., et al., *Comparative study of skeletal response to estrogen depletion at red and yellow marrow sites in rats.* Anat Rec, 1996. **245**(3): p. 472-80.
268. F.M. Lambers, K.K., F.A. Schulte, G. Kuhn and R. Müller *Not only bone resorption rate but also bone formation rate is greater in ovariectomized mice than in sham mice.* Abstracts 37th European Symposium on Calcified Tissues, Glasgow, Scotland, June 26-30,, 2010: p. PP247.
269. Boyd, S.K., et al., *Monitoring individual morphological changes over time in ovariectomized rats by in vivo micro-computed tomography.* Bone, 2006. **39**(4): p. 854-862.
270. Michael Pfeifer, H.W.M., *Bone Loading Exercise Recommendations for Prevention and Treatment of Osteoporosis.* http://www.iofbonehealth.org/health-professionals/special-topics/exercise-recommendations.html.
271. Slemenda, C.W., et al., *Role of physical activity in the development of skeletal mass in children.* Journal of Bone and Mineral Research, 1991. **6**(11): p. 1227-1233.
272. Warburton, D.E.R., C.W. Nicol, and S.S.D. Bredin, *Health benefits of physical activity: the evidence.* CMAJ, 2006. **174**(6): p. 801-809.
273. Rubin, C., et al., *Inhibition of Osteoporosis by Biophysical Intervention*, in *Osteoporosis (Third Edition)*2008, Academic Press: San Diego. p. 581-600.
274. Barengolts, E.I., et al., *Effects of endurance exercise on bone histomorphometric parameters in intact and ovariectomized rats.* Bone and Mineral, 1994. **26**(2): p. 133-140.

275. Brodt, M.D., C.B. Ellis, and M.J. Silva, *Growing C57Bl/6 mice increase whole bone mechanical properties by increasing geometric and material properties.* J Bone Miner Res, 1999. **14**(12): p. 2159-66.
276. Lambers, F.M., et al., *Mouse tail vertebrae adapt to cyclic mechanical loading by increasing bone formation rate and decreasing bone resorption rate as shown by time-lapsed in vivo imaging of dynamic bone morphometry.* Bone, 2011. **49**(6): p. 1340-50.
277. Renno, A.C., et al., *Effects of a progressive loading exercise program on the bone and skeletal muscle properties of female osteopenic rats.* Exp Gerontol, 2007. **42**(6): p. 517-22.
278. Lindsay, R., et al., *Randomised controlled study of effect of parathyroid hormone on vertebral-bone mass and fracture incidence among postmenopausal women on oestrogen with osteoporosis.* The Lancet, 1997. **350**(9077): p. 550-555.
279. Finkelstein, J.S., et al., *The effects of parathyroid hormone, alendronate, or both in men with osteoporosis.* N Engl J Med, 2003. **349**(13): p. 1216-26.
280. Zhou, H., et al., *Anabolic action of parathyroid hormone on cortical and cancellous bone differs between axial and appendicular skeletal sites in mice.* Bone, 2003. **32**(5): p. 513-20.
281. Chow, J.W.M., et al., *Role for parathyroid hormone in mechanical responsiveness of rat bone.* American Journal of Physiology - Endocrinology And Metabolism, 1998. **274**(1): p. E146-E154.
282. Fuchs, R. and S. Warden, *Combination Therapy Using Exercise and Pharmaceutical Agents to Optimize Bone Health.* Clinical Reviews in Bone and Mineral Metabolism, 2008. **6**(1): p. 37-45.
283. McAteer, M.E., et al., *Mechanical stimulation and intermittent parathyroid hormone treatment induce disproportional osteogenic, geometric, and biomechanical effects in growing mouse bone.* Calcif Tissue Int. **86**(5): p. 389-96.
284. Roberts, M.D., T.J. Santner, and R.T. Hart, *Local bone formation due to combined mechanical loading and intermittent hPTH-(1-34) treatment and its correlation to mechanical signal distributions.* J Biomech, 2009. **42**(15): p. 2431-8.
285. Schulte F.A., W.C., Ruffoni D., Lambers F.M., Levchuk A., Webster D., Kuhn G., Müller R. , *The Effects Of Parathyroid Hormone And Bisphosphonate Treatment On The Local Mechanical Control Of Bone Formation And Resorption.* Abstract ASBMR 2012, 2012.
286. Childress, P., et al., *Nmp4/CIZ Suppresses the Response of Bone to Anabolic Parathyroid Hormone by Regulating Both Osteoblasts and Osteoclasts.* Calcif Tissue Int.
287. Sugiyama, T., et al., *Risedronate does not reduce mechanical loading-related increases in cortical and trabecular bone mass in mice.* Bone. **In Press, Uncorrected Proof**.
288. Feher, A., et al., *Bisphosphonates do not inhibit periosteal bone formation in estrogen deficient animals and allow enhanced bone modeling in response to mechanical loading.* Bone. **46**(1): p. 203-7.
289. Jagger, C.J., T.J. Chambers, and J.W. Chow, *Stimulation of bone formation by dynamic mechanical loading of rat caudal vertebrae is not suppressed by 3-amino-1-hydroxypropylidene-1-bisphosphonate (AHPrBP).* Bone, 1995. **16**(3): p. 309-13.
290. Stadelmann, V.A., N. Bonnet, and D.P. Pioletti, *Combined effects of zoledronate and mechanical stimulation on bone adaptation in an axially loaded mouse tibia.* Clin Biomech (Bristol, Avon).

291. Allen, M.R., et al., *Morphological assessment of basic multicellular unit resorption parameters in dogs shows additional mechanisms of bisphosphonate effects on bone.* Calcif Tissue Int. **86**(1): p. 67-71.
292. Keaveny, T.M., et al., *Effects of teriparatide and alendronate on vertebral strength as assessed by finite element modeling of QCT scans in women with osteoporosis.* J Bone Miner Res, 2007. **22**(1): p. 149-57.
293. Cusano, N.E. and J.P. Bilezikian, *Combination antiresorptive and osteoanabolic therapy for osteoporosis: We are not there yet.* Current Medical Research and Opinion. **0**(0): p. 1705-1707.
294. Black, D.M., et al., *The Effects of Parathyroid Hormone and Alendronate Alone or in Combination in Postmenopausal Osteoporosis.* New England Journal of Medicine, 2003. **349**(13): p. 1207-1215.
295. Campbell, G.M., et al., *The bone architecture is enhanced with combined PTH and alendronate treatment compared to monotherapy while maintaining the state of surface mineralization in the OVX rat.* Bone. **In Press, Uncorrected Proof**.
296. Johnston, S., et al., *The Effects of Combination of Alendronate and Human Parathyroid Hormone(1â€“34) on Bone Strength Are Synergistic in the Lumbar Vertebra and Additive in the Femur of C57BL/6J Mice.* Endocrinology, 2007. **148**(9): p. 4466-4474.
297. Samadfam, R., Q. Xia, and D. Goltzman, *Co-Treatment of PTH With Osteoprotegerin or Alendronate Increases Its Anabolic Effect on the Skeleton of Oophorectomized Mice.* Journal of Bone and Mineral Research, 2007. **22**(1): p. 55-63.
298. Yamane, H., et al., *The anabolic action of intermittent PTH in combination with cathepsin K inhibitor or alendronate differs depending on the remodeling status in bone in ovariectomized mice.* Bone, 2009. **44**(6): p. 1055-62.
299. Rittmaster, R.S., et al., *Enhancement of Bone Mass in Osteoporotic Women with Parathyroid Hormone followed by Alendronate.* Journal of Clinical Endocrinology & Metabolism, 2000. **85**(6): p. 2129-2134.
300. Kurland, E.S., et al., *The importance of bisphosphonate therapy in maintaining bone mass in men after therapy with teriparatide [human parathyroid hormone(1–34)]*. Osteoporosis International, 2004. **15**(12): p. 992-997.
301. Black, D.M., et al., *One Year of Alendronate after One Year of Parathyroid Hormone (1â€“84) for Osteoporosis.* New England Journal of Medicine, 2005. **353**(6): p. 555-565.
302. Keller, H. and M. Kneissel, *SOST is a target gene for PTH in bone.* Bone, 2005. **37**(2): p. 148-158.
303. Kramer, I., et al., *Parathyroid hormone (PTH)–induced bone gain is blunted in SOST overexpressing and deficient mice.* Journal of Bone and Mineral Research. **25**(2): p. 178-189.
304. Hoff, A.O., et al., *Increased bone mass is an unexpected phenotype associated with deletion of the calcitonin gene.* J Clin Invest, 2002. **110**(12): p. 1849-57.
305. Yoshitake, H., et al., *Osteopontin-deficient mice are resistant to ovariectomy-induced bone resorption.* Proceedings of the National Academy of Sciences, 1999. **96**(14): p. 8156-8160.
306. Hamrick, M.W., *Increased bone mineral density in the femora of GDF8 knockout mice.* Anat Rec A Discov Mol Cell Evol Biol, 2003. **272**(1): p. 388-91.
307. Baldock, P.A., et al., *Neuropeptide Y Knockout Mice Reveal a Central Role of NPY in the Coordination of Bone Mass to Body Weight.* PLoS One, 2009. **4**(12): p. e8415.

308. Kong, Y.-Y., et al., *OPGL is a key regulator of osteoclastogenesis, lymphocyte development and lymph-node organogenesis.* Nature, 1999. **397**(6717): p. 315-323.
309. Schulte, F.A., et al., *Mechanostat theory is not suspended at the local level despite estrogen depletion in murine trabecular bone.* Bone. **47**(Supplement 1): p. S68-S69.

Acknowedgments

A lot of people have accompanied and helped me during the time of my thesis. Not only in the lab and the institute but also friends at many places for whom I am very thankful.

First of all I would like to thank Prof. Brigitte von Rechenberg and Prof. Ralph Müller who gave me the opportunity to work on this interesting topic.
Gisela Kuhn as our group leader always gave great support. She always had an open door and open ear for all kind of problems.
All the others at the institute gave me a great time and it was fun working with them.

I also want to thank my parents who have always supported me and always believed in me.

All the others, friends and family, near and far: Thank you for being there, being who you are and the time we spent together. At this point I would like to quote a poem of an unknown author:

People come into your life for a reason, a season, or a lifetime. When you figure out which one it is, you will know what to do for each person.

When someone is in your life for a REASON . . . It is usually to meet a need you have expressed. They have come to assist you through a difficulty, to provide you with guidance and support, to aid you physically, emotionally, or spiritually. They may seem like a godsend, and they are! They are there for the reason you need them to be.

Then, without any wrong doing on your part, or at an inconvenient time, this person will say or do something to bring the relationship to an end. Sometimes they die. Sometimes they walk away. Sometimes they act up and force you to take a stand. What we must realise is that our need has been met, our desire fulfilled, their work is done. The prayer you sent up has been answered. And now it is time to move on.

When people come into your life for a SEASON . . . Because your turn has come to share, grow, or learn. They bring you an experience of peace, or make you laugh. They may teach you something you have never done. They usually give you an unbelievable amount of joy. Believe it! It is real! But, only for a season.

LIFETIME relationships teach you lifetime lessons; things you must build upon in order to have a solid emotional foundation. Your job is to accept the lesson, love the person, and put what you have learned to use in all other relationships and areas of your life. It is said that love is blind but friendship is clairvoyant.

Last but not least I must not forget those without whom we would not have gotten any results and would only know a fraction of what we know about life and science: All the mice that support thousands of scientists everyday at their work.

Curriculum Vitae

Name	Claudia Weigt
Date of birth	03. April 1985
Place of birth	Karl-Marx-Stadt (today Chemnitz), Germany
Nationality	German
08 / 1995 – 06 / 2003	Georgius-Agricola-Gymnasium, Chemnitz, Germany
27 / 06 / 2003	Abitur, Georgius-Agricola-Gymnasium, Chemnitz, Germany
10 / 2003 – 02 / 2009	Study of veterinary medicine, Universität Leipzig, Germany
09 / 02 / 2009	Gratuation med. vet. Universität Leipzig, Germany
05 / 2009 – 02 / 2013	Doctoral student of University of Zurich Supervisor: Prof. Dr. Brigitte von Rechenberg Department: Musculosceletal Research Unit (MSRU) / Pferdeklinik
05 / 2009 - 09 / 2011	Doctoral student at Institute for Biomechanics, ETH Zurich, Switzerland
10 / 2011 – recent	Veterinarian at ETH Phenomics Center, ETH Zurich, Switzerland